

Production and Applications of Spore Microcapsules

Wen Cai

PhD

The University of York

The Department of Chemistry

December 2013

Abstract

This thesis involves the preparation of exine shells derived from spores. The exines shells provide a ready source of microcapsules of uniform shape and monodispersed size in the region of 4 to 50 μm . The objective of the research was to fill the exine shells with various functional materials, and to examine qualitatively their bulk properties. Thus, the main production techniques and applications of sporopollenin microcapsules were extensively reviewed, with the objective of shortening the production process in order to develop commercial isolation techniques for sporopollenin exines. The conventional base and acid treatment was simplified and the microcapsules produced by this method were investigated detailed in order to evaluate the yield and quality of the exines. In order to demonstrate the utility of this procedure attempts were made to further simplify by shorter reaction time and limit chemicals applied. The overall result achieved was higher quality and useable exines, produced in a shorter time under less extreme conditions.

The filling of exine microcapsules was studied for a range of materials including dyes and magnetic particles. It was found that, contrary to published data, it was possible to efficiently fill the microcapsules with an absorbate using a large volume of solvent. Dyes that were encapsulated enabled the demonstration of colour change through changes in pH and also temperature. Multicomponents system were also achieved which allowed the demonstration of multifunctionality such as colour and magnetic properties. The use of microcapsules in a chromatography or capture/release vehicle was also demonstrated.

Contents

Abstract	i
Contents	ii
Figure list	vi
Table list	xxii
Acknowledgements	xxiv
Declaration	xxv
1. Introduction	1
1.1 Isolation of Sporopollenin.....	5
1.1.1 Exine shell isolation by base and acid treatment.....	8
1.1.2 Exine isolation by acetolysis and modified acetolysis method.....	13
1.1.3 Exine isolation by methods involving 4- Methylmorpholine N-oxide monohydrate.....	18
1.1.4 Exine isolation by autoclave and sucrose solution.....	23
1.2 Methods used to fill exine shells and their subsequent applications.....	27
1.2.1 Passive encapsulation.....	27
1.2.2 Vacuum encapsulation.....	31
1.2.3 Centrifugation encapsulation method.....	32
1.2.4 Micro-reactor encapsulation method.....	33
1.3 Recovery of encapsulated material from exine microcapsules.....	36
1.4 Application of exine microcapsules.....	39
1.4.1 Food applications.....	39
1.4.2 MRI agents based on exine microcapsules.....	40
1.4.3 Magnetic particles.....	41

1.4.4 Encapsulation of living cells.....	43
1.5 Applications for modified sporopollenin.....	46
1.6 Electrophoretic display techniques.....	48
2. Aims	52
2.1 Dye encapsulation.....	54
2.1.1 Dye encapsulation for display technology.....	54
2.1.2 Chromatographic studies.....	56
2.2 Magnetic microcapsules based on exine and intine capsules.....	57
2.3 pH responsive particles based on exine and intine capsules.....	57
2.4 Thermochromic microparticles based on exine and intine capsules.....	58
2.5 Fluorescent microparticles based on exine and intine capsules.....	59
2.6 Multi-functionalized microparticles base on exine and intine capsules...	60
2.7 Techniques for analysis of the treated exine and intine capsules.....	60
3. Experimental Method	62
3.1 Reagents and Solvents.....	63
3.2 Analytical Techniques.....	63
4. Preparation of Spore Microcapsules	67
4.1 Production of exine and intine capsules.....	68
4.2 Simplified Chm method.....	74
4.3 Bleaching of exine and intine capsules.....	79
4.4 Discussion and conclusion of exine shell isolation.....	82
4.5 Experimental.....	83

5. Encapsulation Technique for Exine and Intine Capsules	87
5.1 The Droplet method.....	88
5.2 Suspension method.....	90
5.3 Effect of concentration of the target material in suspension encapsulation.....	91
5.4 Effect of solvents on encapsulation.....	97
5.5 Effect of temperature on encapsulation in suspension method.....	102
5.6 Conclusion.....	104
5.7 Experimental.....	105
6. Dye Encapsulation	107
6.1 Black particles produced by exine and intine capsules.....	128
6.2 White particles produced by exine and intine capsules.....	130
6.3 Isolation and recovery of dyes by exine and intine capsules.....	134
7. Functional Dye Encapsulation	152
7.1 Fluorescent microcapsules produced from bleached exine and intine capsules.....	153
7.1.1 Conclusion.....	159
7.2 pH responsive microparticles based on exine and intine capsules.....	160
7.2.1 Approach.....	160
7.2.2 Conclusion.....	167
7.3 Temperature responsive microparticles based on exine and intine capsules.....	168
7.3.1 Conclusion.....	183
7.4 Experimental.....	183

8. Magnetic Microcapsules	185
8.1 Synthesis of magnetic nanoparticles inside exine and intine capsules.....	186
8.2 Doping of magnetic nanoparticles onto exine and intine capsules.....	198
8.3 Experimental.....	208
9. Multi-Functional Particles	209
9.1 Conclusion.....	221
9.2 Experimental.....	222
10. Conclusion	223
11. Definition	229
12. Reference	232

Figure List

Figure 1.1	Cross-section of a pollen grain or spore showing the layers present.	3
Figure 1.2	<i>Arabidopsis</i> and mature rice pollen. A and B show SEMs of these species with their corresponding TEMs shown below.	3
Figure 1.3	Illustration for the structures of pollen or spore wall.	4
Figure 1.4	¹³ C-NMR spectrum of <i>Lycopodium clavatum</i> spores treated with organic solvents and base, a) suspended in hot phosphoric acid (80%) for one week and b) for two weeks. (Signals for cellulose are marked by red circles)	10
Figure 1.5	¹³ C-NMR spectrum of <i>Lycopodium clavatum</i> spores treated with organic solvents and base, then treated with hot sulfuric acid (80%) for one week. (Signals for cellulose are marked by a red arrow)	10
Figure 1.6	Summary of base and acid treatment proposed by Sporomex Ltd to produce exine shells.	11
Figure 1.7	SEM images for a) untreated and b) treated <i>Lycopodium clavatum</i> spores. Scale bar in a) 25 μm and b) 50 μm.	12
Figure 1.8	Scanning confocal micrographs for a) untreated and b) treated <i>Lycopodium clavatum</i> spores.	12
Figure 1.9	Summary of an acetolysis method to prepare pollen and spores for light microscopic analysis.	13
Figure 1.10	Procedure of modified acetolysis method	14
Figure 1.11	Images for untreated (left) and isolated pollen grain taken by SEM. A, B is <i>Betula alba</i> . C, D is <i>Ambrosia elatior</i> . E, F is <i>Zea mays</i> and G, H is <i>Pinus pinaster</i> . Scale bar = 10 μm. For C and D, scale bar = 5 μm.	15

Figure 1.12	FT-IR spectra of untreated pollen, A. <i>Betula alba</i> , B. <i>Pinus pinaster</i> , C. <i>Ambrosia elatior</i> and D. <i>Zea mays</i> . The peaks marked by red circles correspond to cellulose	16
Figure 1.13	FT-IR spectra of HF treated pollen. A. <i>Betula alba</i> , B. <i>Pinus pinaster</i> , C. <i>Ambrosia elatior</i> and D. <i>Zea mays</i> .	17
Figure 1.14	The structure of 4-methylmorpholine N-oxide monohydrate	18
Figure 1.15	The procedure of MMNO treatment.	18
Figure 1.16	SEM images of <i>Lilium longiflorum</i> pollen. A) Acetone washed; B) MMNO treated pollen during protoplast release; C) MMNO treated pollen after protoplast release.	19
Figure 1.17	Photomicrographs of <i>L. longiflorum</i> pollen after the treatment with MMNO and carbohydrases in pentacrythritol. A) Cracked exines after release of intine and protoplast; B) intine enclosed protoplast. Scale bar = 50 μm .	20
Figure 1.18	TEM images of <i>L. Longiflorum</i> . a) Separation of exine layer from intine layer (scale bar = 1 μm); b) Protoplast releasing from a small crack in the exine (scale bar = 10 μm); c) Protoplast releasing from a large crack in the exine (scale bar = 10 μm) and d) Magnified region of protoplast marked in c (scale bar = 1 μm).	21
Figure 1.19	Procedures of modified MMNO method. MMNO: 4-O-methylmorpholine N-oxide. CHA: cyclohexylamine. MES: 2-(N-morpholino)ethanesulfonic acid.	22

Figure 1.20	Photomicrographs of pollen and spores before and after modified MMNO enzyme treatment (right column is untreated pollen and left one is treated). A) <i>Betula alba verrucosa</i> ; B) <i>Corylus avellana</i> ; C) <i>Fraxinus excelsior</i> ; D) <i>Taraxacum vulgare</i> (officinale) and E) <i>Lycopodium clavatum</i> . Scale bar = 50 μm .	23
Figure 1.21	Exine isolation process reported by D. Southworth	24
Figure 1.22	Photomicrographs of 1) untreated <i>Calocedrus Decurrens</i> pollen; 2) the pollen during treatment showing the detachment of exine from an intine enveloped protoplast; 3) and 4) a protoplast being released through the cracked intine.	25
Figure 1.23	Ruptured <i>Calocedrus decurrens</i> exine shells from the autoclave method.	26
Figure 1.24	Summary of passive encapsulation method	28
Figure 1.25	Image taken by confocal microscopy of <i>Lycopodium clavatum</i> exine microcapsules over filled with fish oil.	29
Figure 1.26	Photographs of exine microcapsules containing different amounts of fish oil (mass ratio of exine microcapsules to fish oil). A) 1 g g ⁻¹ ; B) 4 g g ⁻¹ and C) 6 g g ⁻¹ . Scale bar = 20 mm	30
Figure 1.27	Procedure of vacuum encapsulation method	31
Figure 1.28	LSCM images of exine microcapsules filled with A) Evans blue; B) Evans blue-stained α -amylase; C) Malachite green and D) Nile red	32
Figure 1.29	Summary of the micro-reactor encapsulation method. Compound A and B are both in the liquid phase and they generate a precipitate of compound C during the process.	33
Figure 1.30	Procedure for encapsulation of Fe ₃ O ₄ nano-particles as described by Paunov <i>et al</i>	34

Figure 1.31	Photomicrograph of Fe ₃ O ₄ encapsulated <i>Lycopodium clavatum</i> exine microcapsules.	35
Figure 1.32	SEM images of Fe ₃ O ₄ encapsulated <i>Lycopodium Clavatum</i> exine microcapsules. The areas highlighted by red circles are claimed to be Fe ₃ O ₄ particles	35
Figure 1.33	SEM images of exine microcapsules isolated from <i>Lycopodium Clavatum</i> a) before incubation and b) after 30 min incubation in plasma.	37
Figure 1.34	Graph showing the intensity of contrast agent released from exines in plasma and buffered aqueous solution as a function of time	38
Figure 1.35	Molecular structure of gadodiamide, commonly marketed under the tradename Omniscan	40
Figure 1.36	MRI microimaging experiment. Four consecutive slides through the agar gel containing exine microcapsules filled with gadodiamide. White regions represent filled microcapsules, with larger regions (highlighted by arrows) representing clumps of filled microcapsules. Frame dimension: 3 x 3 mm	41
Figure 1.37	Fe ₃ O ₄ filled exine microcapsules in the presence of a magnet. a: Fe ₃ O ₄ filled exine microcapsules dispersed in water by shaking. b: Fe ₃ O ₄ filled exine microcapsules moving towards a magnet.	42
Figure 1.38	Fe ₃ O ₄ filled exine microcapsules in the presence of a magnet. a: Fe ₃ O ₄ filled exine microcapsules settled out of an aqueous suspension. b: A fraction of Fe ₃ O ₄ filled exine microcapsules moving towards a magnet.	42
Figure 1.39	Summarized procedure of yeast cell encapsulation	43
Figure 1.40	Photomicrograph of yeast cells encapsulated in exine microcapsules.	44

Figure 1.41	LSCM images of yeast cells encapsulated in exine microcapsules	45
Figure 1.42	SEM images of yeast cells encapsulated in exine microcapsules. Exine microcapsules were treated with liquid nitrogen and cracked open using a pestle and mortar.	45
Figure 1.43	A) A re-dispersed suspension of microcapsules filled with magnetic yeast cells. B) The microcapsules are attracted to the external magnet.	45
Figure 1.44	Reaction condition for the generation of diaminoethylsporopollenin, and possible molecular structure of the product. SP = sporopollenin exine.	46
Figure 1.45	The experiment for dye capture and release by DMSP	47
Figure 1.46	Reaction condition for the generation of CDMSP, and possible molecular structures of the product. SP = sporopollenin exine	47
Figure 1.47	Reaction condition for the generation of CDMSP, and possible molecular structures of the product. SP = sporopollenin exine.	48
Figure 1.48	Scheme of electrophoretic display a) without applied electric field and b) with applied field.	49
Figure 1.49	Structure of red, green, blue and white electrophoretic display based on black& white E-ink.	50
Figure 1.50	Structure of full colour ED based on coloured E-ink.	51
Figure 2.1	Molecular structure altering and optical observation of phenolphthalein in a) pH 0-8 and b) pH 8-10.	58
Figure 2.2	Structure change of crystal violet lactone	59
Figure 3.1	Structure of KC-AC-0002	63
Figure 3.2	Simplified diagram of fluorescence spectroscopy.	66
Figure 4.1	Summary of Chm method.	69

Figure 4.2	SEM images of untreated spores from <i>Lycopodium Clavatum</i> . a) Untreated <i>Lycopodium Clavatum</i> spores, and b) Untreated <i>Lycopodium Clavatum</i> spores under higher magnification.	70
Figure 4.3	SEM images of <i>Lycopodium Clavatum</i> EICs produced by the Chm method. a) EICs. b) EICs under high magnification showing the collapsed architectures.	71
Figure 4.4	TEM images of the EICs showing increasing levels of magnification. Scale bar in a) 5µm, b) 2 µm, and c) 200 nm.	72
Figure 4.5	TEM images of the EICs with a higher magnification of one area revealing intine and an unknown substance. Scale bar in a) 10µm, b) 2 µm.	73
Figure 4.6	FT-IR spectra for a) untreated raw spores, b) CM-2 (EICs), c) SM-1 and d) overlap comparison of a, b and c.	75
Figure 4.7	TEM images of SM-1 . Scale bar of a) 10 µm , and b) 2 µm.	76
Figure 4.8	TEM photograph of SM-1 . Scale bar is 2 µm	77
Figure 4.9	TEM images of DSM-1 . Scale bar of a) 20 µm, b) 5 µm, and c) 2 µm.	78
Figure 4.10	Visual appearance of spores of <i>Lycopodium Clavatum</i> after treatment with the Chm method	79
Figure 4.11	The progression of colour change during bleaching of exines, a-e, from dark brown to pale yellow.	80
Figure 4.12	Visual appearance of bleached EICs (BEIC)	80
Figure 4.13	SEM images of BEICs; a) and b) are taken from same sample, but from different regions of the preparation.	81
Figure 4.14	TEM images of a) BEICs and b) higher magnification image of a). Scale bar of a) 5µm and b) 1 µm.	82
Figure 5.1	Summary of droplet method	89
Figure 5.2	Summary of the suspension method	90

Figure 5.3	Summary of UV-Vis sample preparation for measurement of non-encapsulated RB from a RB encapsulation experiment.	92
Figure 5.4	Calibration curve showing absorbance against concentration for RB in water.	94
Figure 5.5	Amount of RB encapsulated versus the concentration of the RB solution used.	97
Figure 5.6	Photomicrographs of a) empty EICs in toluene and b) polymer absorbate encapsulated by EICs and suspended in toluene. (x400)	101
Figure 5.7	Polymeric absorbate encapsulated in EICs suspended in water. (x400)	102
Figure 5.8	Amount of RB encapsulated per mg of EIC as a function of temperature.	103
Figure 6.1	Photomicrographs of BEICs in a) crossed polars reflective mode and b) crossed polars transmissive mode (x200).	109
Figure 6.2	Structures of the water-insoluble dyes used.	110
Figure 6.3	Structures of the water-soluble dyes used.	111
Figure 6.4	Photomicrographs of the TBBA filled EICs viewed through a) crossed polars reflective mode and b) crossed polars transmissive mode. (x200)	112
Figure 6.5	Photomicrographs of CE-TTP1-51 filled EICs viewed through a) crossed polars reflective mode and b) crossed polars transmissive mode. (x200)	113
Figure 6.6	Photomicrographs of the TYG filled EICs viewed through a) crossed polars reflective mode; b) crossed polars transmissive mode and c) computer enhanced brightness of the image of photomicrograph b. (x200)	114

Figure 6.7	Photomicrographs of CE-TTP1-75 filled EICs viewed through a) crossed polars reflective mode and b) crossed polars transmissive mode. (x200)	115
Figure 6.8	Photomicrographs of RB filled EICs viewed through a) crossed polars reflective mode; b) crossed polars transmissive mode and c) computer enhanced brightness of the image of photomicrograph b. (x200)	116
Figure 6.9	Photomicrographs of SO filled EICs viewed through a) crossed polars reflective mode and b) crossed polars transmissive mode. (x200)	117
Figure 6.10	Photomicrographs of CE-TTP1-67 filled EICs viewed through a) crossed polars reflective mode and b) crossed polars transmissive mode. (x200)	118
Figure 6.11	Photomicrographs of indigo filled EICs viewed through a) crossed polars reflective mode and b) crossed polars transmissive mode. (x100)	119
Figure 6.12	Photomicrographs of the MB filled EICs viewed through a) crossed polars reflective mode; b) crossed polars transmissive mode; c) computer enhanced brightness of the image of photomicrograph a, and d) computer enhanced brightness of the image of photomicrograph b. (x200)	120
Figure 6.13	Photomicrographs of the NBB filled EICs viewed through a) crossed polars reflective mode and b) crossed polars transmissive mode. (x200)	121
Figure 6.14	Visual appearance of the EICs filled by a) TYG, b) RB and c) MB.	122
Figure 6.15	Photomicrographs of TYG filled EICs (suspension method) viewed through a) crossed polars reflective mode and b) crossed polars transmissive mode. (x100)	123

Figure 6.16	Photomicrographs of RB filled EICs (suspension method) viewed through a) crossed polars reflective mode; b) crossed polars transmissive mode and computer enhanced brightness of the image of photomicrograph b. (x100)	124
Figure 6.17	Photomicrographs of MB filled EICs (suspension method) viewed through a) crossed polars reflective mode; b) crossed polars transmissive mode; c) computer enhanced brightness of the image of photomicrograph a, and d) computer enhanced brightness of the image of photomicrograph b. (x100)	125
Figure 6.18	LSCM photomicrographs showing the RB filled EICs viewed on different focal planes a) The encapsulation was carried out using a saturated RB solution and b) the encapsulation was carried out using a low concentration of RB solution. The sample was excited using a laser at 543 nm.	126
Figure 6.19	LSCM photomicrographs showing the TYG filled EICs viewed on different focal planes a) The encapsulation was carried out using a saturated TYG solution and b) the encapsulation was carried out using a low concentration of TYG solution. The sample was excited using a laser at 488 nm.	127
Figure 6.20	SEM image of <i>Clavatum</i> exines (40 μ m).	128
Figure 6.21	Photomicrographs of the <i>Clavatum</i> exines (40 μ m) filled by a) TYG; b) RB; c) MB with crossed polars transmissive mode; d) computer enhanced brightness of the image of photomicrograph a; e) computer enhanced brightness of the image of photomicrograph b and f) computer enhanced brightness of the image of photomicrograph c. (x200)	128
Figure 6.22	Procedure used to produce black EICs.	129

Figure 6.23	Photomicrograph of black EICs in water viewed through parallel polars transmissive mode. (x400)	130
Figure 6.24	Photomicrograph of empty BEICs in water viewed through parallel polars transmissive mode. (x400)	130
Figure 6.25	Photographs of the white EICs a) dry and b) suspended in water.	131
Figure 6.26	Photomicrographs of the white EICs viewed through a) crossed polars reflective mode and b) crossed polars transmissive mode. (x200)	132
Figure 6.27	Photomicrographs of empty BEICs in, a) 40 ° crossed polars and b) crossed polars, reflective mode.	133
Figure 6.28	Photomicrographs of the white EICs in crossed polars reflective mode.	133
Figure 6.29	Graphical representation of the spores ‘column’ used in this study.	135
Figure 6.30	Photographs showing a comparison of the initial aqueous solutions (left) and filtrates (right) of a) RB, b) MB, c) SO, d) TYG, e) NBB and f) CT69 (in acetone)	137
Figure 6.31	Molecular structures of dyes that were isolated compared to dyes that were not isolated.	138
Figure 6.32	Photographs showing comparisons of the initial solutions of RB (left) and the filtrates (right) for a) Acetone, b) Ethanol and c) DCM	139
Figure 6.33	Photographs showing a) the deionized water washings, b) ethanol washings and c) initial 0.1g.L ⁻¹ aqueous solution of RB	139
Figure 6.34	Photographs of a) initial ethanol filtrate containing little SO, b) subsequent ethanol washings and c) HCl washing continuing to release SO.	142
Figure 6.35	Protonation of the exine shell and release of dye (D ⁺).	142

Figure 6.36	Photographs showing the initial solutions of RB and the resulting filtrates using a) acetone and b) ethanol.	143
Figure 6.37	Photograph showing the initial solution of NBB in acetone (left) and the clear filtrate from the HCl pretreated exine “column” (right).	143
Figure 6.38	Photograph showing the initial solution of NBB in acetone (left) and the filtrate from the DCM pretreated exine “column” (right).	144
Figure 6.39	Proposed mechanism for the interaction of A) the untreated sporopollenin and dye for capture of cationic dyes. B) HCl pretreated sporopollenin and dye for capture of anionic dyes.	144
Figure 7.1	Molecular structure of Rhodamine B (RB).	153
Figure 7.2	Photomicrographs of samples of <i>Lycopodium clavatum</i> under a 365 nm UV lamp. a) Non-bleached EICs, b) BEICs, and c) untreated spores.	154
Figure 7.3	Emission spectra of bleached EICs from two different batches (BE-1 and BE-7), Spectrum B is an expansion of the 370-650 nm range in spectrum A. The excitation wavelength is 365 nm, the peak emission wavelength for BE-7 is 444 nm and for the BE-1 449 nm	155
Figure 7.4	Graph A: Fluorescence emission spectra of BEICs treated with aqueous solutions of RB at different concentrations. Graph B: Expansion of the region 370–570 nm of graph A. Excitation wavelength 365 nm	156
Figure 7.5	UV spectrum of 0.01 gL ⁻¹ aqueous solution of RB	158
Figure 7.6	Emission spectra of aqueous solutions of RB at different concentrations. Excitation wavelength 365 nm	159
Figure 7.7	Molecular structure altering and optical observation of phenolphthalein in the pH 8-10.	161

Figure 7.8	The appearance of phenolphthalein based pH responsive EICs (pH-EICs).	161
Figure 7.9	Photomicrographs of dry phenolphthalein filled EICs, a) parallel polars in transmissive mode and b) crossed polars in reflective. (x400)	162
Figure 7.10	Photomicrographs of a) pH-EICs and b) BEICs suspended in deionized water. (x400).	163
Figure 7.11	The appearance of BEIC in an aqueous solution of phenolphthalein after shaking.	163
Figure 7.12	Photograph of pH-EICs in pH 9 solution.	164
Figure 7.13	Photomicrographs of pH-EICs in a NaOH aqueous solution (pH 9). (x400)	165
Figure 7.14	Photomicrographs of pH-EICs; a) before pressing, and b) after being pressed. (x100)	166
Figure 7.15	Photograph of an aqueous solution (pH 6) with pH EICs suspended.	167
Figure 7.16	Photomicrographs of pH-EICs in a solution after the pH was changed from 9 to 6. (x200)	167
Figure 7.17	Photographs of a) TCS-1 and b) TCS-2 at room temperature, and c) TCS-1 and d) TCS-2 after the thermal stimuli.	169
Figure 7.18	Photomicrographs of TCS-1 in reflective mode with crossed polars. a) TCS-1 at room temperature and b) TCS-1 at 55 °C. (x400)	171
Figure 7.19	Photomicrographs of TCS-2 in reflective mode with crossed polars. a) TCS-2 at room temperature, and b) TCS-2 at 55 °C. (x400)	172
Figure 7.20	Photomicrographs of TCS-1 across a temperature range in reflective mode with crossed polars.	173

Figure 7.21	Photomicrographs of TCS-2 across a temperature range in reflective mode with crossed polars.	174
Figure 7.22	Four samples of TCS-2 were heated at different temperature for 1 h, all photographs were taken at room temperature.	175
Figure 7.23	Photomicrographs of TCS-2 across a temperature range from room temperature to ninety °C. The upper images were taken in transmissive mode with parallel polars, and the lower images were taken in reflective mode with crossed polars.	176
Figure 7.24	The comparison for the TCS-2 samples before and after being heated at 55 °C for different lengths of time. All of the photographs were taken at room temperature.	177
Figure 7.25	Illustration for the directions of evaporating hexadecanol movement in a cell with different orientations; a) the cell laid flat, b) the cell laid vertically.	179
Figure 7.26	Re-encapsulation of 1-hexadecanol to regenerate irreversible TCS-2 EICs.	180
Figure 7.27	Test for the thermochromic reversibility of refTCS-2, a) and c) were taken at room temperature, and b) was taken at roughly 60 °C.	180
Figure 7.28	Irreversible TCS-2 treated with acetone; a) Irreversible TCS-2, b) Irreversible TCS-2 was suspended in acetone without hexadecanol, and c) resTCS-2.	181
Figure 7.29	Test for the thermochromic reversibility of resTCS-2; a) and c) were taken at room temperature, and b) was taken at roughly 60 °C.	182
Figure 7.30	Photographs of the same TCS-1 sample, a) before and b) after 2 years.	182

Figure 8.1	Photographs of empty BEICs and MS I. a) Dried bleached EIC; b) Dried MS I; c) BEIC suspended in water and d) MS I suspended in water.	187
Figure 8.2	Photomicrographs for MS I in a) transmissive mode with parallel polars, b) reflective mode with crossed polars (x400).	188
Figure 8.3	Photomicrograph of MS I in toluene in transmissive mode with parallel polars (x 400).	189
Figure 8.4	Photomicrograph of empty BEICs in toluene in transmissive mode with parallel polars (x400).	190
Figure 8.5	TEM images of MS I, a) the middle part of a slightly flattened MS I and b) close up for the red square marked area in a. Scale bar in a) 1 μm and b) 200 nm.	191
Figure 8.6	TEM photograph for the close up of Fe_3O_4 magnetic nanoparticles in MS I. Scale bar 200 nm.	192
Figure 8.7	Pictures taken from a video of MS I moving by application of a magnet	193
Figure 8.8	Photographs of MS I suspended in water and subjected to a magnetic field as a function of time (seconds)	193
Figure 8.9	General inspection of MS I when the magnet is rotated. ‘N’ and ‘S’ represent the north and south poles of the magnet, respectively.	194
Figure 8.10	Photomicrograph of MS I rotating in water by a magnet.	195
Figure 8.11	Isolation of MS I from BEIC in the absence of solvent.	196
Figure 8.12	Simplified diagram showing the isolation of MS I from empty BEICs in the absence of solvent	197
Figure 8.13	Isolation of MS I from normal BEIC in water.	197
Figure 8.14	Simplified diagram showing the isolation of MS I from empty BEICs in solvent	198
Figure 8.15	Photographs for MS II.	199

Figure 8.16	Photographs showing purification of MS II, the black powder highlighted by red circle is thought to show an area composed of free magnetic nanoparticles.	200
Figure 8.17	Photomicrographs of MS II a) in transmissive mode with parallel polars and b) in reflective mode with crossed polars.	201
Figure 8.18	Photomicrographs of MS II in toluene in transmissive mode with parallel polars.	202
Figure 8.19	TEM images of MS II showing the nanoparticles on the surfaces of the exine walls. Scale a) 5 μ m and b) 1 μ m.	203
Figure 8.20	Moving MS II by a magnetic field in a sample vial.	204
Figure 8.21	Pictures taken from a video of MS II being collected by a magnet in a solvent (water).	205
Figure 8.22	Isolation of MS II from BEIC by a magnet without solvent.	206
Figure 8.23	Isolation of MS II from BEICs in solvent (water) by a magnet.	206
Figure 8.24	MS II rotation by magnetic field under microscope.	207
Figure 9.1	Photograph of cmEICs.	212
Figure 9.2	Photomicrographs using crossed polars in reflective mode for; a) empty bleached EICs, b) MS II, c), and d) cmEICs. (x400)	213
Figure 9.3	Photomicrograph of cmEICs with a) transmissive mode with parallel polars, b) reflective mode with crossed polars and c) computer enhanced brightness of the image of photomicrograph b. (x400)	214
Figure 9.4	cmEICs moving in the presence of a magnet	215
Figure 9.5	Photograph of tmEICs at room temperature	215

Figure 9.6	Photomicrographs of a single exine (circled) of tmEICs a), the tmEICs with both RB and LTM encapsulated, b) and c) tmEICs where encapsulation did not occur are highlighted in a difference in colour. (x400)	216
Figure 9.7	Photomicrograph of a) and b) tmEICs suspended in water, and c) empty bleached EICs suspended in water with parallel polars in transmissive mode.	217
Figure 9.8	Photomicrograph of a) tmEICs suspended in water with crossed polars using reflective and b) computer enhanced brightness image of a). (x400)	219
Figure 9.9	Photographs of tmEICs heated from room temperature to 50 °C.	220
Figure 9.10	Photographs of the separation of tmEICs and yellow EICs by a magnet.	220
Figure 9.11	Photographs of the separation of tmEICs and yellow BEICs by a magnet.	221

Table list

Table 1.1	Diameters of a range of pollen and spores (including bacterial spores)	7
Table 1.2	Results of base and acid treatments applied to <i>Lycopodium clavatum</i> spores.	9
Table 4.1	Summary of reagent, quantities used and yield for BEICs.	86
Table 5.1	Table of reference samples (Ref n) versus quantity, concentration and UV-vis absorbance of RB in water used as calibration data for the encapsulation experiments.	93
Table 5.2	RB left in the solution B.	95
Table 5.3	RB encapsulated by EICs (mg mg^{-1}) by different concentrations of aqueous RB solutions.	96
Table 5.4-1	Appearance of EICs of <i>Lycopodium clavatum</i> in different solvents, when view from the top and side (x400)	99
Table 5.4-2	Appearance of EICs of <i>Lycopodium clavatum</i> in different solvents, when view from the top and side (x400)	100
Table 5.5	Results of the experiments for temperature effect in RB encapsulation with 0.1 g L^{-1} RB solution with water.	103
Table 5.6	Summary of BE-1 used in aqueous RB solutions with different concentrations.	105
Table 5.7	Summary of BE-1 used in the experiment to encapsulate RB with different temperatures.	106
Table 6.1	Comparison of the capture efficiency of raw spores and exines with different pre- and post-packing treatments.	136
Table 6.2	Comparison of initial solutions of RB and filtrates for a range of solvents. All the initial solutions have a concentration of 0.1 g.L^{-1}	141
Table 6.3	Summary of reagents used in encapsulations of water-insoluble dyes via the droplet method.	145

Table 6.4	Summary of reagents used in encapsulations of water-soluble dyes via the droplet method.	146
Table 6.5	Summary of reagents used in encapsulations of water-soluble dyes via the droplet method (40 μ m exine microcapsule).	147
Table 6.6	Summary of reagents used in encapsulations of water-soluble dyes via the suspension method.	148
Table 6.7	Experimental detail of dye isolation using EIC “columns”.	150
Table 6.8	Experimental detail of dye isolation using pretreated EIC “columns”	151

Acknowledgements

First and foremost, I offer my sincerest gratitude to my supervisor, Prof. John W. Goodby, for all I have learned from him and for his continuous help and support in all stages of my research and thesis. I also would like to express my gratitude to Dr. Stephen Cowling, who has helped me a lot with my academic writing and experimental studies. It is their guidance that I will never forget.

I wish to sincerely thank Dr. Charles Bradbury for his advice and for helpful experimental guidance; I learned a great deal from him. Furthermore, I would never forget to deeply thank Dr. Edward Davis, who is very friendly and helped me to start my research career. It is always very enjoyable and useful to discuss my research with him.

I would also like to thank Katrina Bakker and Dr. Emily Bevis for their great help with my thesis and English skills. Moreover, I have particularly benefitted from Katrina Bakker's rigorous academic attitude.

I am grateful to all of the technical staff that I have worked with; Thanks to Meg Stark, Stephen Hau, Mike Keogh, Karl Heaton, Heather Fish, and Dr. Laurence Abbott and Dr. John Moore for useful discussions regarding fluorescence studies.

It is my pleasure to have worked in this very friendly research group, thanks to all of the members for providing this friendly atmosphere in both the laboratory and the office: Dr. Richard Mandle, Dr. Martin Bates, Dr. Verena Gortz, Dr. Isabel Saez, Dr. Edward Davis, Dr. Emily Bevis, Katrina Bakker, David Stewart, Kirsty Holdsworth, Charlie Wand, Tiantian Ma, Tingjun Zhong, Xiang Jia.

Finally, I would like to offer my sincerest gratitude to my parents, NengCai and WenXiang Yu. Without their support and encouragement, my thesis and research would never have been completed.

Declaration

I am hereby to certify that this thesis is a presentation of my original research work and that I am the sole author. All direct and indirect sources are acknowledged as references.

Wen Cai

16th December 2013

1. Introduction

Nature provides a fantastic range of materials for us to use and modify. A good example of a useful natural material is wood (eg. paper, building materials, furniture). The range of natural materials being investigated for applications is rapidly increasing through the progress of modern science, although due to the complex structure and limit of modern analytical approaches knowledge of exact chemical composition of many natural remains a mystery. Sporopollenin is an example of a natural material that has remarkable properties. It is a biopolymer, usually found in the outer walls of spores and pollen. Spores and pollens are from part of the reproductive cycles of higher plants, mosses, some green algae and ferns. Some bacteria and fungi also possess sporopollenin outer walls.^{1,2}

Sporopollenin is able to withstand harsh chemical and physical conditions, which other plant materials and even many synthetic polymers cannot. It can resist almost all methods of degradation, including acid and base decomposition and bio-degradation.^{3,4} Sporopollenin is insoluble in most common organic and inorganic solvents.^{5,6} Furthermore, it remains stable even when exposed to high pressures and both high and low temperatures.⁷ Shaw and Brooks stated “Sporopollenins are probably the most resistant organic materials of direct biological origin found in nature and in geological samples”.⁷ This is early evidence that sporopollenin is not one single molecule, but classes of very similar molecules. One of the most powerful pieces of evidence for sporopollenin’s stability is that intact spores have been found in 500 million year old rock samples.⁸

A cross-section through a pollen grain or spore is shown in Figure 1.1. Although pollens and spores participate in different re-productive cycles, their structures and compositions can be considered to be similar for the purposes of this work.

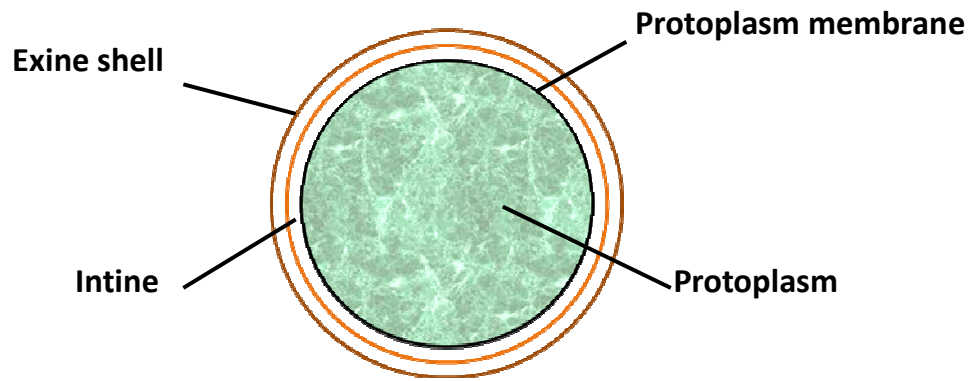
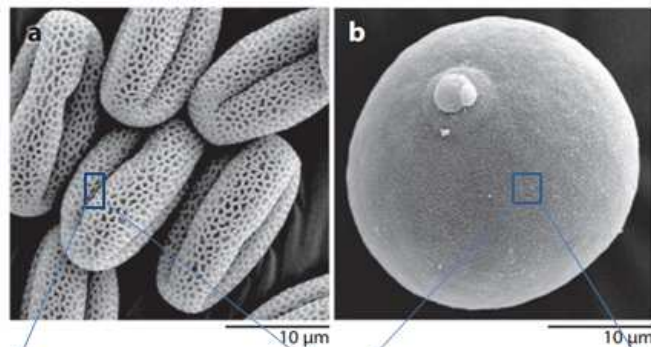


Figure 1.1 Cross-section of a pollen grain or spore showing the layers present.

Although the surface of pollen grains and spores from various species may appear different under the scanning electron microscope (SEM), transmission electron microscopy (TEM) demonstrates that the layers present within their walls are broadly similar (Figure 1.2).⁹

SEM:



TEM:

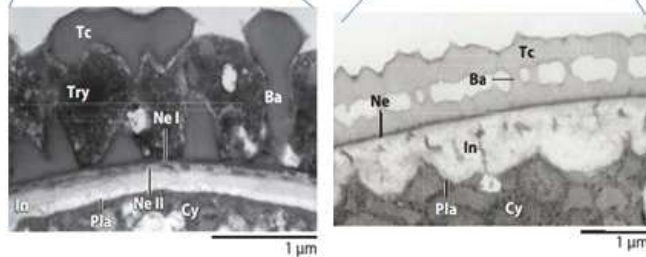


Figure 1.2 *Arabidopsis* and mature rice pollen. A and B show SEMs of these species with their corresponding TEMs shown below.⁹⁾

Internal structures, such as the nuclei, cytoplasm and membrane structures, are found within the protoplast. All pollen and spores possess protoplasts with similar compositions, although different species may have different ratios of components within the protoplast. Protoplasts are composed of five classes of substance: water, electrolytes, proteins, lipids and carbohydrates.¹⁰ Pollen and spore protoplast are delicate, and are

therefore covered by a wall to protect their fragile organelles, which are small structures within a cell that are essential for their function (e.g. nucleus, mitochondria, lysosome and Golgi apparatus).¹¹

Pollen and spore walls are constructed of two layers: the exine and the intine. The intine lies between the exine and the protoplast membrane. The intine is composed of cellulose, pectin and various proteins.¹² The outermost layer of pollen and spores is the exine. This provides a physical barrier to separate the delicate pollen or spore contents from the surrounding environments. The exine is composed of sporopollenin and can be divided into two sub-layers (sexine and nexine) as shown in Figure 1.3. The outer layer is called the sexine, and usually possesses a distinctive architecture. Examples of two possible types of architecture are shown in Figure 1.3, although many more are possible. This layer provides each species of pollen and spore with its distinct morphology.

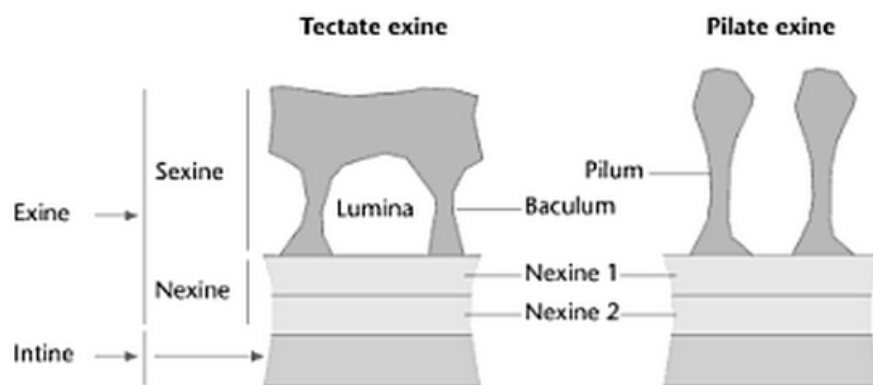


Figure 1.3 Illustration for the structures of pollen or spore wall.¹³

The layer that lies between the sexine and intine is called the nexine. This can also be divided into two sublayers; however, unlike the sexine, these sublayers possess no visible architecture. The sexine usually fully covers the intine and protoplast. Micro-scale pores traverse the sexine and nexine layers in some species (e.g. rye), and the exine walls of most species possess nano-scale channels.¹⁴ These facilitate the passage of materials between the interior and exterior of the spore or pollen grain.

The sporopollenin that makes up the exine has a complex molecular structure that is not yet fully understood. Furthermore, its composition varies between genera. For example, sporopollenin from *Typha angustifolia L.* has been dissolved in 2-aminoethanol, but the sporopollenins from other genera do not dissolve in this solvent.⁶ Abstracting 'pure' sporopollenin for analysis has been found to be particularly challenging. This is because

methods used either alter its chemical composition or do not remove non-sporopollenin material, e.g. theintine.¹⁵

Historically, sporopollenin was largely considered to be a biopolymer derived from carotenoids and carotenoid esters. This was because some polymers of carotenoids display similar results to sporopollenin when analyzed by infrared spectroscopy and pyrolysis-gas chromatography.¹⁶

However, these carotenoid precursors synthesized by plants were not found to be incorporated into the sporopollenin exine during pollen development.¹⁷ These experiments, known as tracer experiments, did however demonstrate the presence of phenolic groups. Further analysis using a host of analytical techniques has revealed additional functional groups. Solid state NMR and Fourier transform-infrared (FT-IR) spectroscopy indicated that sporopollenin contains long aliphatic chains in addition to aromatic rings.^{17,18}

Although the exact molecular structure of sporopollenin is unknown and may vary from species to species, the presence of the following functional groups has been confirmed: phenolic groups, carboxylic acids, ethers, alcohols and unsaturated hydrocarbons.^{8, 19, 20, 23} These functional groups have already been used in the modification of sporopollenin (see section 1.2.9).

1.1 Isolation of sporopollenin

Due to the remarkable chemical and physical stability of sporopollenin, and the natural capsule-like structure of pollen and spore exine walls, intact exine shells have been evaluated as potential microcapsules. Pollens and spores range in diameter from approximately 1 μm to 250 μm including bacteria and fungi. Table 1.1 shows the diameters of a small sample of pollens and spores, which could be used as potential microcapsules. By removing non-exine material, microcapsules can be prepared from pollen and spores. Moreover, pollen and spores from different species have different shapes and wall architectures. In principle, a wide range of microcapsules could be synthesized with characteristics to match various applications.

As previously discussed, pollens and spores contain a wide range of biological structures, i.e. the intine and protoplast, in addition to the sporopollenin exine. In order

to produce microcapsules from pollen and spores, this non-sporopollenin material must be removed. This is challenging and many processes have been proposed to achieve this. These methods can be broken down into four groups: acid and base treatments, acetolysis, 4-methylmorpholine N-oxide monohydrate (MMNO) with enzyme treatment, and predominately physical treatments. All of these treatments can isolate exine material from pollen and spores, but the chemical structure of the sporopollenin exine shells recovered via each of these methods is likely to be different. For example, treatments involving hydrochloric acid have been found to result in chlorination of sporopollenin.²⁵ It is important to note that not all methods will remove all of the non-sporopollenin material. In addition, some methods produce intact exine shells, whereas others rupture the shells.^{24, 39}

Table 1.1 Diameters of a range of pollen and spores (including bacterial spores)^{21,22}

Name	Diameter /μm	Name	Diameter /μm
<i>Bacillus subtilis</i>	1.2	<i>Myosotis</i>	2.4-5
<i>Aspergillus niger</i>	4	<i>Penicillium</i>	3.0-5.0
<i>Ganoderma</i>	5-6.5	<i>Mimosa pudica</i>	9
<i>Macropiper excelsum</i>	10	<i>Piper yzabalanum</i>	12
<i>Cyclamen hederifolium</i>	13	<i>Agrocybe</i>	10.0-14.0
<i>Calluna vulgaris</i>	15	<i>Theobroma cacao</i>	16
<i>Juniperus communis</i>	17	<i>Anemone hupehensis</i>	18
<i>Delosperma taylori</i>	19	<i>Asperula 'sintensis'</i>	20
<i>Lycopersicum esculentum</i>	20	<i>Portulaca grandiflora</i>	20
<i>Fraxinus ornus</i>	21	<i>Nemophila maculata</i>	22
<i>Viburnum bodnantense</i>	23	<i>Robinia pseudoacacia</i>	24
<i>Lycopodium clavatum</i>	25	<i>Symphytum officinale</i>	25
<i>Anemone coronaria</i>	26	<i>Betula pendula</i>	28
<i>Helianthus annuus</i>	30	<i>Brunnera macrophylla</i>	32
<i>Cephalotaxus harringtonia</i>	33	<i>Nicotiana tabacum</i>	34
<i>Helleborus niger</i>	35	<i>Lychnis flos-cuculi</i>	36
<i>Eremurus himalaicus</i>	38	<i>Molucella laevis</i>	40
<i>Brunfelsia americana</i>	43	<i>Pachystachys lutea</i>	45
<i>Juglans regia</i>	48	<i>Colchicum hungaricum</i>	50
<i>Hyacinthoides non-scripta</i>	53	<i>Clerodendrum bungei</i>	55
<i>Calochortus superbus</i>	58	<i>Fritillaria imperialis</i>	60
<i>Convolvulus arvensis</i>	63	<i>Armeria maritima</i>	65
<i>Pinus taiwanensis</i>	66	<i>Clerodendrum splendens</i>	70
<i>Lonicera periclymerium</i>	75	<i>Passiflora caerulea</i>	77
<i>Averrhoa carambola</i>	80	<i>Eucharis amazonica</i>	83
<i>Pinus nigra v. pallasiana</i>	85	<i>Pinus coulteri</i>	88
<i>Zea mays</i>	95	<i>Lilium</i>	100
<i>Dionaea muscipula</i>	110	<i>Cucubita pepo</i>	120
<i>Luffa cylindrica</i>	130	<i>Hymenocallis</i>	140
<i>Hymenocallis littoralis</i>	150	<i>Oenothera biennis</i>	160
<i>Calliandra haematocephala</i>	170	<i>Oenothera macrocarpa</i>	190
<i>Pavonia x gledhillii</i>	200	<i>Cuburbita</i>	250

1.1.1 Exine shell isolation by base and acid treatment

A combination of acid, base and organic solvent treatments are most commonly used to produce intact exine shells from spores. This treatment can be broken down into three steps:

Step 1: The spores are stirred in organic solvent and heated to reflux to remove surface lipids and some protoplast material.

Step 2: Spores are stirred in aqueous base solution and heated to reflux to remove almost all of the protoplast and some of the intine material.

Step 3: Spores are stirred in boiling concentrated acid to remove any remaining intine and protoplast.

Filtration and washing is usually performed between each step. This method relies on the chemical stability and insolubility of sporopollenin to successfully isolate exine shells.

This method was first reported by Zetzsche *et al.*^{23,24} However, the cellulose layer (intine) of the spores was difficult to completely remove. A range of different acids were used in an attempt to remove the intine from *Lycopodium clavatum* spores, which had previously had their protoplast removed as shown in Table 1.2. Although acids were largely successful at removing the intine, hydrochloric acid and sulfuric acid resulted in both chlorination and sulfination of the sporopollenin structure. This illustrates that the acid used to eliminate the intine and protoplast must be selected with care and that warm 85% phosphoric acid could be the most appropriate acid to use. These results are all relative to *Lycopodium clavatum* and there is no evidence to suggest that this methodology would give rise to the same results in other species.

Table 1.2 Results of base and acid treatments applied to *Lycopodium clavatum* spores.²⁵

Acid or base used	Result
Cuprammonium hydroxide	Some non-sporopollenin material remained
40% hydrochloric acid	Chlorine found to have contaminated sporopollenin
72% sulphuric acid	Sulfur found to have contaminated sporopollenin
Warm 85% phosphoric acid	Cellulose reported to have been removed

Conversely, Shaw *et al.* reported that treating spores with phosphoric acid does not remove all non-sporopollenin material.²⁶ *Lycopodium clavatum* spores were treated with organic solvents and base, and then heated to reflux for 1 week in 80% phosphoric acid.¹³ ¹³C-NMR analysis revealed a strong cellulose signal, indicating the presence of intine material (Figure 1.4a). After two weeks of continuous reflux in acid, the cellulose signal diminished, but did not disappear completely (Figure 1.4b). This indicates that the intine was not completely removed by this acid treatment.²⁶ Sulfuric acid (80 %) was used instead of phosphoric acid. Spores were treated with sulfuric acid at 80-90 °C for one week and the cellulose signal did disappear upon NMR analysis (Figure 1.5). However, as previously mentioned, this treatment is likely to result in sulfination of the sporopollenin.

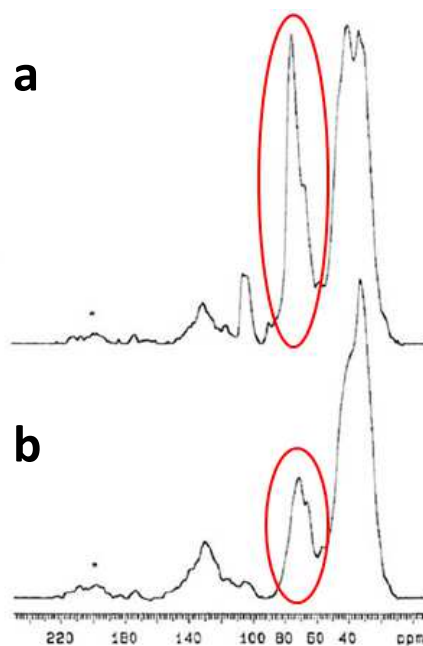


Figure 1.4 ^{13}C -NMR spectrum of *Lycopodium clavatum* spores treated with organic solvents and base, a) suspended in hot phosphoric acid (80%) for one week and b) for two weeks. (Signals for cellulose are marked by red circles)²⁶

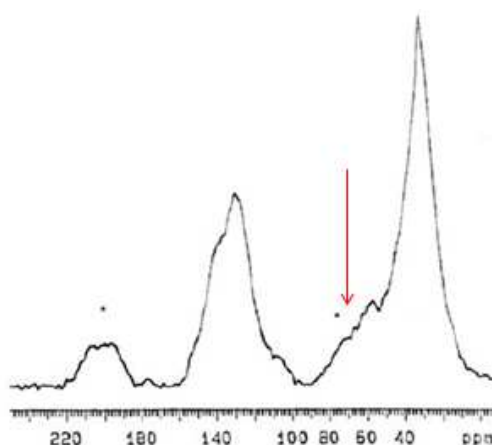


Figure 1.5 ^{13}C -NMR spectrum of *Lycopodium clavatum* spores treated with organic solvents and base, then treated with hot sulfuric acid (80%) for one week. (Signals for cellulose are marked by a red arrow)²⁶

In more recent years, phosphoric acid (in conjunction with organic solvents and base treatments) has become the most popular method to produce exine shells. Sporomex Ltd produces exine shells from spores for commercial applications via the treatments summarized in Figure 1.6.²²

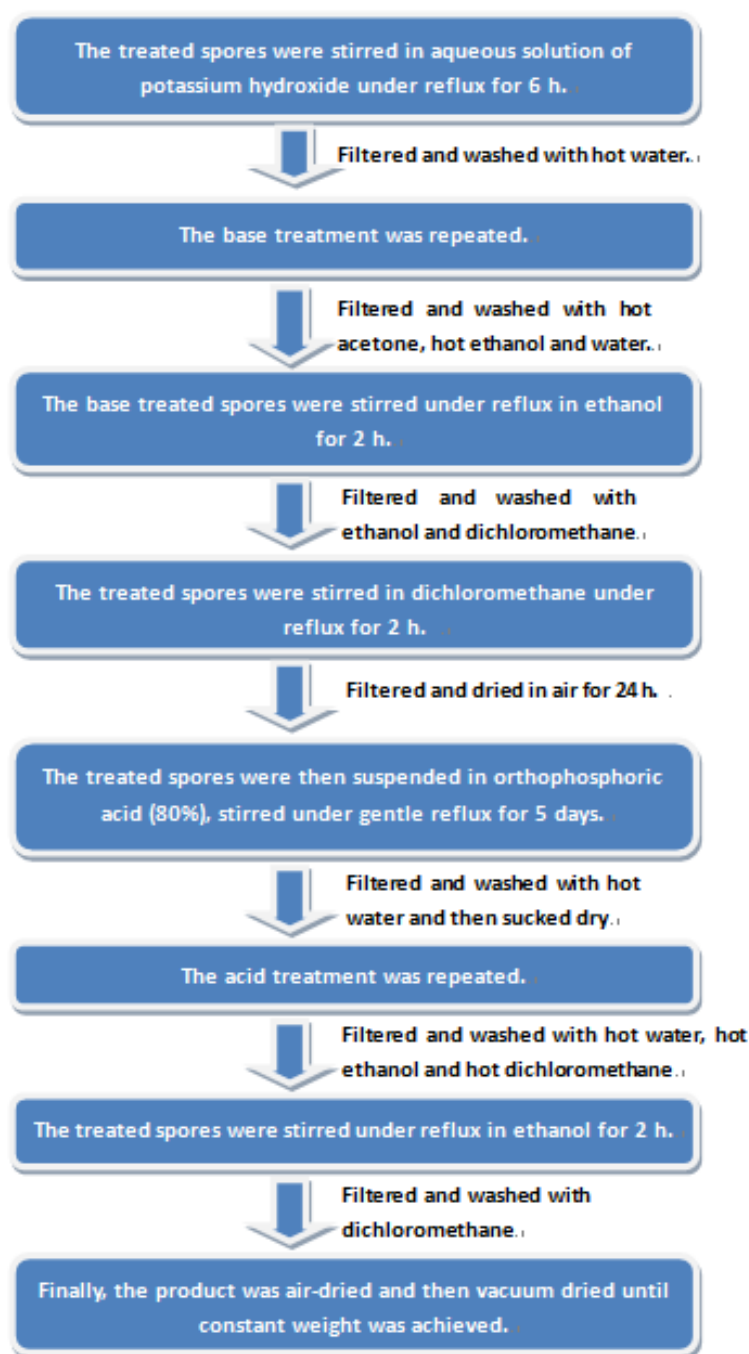


Figure 1.6 Summary of base and acid treatment proposed by Sporemex Ltd to produce exine shells.

Figure 1.7 shows the results of SEM analysis of untreated *Lycopodium clavatum* spores, and those treated by the method summarized in Figure 1.6. The untreated spores have a rounded appearance however, after base and acid treatment, they have become deflated. Figure 1.8 shows laser scanning confocal micrographs (LSCM) for both an untreated and treated *Lycopodium clavatum* spore. The blue area in image 1.8 indicates the protoplast inside the spore and the red area highlights the spore wall. Due to the low

resolution of this technique, it is not possible to distinguish between the intine and exine. After treatment, image 1.8b, the blue area (indicating protoplast) has disappeared, revealing that the spore is composed almost entirely of exine. Due to the low resolution of the image, it is difficult to confirm the presence or absence of intine, though it is likely to have been removed as the author claims.²⁸ There are still fragments of material remaining in spore (see left of cavity). The exact nature of this material is difficult to identify, but could be protoplast material, cellulose fragments or chemicals used for isolation.

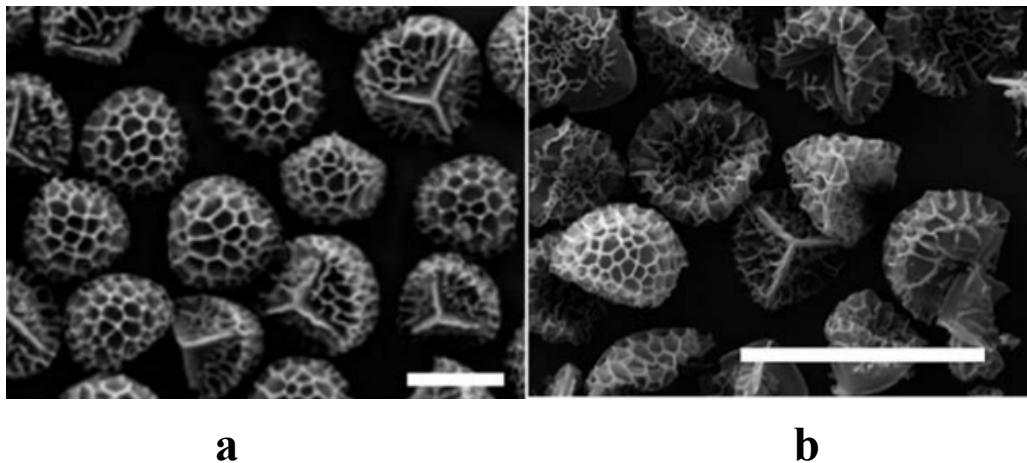


Figure 1.7 SEM images for a) untreated and b) treated *Lycopodium clavatum* spores. Scale bar in a) 25 μm and b) 50 μm .²⁷

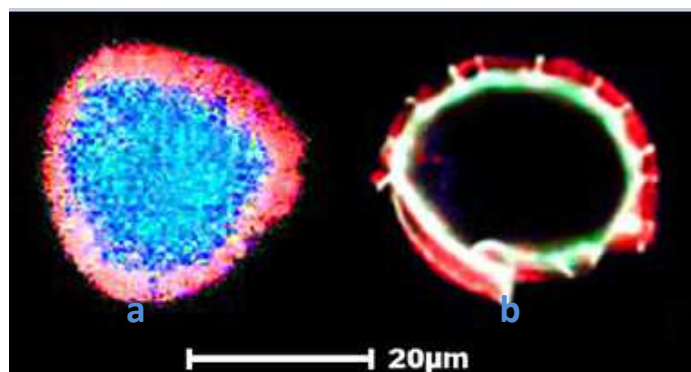


Figure 1.8 Scanning confocal micrographs for a) untreated and b) treated *Lycopodium clavatum* spores.²⁸

Among the four methodologies described (base and acid, acetolysis, MMNO with enzymes and physical treatments), the base and acid treatment has the longest reaction time. It has already been demonstrated that the acid treatment changes the chemical composition of the sporopollenin, which is further highlighted by the colour change

from a very pale yellow powder before treatment to a brown powder after treatment.

The results have clearly demonstrated that this acid treatment does not damage the structural integrity of the exines while removing the biological fragments. Interestingly the isolated microcapsules are not harmful to human health, as discussed in section 1.4.1, and the exceptional chemical and physical properties of the spores are retained.

1.1.2 Exine isolation by acetolysis and modified acetolysis methods

Acetolysis is the traditional method used to prepare pollens and spores for analysis by light microscopy, and was initially reported by Erdtman *et al.*²⁹ This technique produces intact exine shells that have had all non-sporopollenin material removed. The main step in this process involves the treatment of pollens and spores with acetolysis fluid, made up of one part concentrated sulfuric acid to nine parts acetic anhydride by volume.³⁰ It is possible to combine acetolysis with other processes, such as pre-treatment with potassium hydroxide or glacial acetic acid, to fit the requirements to different species.^{31,32} A good example for this method is a combination of chlorination and acetylation, and the procedure is summarized in Figure 1.9.³³

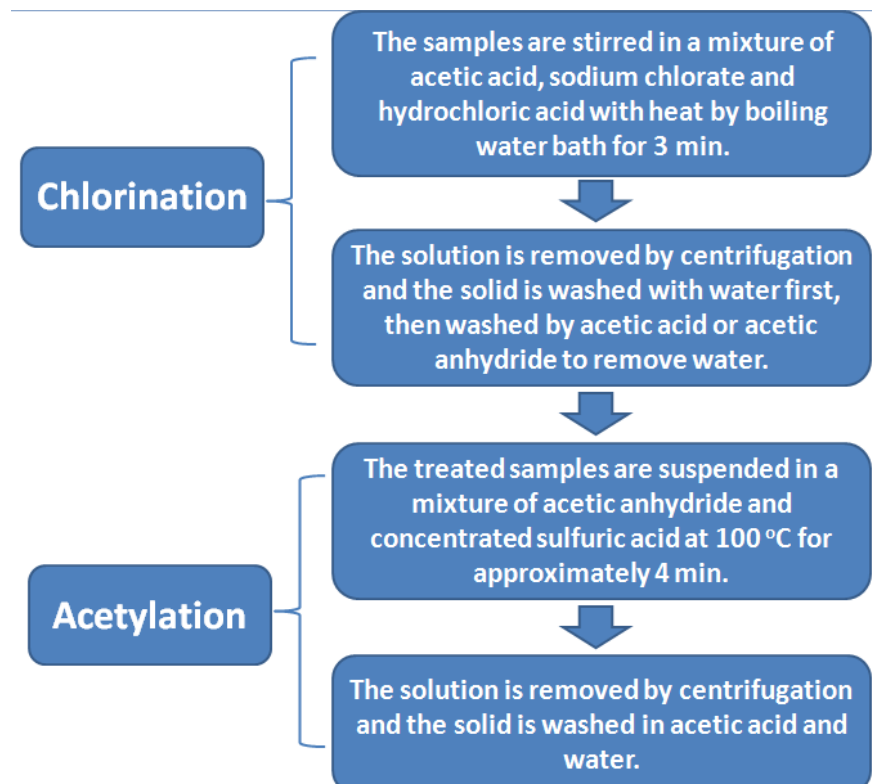


Figure 1.9 Summary of an acetolysis method to prepare pollen and spores for light microscopic analysis.³³

This method is similar to the base and acid treatment in that it uses acid in an attempt to remove non-sporopollenin material. Acetolysis is a quick, easy, well-studied method that is simple to perform on a small scale. It has been used successfully on a wide range of pollens and spores, and removes almost all non-sporopollenin material.²⁹⁻³³ The most significant drawback of this method is that it produces very dark brown exine shells, which would not be suitable for food, pharmaceutical or optical applications.

Acetolysis does not always remove all non-sporopollenin material; the degree to which the intine is removed in each species is not well studied. Dominguez *et al.* performed a modified acetolysis in an attempt to remove additional polysaccharidic material not removed by conventional acetolysis (this material is largely located in the intine). The procedure used is outlined in Figure 1.10.³⁴ Initially, acetolysis was used to produce almost empty pollen, still containing some intine residue. Hydrogen fluoride in pyridine was subsequently used to remove the remaining contents, as demonstrated by FT-IR.³⁴

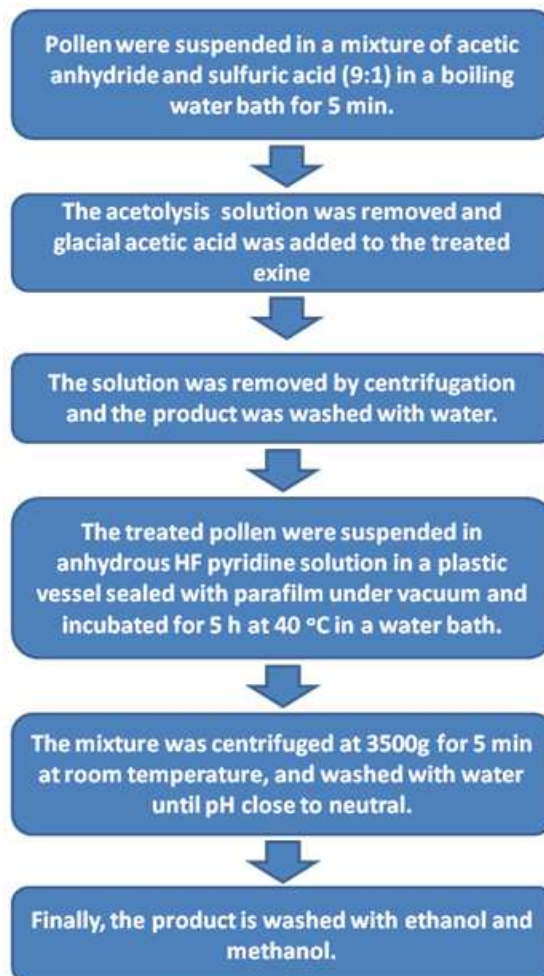


Figure 1.10 Procedure of modified acetolysis method.³⁴

The modified acetolysis method was used to isolate sporopollenin from *Betula alba*, *Ambrosia elatior*, *Zea mays* and *Pinus pinaster* pollen(see Figure 1.11).³⁴ From these SEM images, it is clear that untreated and treated pollens have different appearances whereby the untreated pollens are rounded and the treated pollens are deflated or somewhat deformed. Due to the structure of *Pinus pinaster* pollen (Figure 1.11 G and H), the saccuses beside the major body of pollen make the changes in morphology of the pollen difficult to observe.

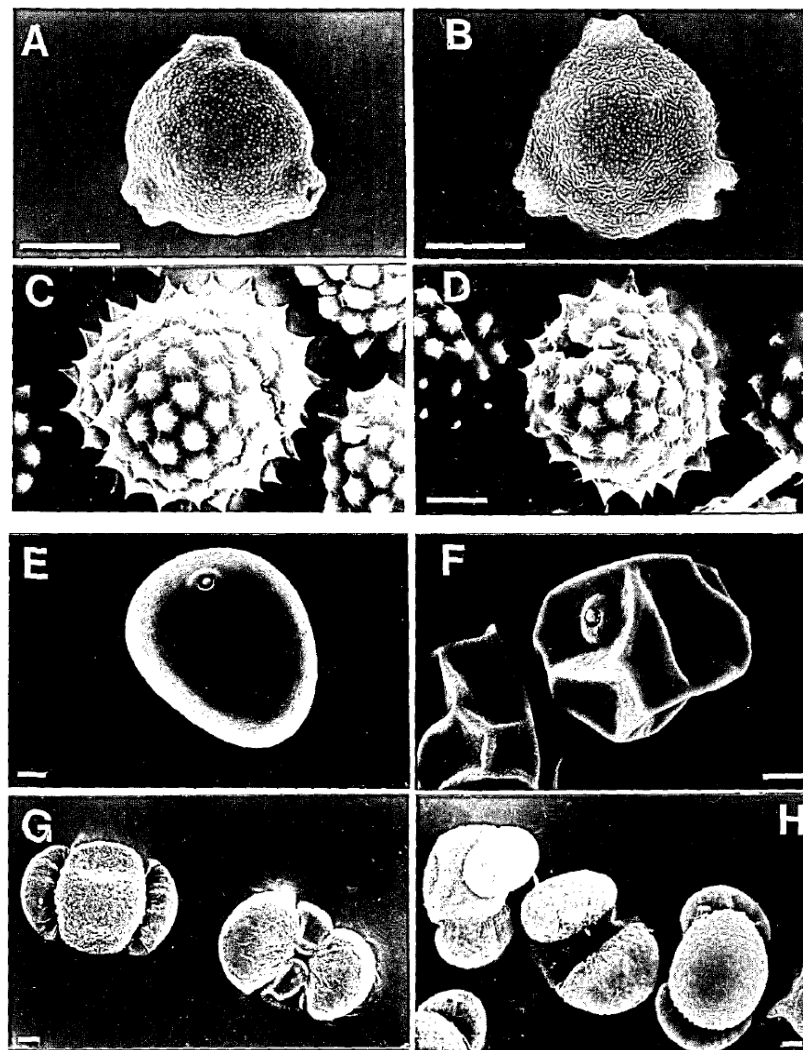


Figure 1.11 Images for untreated (left) and isolated pollen grain taken by SEM. A, B is *Betula alba*. C, D is *Ambrosia elatior*. E, F is *Zea mays* and G, H is *Pinus pinaster*. Scale bar = 10 μm.

For C and D, scale bar = 5 μm.³⁴

SEM images alone are insufficient to demonstrate that polysaccharides (including cellulose found in the intine) have been completely removed *via* this modified

acetolysis method. Additional analysis is required to determine the presence or absence of these polysaccharides. Dominguez *et al.* attempted to demonstrate the removal of the intine by FT-IR analysis of untreated pollen and treated pollen using the modified acetolysis method. Figure 1.12 shows the FT-IR analysis where the authors claim that peaks marked by red circles correspond to the intine. After the modified acetolysis treatment these peaks are absent (Figure 1.13). Based on the comparison between the FT-IR spectra before and after treatment, the authors concluded that the intine was successfully removed by this treatment. However, FT-IR is not a suitable technique to convincingly detect intine material due to the complex chemical composition of pollen. The peaks for intine material may overlap with other pollen material. For example, both sporopollenin and the cellulose intine possess hydroxyl groups. Therefore, TEM would be required to definitively demonstrate the presence or absence of intine material.

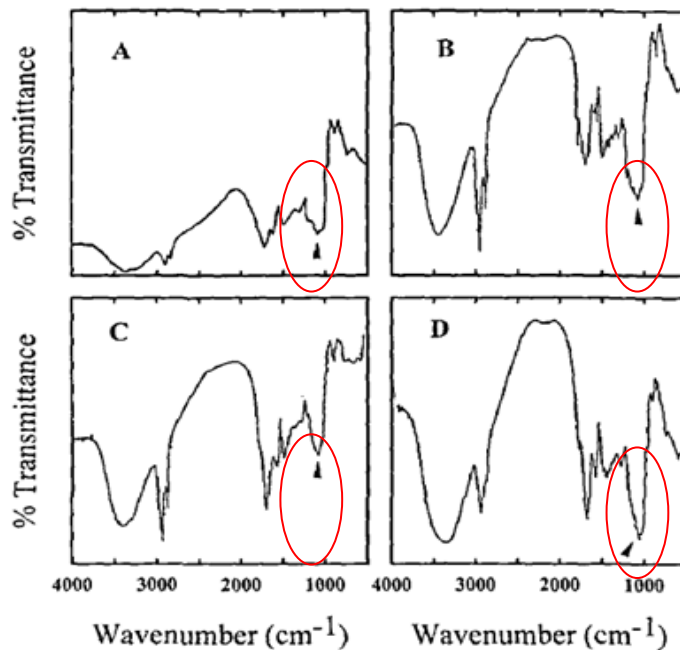


Figure 1.12 FT-IR spectra of untreated pollen, A. *Betula alba*, B. *Pinus pinaster*, C. *Ambrosia elatior* and D. *Zea mays*. The peaks marked by red circles correspond to cellulose.³⁴

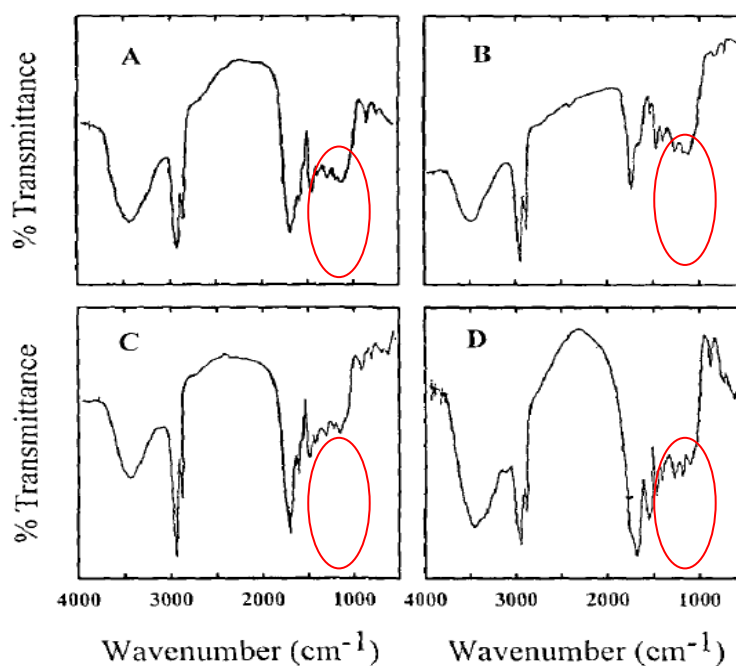


Figure 1.13 FT-IR spectra of HF treated pollen. A. *Betula alba*, B. *Pinus pinaster*, C. *Ambrosia elatior* and D. *Zea mays*.³⁴

Due to the extremely acidic nature of anhydrous hydrogen fluoride (pKa of HF is 3.15 and HCl is -7), this isolation technique is quicker than the base and acid method (section 1.1.1). Hydrogen fluoride is hazardous to handle, making the method dangerous to reproduce. Furthermore, hydrogen fluoride could remain inside the exine shell after treatment, even after careful washing. In addition, the chemical structure of sporopollenin may be altered by this treatment. The presence of fluorine in the HF treated pollen could have been detected by elemental analysis. However, no such analysis appears to have been performed.

1.1.3 Exine isolation by methods involving 4-Methylmorpholine N-oxide monohydrate

In 1985, Leowus *et al.* reported a method to release intact protoplasts from pollen grains, leaving grains with cracked walls (possibly with intine attached) behind.³⁵ The basic procedure utilizes 4-methylmorpholine N-oxide monohydrate (MMNO), the structure for which is shown in Figure 1.14. The methodology is described in Figure 1.15.³⁵

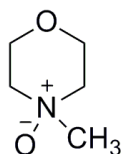


Figure 1.14 The structure of 4-methylmorpholine N-oxide monohydrate

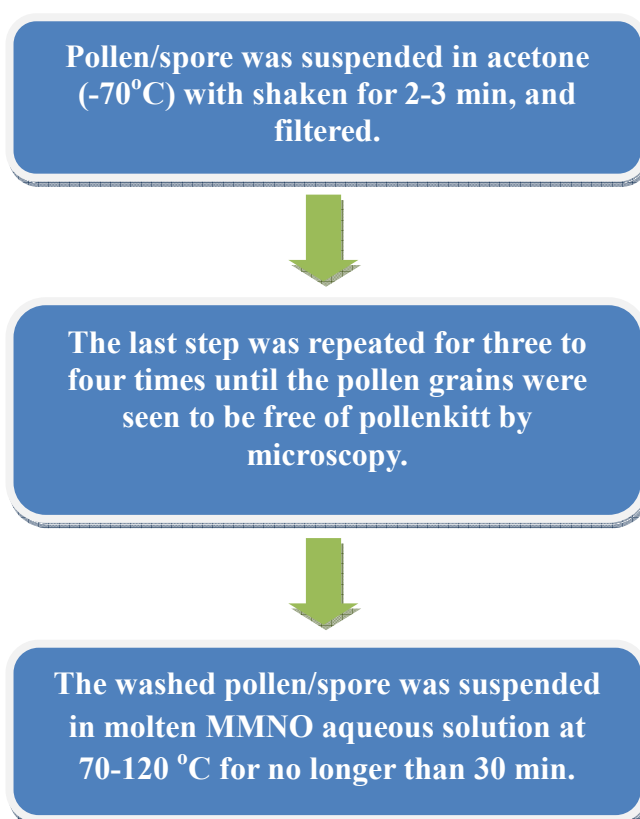


Figure 1.15 The procedure of MMNO treatment. Pollenkitt: a viscous liquid coating on surface of some pollen grains, play important role in pollen dispersion and adhesion.³⁶

MMNO is widely used to dissolve cellulose and other polysaccharides. This method (Figure 1.15) has been applied to pollen from *Lilium longiflorum* and uses less hazardous chemicals than in the previously discussed method (section 1.1.2). Loewus *et al.* claimed that it dissolved exine and intine from this species of pollen.³⁵

Figure 1.16 demonstrates how the pollen changes during various steps in the MMNO treatment. Comparing the structures of the pollen in Figure 1.16A to C, the exine shell is clearly changed after treatment with MMNO. However, it isn't clear whether the exine dissolves (as the authors claim) or decomposes during this treatment. Treatment with MMNO appears to weaken the pollen wall, causing it to fracture, facilitating the release of protoplasts. It is possible that some regions of the wall may break first due to inherent structural weakness, such as a thinner region of the exine.

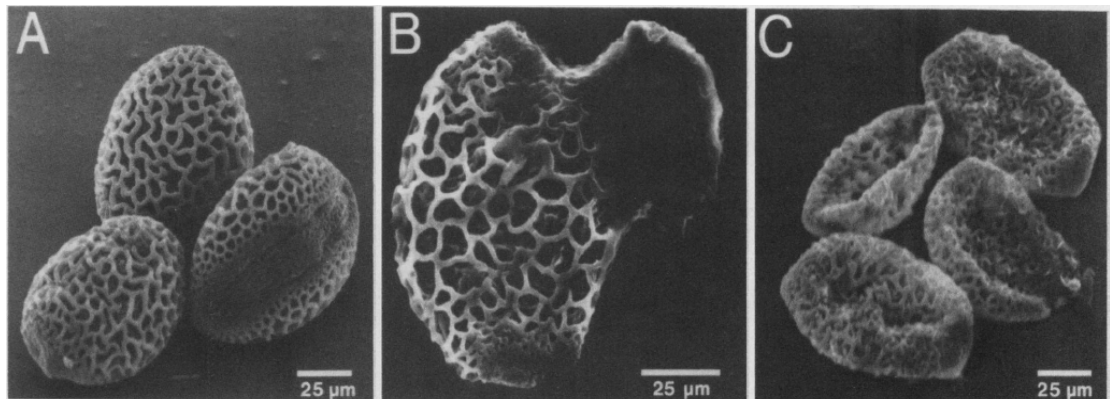


Figure 1.16 SEM images of *Lilium longiflorum* pollen. A) Acetone washed; B) MMNO treated pollen during protoplast release; C) MMNO treated pollen after protoplast release.³⁵

Although this MMNO technique damages the exine shell, it is still an interesting method to separate components of pollens and spores, especially when it is enhanced by the addition of other procedures. These include: MMNO with cyclohexylamine in sucrose; MMNO in sucrose under alkaline conditions and MMNO plus carbohydrases in pentaerythritol.³⁷ These modifications provide approaches to obtain similar results to the unmodified MMNO method, but use lower temperatures and leave behind largely intact intine layers.

A further development of the MMNO method using carbohydrases and pentaerythritol involves the use of an enzyme treatment, which is known to digest cellulose. Given that the intine layer is largely composed of cellulose, it is expected that this will lead to digestion of the intine layer. The following steps were described to isolate protoplast from *L. longiflorum*.³⁷

- Pollen was suspended in a mixture of pentaerythritol, 2-[N-morpholino]-ethanesulfonic acid and CaCl_2 at 20 °C until fully swollen (ca.15-20 min).
- 60% aqueous MMNO solution, cellulysin, macerase and bovine serum albumin were added to the suspension and it was gently shaken in a water bath at 25 °C for at least 1 hour.
- Finally, MMNO and carbohydrases were removed by vacuum filtration and the solids were washed with CaCl_2 solution.

The above procedure was reported to isolate protoplast from *L.longiflorum*. It resulted in the separation of the intine and protoplast from the exine shell (Figure 1.17). Similar to the MMNO method described previously, the protoplast and intine were released by cracking the exine shell (Figure 1.17 a). However, it was reported that further enzyme treatment resulted in the release of protoplast from the intine.³⁷

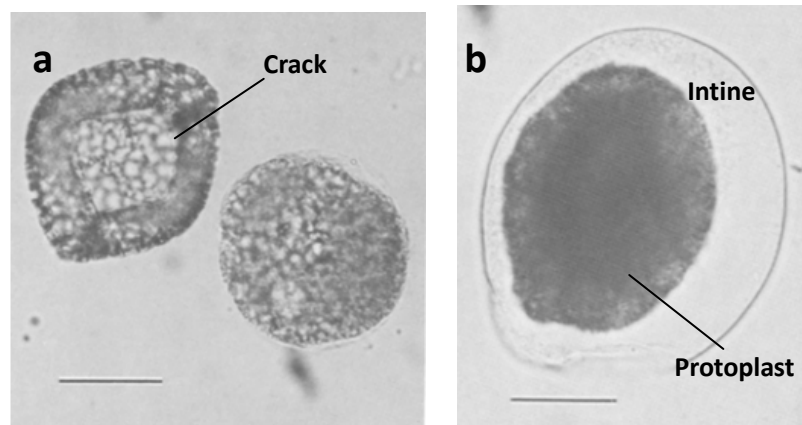


Figure 1.17 Photomicrographs of *L. longiflorum* pollen after the treatment with MMNO and carbohydrases in pentacrythritol. A) Cracked exines after release of intine and protoplast; B) intine enclosed protoplast. Scale bar = 50 μm ³⁷

TEM was used to analyze the mechanism of exine shell isolation by the modified method (Figure 1.18). Figure 1.18(a) shows that the intine layer is initially separated into two parts, one part is still attached to the inner surface of the exine shell and the other part remains attached to the protoplast membrane. After this separation the protoplast is then released from a crack in the exine shell (Figure 1.18(b) and (c)). Figure 1.18(d) is a magnified region of the protoplast from 1.18(c) showing an intact intine layer attached to the protoplast membrane.

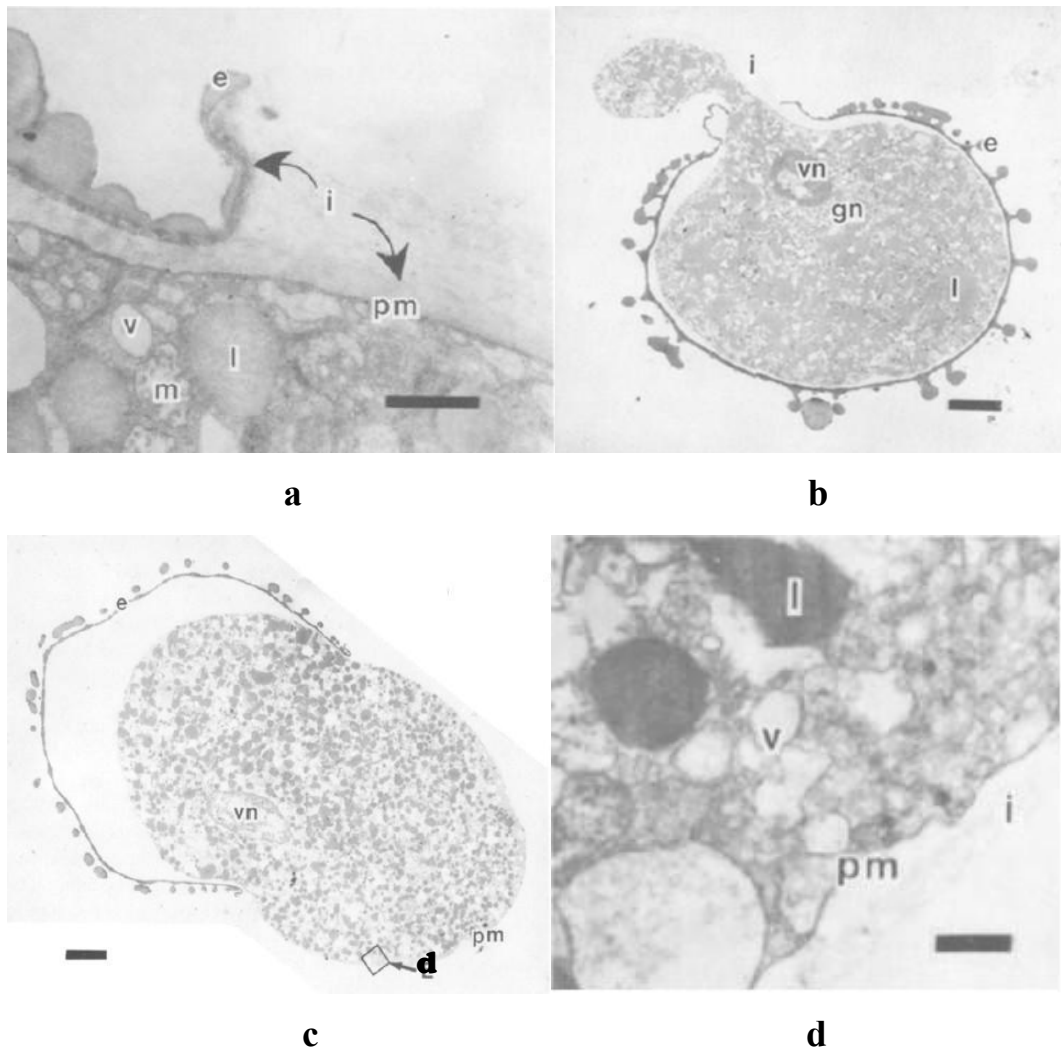


Figure 1.18 TEM images of *L. Longiflorum*. a) Separation of exine layer from intine layer (scale bar = 1 μm); b) Protoplast releasing from a small crack in the exine (scale bar = 10 μm); c) Protoplast releasing from a large crack in the exine (scale bar = 10 μm) and d) Magnified region of protoplast marked in c (scale bar = 1 μm).

Key: *e* exine; *i* intine; *l* lipid body; *m* mitochondrion; *gn* generative nucleus; *vn* vegetative nucleus; *pm* plasma membrane; *v* vesicle.³⁷

This modified MMNO treatment separates the exine layer and intine layer by gentle chemical treatment. Due to a reduction in the amount of MMNO utilised and highly selective enzymes, the sporopollenin is isolated from the pollen with minimum effect to its chemical structure. However, this method is principally used to obtain intact protoplast and intine rather than empty exine shells so physical damage to the exine is inevitable. Eventually, this method was further modified by Tarlyn *et al.* in 1993 to produce intact exine shells.³⁸

The modified method is described in Figure 1.19. In this method the spores are treated in a tissue grinder rather than subjected to heat treatment. This process gently removes fragmented intine and protoplast without physical damage to the exine shell.

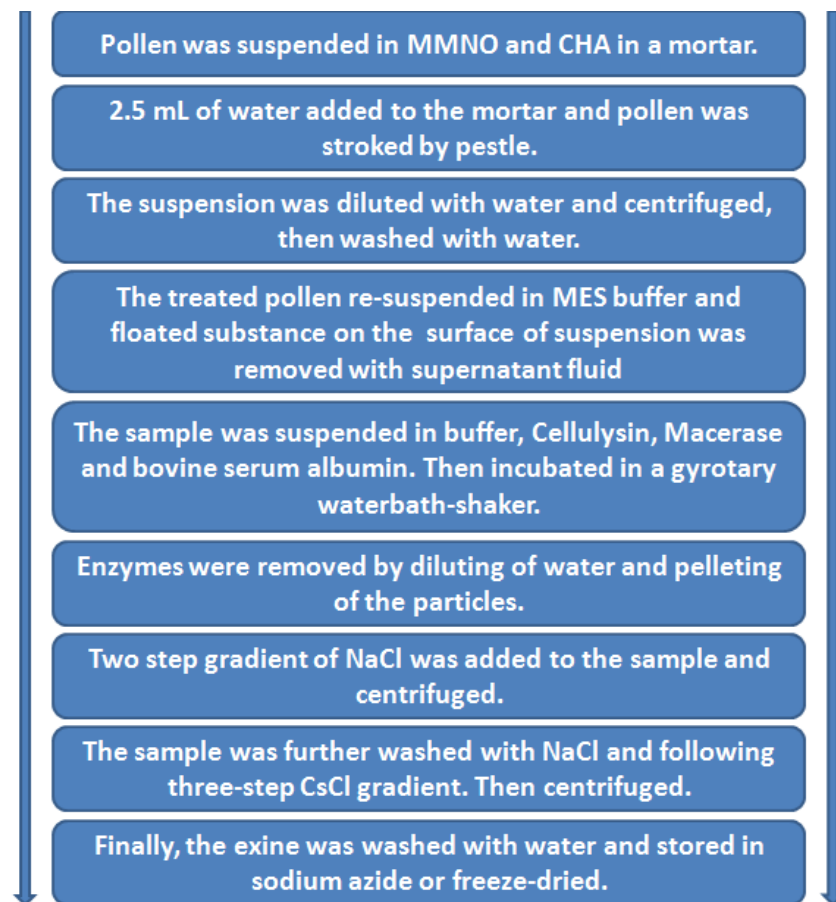


Figure 1.19 Procedures of modified MMNO method. MMNO: 4-O-methylmorpholine N-oxide. CHA: cyclohexylamine. MES:2-(N-morpholino)ethanesulfonic acid.³⁸

Centrifugation is a technique frequently utilized in biology experiments to separate substances by mass. In this method, it is used to separate enzyme, residual protoplast composition and decomposed intine material from the emptyexine shells.This method also allows for the separation of exine shells with differing degrees of biological material removed.

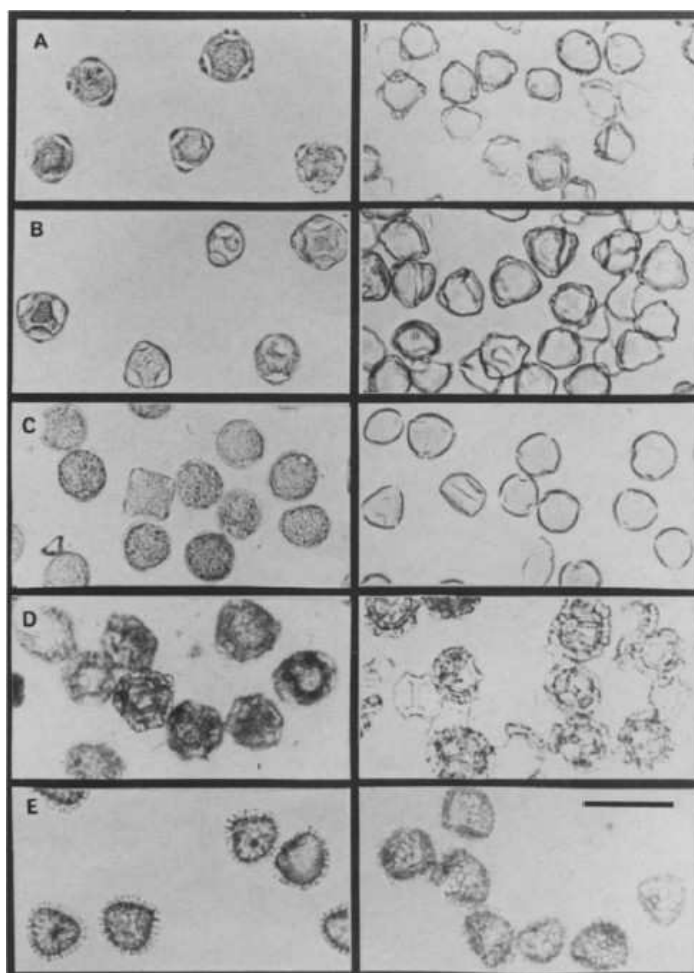


Figure 1.20 Photomicrographs of pollen and spores before and after modified MMNO enzyme treatment (right column is untreated pollen and left one is treated). A) *Betula alba verrucosa*; B) *Corylus avellana*; C) *Fraxinus excelsior*; D) *Taraxacum vulgare* (officinale) and E) *Lycopodium clavatum*. Scale bar = 50 μm .³⁸

Optical microscopy was used to demonstrate the difference between untreated and treated pollens and spores (Figure 1.20). The centres of the treated pollens and spores are much more transparent than before treatment which indicates that the biological material has been removed from within the pollen or spore. However, optical microscopy alone is not a reliable method to identify the presence of intine.

1.1.4 Exine isolation by autoclave and sucrose solution

A method to isolate sporopollenin for analysis was reported by Southworth in 1988.³⁹ The procedure is outlined in Figure 1.21. This method uses an autoclave in conjunction with a sucrose solution in order to separate the exine shell from the protoplast and intine over a period of roughly two days. Sucrose does not react with sporopollenin, therefore, this method can be used to achieve chemically unaltered

sporopollenin. This is in contrast to all other methods (see sections 1.1.1, 1.1.2 and 1.1.3), which probably change the chemical composition of sporopollenin.

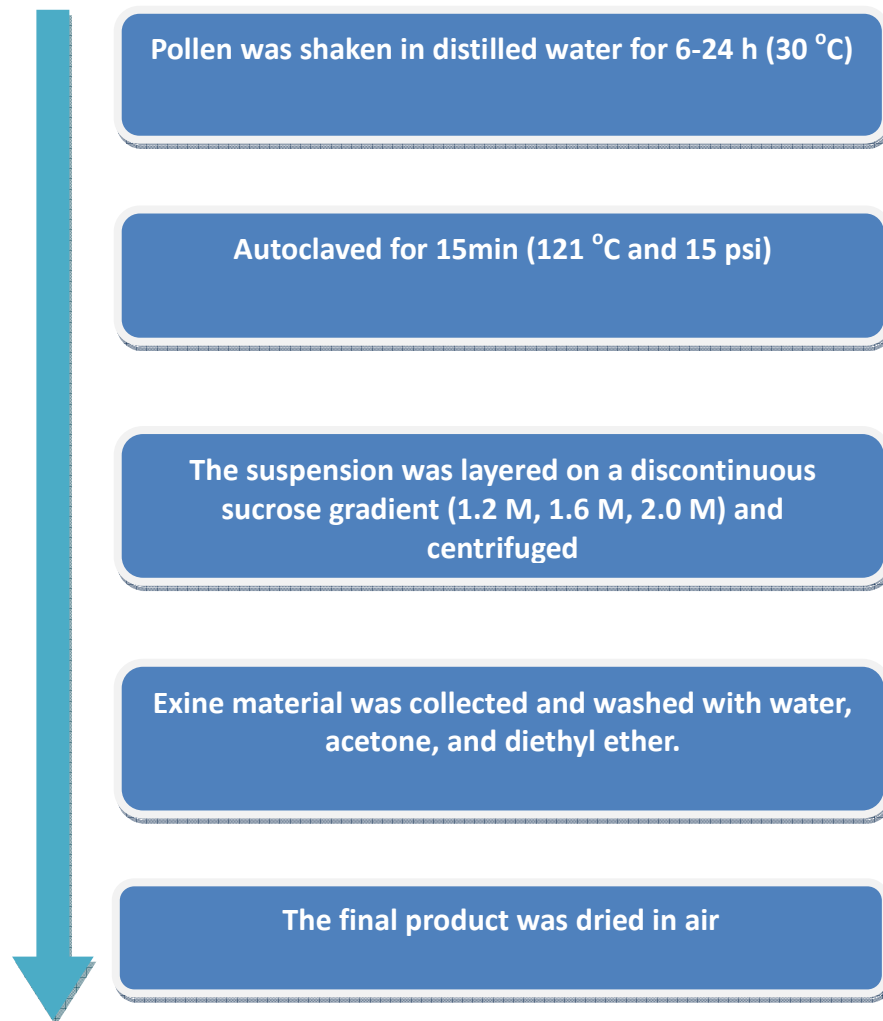


Figure 1.21 Exine isolation process reported by D. Southworth.³⁹

This treatment works to separate the exine from the intine and protoplast. Shaking pollen in water (30 °C) separates the exine from the intine by swelling the intine layer. Autoclaving dissolves the polysaccharide intine, and as a result produces cracked exine shells and protoplasts. This process is summarized in Figure 1.22.

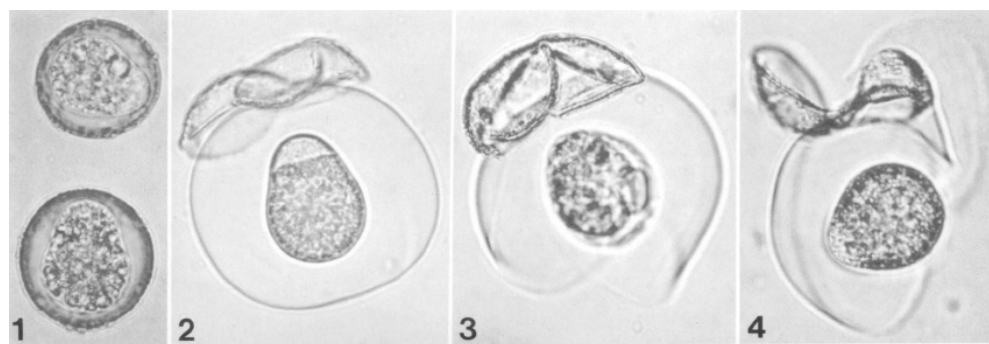


Figure 1.22 Photomicrographs of 1) untreated *Calocedrus Decurrens* pollen; 2) the pollen during treatment showing the detachment of exine from an intine enveloped protoplast; 3) and 4) a protoplast being released through the cracked intine.³⁹

The product of this method was analyzed by SEM (Figure 1.23). The very small spheres observed on the surface of these cracked exine shells are called orbicules and have the same chemical composition as the exine shell. The exine shells were collected by centrifugation, which also removed any free intine and protoplast fragments. However, SEM cannot be used to assess the extent to which intine and protoplast material is still bound to the exine shells. Instead, TEM analysis would be required to evaluate this further. Sporopollenin is very unlikely to be chemically altered by this technique as no chemical treatments are applied.

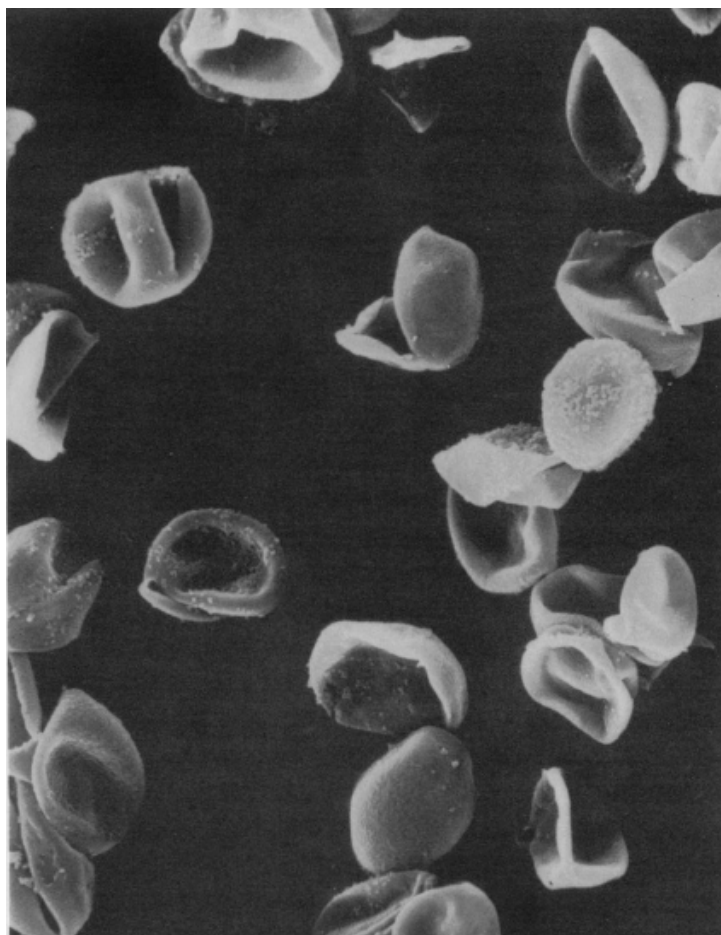


Figure 1.23 Ruptured *Calocedrus decurrens* exine shells from the autoclave method.³⁹

Although this process produces cracked exine shells, they are likely to be largely uncontaminated by intine and protoplast material. This is likely to be the only published method that produces chemically unaltered sporopollenin, which is useful for chemical analyses. This method uses a physical approach to isolate exine shells in a similar fashion to MMNO treatments (see section 1.1.3). Furthermore, the autoclave method is simpler than most of the other methods described. Although acetolysis is faster than this treatment, it alters sporopollenin's chemical structure.

Unfortunately, this method will always produce cracked exine shells, which aren't suitable as microcapsules. However, these shells could still be used for surface modification techniques, such as ligand exchange.⁴⁰ We cannot be certain this technique synthesizes exine shells free from all intine material. If an autoclave technique could be developed that produced intact exine shells, this would have great potential to produce intact, chemically unaltered exine shells (something no technique has yet achieved).

1.2 Methods used to fill exine shells and their subsequent applications

Intact exine shells have been isolated from *Lycopodium clavatum* spores via a base and acid treatment and directly utilized as microcapsules. In this instance, the exine shell is referred to as an exine microcapsule. Exine shells have many properties that make them excellent microcapsules. Compared to commercially produced microcapsules, exine microcapsules have a remarkably narrow size distribution.⁴¹ Synthesizing microcapsules with such a narrow size distribution is challenging and costly, making exine microcapsules desirable. The remarkable resistance of the exines to chemical and physical degradation is retained after a base and acid treatment. Therefore, these exine microcapsules have been deployed in challenging environments, such as biological environments, e.g., in plasma. Exine microcapsules behave like a sponge: they are excellent at absorbing and then releasing encapsulated materials. It is proposed that the exine shells absorb material via nano-channels and capillary effects.⁴²

To date, *Lycopodium clavatum* spores have been most widely used as microcapsules. *Lycopodium clavatum* is inexpensive and can be purchased in large quantities (> 1 kg). Pollen is more expensive and can only usually be bought in smaller quantities (< 10 g). In comparison to pollen, *Lycopodium clavatum* is particularly well studied and there is a wealth of published information on its chemical and structural composition.²⁵

A variety of methods have been employed to fill exine microcapsules with a wide range of materials. These filled microcapsules have been utilized in a number of different applications.

1.2.1 Passive encapsulation

The simplest method of encapsulation reported is the passive encapsulation technique. Encapsulation is achieved by stirring exine microcapsules in the material to be encapsulated. This process can take place with or without solvent depending on the nature of the material used (Figure 1.24). This method relies on the target material moving through the nano-channels in the exine microcapsule wall via capillary action. The method can be optimized depending on the nature of the material used by altering the temperature of encapsulation.⁴³ Solvents are claimed to improve the rate of absorption of material by exine microcapsules by improving their passage through the

exine via capillary action. However, the mechanism by which this takes place has not been fully studied.²²

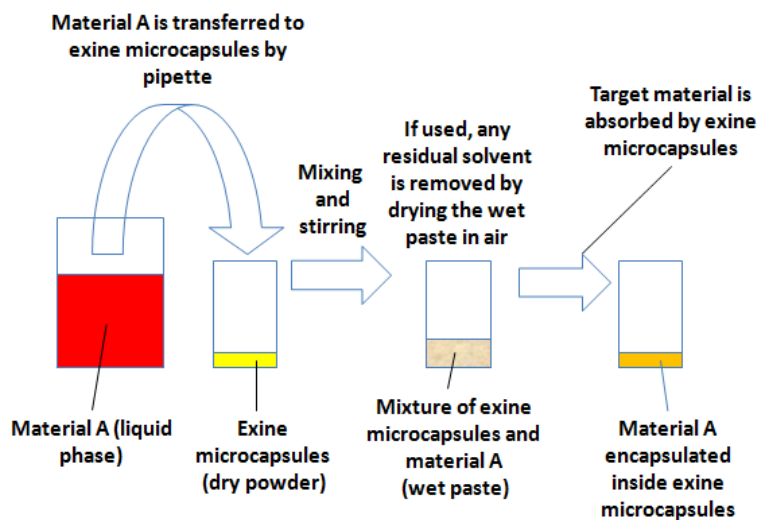


Figure 1.24 Summary of passive encapsulation method.

Barrier *et al.* reported that fish oil can be encapsulated inside *Lycopodium clavatum* exine microcapsules by the passive encapsulation method. No solvents were used and the liquid fish oil was kept at room temperature during encapsulation. The resultant microcapsules were analyzed by laser scanning confocal microscopy (LSCM) (Figure 1.25).⁴³ In this Figure, the red regions represent the exine shell, and the blue region the fish oil. Most of the fish oil is clearly encapsulated by the exine microcapsules; however, some fish oil remains on their surfaces (highlighted by the yellow ring in Figure 1.25).

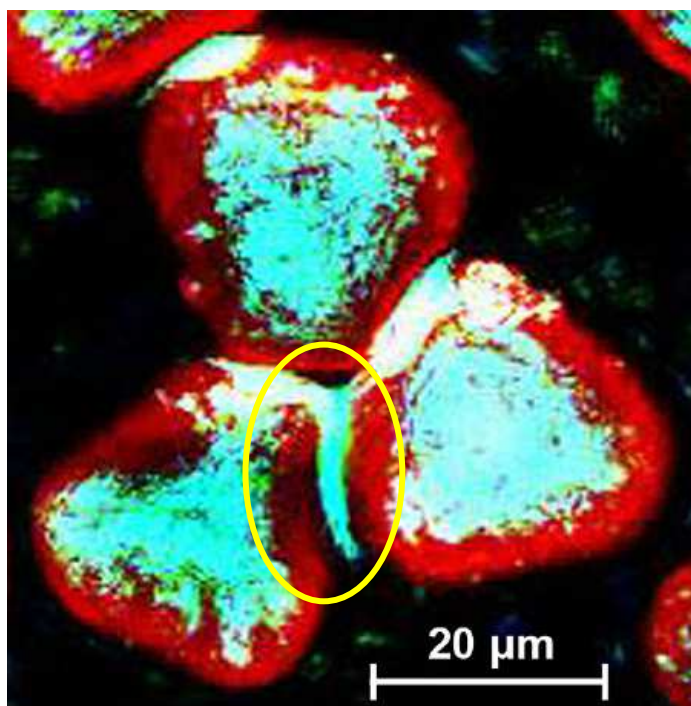


Figure 1.25 Image taken by confocal microscopy of *Lycopodium clavatum* exine microcapsules overfilled with fish oil.⁴³

If the target material is not aliquid at room temperature, it may be melted and/or dissolved in a solvent. For example, cocoa butter (melting point approximately 35 °C) was melted prior to passive encapsulation in *Lycopodium clavatum* exine microcapsules. Good encapsulation of cocoa butter was only observed at ratios of 1:1 of cocoa butter to exine microcapsules. When compounds are melted in order to be encapsulated it is not always possible to wash off the excess material from the exines. The uptake of material into the exines is not a homogeneous process and it is common for some exines to absorb more material than others. One major limiting factor in this process is the melting point of the material to be encapsulated. If the melting point is too high it becomes more difficult to handle and there is also a greater opportunity for decomposition to occur prior to encapsulation.

Solution encapsulation offers a facile approach to filling the exines and overcomes many of the issues of melt encapsulation. Using this approach ensures that the exine microcapsules cannot be overfilled. The encapsulation process can be completed at room temperature, thus the problem from high temperature is solved too. Moreover, viscosity of the solvents and solutions is also not an issue, which was one of the

problems faced in melt encapsulation. However, the limiting factor in the solvent approach is solubility. Some compounds that would be desirable for encapsulation have very low solubilities in common solvents.

Figure 1.26 shows exine microcapsules filled with fish oil at concentrations of 1, 4 and 6 g g⁻¹ (mass ratio of exine microcapsules to fish oil).⁴³ At concentrations of 1 g g⁻¹, encapsulation appears most successful. However, although the authors described these filled microcapsules as a free-flowing powder, it is obvious that some of the microcapsules stick together. This suggests that some fish oil remains on the surface of the microcapsules and total encapsulation is not achieved at this ratio. At higher ratios of fish oil (4 and 6 g g⁻¹), poor encapsulation is observed and a significant amount of material remains on the exine surface, leading to sticky solids. From these photographs, concentrations below 1 g. g⁻¹ are most suitable for the passive encapsulation of fish oil.

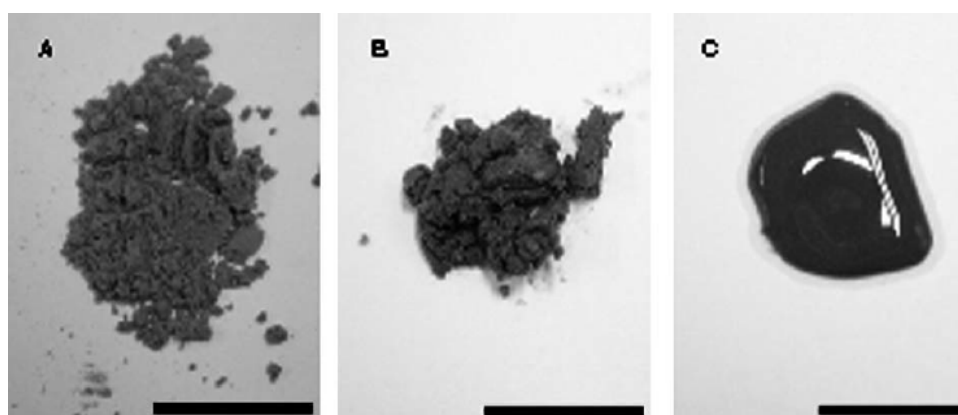


Figure 1.26 Photographs of exine microcapsules containing different amounts of fish oil (mass ratio of exine microcapsules to fish oil).

A) 1 g g⁻¹; B) 4 g g⁻¹ and C) 6 g g⁻¹. Scale bar = 20 mm⁴³

The passive encapsulation method is simple to carry out and appears to be suitable for the encapsulation of most materials, which are liquid, molten or in solution. However, the ratio of target material to exine microcapsules that can be achieved is poor compared to other encapsulation methods. Passive encapsulation leaves target material behind on the surface of the exine making this technique unsuitable for many applications, e.g. optical displays.

1.2.2 Vacuum encapsulation

The most widely reported encapsulation technique for exine microcapsules is vacuum encapsulation. This technique is a modification of the passive encapsulation technique and was first suggested by Mackenzie *et al.*⁴³ Instead of merely stirring exine microcapsules in the material to be encapsulated, a vacuum is applied to the mixture to enhance encapsulation. The procedure is summarised in Figure 1.27.⁴³

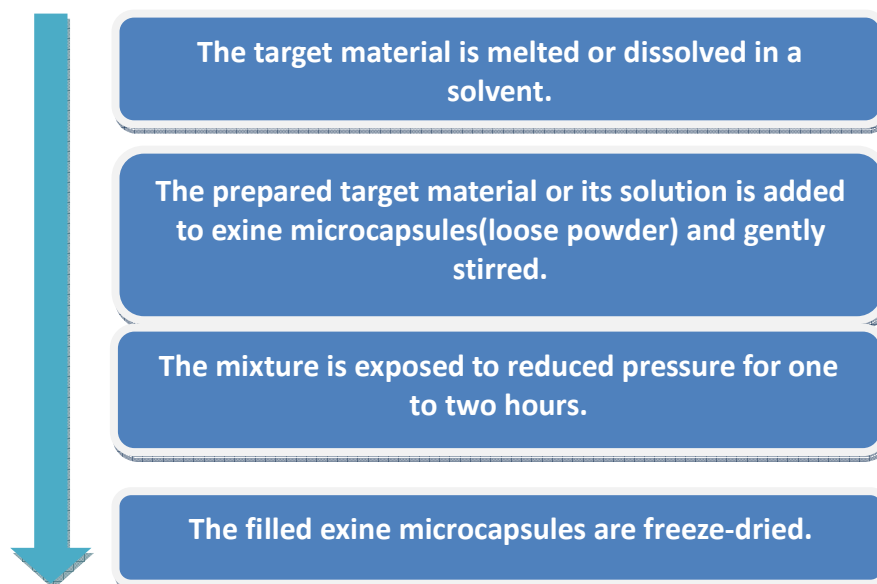


Figure 1.27 Procedure of vacuum encapsulation method.⁴³

Vacuum encapsulation has been used to encapsulate a range of target materials such as dyes, fish oil and cocoa butter.⁴³ Dyes encapsulated include Evans blue, Evans blue-stained α -amylase (an enzyme), Malachite green and Nile red. The filled exine microcapsules were analyzed by laser scanning confocal microscopy (LSCM), see Figure 1.28. The images clearly show that the dyes are incorporated into the microcapsules although there may be some remaining on the surface for Evans blue-stained α -amylase and Malachite green. The distribution of the dye within the exine microcapsule varies for each dye, but this is not discussed or explained in the literature.

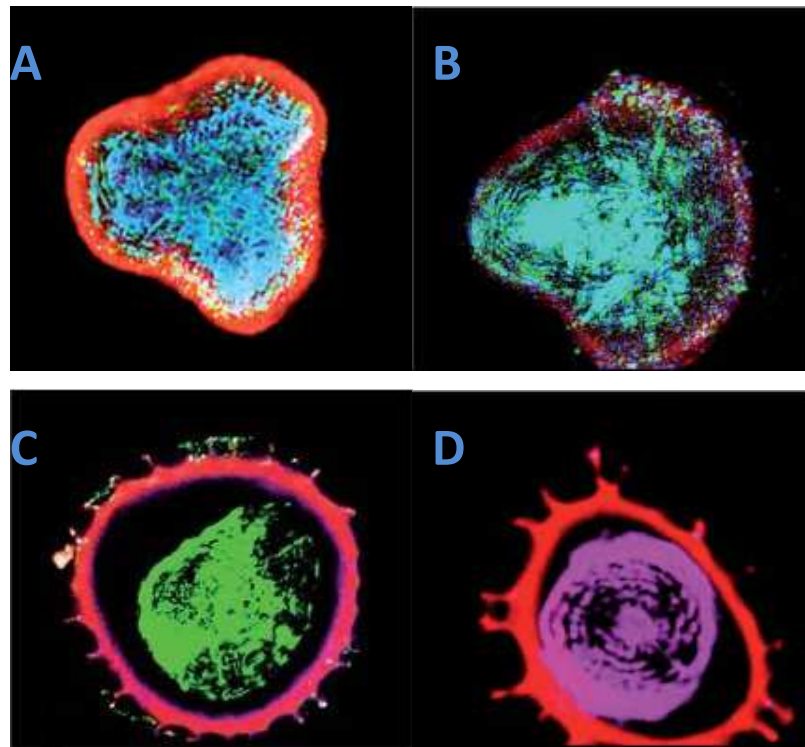


Figure 1.28 LSCM images of exine microcapsules filled with A) Evans blue; B) Evans blue-stained α -amylase; C) Malachite green and D) Nile red.⁴³

The vacuum encapsulation method appears to be a facile route for encapsulation. The experiments reported in the literature are mainly performed at room temperature, but there is evidence that heat can be applied if required to melt target materials in order to enable encapsulation.⁴³

1.2.3 Centrifugation encapsulation method

The passive encapsulation method has also been modified with a view to improving the levels of encapsulation by using centrifugation. The procedure is reported to be quick and involves mixing either a liquid material or a solution of the material in an organic solvent with exine microcapsules and then centrifuging.⁴³ This method was utilized to encapsulate an enzyme, alkaline phosphatase (ALP) into exine microcapsules. A solution of ALP was centrifuged with exine microcapsules for 10 min under 10,000 g (gravitational acceleration) at 4 °C. It is claimed that this process is efficient and that there was almost no free ALP on the outside of the exine microcapsules.

1.2.4 Micro-reactor encapsulation method

Passive, vacuum and centrifugation encapsulations all require the material for encapsulation to be in a liquid phase during the encapsulation process. High melting point and low solubility materials are difficult to encapsulate by these methods. Paunov *et al.* have reported a method that utilizes exine microcapsules as micro-reactors. They are used to synthesize target compounds within the exine shells, which by standard methods of synthesis would be challenging.⁴⁴ This method cleverly bypasses the problem caused by low solubility and high melting point materials. Figure 1.29 summarizes this method whereby a solution of compound A was stirred with exine microcapsules to initiate encapsulation, followed by washing with solvent to remove any residual compound A, and then these filled microcapsules were transferred into a solution of compound B. Compound A and B reacted with each other inside the microcapsule and formed a precipitate of the target material (compound C) which was insoluble. The filled microcapsules were subsequently washed with solvent to remove any unreacted starting materials.

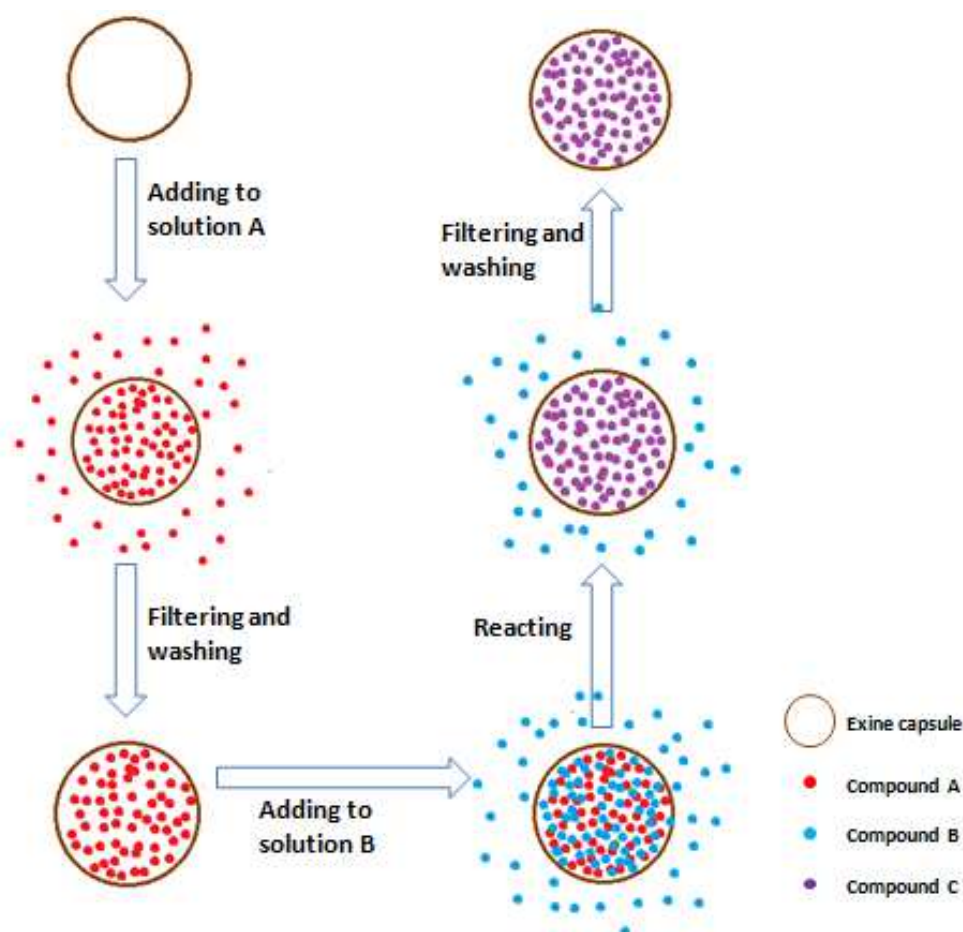


Figure 1.29 Summary of the micro-reactor encapsulation method. Compound A and B are both in the liquid phase and they generate a precipitate of compound C during the process.⁴⁴

This micro-reactor encapsulation method was used to encapsulate Fe₃O₄ nano-particles into exine microcapsules.⁴⁴ The procedure for formation and encapsulation of Fe₃O₄ is given in Figure 1.30.

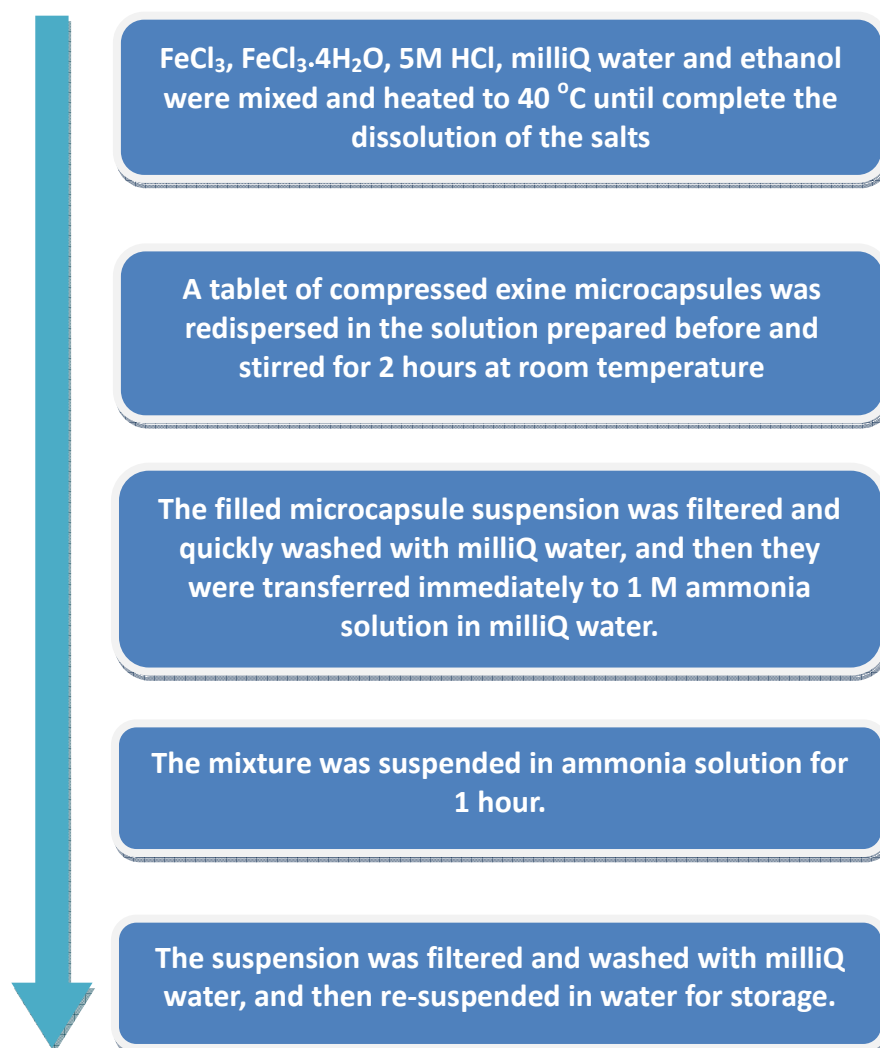


Figure 1.30 Procedure for encapsulation of Fe₃O₄ nano-particles as described by Paunov *et al.*⁴⁴

The Fe₃O₄ nano-particle filled exine microcapsules were analyzed by optical microscopy and SEM. Under optical microscopy, these filled microcapsules were observed using a very bright light source and some brown spots can be seen that appear to be inside the microcapsules (Figure 1.31).⁴⁴ These brown spots were claimed to be the encapsulated magnetic nanoparticles. Unfortunately, no image of empty exine microcapsules was presented for comparison.

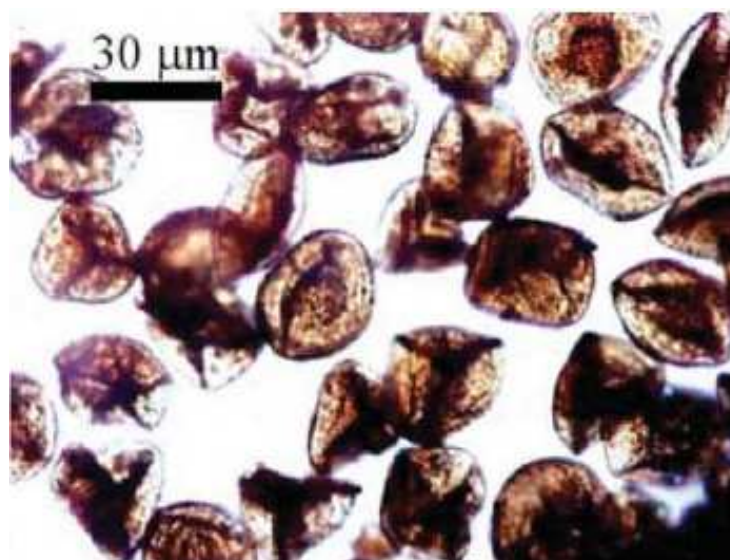


Figure 1.31 Photomicrograph of Fe_3O_4 encapsulated *Lycopodium clavatum* exine microcapsules.⁴⁴

SEM images of Fe_3O_4 encapsulated exine microcapsules are presented in Figure 1.32.⁴⁴ Clumps of material were observed on the inner surfaces of several cracked exine microcapsules and the authors claim these clumps were Fe_3O_4 nano-particles, therefore encapsulation was considered a success.

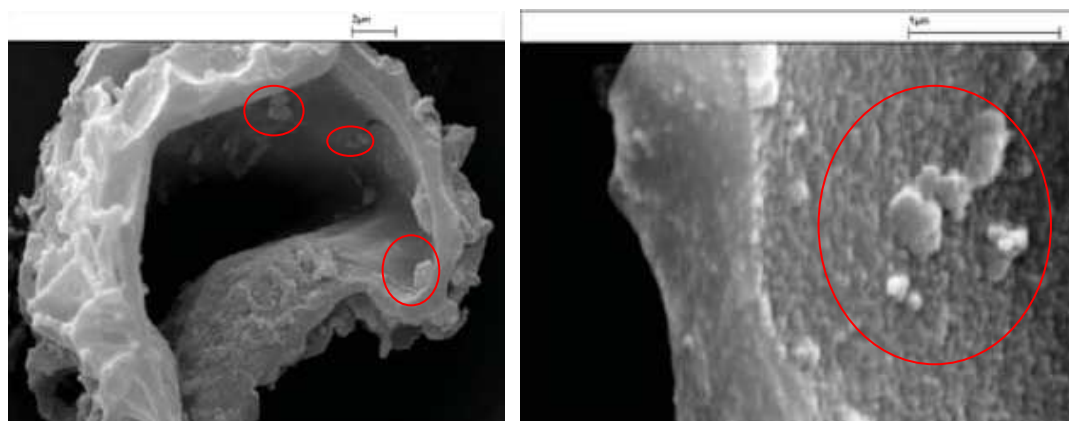


Figure 1.32 SEM images of Fe_3O_4 encapsulated *Lycopodium Clavatum* exine microcapsules. The areas highlighted by red circles are claimed to be Fe_3O_4 particles.⁴⁴

The main advantage of this method is that it is able to encapsulate target materials into exine microcapsules, which have high melting points and are poorly soluble in common solvents. However, in order to synthesize the target compound within exine microcapsules, reactants must be available that are highly soluble or have a low melting point. The amount of target material encapsulated is dependent on the yield and

selectively of the reaction used to produce it. This may cause difficulties in the encapsulation process if a sufficient amount of target material cannot be synthesized.

1.3 Recovery of encapsulated material from exine microcapsules

It is often desirable to recover encapsulated material from microcapsules and there are numerous applications of this technology. For example, encapsulated fragrances printed onto paper may be released by scratching, i.e. Scratch and Sniff paper.⁴⁵ By encapsulating drugs inside microcapsules they may be released in a controlled fashion over time in the body.^{46,47,48}

Barrier *et al.* reported a method to recover encapsulated materials from exine microcapsules by solvent extraction.⁴³ This method uses a solvent able to dissolve the encapsulated target material, which leeches out of the exine microcapsule. The target material in solution and the exine microcapsules are then separated by filtration.

An example of the solvent extraction method is the recovery of fish oil from exine microcapsules.⁴³ Chloroform was used as the extracting solvent and 96–99% of encapsulated fish oil was successfully recovered from the exine microcapsules. The recovered oil was assessed by peroxide value titration (a measure of oxidation) and the result indicated that neither the exine encapsulation nor recovery process was deleterious to fish oil.

Another example of the solvent extraction method is the recovery of an enzyme, alkaline phosphatase (ALP) from exine microcapsules.⁴³ ALP was recovered by extraction in phosphate buffered saline (PBS): ALP filled exine microcapsules were shaken in PBS for 30 s, filtered by 0.4 µm-pored syringe-tip filter and washed with PBS several times. Subsequently, the activity of ALP was demonstrated by the comparison of fresh ALP solution and recovered ALP solution. After ALP was recovered, its activity only reduced by 1-3 %. Thus, encapsulation followed by solvent extraction does not significantly reduce the activity of this enzyme.⁴³

Encapsulated target materials (i.e. fish oil and ALP) have been successfully released from exine microcapsules. This demonstrates that encapsulated materials can be stored in exine microcapsules and then released on demand. Results indicate that encapsulation

followed by solvent extraction using *Lycopodium clavatum* exine microcapsules does not alter the encapsulated target materials or damage the exine microcapsules.⁴³

Many of the potential applications for exine microcapsules are in biological or medicinal areas, in which organic solvent extraction would not be appropriate. Therefore, for release of encapsulated material *in vivo* the extraction must take place in an aqueous environment.

An alternative method to release encapsulated material from exine microcapsules is exine digestion. Although sporopollenin is a chemically stable material, a recent experiment reported by Lorch *et al.* demonstrated that sporopollenin exine microcapsules are digested *in vitro* in human blood plasma.⁵⁵ Figure 1.33 shows an obvious difference between the exine microcapsules before and after 30 min incubation in blood plasma. After incubation, most exine microcapsules appeared damaged and cracked (Figure 1.33b), thus providing an opportunity to release the encapsulated target material, in this case a magnetic resonance imaging (MRI) contrast agent.

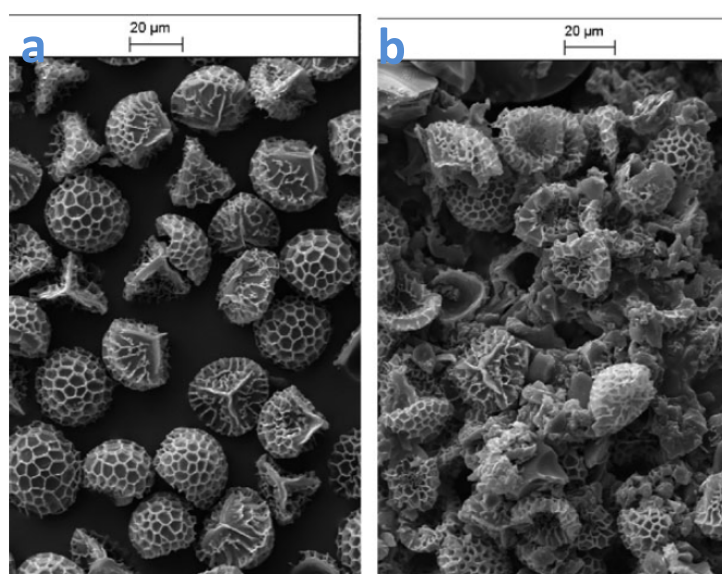


Figure 1.33 SEM images of exine microcapsules isolated from *Lycopodium Clavatum* a) before incubation and b) after 30 min incubation in plasma.⁵⁵

In the method reported by Lorch *et al.* an MRI contrast agent was encapsulated in *Lycopodium clavatum* exine microcapsules.⁵⁵ These microcapsules were suspended in either blood plasma or a buffer solution. The relaxivity of these suspensions were

measured every ten minutes and compared. The relaxivity provides a measure of the amount of MRI contrast agent in suspension as opposed to being encapsulated.⁵⁵ Results suggest that no contrast agent was released from exine microcapsules suspended in buffer solution (Figure 1.34). However, the results are particularly noisy so it is possible that a small amount of MRI contrast agent was released. In contrast, the relaxivity of the plasma suspension changed significantly during the course of the experiment (four hours), indicating the release of MRI contrast agent from the exine microcapsules. The results show a large difference in relaxivity even during the first twenty to thirty minutes, indicating rapid digestion of the microcapsules in plasma.

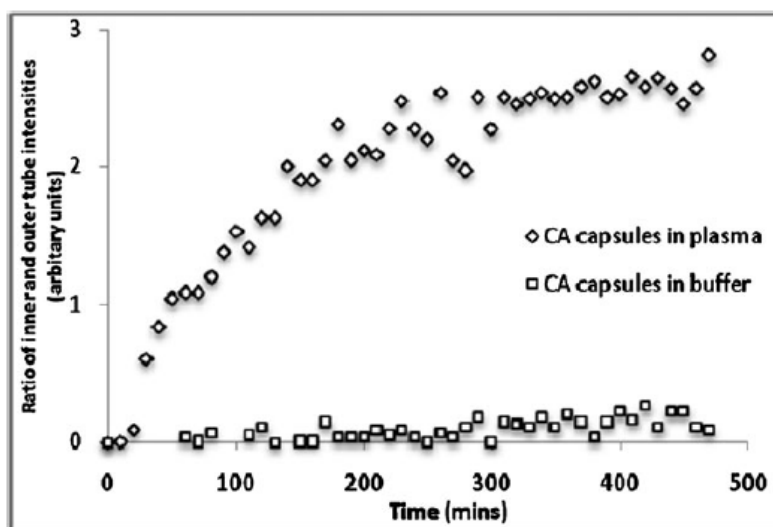


Figure 1.34 Graph showing the intensity of contrast agent released from exines in plasma and buffered aqueous solutions as a function of time.⁵⁵

Compared to the solvent extraction process, plasma degradation does significantly damage exine microcapsules meaning that they cannot be recycled for repeated uses. The mechanism of sporopollenin degradation in blood plasma is unknown, although the authors suggest that enzymes may be involved in the digestion process. Encapsulating an MRI contrast agent in exine microcapsules delays the contact between the encapsulated material and the blood. This could be useful in human diagnostic MRI studies, where a contrast agent needs to be observed over a period of time. Influencing the rate and quantity of a contrast agent to be released from an exine microcapsule would be challenging as this would involve altering the structure of the microcapsule or influencing its surrounding environment (i.e. the blood plasma).

1.4 Application of exine microcapsules

1.4.1 Food applications

Microencapsulation is widely utilized in the food industry and the nature of the microcapsules and techniques to produce them are always a focus of research and development. Microcapsules encapsulate a range of solid and liquid foodstuffs and protect these from their surrounding environment. For example, microcapsules can protect reactive, sensitive or volatile additives, such as vitamins and flavours.⁴⁹ They can be used to mask unpleasant flavours, e.g. fish oil.⁵⁰ Liquid encapsulants may be converted to a solid form by encapsulation and this can make them easier to handle and transport.⁴⁸ In addition, microencapsulation can be used to improve the effectiveness of some food additives.⁴⁸

Microcapsules synthesized from maltodextrins, gum Arabic and soy protein have been used to encapsulate a broad range of food stuffs.⁵¹⁻⁵² Recent research has investigated the suitability of exine microcapsules to encapsulate foodstuffs. Cod liver oil and sunflower oil were encapsulated inside exine microcapsules to mask their unpleasant flavours. Exine microcapsules (1.0 g) were stirred with sunflower oil (0.5 g) and cod liver oil (0.5, 1, 2 and 4 g), and then subjected to a vacuum (10 hPa) for two hours to facilitate passive encapsulation. Twenty volunteers from a range of age groups tasted these microcapsules (as well as a blank sample made up with water) and were asked to distinguish between the encapsulated materials.²⁸ The authors reported that, at or below a 1:1 ratio of microcapsules to sunflower oil or cod liver oil, volunteers were unable to differentiate these oils from the blank, indicating successful taste masking. At higher cod liver oil to microcapsule ratios (2:1 and 4:1) the oil was recognized. The authors suggested this was due to oil being left on the surface of the microcapsules after vacuum encapsulation, which was supported by LSCM evidence (Figure 1.25) as well as photographs indicating the appearance of microcapsules at these higher loadings (Figure 1.26). These results indicate that exine microcapsules are safe for human consumption and can mask the taste of edible oils loaded in a ratio of 1:1. This method may be applicable to other foods.

1.4.2 MRI agents based on exine microcapsules

Magnetic resonance imaging (MRI) is an important diagnostic tool in medicine. Contrast agents are often injected into the blood of a patient in order to produce more diagnostically useful images. By encapsulating contrast agents within microcapsules (for example those synthesized from poly (lactide-co-glycolide)) their lifetime within the circulatory system may be prolonged. This effect is also sometimes achieved by modifying the chemical structure of the contrast agent.⁵³⁻⁵⁴ Research has shown that an MRI contrast agent can be encapsulated inside exine microcapsules, and that these microcapsules break down within the blood to release the contrast agent.⁵⁵

Lorch *et al.* demonstrated the encapsulation of a gadolinium (III) MRI contrast agent (Gadodiamide, Figure 1.35) within an exine microcapsule.⁵⁵ The encapsulation of the gadodiamide was achieved by vacuum encapsulation and successful encapsulation was demonstrated by an MRI microimaging experiment. Bright areas within Figure 1.36 show the gadodiamide encapsulated inside exine microcapsules, supported by an agar gel.⁵⁵ Meanwhile, a similar microimaging experiment repeated upon empty exine microcapsules demonstrated that they are not highlighted by this imaging technique.

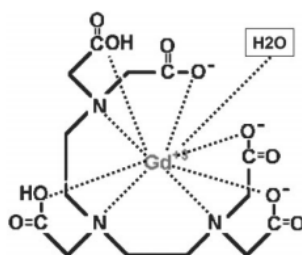


Figure 1.35 Molecular structure of gadodiamide, commonly marketed under the trade name Omniscan.⁵⁶

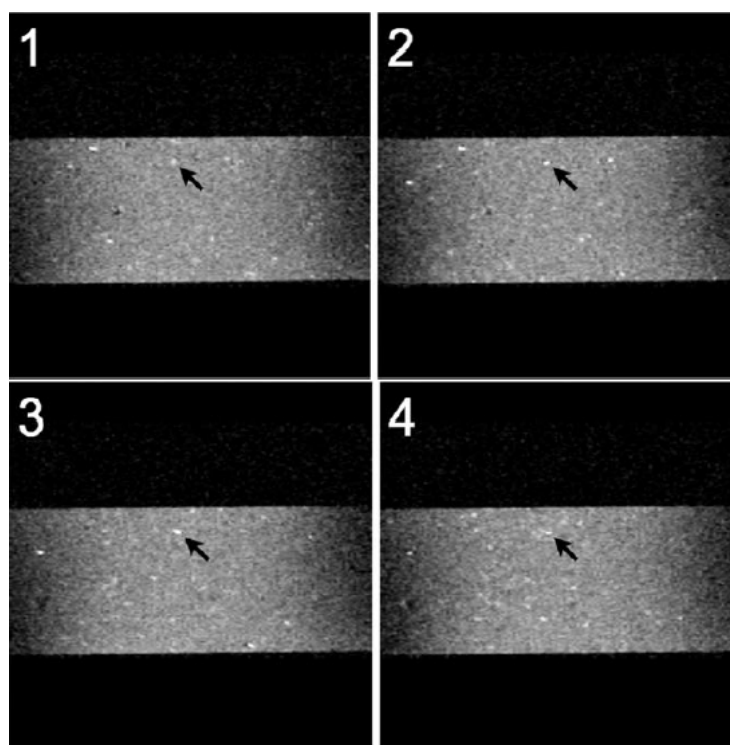


Figure 1.36 MRI microimaging experiment. Four consecutive slides through the agar gel containing exine microcapsules filled with gadodiamide. White regions represent filled microcapsules, with larger regions (highlighted by arrows) representing clumps of filled microcapsules. Frame dimension: 3 x 3 mm.⁵⁵

As already demonstrated in section 1.3, the exines were digested in plasma leading to the steady release of the MRI agent. This discovery has led to further focus on exine microcapsules and their use with other metallo drug and imaging agents.⁵⁵

1.4.3 Magnetic particles

Magnetic microcapsules are often used to transport a ‘package’ (e.g. anticancer drugs) to a targeted region (e.g. any body tissue).⁵⁷ These drug carriers contain magnetic particles with sub-micron dimensions. These may be coated with a biocompatible polymer or distributed throughout the structure of a porous biocompatible polymer microparticle.⁵⁸ Exine microcapsules synthesized from *Lycopodium clavatum* spores have been filled with magnetic nanoparticles.

As previously discussed, the encapsulation of Fe_3O_4 nanoparticles was achieved by the micro-reactor encapsulation method (section 1.2.4). The magnetic properties of the Fe_3O_4 filled exine microcapsules were demonstrated by moving the microcapsules in

suspension using a magnet (Figure 1.37).⁴⁴ The microcapsules were suspended in water and dispersed by shaking. A magnet was placed next to the sample vial and most of the microcapsules moved towards the magnet. However, a small number of Fe_3O_4 filled exine microcapsules were not attracted by the magnet and remained at the bottom of the vial. It is possible that these microcapsules did not feel sufficient attraction from the magnet to move. In contrast, if the suspension was not shaken, the microcapsules moved to a much lesser degree in the presence of a magnet (Figure 1.38).⁴⁴

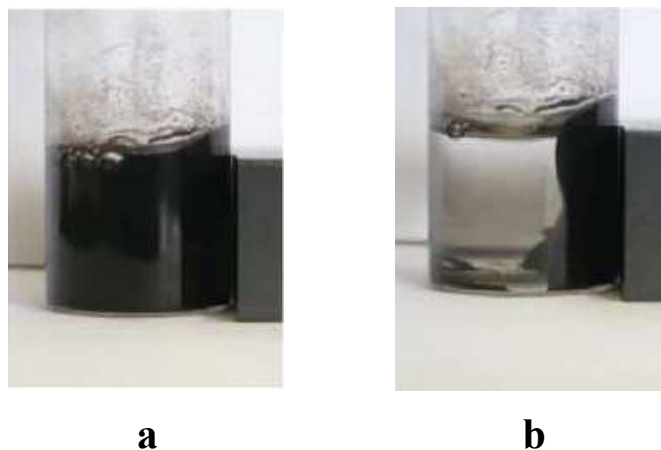


Figure 1.37 Fe_3O_4 filled exine microcapsules in the presence of a magnet. a: Fe_3O_4 filled exine microcapsules dispersed in water by shaking. b: Fe_3O_4 filled exine microcapsules moving towards a magnet.⁴⁴

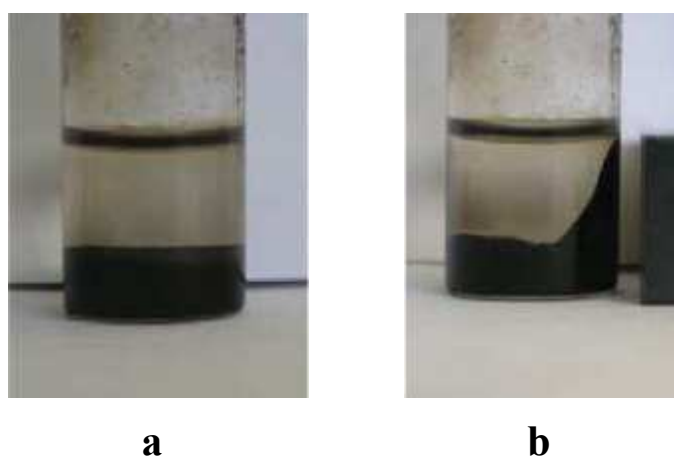


Figure 1.38 Fe_3O_4 filled exine microcapsules in the presence of a magnet. a: Fe_3O_4 filled exine microcapsules settled out of an aqueous suspension. b: A fraction of Fe_3O_4 filled exine microcapsules moving towards a magnet.⁴⁴

The magnetic properties of these Fe₃O₄ filled exine microcapsules were only demonstrated in the presence of solvent and no information was given about their bulk properties.

1.4.4 Encapsulation of living cells

Microencapsulation technology has been used to encapsulate living materials, such as rat pancreatic cells and bifidobacteria (bacteria found in yogurt).^{59,60} These encapsulated living cells have been used in many applications. For example, rat pancreatic cells were encapsulated in a microcapsule and transplanted into mice. Encapsulation was used to limit the undesirable immune response usually observed when transplanting living cells between organisms.⁶⁰ *Bifidobacterium adolescents* was encapsulated inside alginate-coated gelatin microspheres and subjected to a simulated gastro-intestinal environment (pH 2). Encapsulation was found to significantly prolong the life of these beneficial probiotic bacteria, therefore demonstrating that microencapsulation has the potential to increase the survival of living cells in a hostile environment, such as the gastro-intestinal system.⁶¹

Another example of encapsulation of living organisms is the encapsulation of yeast cells. These cells were encapsulated into exine microcapsules using a vacuum encapsulation method with aiding of Tween 20 (see Figure 1.39) and ethanol, which is summarized in Figure 1.40.⁶²

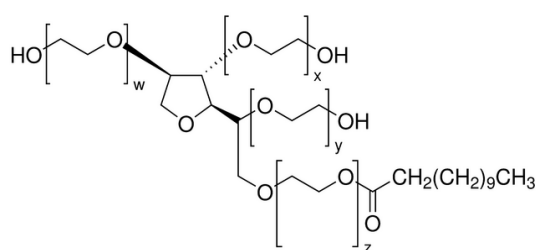


Figure 1.39 Molecular structure of Tween 20.⁶³

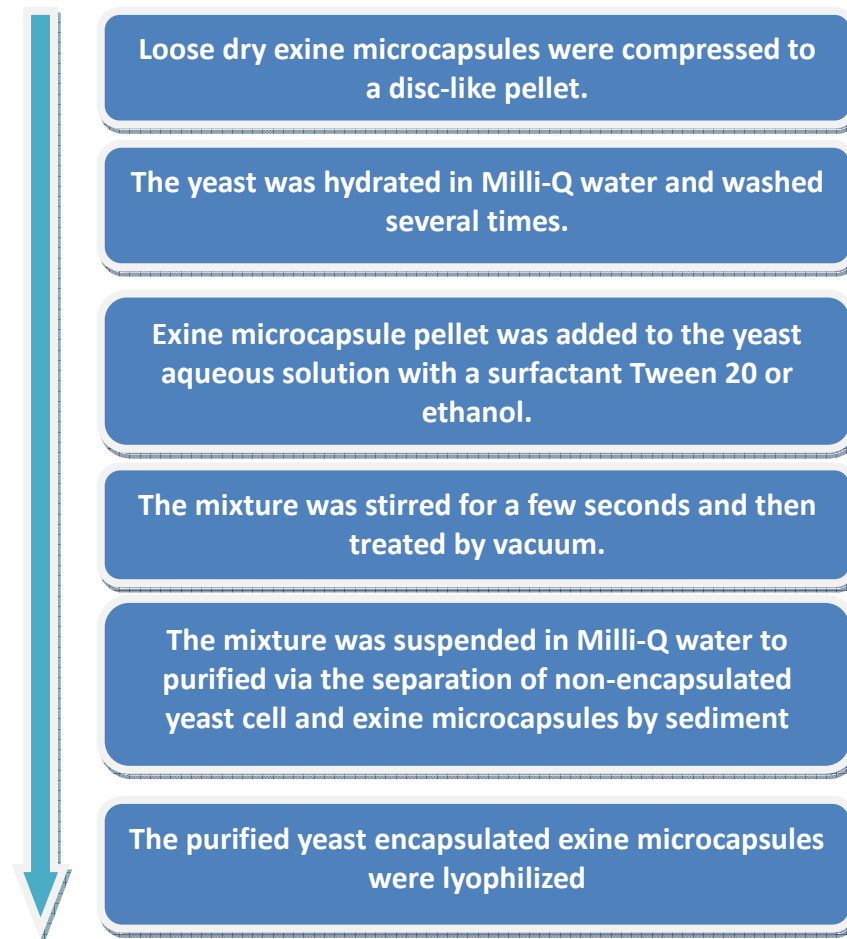


Figure 1.40 Summarized procedure of yeast cell encapsulation.⁶²

In this article the authors claim that the large yeast cell entered the microcapsules *via* opening and closing of the trilete scar on the proximal face of the spore. The scar is described to open upon compression of the exine and closed by swelling using liquid media.⁶² Limited evidence of encapsulation is presented (Figures 1.41 - 1.43) and the proposed mechanism by which yeast cells enter the microcapsules is purely theoretical. The authors provide many supporting pieces of evidence to prove yeast cells were successfully encapsulated into exine microcapsules. Firstly, the yeast filled exine microcapsules were analyzed by light microscopy (Figure 1.41). This image shows a number of exine microcapsules containing some yeast cells inside, but the limited transparency of the exine shell makes it difficult to be conclusive. Subsequently, the yeast encapsulated exine microcapsules were exposed to a solution of fluorescein diacetate and analyzed by a laser scanning confocal microscopy (Figure 1.42). Figure 1.42 shows a series of images of sections through a yeast filled exine microcapsule. A cluster of yeast cells is clearly visible right in the middle of the microcapsule. Direct

evidence for yeast encapsulation was provided by SEM. The yeast filled microcapsules were frozen by liquid nitrogen and ground to crack the exine shells to enable the contents of the interior to be viewed. Figure 1.43 shows a cracked exine shells containing a couple of yeast cells inside.

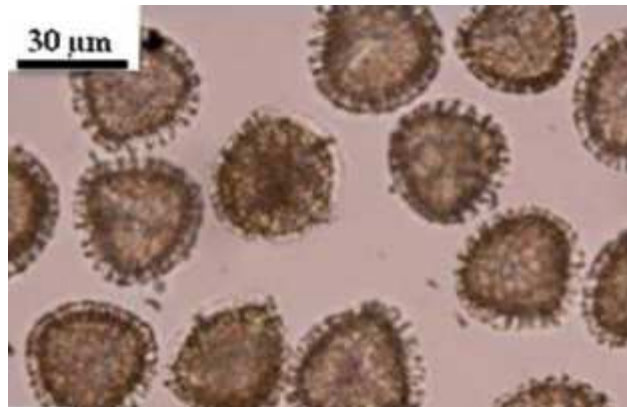


Figure 1.41 Photomicrograph of yeast cells encapsulated in exine microcapsules.⁶²

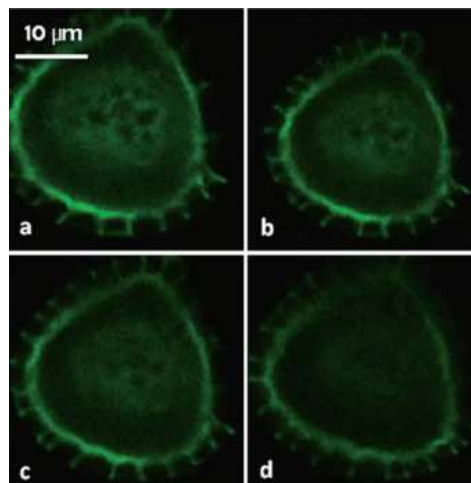


Figure 1.42 LSCM images of yeast cells encapsulated in exine microcapsules.⁶²

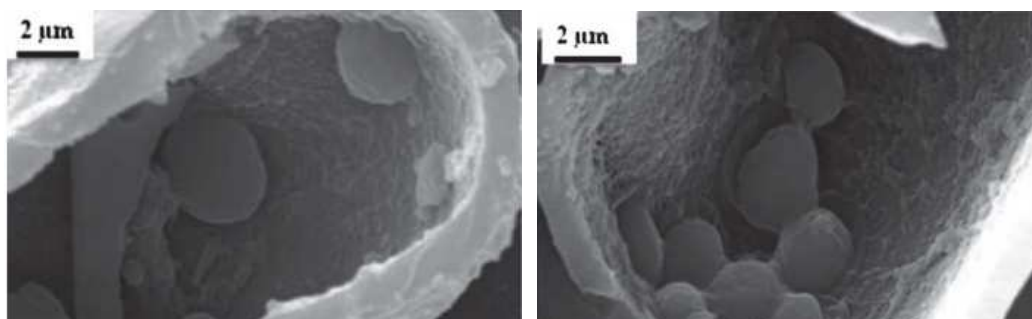


Figure 1.43 SEM images of yeast cells encapsulated in exine microcapsules. Exine microcapsules were treated with liquid nitrogen and cracked open using a pestle and mortar.⁶²

To further confirm encapsulation of yeast cells, these cells were coated with magnetite nanoparticles, making the yeast magnetic. These cells were encapsulated inside exine microcapsules and the magnetic properties of these microcapsules demonstrated. These filled microcapsules were suspended in solution and an external magnetic field applied. As shown in Figure 1.44, these microcapsules moved towards the magnet, providing further evidence of successful encapsulation.

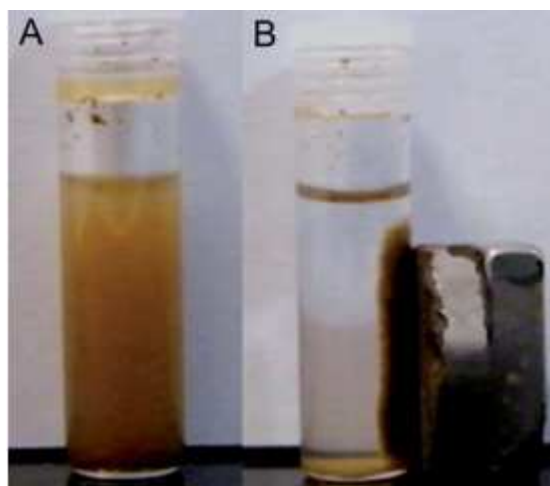


Figure 1.44 A) A re-dispersed suspension of microcapsules filled with magnetic yeast cells. B) The microcapsules are attracted to the external magnet.⁶²

Although the encapsulation of live cells has many promising applications, limited work has been carried out in order to demonstrate that exine microcapsules may be suitable for these applications.

1.5 Applications for modified sporopollenin

As stated in section 1, Sporopollenin is a complex material that forms the structure of the exine shell but its chemical structure is as yet unclear, although a range of functional groups have been identified by analytical techniques. Attempts have been made to modify these functional groups. For example, 1,3-diaminoethane was reacted with sporopollenin to yield diaminosporopollenin (DMSP), with the reaction conditions and possible molecular structure of the product formed shown in Figure 1.45.⁶⁴

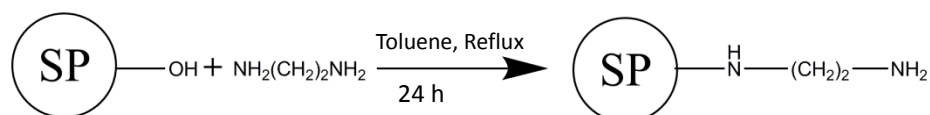


Figure 1.45 Reaction condition for the generation of diaminoethylsporopollenin, and possible molecular structure of the product. SP = sporopollenin exine.⁶⁴

Modified sporopollenin has been studied as a solid support for ligand and ion exchange. A typical application of these solid supports is chromatography. For example, it has been reported that DMSP was used to capture methylene blue from an aqueous solution.⁶³ The captured methylene blue was released from the DMSP by solvent washing. The capture and release of methylene blue by DMSP is summarized in Figure 1.45. DMSP was packed into a column and conditioned with doubly-distilled water and 0.5M HCl, loaded with methylene blue dye and then stripped using 0.5M NH₃ and methanol to remove the dye.⁶³ This result suggests that higher concentrations of methylene blue loaded onto the column lead to higher concentrations of methylene blue absorbed onto DMSP. However, the maximum capacity of the DMSP for methylene blue was not discussed.

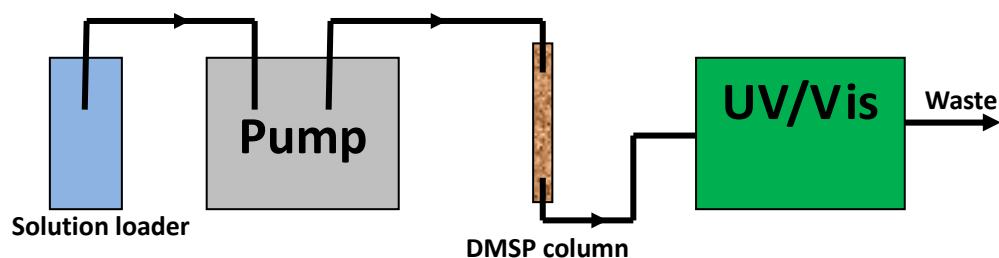


Figure 1.46 The experiment for dye capture and release by DMSP.⁶⁵

DMSP can be further modified by reaction with ethyl bromoacetate to produce carboxylated diaminoethylsporopollenin (CDMSP). The exact mode of bonding is unclear as the carboxylic acid has several potential binding locations (Figure 1.47).⁶⁶ Both CDMSP and DMSP were used to capture crystal violet lactone using a procedure similar to that described in Figure 1.46.⁶⁶ CDMSP was found to capture a greater percentage of the crystal violet lactone loaded onto a column compared to DMSP. The authors claim that the ability of the modified sporopollenin (CDMSP) to capture ionic compounds is greater than untreated sporopollenin.

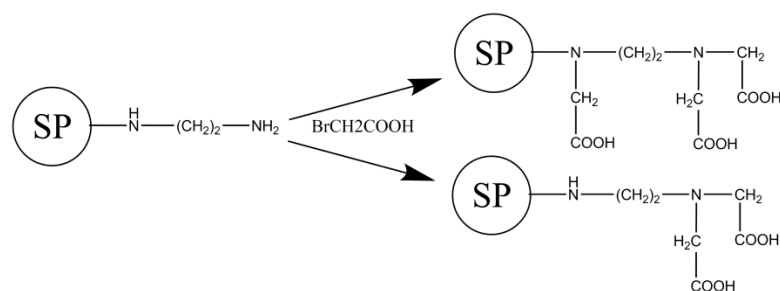


Figure 1.47 Reaction condition for the generation of CDMSP, and possible molecular structures of the product. SP = sporopollenin exine.^{66,22}

In addition to chromatography, sporopollenin has been modified with a range of other moieties. For example, sporopollenin has been bound to a calixarene in order to sequester toxic and harmful sodium dichromate from aqueous solutions.⁶⁷ In similar studies, Schiff bases were immobilized on sporopollenin in an attempt to recover vanadium and ruthenium from solution.^{68,69} *Lycopodium clavatum* spores were treated with *Candida rugosa* lipase using a modified passive encapsulation method in an attempt to immobilize this enzyme on the sporopollenin surface.⁷⁰ Limited evidence (a single SEM) was provided to confirm immobilization. Although the kinetic activity of the enzyme decreased, immobilization successfully improved its thermal stability compared to free lipase. These authors also modified sporopollenin in order to bind the protein hemoglobin.⁷¹

1.6 Electrophoretic display techniques

The electrophoretic display (ED) is a technology that has gained prominence in portable e-reader devices such as Kindle.⁷² Commercially viable displays are all monochrome, ie, they operate in black & white mode although a full-colour ED has been invented.⁷³ Compared to liquid crystal displays (LCD) and plasma displays (PD), ED requires low power for operation although response times are much slower. These EDs do not require a backlight because they operate using light scattering in a similar way to text on a page in a book and these devices are also bistable meaning that image retention is possible without continual use of an applied field.⁷⁴ The light scattering properties of EDs also mean that readability of the display improves in direct sunlight whereas other display types become more difficult to read.

The essential component of a typical e-reader using an electrophoretic display is electronic ink (E-ink). E-ink can be briefly described as a conductive colloid comprising

of microcapsules that are filled with positively and negatively charged black and white dyes or pigments.⁷⁵ Each of these microcapsules represents a single pixel within the device and as such the size of the microcapsules limits the resolution of the display (Figure 1.48a). Under an applied field the charged particles migrate towards the external electrodes using electrophoresis, ie, the negatively charged particles move towards a positive electrode and positively charged particles move towards the negative electrode. An example of this migration is shown in Figure 1.48b.

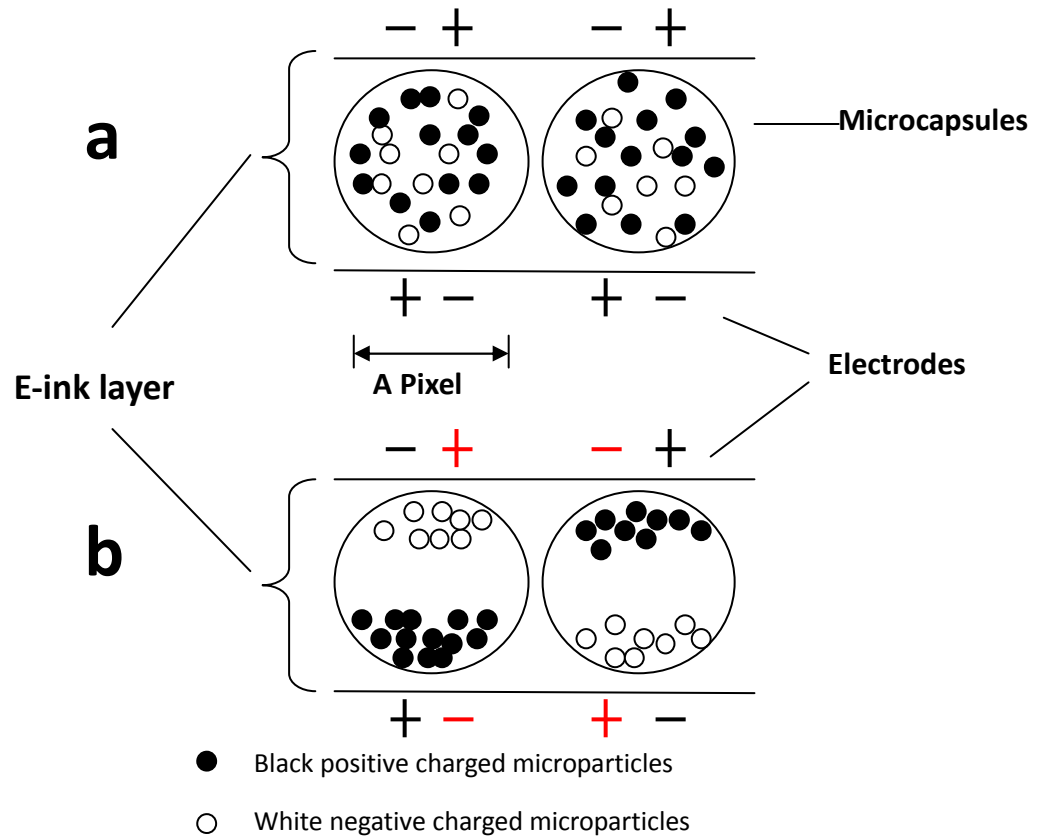


Figure 1.48 Scheme of electrophoretic display a) without applied electric field and b) with applied field. Red colour in b) represent electric field applying.

Many different methods were proposed to produce full-colour ED, but they can be broken down into two main types. The first type is essentially an extension to the classical black & white ED whereby colour filters are incorporated into the display structure.⁷⁶ A typical coloured device based on this technology is presented in Figure 1.50. In this system it is the colour filters that give colour because the microparticles used are always black and white. However, the limitation of this type of electrophoretic device is largely dependent on the quality of the colour filters that are used because they absorb part of the transmitted and reflected light beam. Hence, this reduces the

effectiveness of the display.⁷⁶ Furthermore, there are no barriers between the subpixels and light scattering of the particles may cause colouration of neighboring sub-pixels.⁷⁷

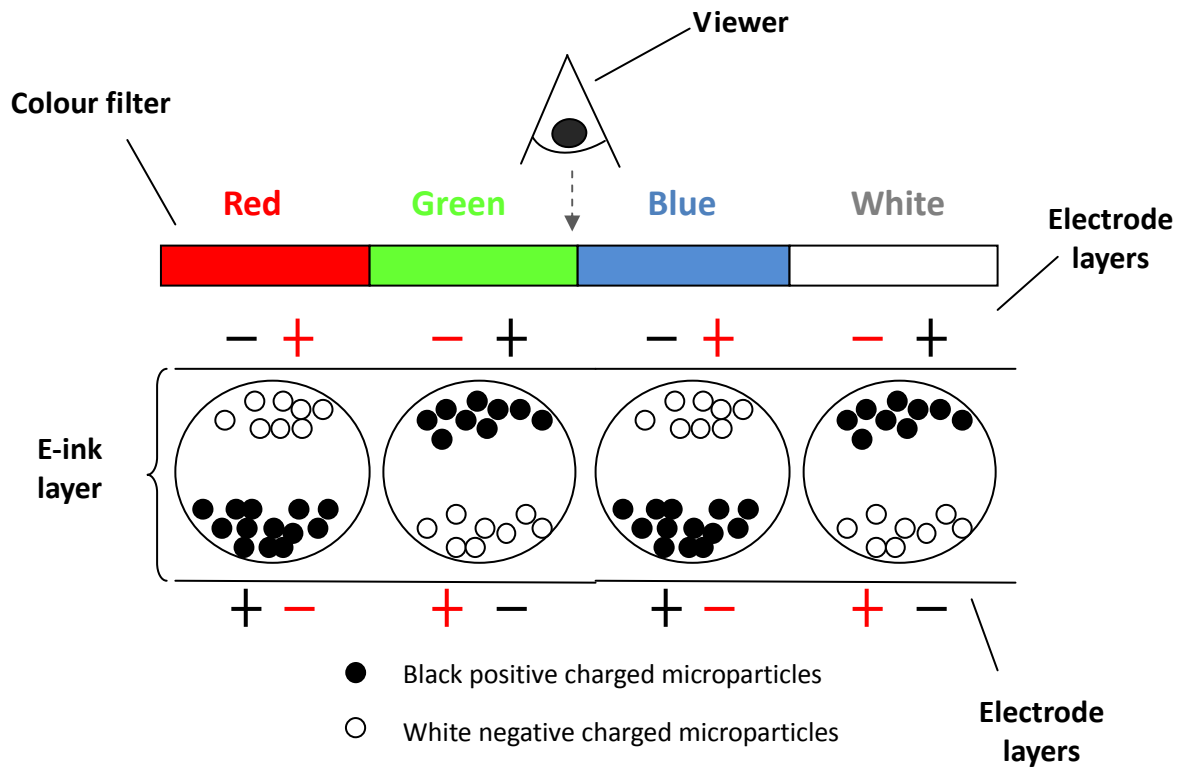


Figure 1.50 Structure of red, green, blue and white electrophoretic display based on black & white E-ink.⁷⁸

Another type of full-colour EDs use coloured E-ink where the black and white microparticles in microcapsules are replaced by single coloured microparticles (e.g red, green and blue microparticles). A good example for structure of this type of ED is demonstrated in Figure 1.51. In classical white & black ED, microparticles vertically move between bottom and top. However, movement of microparticles in this full-colour ED (Figure 1.51) changed from vertical to horizontal, they move between left and right. In this system, light beam will pass through all layers and yield white reflected light when all microparticles are attracted and hide in one side; colour appearance are observed when corresponding coloured microparticles are moved to suspend in the carrier fluid (Figure 1.51).

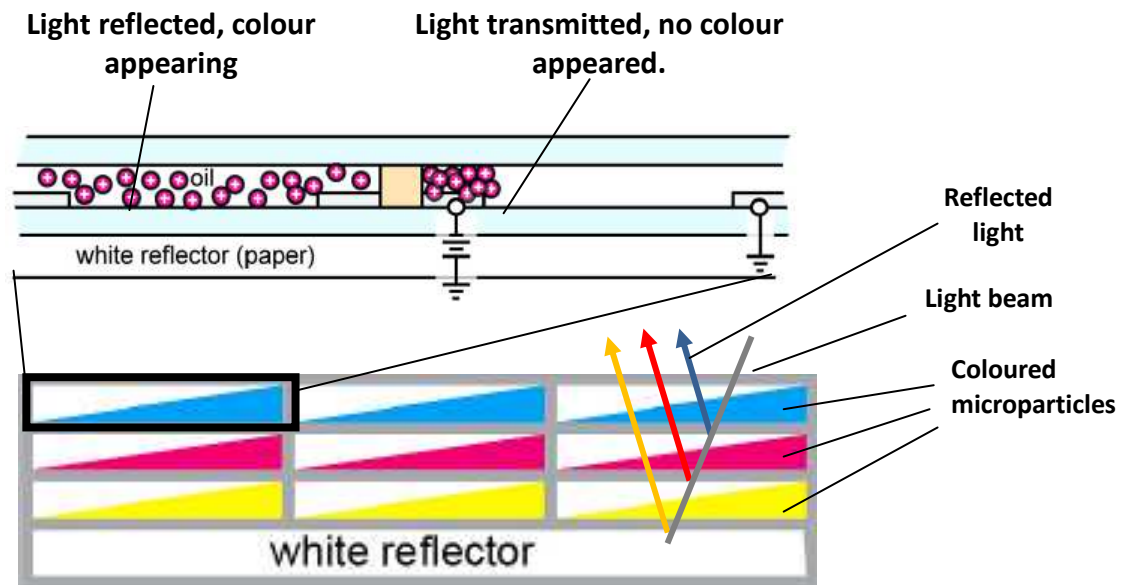


Figure 1.51 Structure of full colour ED based on coloured E-ink.⁷⁹

This type of display has the advantage of improved brightness and contrast due to the absence of coloured filters over the aforementioned display type. Although this device concept has the potential to eradicate the sub-pixel colouration problem it must be noted that there are other challenges that are encountered such as the difficulty patterning the sub-pixels and aligning them with an appropriate thin film transistor at each sub-pixel.⁷⁶ Therefore, most full-colour ED in the market still use the colour filter method to exhibit colour.

2. Aims

Sporopollenin is a robust material that can resist a variety of chemical and physical degradation processes, and it is an innate microcapsule that can be obtained from pollens and spores with relative ease. Exine shells have shown high potential for microencapsulation applications and much related research has been reported by Mackenzie *et al.*^{19,22, 28,43} In this project, systematic studies of various applications of exine microcapsules were carried out. The research was divided into two strands focussing on the preparations of exine microcapsules from raw *Lycopodium Clavatum* spores, and the development of encapsulation techniques with a view to use in various applications, respectively.

Lycopodium clavatum was selected as the source of the exine microcapsules because it is readily available, well studied and frequently applied in exine microcapsule research. Currently, the most popular exine microcapsule isolation technique is base and acid treatment, but this is a time consuming process that takes roughly two weeks to complete. Thus, the first intention of this project is to modify the common base and acid treatment to introduce simpler steps that are also less time consuming.

In the common base and acid treatment, the long experimental time is due to the stubborn and difficult removal of the intine layers. Organic solvent and base treatments are able to remove all of the protoplast and most of the intine within no more than 5 days. However, the removal of the remaining intine *via* acid suspension takes at least one week to complete. As mentioned in section 1.1.1, the use of a phosphoric acid suspension may not remove the intine material completely. Nevertheless, some applications allow a certain degree of flexibility with respect to the purity of sporopollenin in the exine microcapsules. A small amount of residual intine material is not expected to interact with many encapsulated materials and therefore will have little influence on certain applications. Therefore, one of the first aims is to investigate the effects of reducing or removing the acid treatment stage in order to minimize the experimental time. Due to the expected increased presence of residual intine material, the microcapsules produced from this simplified base and acid treatment will be referred to as exine and intine microcapsules (EIC).

Furthermore, suspensions of spores in solvents are usually achieved by mechanical stirring, but this may be replaced by other methods, such as ultrasonic agitation. This

approach has never been reported for *Lycopodium clavatum* spores, but is used to enhance dissolution of intine material and protoplasts. Thus, an ultrasonic bath will be used to investigate if it is possible to reduce further the experiment time. In addition to investigating the time of the procedure, the stability of *Lycopodium clavatum* exine microcapsules to ultrasonic sound will be studied.

2.1 Dye encapsulation

Dyes exist in a broad range of colours and, in many cases, the tone or shade colour that is observed is dependent upon the concentration of the dye used. This means that the amount of dye encapsulated by bleached EICs (BEICs) can be measured quantitatively by examining the colour of the filled BEIC. Hence, the results obtained from different methods and conditions of encapsulation can be easily compared *via* visual comparison. The dyes for encapsulation in this work will be divided into three groups: cationic, anionic and non-polar, this will allow for investigations of dyes with differing affinities for the BEICs. It should be noted that the different affinities of the dyes will also produce different colour intensities across the series of dyes as a whole, i.e., the dye intensities will not scale uniformly as a function of concentration across the materials studied.

In the proposed experiments, the dyes will firstly be encapsulated into BEICs by a droplet method (passive method, see Chapter 1) to compare the dyes and to select the optimum dyes for applications from the colours of the BEICs. The following criteria will be used to assess the BEICs; the amount of dye encapsulated, and the intensity of the colour and consistency of colour for individual BEICs. Once this initial screening has been completed, the selected dyes will be encapsulated into BEICs by the suspension method (this method is introduced in Chapter 5) because it can produce BEICs on a large scale more easily than the droplet method, and also can achieve a better consistency of colour for the products.

2.1.1 Dye encapsulation for display technology

One area of BEIC encapsulation research that has not yet been explored is their potential for use in display technologies, such as E-paper. Currently, E-paper technology works by the electrophoretic movement of microparticles, but at this time they are only available as black and white displays because the particles are only available in black or

white. If coloured BEICs are able to move electrophoretically they could, in principle, replace the current microparticles in E-paper in order to produce a full colour display. In order to make the BEICs responsive to an applied electric field, the surface of the EICs will be charged through chemical modification, or attempts will be made to encapsulate ionic dyes. At this stage it is acknowledged that the size of the BEIC based on *Lycopodium clavatum* (25 µm) may limit resolution for handheld displays such as those found in e-books. However, the aim of this work is to investigate the possibilities for the exploitation of exine microcapsules and not to focus on optimization for a single final application. Furthermore, there are examples of smaller exine microcapsules that could potentially be investigated for such applications, but this is beyond the scope of this current work.

In order to build a colour display (e.g horizontal electrophoretic display, see Figure 1.51) the dyes encapsulated by BEICs need to include five colours: red, yellow, blue, white and black.⁷⁹ Red, yellow and blue dyes are all commercially available. However, soluble white dyes cannot be easily obtained commercially, so white BEICs will be targeted by the attempted encapsulation of titanium dioxide. Titanium dioxide is an inorganic pigment that has limited solubility in common solvents. If it can be encapsulated into or coated onto BEICs, this experiment would also demonstrate the possibilities of utilizing BEICs in the removal of small insoluble particles from solvents. If successful, this experiment will demonstrate that the materials that could be adsorbed would not be limited by their solubility or insolubility. Therefore BEICs could be used as adsorbant materials for spill clean-up procedures etc.

Studies will be carried out to investigate the quantity of black dye that can be incorporated into BEICs but due to the poor solubility of most commercially available black dyes, direct encapsulation may be inadequate to produce a visually black particle. Therefore, another approach will be to investigate the encapsulation of more than one dye, i.e., as a dye mixture, into a single BEIC focussing on the uptake of a mixture of red, blue and yellow dyes. Fundamental questions that may arise in this study include whether the dyes mix well enough to give a black dye mixture and also whether the exine is capable of encapsulating all three in appropriate ratios to give a black mixture, or if preferential absorption or chromatography takes place.

The coloured BEICs will be mainly analyzed via light microscopy. This technique can rapidly reveal if there is any non-encapsulated material contaminating the products and also identify the consistency in distribution of colour in the BEICs, ie, do all BEICs encapsulate the dye to the same extent. The amount of dye encapsulated will be monitored via UV-Vis spectroscopy. Additionally, some of the dyes (e.g. Rhodamine B (RB) and thiazole yellow G (TYG)) are fluorescent and they will be examined by laser scanning confocal microscopy (LSCM) to identify their distribution in the BEICs.

2.1.2 Chromatographic studies

Shaw *et al.* reported that sporopollenin could be used as a solid ion/ligand exchange reagent after modification (e.g. addition of amino groups and carboxylic acid groups, see section 1.5). As part of this research project, raw *Lycopodium Clavatum* spores, low pressure treated *Lycopodium Clavatum* spores (raw *Lycopodium Clavatum* spores that have been stored under low pressure) and EICs will be investigated for use as ion exchange reagents without any modifications. In order to carry out the experiments, these particles will be packed into a pipette in the form of a mini chromatography column (for the purpose of this work this setup will be referred to as a spore or EIC “column”). A solution of ionic material will be passed through this “column” with the intention that the EICs will isolate this material from its solution. RB is a cationic compound and it is already known that it can be encapsulated into EICs, so it will be used as proof of principle in this experiment. The amount of RB left in the solution will be determined through comparison of intensity of absorption by UV-Vis spectroscopy.

In order to investigate the mechanism of this potential ionic exchange reagent, cationic, anionic and non-polar materials will be examined in a variety of solvents under neutral, acidic and basic environments. Specific dyes to be used in this research include three cationic materials (RB, methylene blue (MB) and safranin O (SO)), two anionic materials (TYG and Naphthol blue black (NBB)) and one non-polar material (CT69, 1,5-bis-(4-decyl-phenylamino)-anthraquinone). The efficiency of isolation on the EICs will easily be observed through visual inspection ie, does the column become coloured while the solution becomes clear. The pH will be investigated to determine if a change in pH can aid capture or release of the dyes and to determine if different pH environments will affect which dyes are captured and those that are not.

Solvent effects are important to consider because the interaction between solvent, encapsulation material and EICs will affect the encapsulation process. In order to investigate and understand this interaction, attempts will be made to isolate RB from a wide range of common solvents (e.g. water, ethanol, acetone etc.). The aim is to identify if EICs can act as capture and release agents that operate as a function of solvent.

2.2 Magnetic microcapsules based on exine and intine microcapsules

Magnetic vessels are frequently studied as an approach for drug delivery and Paunov *et al.* reported a novel magnetic vessel made from exine microcapsules.⁴⁴ In recent exine encapsulation research, insoluble materials are usually considered unable to be encapsulated by exine shells. Therefore, this magnetic exine vessel was prepared by synthesis of Fe₃O₄ nanoparticles directly inside the exine capsules, as mentioned in section 1.2.4. Attempts will be made to use the EICs prepared by the Chm-method (see chapter 4) to prepare magnetic particles following this published method and these products will be used as a reference material. Attempts will be made to directly encapsulate pre-prepared magnetic nanoparticles (γ -Fe₂O₃) into or onto EICs. In this way the nanoparticles could be characterised and evaluated prior to encapsulation and their behaviour pre- and post-encapsulation can be compared. The properties of EICs filled with magnetic nanoparticles from both methodologies can also be compared along with the size and distribution of nanoparticles within the EICs themselves.

2.3 pH responsive particles based on exine and intine capsules

The semi-transparent wall of BEICs allows the optical properties of the encapsulated material to be observed. In addition, the filled BEICs remain open to the environment and chemical exchange may continue between the inside of the BEICs and the outer environment. Therefore, the nature of the chemical environment can affect the encapsulated material. If the external environment stimulates a colour change of the encapsulated material, this can be easily observed visually. Therefore, pH responsive materials are considered suitable candidates to demonstrate this process.

Thus, phenolphthalein will be encapsulated into the BEICs. This common pH indicator is readily available and well studied. The structure of phenolphthalein changes when exposed to different pH resulting in a two-colour system. The reversible colour change and corresponding pH of phenolphthalein is summarized in figure 2.1. For this reason

phenolphthalein is considered a suitable material for the BEICs to produce pH responsive microparticles or pH micro-indicators.

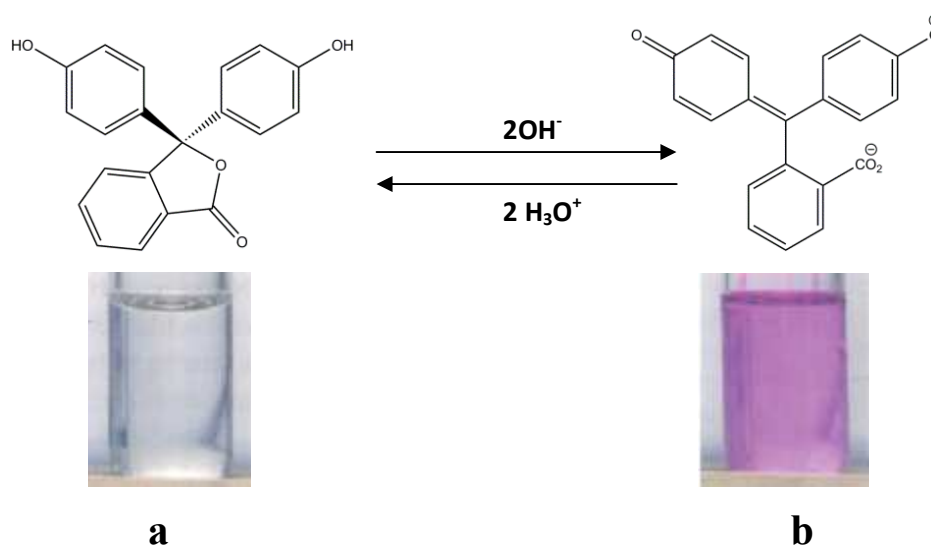


Figure 2.1 Molecular structure and associated colour of phenolphthalein at a) pH 0-8 and b) pH 8-10.⁸⁰

The response of the phenolphthalein filled BEICs will be tested at differing pH values and the colour change will be monitored visually. Phenolphthalein colour change is reversible as a function of pH so each of the prepared BEICs will be treated at different pH to see if this reversibility is maintained after encapsulation.

2.4 Thermochromic microparticles based on exine and intine capsules

Thermochromic dyes change colour as a function of temperature and hence they can be used as temperature sensors. The encapsulation of thermochromic materials by BEICs may demonstrate a novel approach to produce thermochromic particles, which may have potential in applications such as temperature indicators and temperature markers.

Crystal violet lactone is a thermochromic dye and will be encapsulated by BEICs to investigate if it is possible to produce thermochromic particles. Crystal violet lactone is a cheap and well-understood compound that belongs to a family of materials known as leuco dyes. Leuco dyes such as crystal violet lactone exhibit two molecular structures based on chemical interactions where one form is colourless and the other coloured. For example, the structure of crystal violet lactone is altered in the presence of H^+ (Figure 2.2). When it interacts with a H^+ donor, such as phenolphthalein, it will accept H^+ and is switched to the coloured form, which is blue. This process is irreversible. However, the

process becomes reversible thermally by the addition of hexadecanol. Hexadecanol provides an opportunity for protonated crystal violet lactone to re-form its colourless (leuco) form when it is above its melting point. Therefore to investigate if it is possible to produce thermochromic BEICs three components will be required to be encapsulated: crystal violet lactone, phenolphthalein and hexadecanol. Studies will be carried out to investigate if it possible to encapsulate the three components in the correct ratios to be able to produce a thermochromic particle; secondly if the thermochromic response is evident and occurs at the same temperature as the leuco dye mixture; thirdly if the process occurs reversibly within the BEICs and whether any effects are short term or long term.

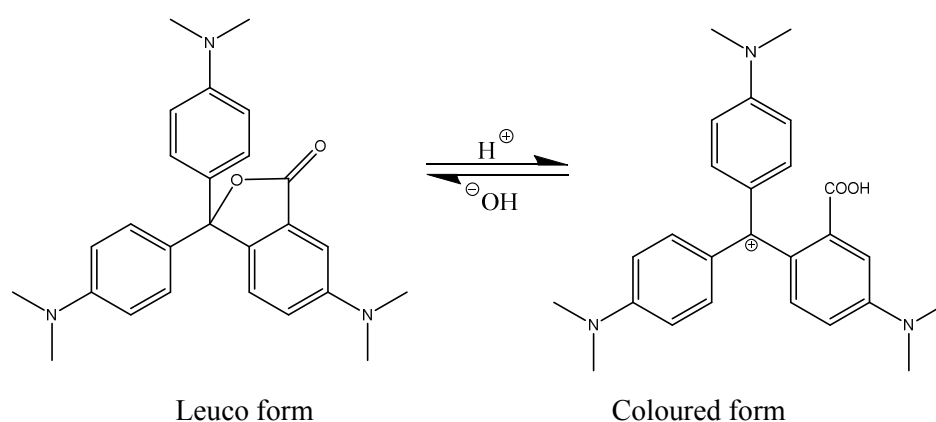


Figure 2.2 Structure change of crystal violet lactone.^{81,82}

2.5 Fluorescent microparticles based on exine and intine capsules.

Fluorescence is a function that can be easily incorporated into BEICs to produce fluorescent microparticles. It can be simply achieved by the encapsulation of fluorescent dyes. The antioxidant property of BEICs should protect the fluorescent material and extend its lifetime.

The major composition of BEICs, sporopollenin, is known to exhibit fluorescence, thus it may affect the fluorescent properties of encapsulated material. Therefore, the fluorescent material encapsulated BEICs will be analyzed via fluorescence spectroscopy and this study will investigate the degree of influence from the sporopollenin on the fluorescence of the encapsulated fluorescent material. The concentration of the fluorescent dye will be varied to investigate if the fluorescence is sensitive to concentration.

Rhodamine B (RB) will be used as the fluorescent material in this research since it is a well-documented fluorescent dye and frequently utilized in other fluorescence research which will allow for points of reference for any studies.

2.6 Multi-functionalized microparticles base on exine and intine capsules

To further extend the work and to produce microparticles that have greater functionality, studies will be carried out to encapsulate several components. It is important when combining two functional materials that they do not interact with each another and disrupt their functionality. Therefore, the choice of components must be carefully considered. For this purpose attempts will be made initially to combine colour and magnetic nanoparticles in EICs and the properties of these will be compared to the sole component EICs.

Attempts will also be made to extend this study and increase the complexity of the system by encapsulating thermochromic dyes, fluorescent dyes and magnetic materials in the same EICs. To achieve this degree of complexity, the filling procedure may become important and so the sequence of filling will be investigated. For example, if the sequence of encapsulation order is: 1. Thermochromic dye; 2. Fluorescent dye; 3. Magnetic material. In the second stage, encapsulation of fluorescent dye, the pre-encapsulated thermochromic dye may leach out and lead to reduced functionality. Therefore the sequence of encapsulation is important and investigation will be carried out to determine the optimum sequence.

2.7 Techniques for analysis of the treated EICs

Optical microscopy will be used to examine all of the EICs prepared in this work because it is a simple technique for the rapid screening of samples. For the purpose of this project the EICs will be examined using transmission and reflective microscopy. Since the walls of the exines are transparent it is possible to see if dyes have been encapsulated and also to see any colour changes that occur with temperature or pH.

For more detailed analysis of the EICs, samples will be examined using a combination of SEM, TEM and confocal microscopy. These techniques will allow the location of the encapsulated material to be identified along with the structural nature and integrity of

the capsule after treatments compared to the virginal material.

Additional techniques will be used for specific analyses such as UV-vis or fluorescence spectroscopy to evaluate the nature of the dyes pre- and post-encapsulation.

3. Experimental Methods

3.1 Reagents and Solvents

All solvents were supplied by Fluka, except diethyl phthalate which was purchased from Sigma-Aldrich and were used as supplied.

All reagents used in this work were supplied by Sigma-Aldrich and were used without purification. Norland optical glue (NOA76) was supplied by Norland Products and the photoinitiator (Irgacure 184) was supplied by Ciba-Geigy. *Lycopodium Clavatum* exines 25 μm and 40 μm were kindly donated by Sporomex Ltd, Maghemite nano-particles ($\gamma\text{-Fe}_2\text{O}_3$, 10nm) were donated by Liquids research, and *N,N'*-(2,2'-(ethane-1,2-diylbis(oxy))bis(ethane-2,1-diyl))bis(*N*-allylprop-2-en-1-amm onium chloride) (KC-AC-0002 purchased from Kingston Chemicals) See Figure 3.1.

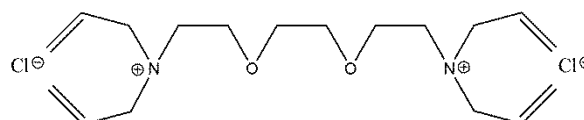


Figure 3.1 Structure of KC-AC-0002

3.2 Analytical Techniques

Ultraviolet-Visible spectroscopy (UV-Vis)

All UV-Vis spectra were recorded using a double beam Shimadzu UV-2401PC Spectrophotometer.

Solutions were all measured in index matched quartz cuvettes with a path length of 1 cm. The majority of dyes were water soluble and hence measurements were carried out in aqueous solution unless otherwise stated.

Solid samples were measured using sandwich cells that were prepared using 1" square pieces of microscope slide glass sealed together using optical glue. The glue was cured by placing under a UV lamp for one hour. Air was used as the reference specimen for all solid samples.

Fourier-transform infrared spectroscopy (FT-IR)

All infrared spectra were recorded using a Shimadzu IR Prestige-21 Fourier Transform

infrared Spectrophotometer with a Specac “Golden-Gate” diamond ATR IR insert.

Light microscopy

Normal light microscopy sample preparation process was used to investigate all samples, where for each specimen a glass microscope slide was employed without any special treatments.

All samples were analyzed using a Zeiss Axioskop 40Pol microscope, but the thermochromic EICs were confined in a Mettler FP82HT hot stage controlled using a Mettler FP90 central processor.

All photomicrographs were captured using a 21 MP Infinity X camera operating with Infinity-X capture software.

Laser scanning confocal microscopy (LSCM)

Laser scanning confocal microscopy was carried out in the Biology Technology Facility using a fully automated Zeiss LSM 510 meta attached to a Zeiss Axioplan 2 upright microscope. The samples were viewed using a Plan Neofluar 20x/0.5 objective. Images were taken with 2 X digital zoom using LSM 510 software.

All samples were suspended in deionized water with a glued cover slip (glass) on a standard microscope slide.

Excitation wavelength of RB sample used was 543 nm.

Excitation wavelength of TYG sample used was 488 nm.

Scanning electron microscopy (SEM)

Scanning electron microscopy was carried out using a JEOL JSM-6490LV scanning electron microscope within the Biology Technology Facility at The University of York operating in a high vacuum mode.

The samples were mounted on sticky carbon tabs and then sputter coated with ca. 7 nm of Au/Pd nanoparticles.

Transmission electron microscopy (TEM)

Transmission electron microscopy was carried out in the Biology Technology Facility at The University of York using a FEI Tecnai 12 Bio TWIN transmission electron microscope operating at 120 kV.

The samples were prepared by two methods as follows:

Method I: The samples were fixed in glutaraldehyde (2.5%) and formaldehyde(4 %) in phosphate buffer (100mM) overnight and then washed with buffer solution. Post-fixation the sample was treated with osmium tetroxide for 3 h and subsequently washed with water. The washed sample was exposed to uranyl acetate (1%) for 1h 30min in the dark and then washed with water. The sample was dehydrated through an acetone series and embedded in Spurr resin. 70 nm Sections were cut from the sample using a Leica Ultracut microtome and were stained with saturated uranyl acetate in ethanol (50%) and Reynolds lead citrate for 10mins each.

The following samples were prepared by method I: Raw *Lycopodium Clavatum* spores, empty *Lycopodium Clavatum* exines (batch No.: **CM-2**, see chapter 4), bleached empty *Lycopodium Clavatum* exines (batch No.: **BE-2** and **BE-7**, see chapter4)

Method II: Without any solvent or water-base chemical treatment, the samples were directly added to the Spurr resin and cut into 70 nm sections using a Leica Ultracut microtome.

The following samples were prepared by method II:MSI (batch No.: **MSI-1**, see chapter 8) and MS II (batch No: **MSII-2**, see chapter 8)

Ultrasonication

Ultrasonication of samples was carried out in a 50 Watt Eumax UD50SH-2L ultrasonic bath.

Fluorescence spectroscopy

Fluorometry was carried out using a Hitachi F-4500 FL fluorescence spectrophotometer with standard sample holder (liquid sample) and front face sample holder (solid sample). Figure 3.2 shows the configuration of the fluorescence spectrometer used in this work.

Excitation wavelengths were varied depending on the sample investigated.

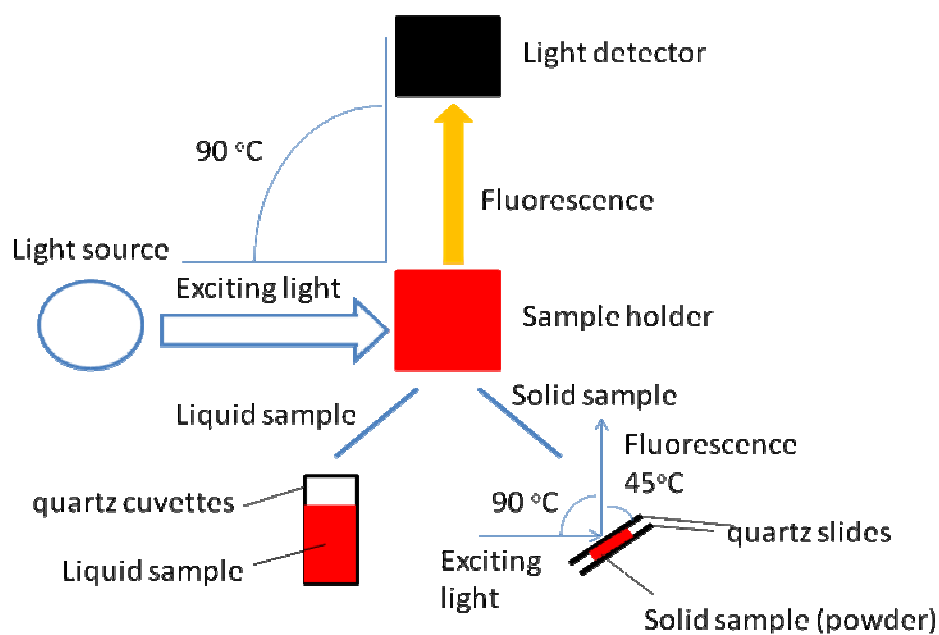


Figure 3.2 Simplified diagram of fluorescence spectroscopy.

Solutions were measured in quartz cuvettes (Path length: 1 cm).

Solid sample preparation: A few grains of a sample were placed in the middle of a small quartz slide (1" square) and sandwiched by a second piece of quartz. The cell was sealed using tape around the edges so that they could be opened, cleaned and reused.

4. Production of Spore Capsules

The major purpose of this project is the development of exine shells for a range of applications, often involving encapsulation of materials. However, the presence of intine and protoplast material inside the spores may strongly affect the encapsulation by the exine microcapsules, as well as potentially influencing the properties of the encapsulated material. Therefore, it was decided that as much as possible of the non-sporopollenin material contained in the spores would be removed in process of leaving an intact exine shell behind.

Four methods for removal of biological material from the spores were discussed in the introduction. The acetolysis method does not completely remove the intine layer from pollens and spores, and the use of sulfuric acid alters the molecular structure of the exine shells.³³ There are no reports on the production of exine shells on a large scale. A modified acetolysis method, which combines treatment with hydrogen fluoride, was considered too hazardous to carry out on a large scale.³⁴ Exine shells produced by both the 4-methylmorpholine N-oxide monohydrate (MMNO)³⁵ and the autoclave³⁹ methods did not remain intact. The modified MMNO method using a tissue grinder and enzyme treatments can produce intact exine shells but it is unclear on the degree of intine material removed during this process.³⁸ Additionally, this process has never been used to produce exine shells on a large scale. A base and acid treatment has been reported, but was shown to alter the chemical composition of sporopollenin by introduction of elements such as potassium into the structure.²² One of the negative aspects of this procedure is the length of time to produce empty exines however, this method produces intact exine shells, and on a large scale. Moreover, the exine shells produced by the base and acid treatment are available commercially, and are already used as microcapsules in published research.^{43, 44, 55} Therefore, the base and acid treatment was selected as the preferred technique for the preparation of microcapsules in this work.

4.1 Production of exine and intine capsules

Of the two major disadvantages of the base and acid method for production of exine shells, the changing of the molecular structure of sporopollenin cannot be prevented because of the chemical activity of the acid and base. However, the production time may be reduced via modification of the procedure. In this method, acid and base treatments are both effective steps to remove intine and protoplast, and both steps are

essential for their complete removal. However, it was noted that when only the base treatment step was performed a small amount of intine material remained inside the exine shells. For many applications it is not critical to remove all of the intine material, and therefore the base and acid method was modified to significantly in order to reduce the production time by eliminating the acid treatment, thereby reducing the procedure by at least 5 days.

This simplified preparation method of spore capsules was named the Chm method and for the purpose of this work the microcapsules were called exine and intine capsules (EICs) due to the presence of a small amount of intine. The sequence of events for the Chm method is summarized in Figure 4.1. The microcapsules, based on *Lycopodium clavatum*, used in this body of work were all prepared using the Chm method.

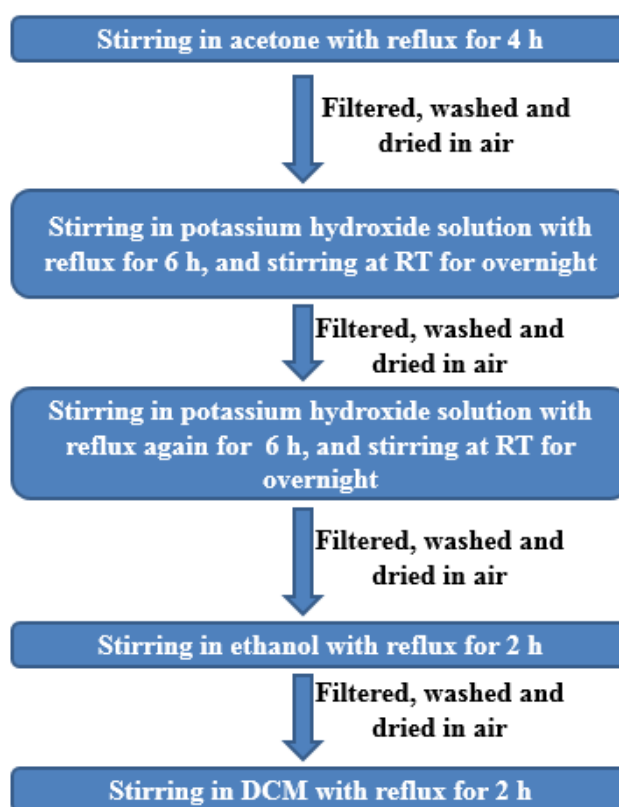


Figure 4.1 Summary of Chm method.

The EICs produced were analyzed by scanning electron microscopy (SEM) and compared with untreated spores, which revealed that there was no apparent damage to the spores using this method of preparation. Figure 4.2 shows that untreated spores appear rounded when observed under vacuum as they are fully filled with protoplast.

After treatment with the Chm method, the protoplast is removed and so the EICs now appear completely collapsed (Figure 4.3). Furthermore, four intact EICs are observed in Figure 4.3b demonstrating the typical morphology of the microcapsules.

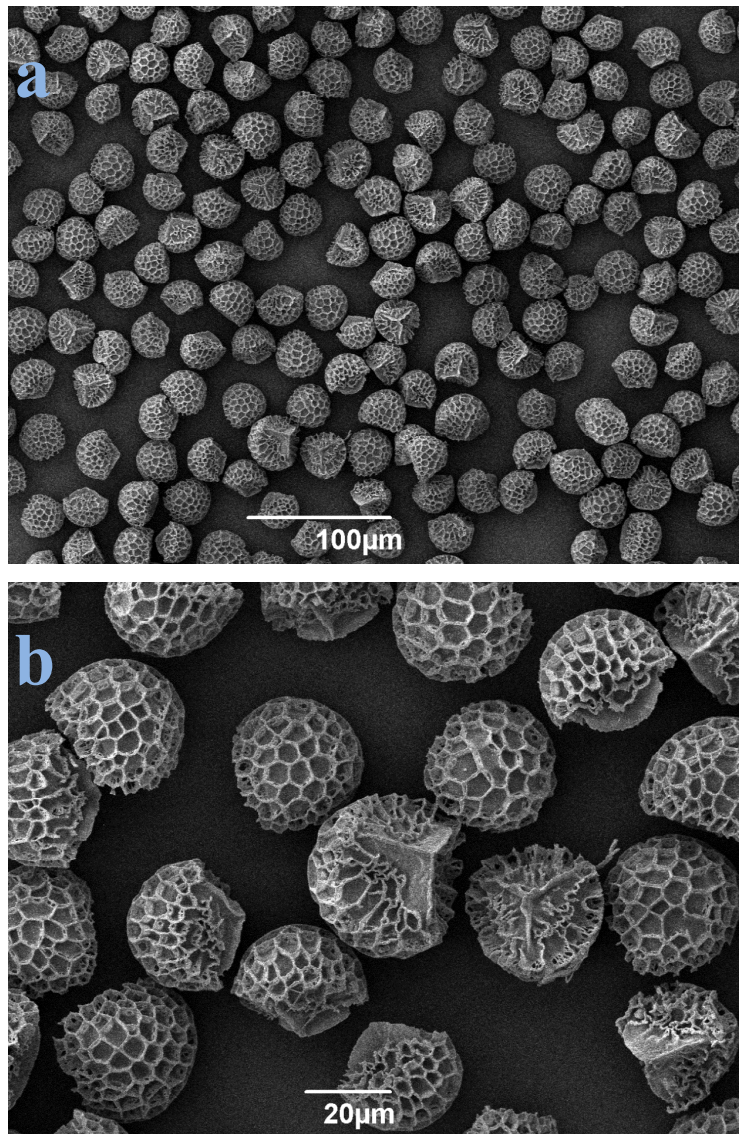


Figure 4.2 SEM images of untreated spores from *Lycopodium Clavatum*. a) Untreated *Lycopodium Clavatum* spores, and b) Untreated *Lycopodium Clavatum* spores under higher magnification.

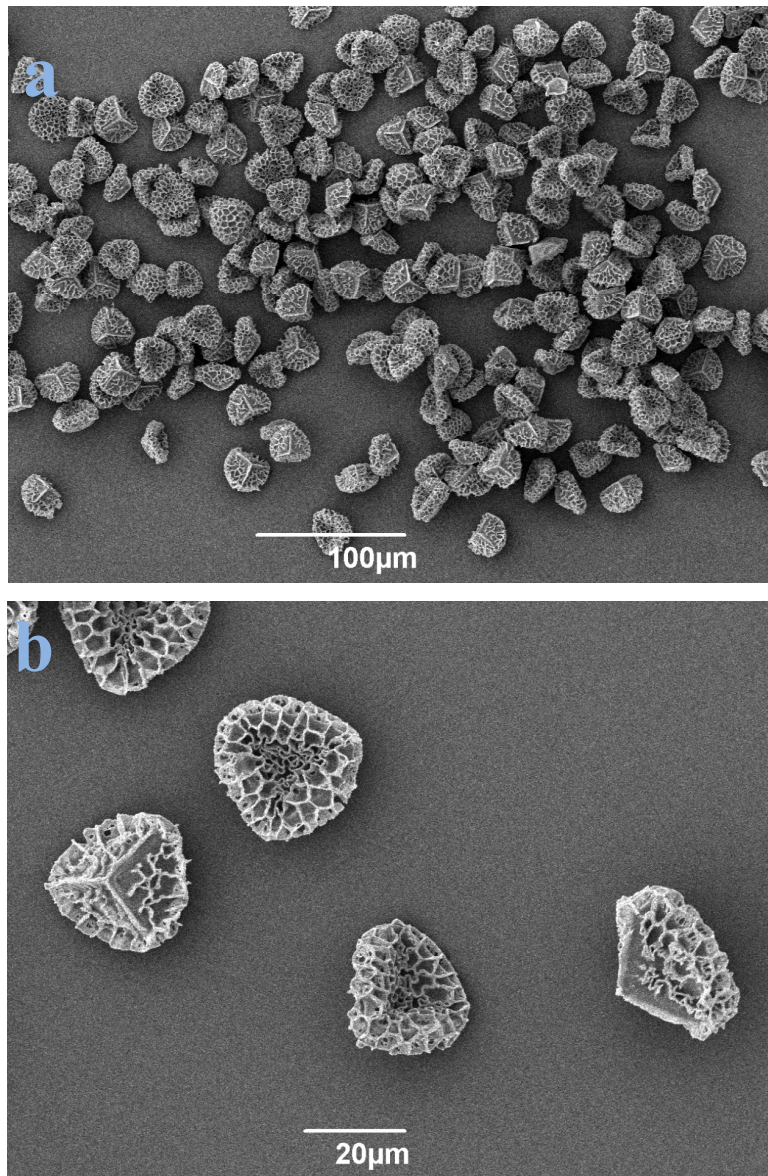


Figure 4.3 SEM images of *Lycopodium Clavatum* EICs produced by the Chm method. a) EICs.
b) EICs under high magnification showing the collapsed architectures.

The amount of intine and protoplast removed from the EICs was analyzed by transmission electron microscopy (TEM). Figure 4.4 shows a sequence of images of a cross-section of an EIC with increasing levels of magnification. The exine shell and a very small amount of intine material are clearly visible demonstrating the extent of removal using the Chm methodology. Figure 4.5 shows a cross-section of another EIC and this reveals the presence of intine material and some unknown substance within the exine shell.

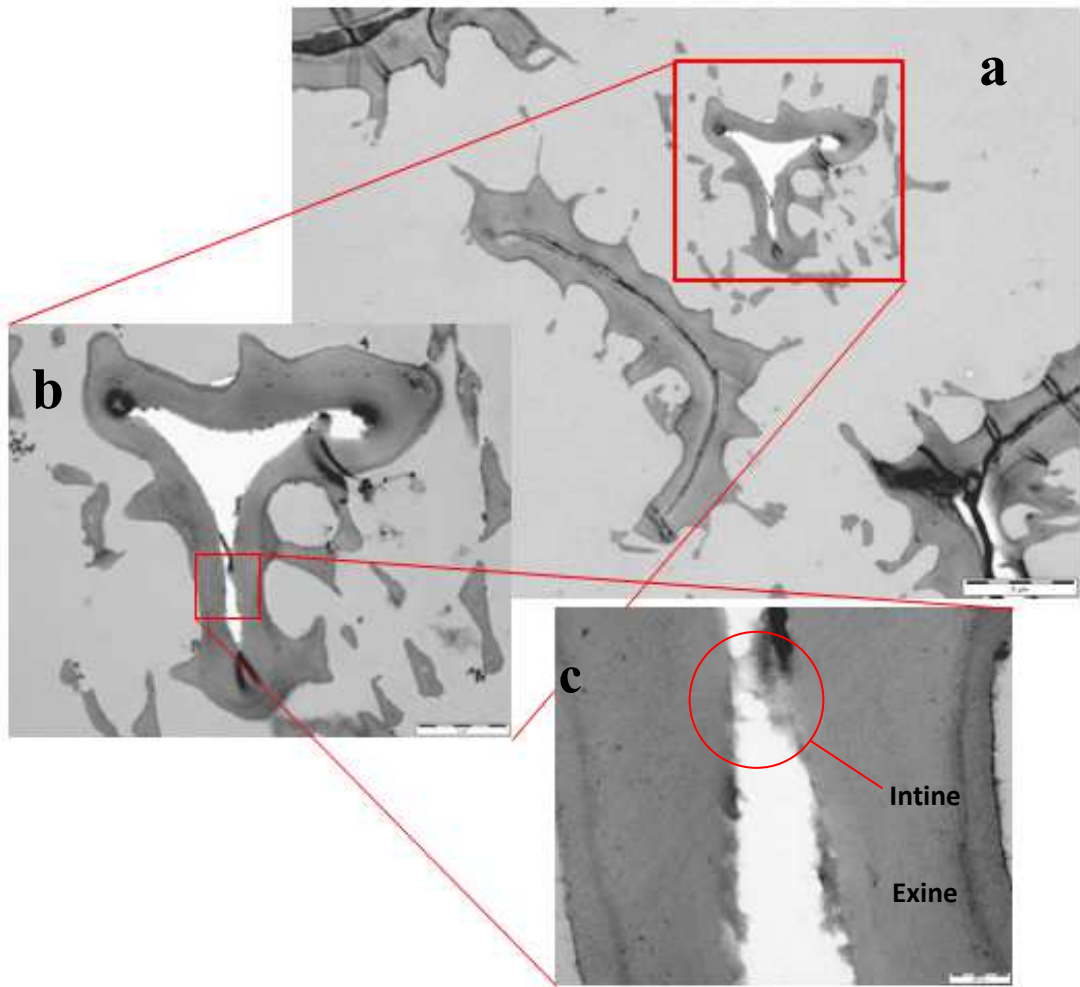


Figure 4.4 TEM images of the EICs showing increasing levels of magnification. Scale bar in a) 5 μm, b) 2 μm, and c) 200 nm.

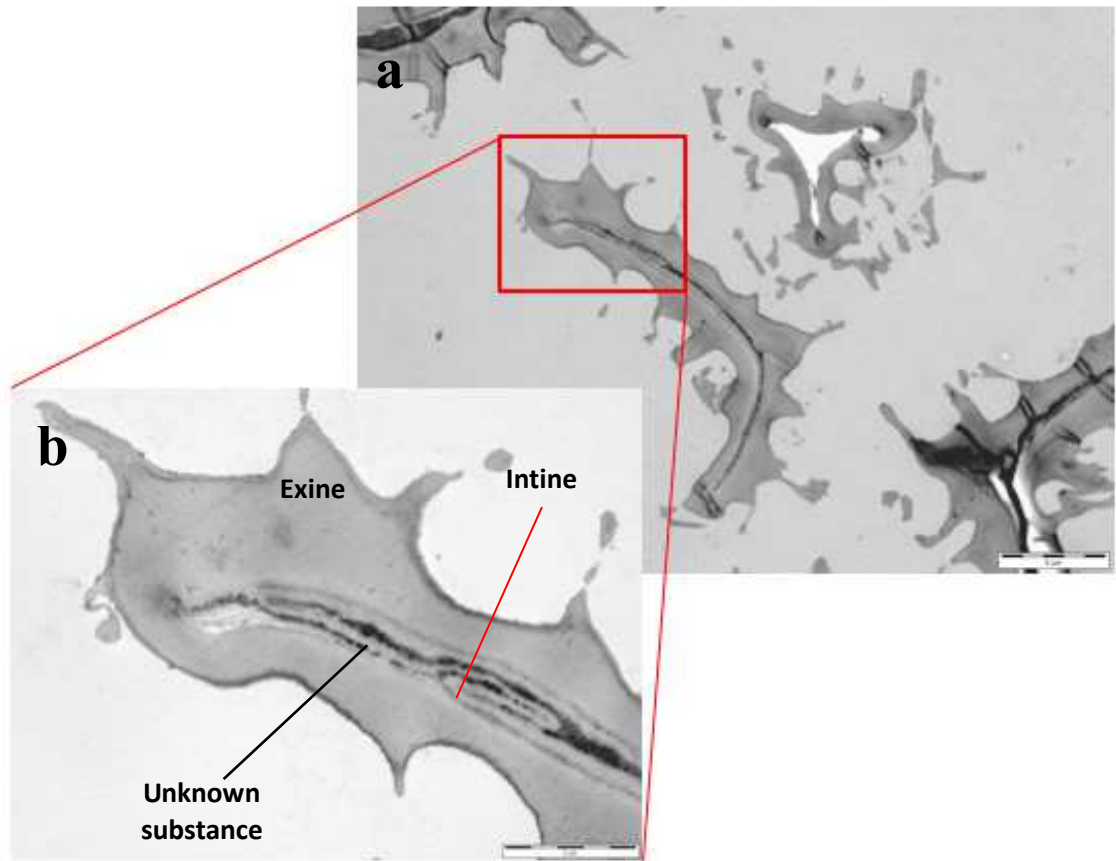


Figure 4.5 TEM images of the EICs with a higher magnification of one area revealing intine and an unknown substance. Scale bar in a) 5 μm and b) 2 μm .

Protoplast cannot survive the harsh conditions used in the Chm method so the dark unknown substance observed in Figure 4.5 was not residual protoplast. However, this substance exhibits a strong similarity to either the sporopollenin or intine material, existing solely in the interior of the EIC. It is also possible that the unknown substance is residual potassium hydroxide from the preparation of EICs that has become trapped within the exine due to strong ionic interactions. However, after numerous washing procedures, it might be expected that the ionic materials will be adsorbed in the aqueous wash. In order to test this possibility a small amount of EICs (CM-2) was placed on a pH indicator paper and a few droplets of water were added to wet EICs and pH paper. The indicator changed to dark blue indicating the wash was basic. The EICs were also stirred in water for 2 h and the pH tested again, with the same result. Furthermore, when empty bleached EICs were shaken in aqueous phenolphthalein solution, the solution changed to purple again indicating that the aqueous solution was basic. Thus these simple experiments support the view that the material trapped in the exine shells is likely to be potassium hydroxide. An attempt was made to further confirm this by mass

spectroscopy, but the single ion was too difficult to observe.

Thus, it can be concluded that the Chm-method is able to remove the majority of non-sporopollenin material from *Lycopodium clavatum* spores leaving the exine shells intact. TEM analysis indicated that only a small amount of intine remained after treatment, with the potential that some residual potassium hydroxide is also present.

4.2 Simplified Chm method

In order to further improve the Chm method for the preparation of EICs it was speculated that replacement of magnetic stirring of the spores with agitation using an ultrasonic bath would improve the rate of removal of the intine and protoplast material. This method was named the S-method. The *Lycopodium clavatum* spores were treated with aqueous potassium hydroxide (0.12 g mL^{-1}) under reflux for 2 h, then DCM at 35 °C for 0.5 h, followed by a solution of ethanol and water (1:1, 70 °C) for 0.5 h immersed in an ultrasonic bath (**SM-1**).

SM-1 was analyzed by FT-IR and compared to the EICs produced by the Chm-method (Figure 4.6). Despite the difference in exposure time there does not appear to be a significant difference in the IR spectra of the two sets of EICs. This evidence gave some reassurance that the S-method was not leaving behind additional material compared to the Chm method.

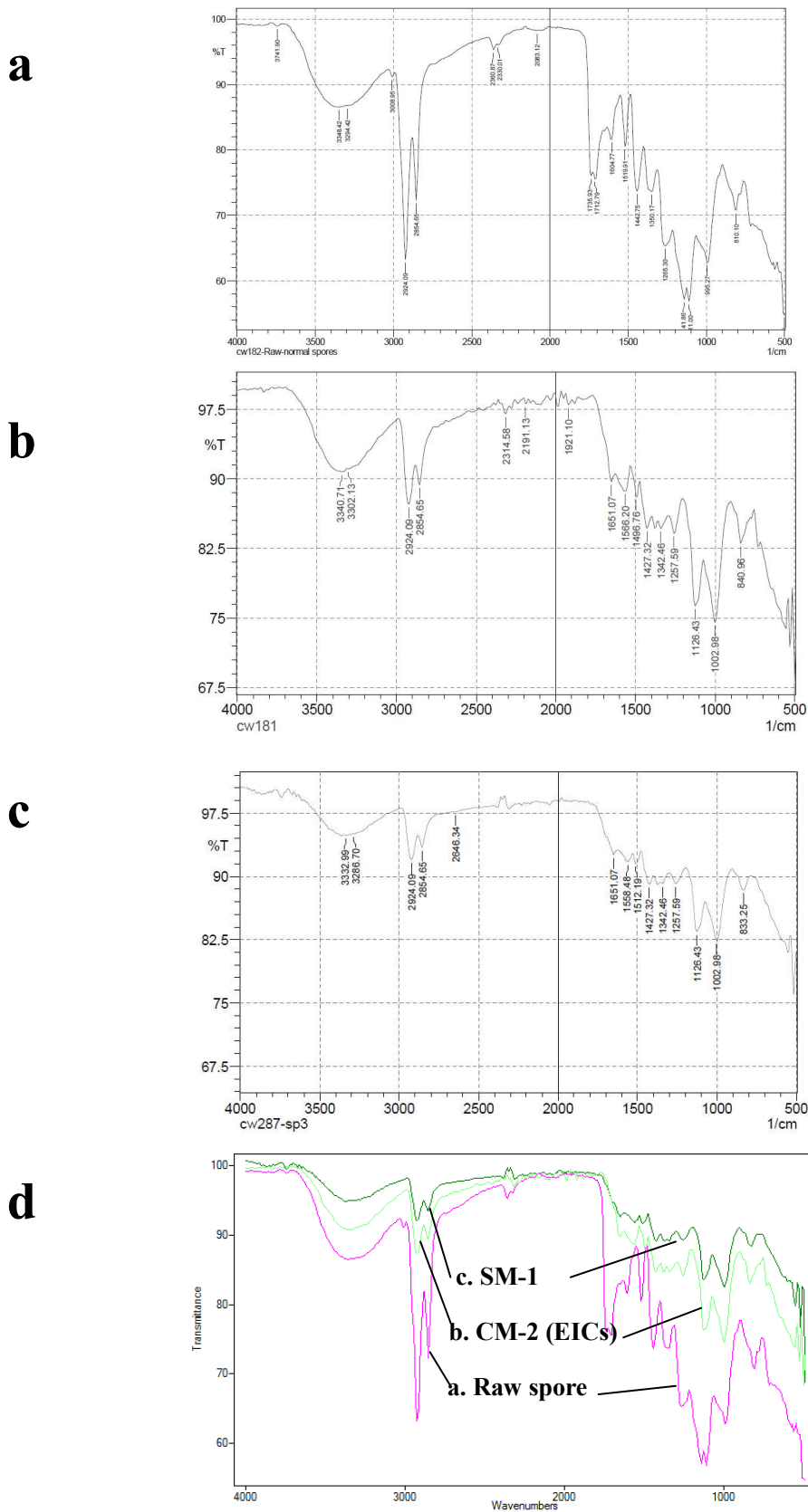


Figure 4.6 FT-IR spectra for a) untreated raw spores, b) **CM-2** (EICs), c) **SM-1** and d) overlap comparison of a, b and c.

There was hardly any notable difference between **SM-1** and **CM-2** (EICs produced by Chm-method by FT-IR, therefore **SM-1** was further analyzed by TEM (Figures 4.7 and 4.8). Figures 4.7 and 4.8 were taken in different areas of the same sample. Clearly the TEM analysis reveals that the same composition of EIC is observed for samples prepared using both the Chm and S-methods.

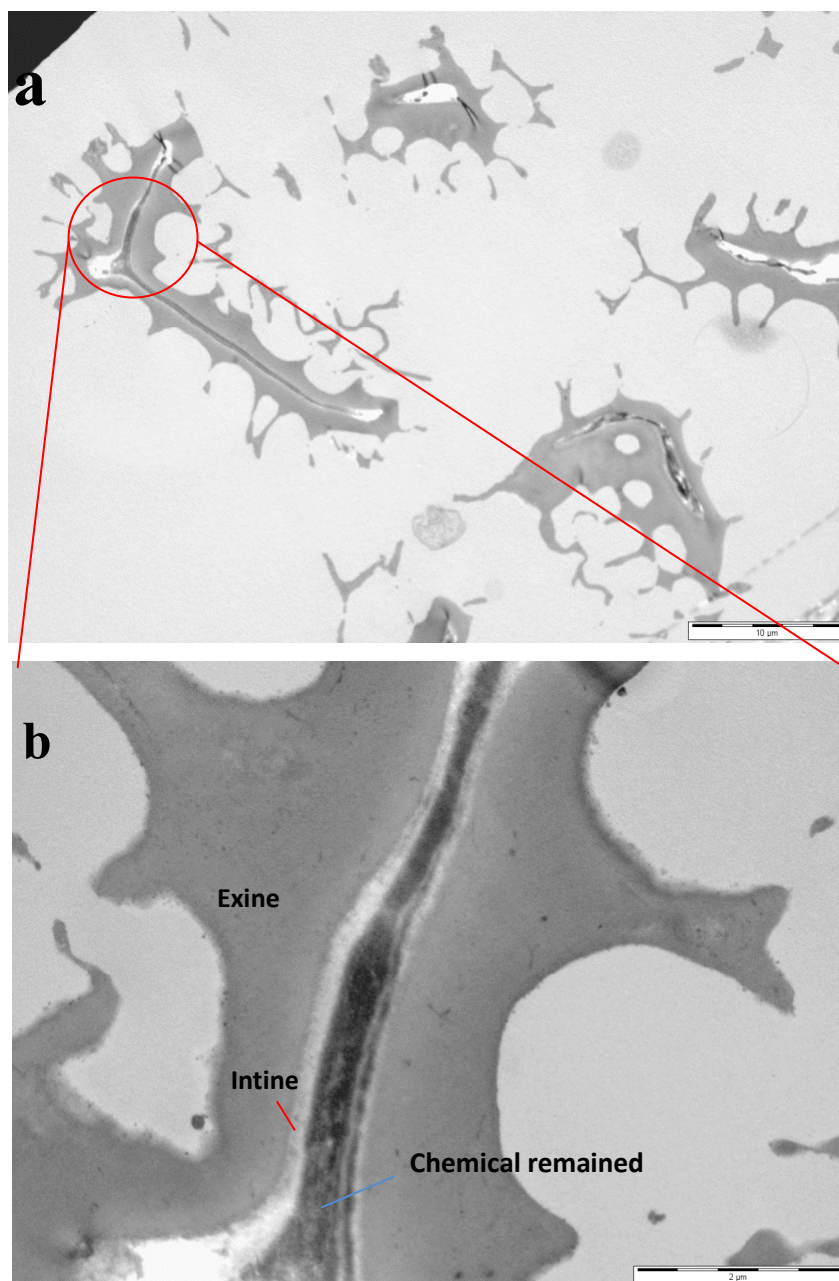


Figure 4.7 TEM images of **SM-1**. Scale bar of a) 10 μm, and b) 2 μm.

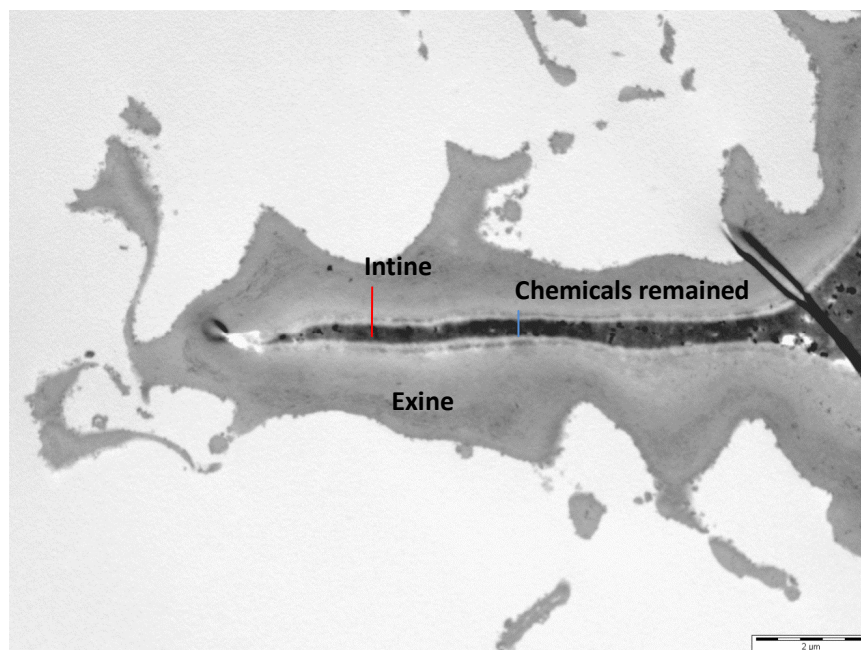


Figure 4.8 TEM photograph of **SM-1**. Scale bar is 2 μm.

The spores treated by the S-method are not considered suitable for use as microcapsules for some applications, such as food encapsulation and drug encapsulation, due to the residual intine material and chemicals; the residual contents may cause unknown risk to the encapsulated food and drugs. However, the encapsulation of materials carried out by capillary action and passive absorption into the exine shells should not be affected by remaining intine material. Therefore, the microcapsules produced by the S-method potentially may still be suitable for non-medical or non-food use, ie, in applications such as displays.

The TEM images of **SM-1** demonstrate the potential of the S-method for producing real double layer microcapsules (intact exine and intine layer). The S-method was further modified in an attempt to prepare EICs with little or no damage to the intine layer (DS-method). Only organic solvents (acetone, ethanol and DCM) were used to treat *Lycopodium clavatum* spores in this method, thereby avoiding acid and base treatments. Ultrasonication was used to aid the solubility of all non-sporopollenin material.

DSM-1 in Figure 4.9 shows the EICs prepared using a further simplified method (DS-method, see section 4.5), which were analyzed by TEM. Figure 4.9a shows a typical representation of the sample where most cross-sections of the treated spores appear to have residual protoplast. Figure 4.9b is a magnified region of Figure 4.9a

showing a treated spore with both intine and protoplast material present, however, the intine layer appears to be partially detached from the exine shell as shown in Figure 4.9c.

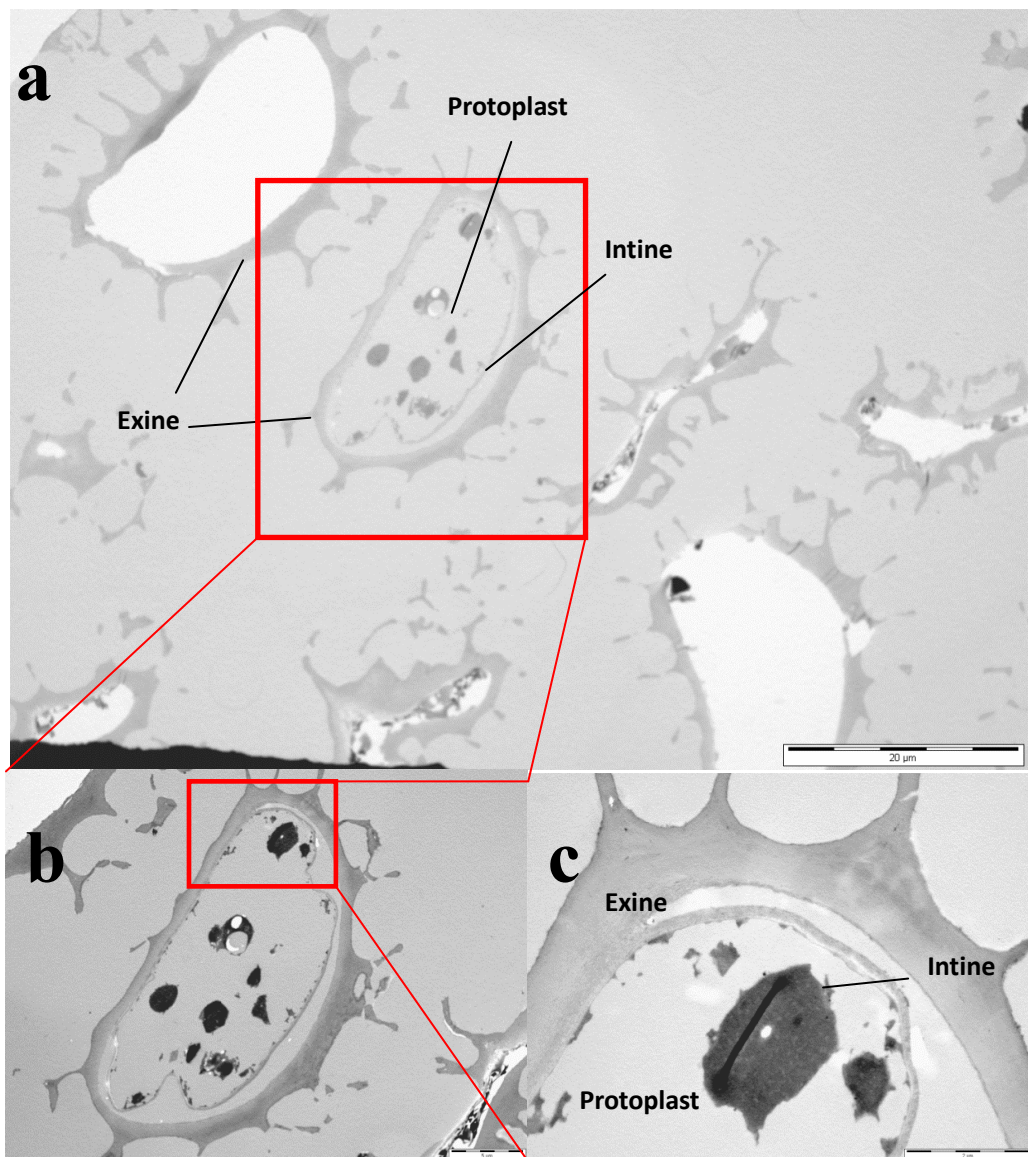


Figure 4.9 TEM images of **DSM-1**. Scale bar of a) 20 µm, b) 5 µm, and c) 2 µm.

Although Figure 4.9a shows that some of spores treated by this method maintain a large proportion of intine and protoplast, some spores also appear completely empty of non-sporopollenin material. This inconsistency suggests that either the DS-method is capable of emptying spores of non-sporopollenin material over time or that the intine and protoplast material is removed during the cross-sectioning process and remains relatively unaffected by solvent treatment.

In summary, the S- and DS-methods were not able to demonstrate removal of just protoplast leaving exine shells with intact intine layers. The S-method was a little too harsh whereas the DS-method was not harsh enough.

4.3 Bleaching of exine and intine capsules

The appearance of untreated *Lycopodium Clavatum* spores is as a pale yellow powder, but this changes to brown after treatment by the Chm method (see Figure 4.10). In order for EICs to be useful in applications where colour is important, such as in optical displays, it is necessary for the EICs to be white or transparent.



Figure 4.10 Visual appearance of spores of *Lycopodium Clavatum* after treatment with the Chm method

An approach described by Atkin *et al.* uses sodium hypochlorite to bleach the exine microcapsules produced by the base and acid method.⁸³ This approach was applied to the EICs that were produced by the Chm-method, but with a slight modification. The modified method still used sodium hypochlorite as the bleaching agent, however, the reaction time and temperature were adjusted depending on the concentration of active chlorine in each batch of sodium hypochlorite solution. It was found that optimum conditions required stirring in sodium hypochlorite with a 7 % active chlorine content at 35 °C for up to 2h (**BE-1**).

It was not always necessary to treat the EICs for a full 2h because the progress of the reaction could be monitored visually, and the bleaching was complete when the suspension turned yellow-white. The progression of the colour change during the reaction in **BE-1** is presented in Figure 4.11. The bleached EICs were filtered and washed immediately once this colour change had occurred (see Figure 4.11e). It was noted that if the treatment was continued beyond this point, the EICs sometimes started

to decompose and crack. At low concentrations the bleached EICs (BEICs) appear white, but at high concentrations they appear to be yellow (see Figure 4.12).

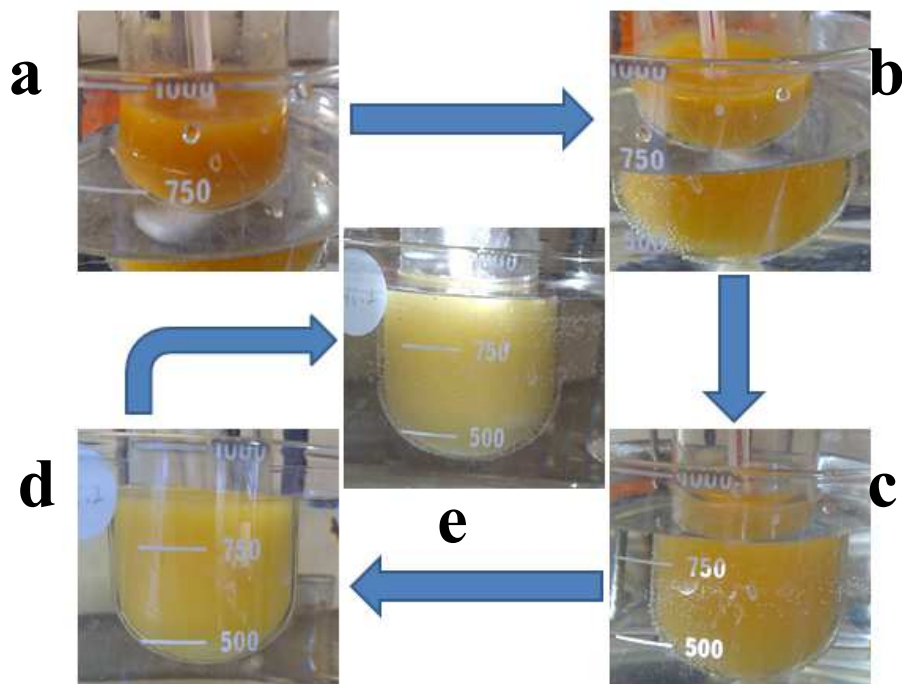


Figure 4.11 The progression of colour change during bleaching of exines, a-e, from dark brown to pale yellow.



Figure 4.12 Visual appearance of bleached EICs (BEIC).

A sample of BEICs was analyzed by SEM and a few images were taken from different areas of the same sample (Figure 4.13). These images indicate that the BEICs have a very similar appearance to the empty EICs and no apparent damage to their overall structure was observed.

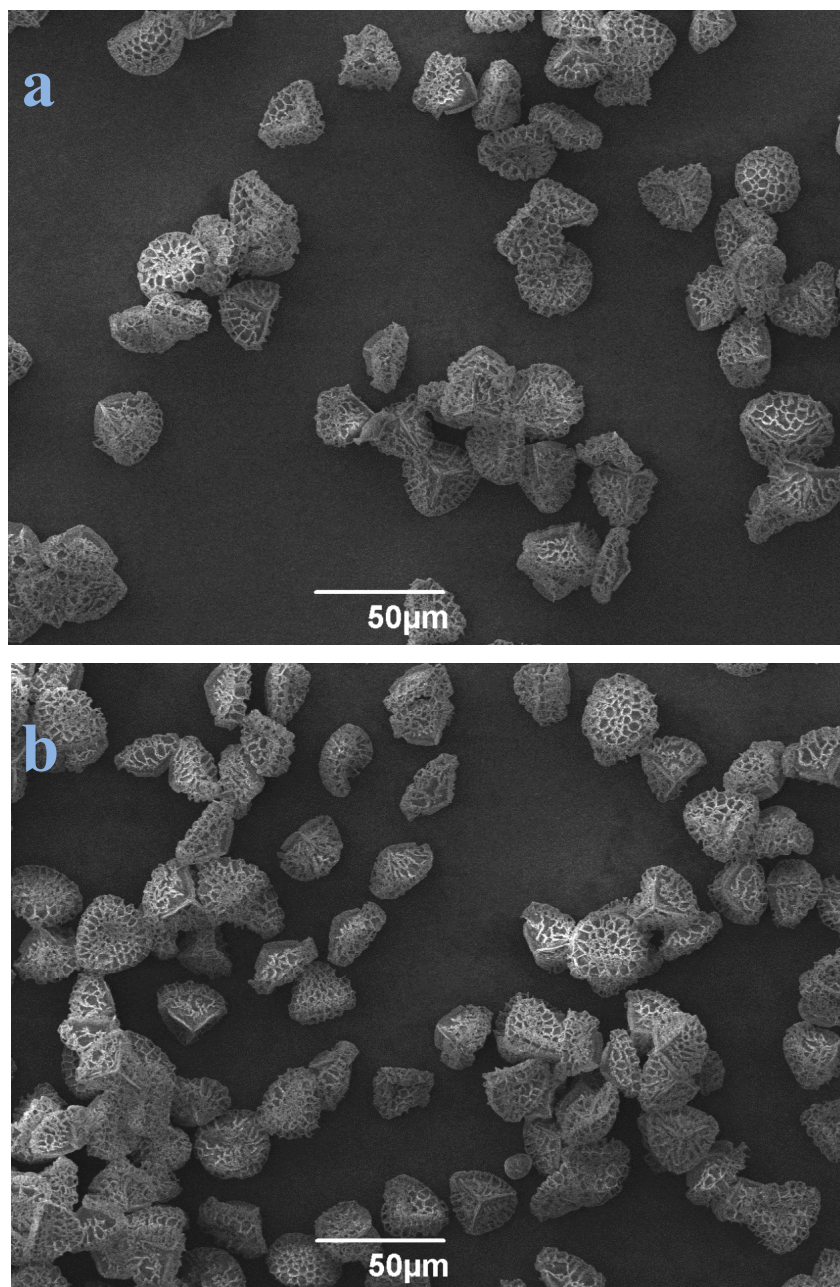


Figure 4.13 SEM images of BEICs; a) and b) are taken from same sample, but from different regions of the preparation.

The aqueous solution of sodium hypochlorite also acts as a base and so the residual intine material in BEICs may be further removed by the bleach treatment, which was confirmed by TEM analysis. However, this process not only decomposes intine material, but also causes some damage to the internal structure of the exine material, as shown in Figure 4.14. The TEM images show some residual material in the BEICs that could be due to residual intine material or an impurity related to the bleaching treatment, for example an inorganic material.

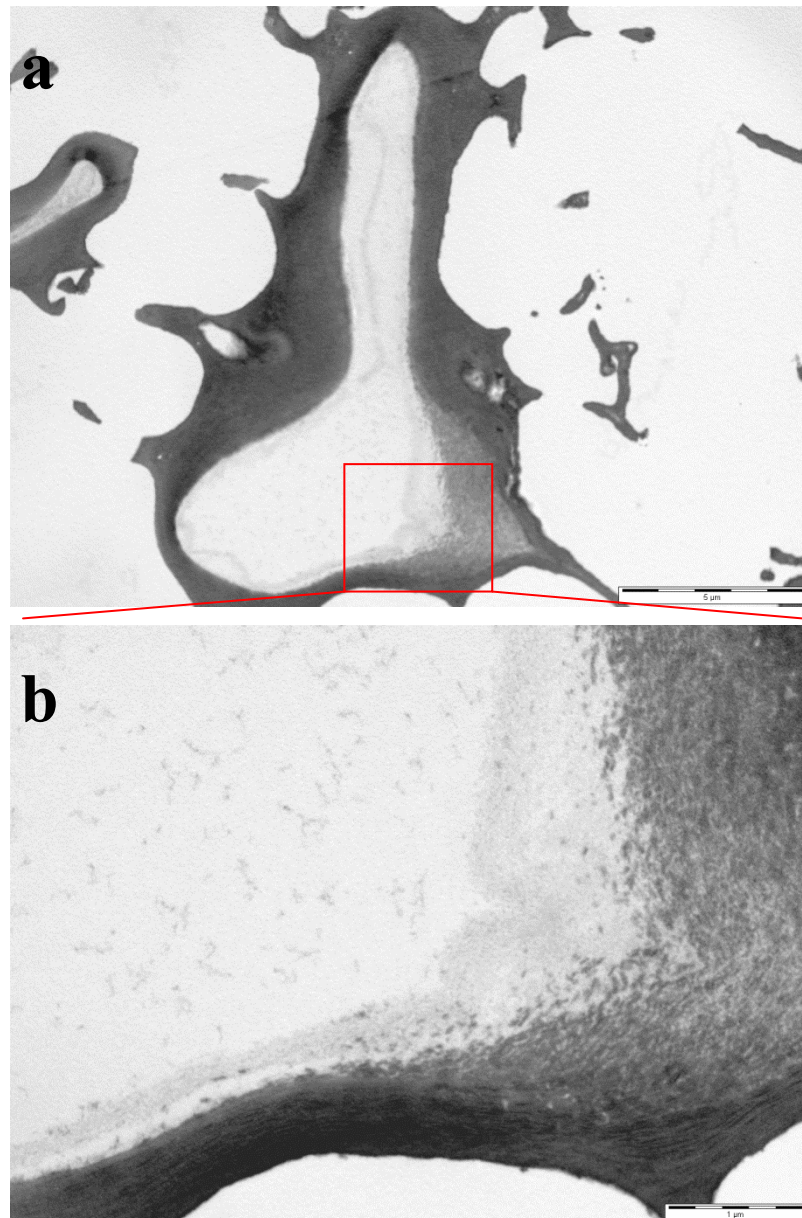


Figure 4.14 TEM images of a) BEICs and b) higher magnification image of a). Scale bar of a) 5 μ m and b) 1 μ m.

The bleach treatment is an inconsistent process with varying shades of whiteness observed in the resulting BEICs. This variation may be due to different concentrations of active chlorine in the sodium hypochlorite solution or it could be due to residual material remaining inside the BEICs.

4.4 Discussion and conclusion of exine shell isolation

All of the techniques used for the preparation of spore capsules in this project are based on the literature acid and base treatment,²² but all exclude acid treatment in order to shorten the time of the experiment and to simplify the procedure. The major

microcapsule production method, the Chm-method, successfully produced intact spore microcapsules (EICs) with all of protoplast and part of intine removed. Moreover, these EICs were successfully bleached by sodium hypochlorite without significant damage to exine shells. However, the washing process requires further improvement due to the small amount of residual material remaining inside the BEICs.

The S-method used an ultrasonic bath to further shorten the experiment time. The resulting spores have a more intact intine layer and so a larger amount of intine material remains than for the EICs prepared by the Chm method. It is proposed that the intact intine layer may aid the release of encapsulated material, due to the autoclave and sucrose method (see Chapter 1) used to swell the intine layer and rupture the exine shells. Therefore, the S-method, and its treated spores, is considered to have good potential for future development.

The subsequent research (DS-method) demonstrates the removal of intine and protoplast from the spores without harsh chemical treatments (e.g acid and base). The result shows the potential to use only common organic solvents, aided by an ultrasonic bath, to achieve similar effects to the MMNO treatment, which can detach the intine from the exine shell. Therefore, this method may be improved by the addition of an enzyme treatment as an alternative to the MMNO method, and the gentle nature of the treatment is expected to maintain the initial chemical structure of sporopollenin.⁸⁴

4.5 Experimental

The first batches of EICs (**CM-1**) and BEICs (**BE-1**) were produced by Dr. Charles K Bradbury and the author. The methods employed are outlined in the sections that follow.

Chm Method (CM-1)⁸⁵

Clavatum Lycopodium spores (250 g) in acetone (1.3L) were heated under reflux for 4 h. The mixture was cooled to 40 °C and then filtered. The isolated spores were washed with acetone (300 mL) and dried. Yield 239 g.

KOH (51 g) in water (850 mL) was then added to the treated spores (239 g) under an argon atmosphere with stirring. The reaction mixture was heated under reflux for 6 h, cooled and then left to stir at RT overnight. The reaction mixture was filtered in four

portions and each portion was washed with hot water (5 x 400 mL) until the washings became colourless. The orange-brown cake was left to dry overnight.

The damp cake (280 g) was suspended in 6 % aqueous KOH (750 mL) and the procedure from the above paragraph was repeated again, except that the cake was washed, not only with hot water (total 8 L), but also sequentially with EtOH (2 x 500 mL at 60 °C), water (2 x 500 mL at 80 °C) and finally with warm EtOH (2 x 500 mL).

EtOH (650 mL) was then added to the product under an argon atmosphere. The mixture was heated to reflux with stirring for 2 h. After cooling to ca. 40 °C, the brownish-yellow product was isolated by filtration, and washed with EtOH (2 x 500 mL), and then with DCM (2 x 500 mL) and lastly air dried.

Finally DCM (600 mL) was added to the product from above. The slurry was heated under reflux, with stirring, for 2h. After cooling to RT, the product was filtered, washed with DCM (250 mL) and dried in air overnight. Yield 76 g, 30.4 %.

CM-2

The procedure was carried out in an analogous way to the Chm method. The following quantities were used: Untreated *Lycopodium Clavatum* spores (50.26 g), acetone (200 mL), aqueous potassium hydroxide solution (5.9%; 200 mL), ethanol (130 mL) and dichloromethane (200 mL). Yield 14.33 g (29 %)

CM-3

The procedure was carried out in an analogous way to the Chm method. The following quantities were used: Untreated *Lycopodium Clavatum* spores (104.51 g), acetone (500 mL), aqueous potassium hydroxide solution (5.9%; 1 L), ethanol (600 ml) and dichloromethane (600 mL). Yield 32.62 g (31 %)

S-method-1 (SM-1)

Untreated *Lycopodium clavatum* spores (0.58 g) were stirred in 12% aqueous solution of KOH (10 mL) and heated under reflux for 2 h. The treated spores were filtered and washed with ethanol (10 mL), water (30 mL), ethanol (30 mL), ethanol and water (1:1) solution (30 mL), acetone and water (1:1) solution (30 mL), and acetone (30 mL). The

resultant spores were transferred to DCM (30 mL) and the mixture was sonicated for 0.5 h at 35 °C. The product was filtered and washed with DCM (10 mL), ethanol (20 mL) and acetone (10 mL). The treated spores were then sonicated in ethanol and water (1:1) solution (30 mL) at 70 °C for 0.5 h. The suspension was filtered and washed with water (10 mL), ethanol (10 mL) and acetone (10 mL). Then the product was dried in air. The production of EICs by this method results in removal of the bio-content, so the, although inconsistent, yield was always lower in comparison to the other methods. Yield 0.22g (38%)

DS- method-1 (DSM-1)

Untreated *Lycopodium clavatum* spores (2 g) were added into a solution of acetone and water (1:1) (100 mL) and treated by ultrasonication at 70 °C for 0.5 h. The spores were filtered and washed with water (50 mL), water and ethanol (1:1) solution (50 mL), ethanol (50 mL), acetone and water (1:1) solution (50 mL) and acetone (50 mL). The treated spores were air dried and then added into an ethanol and water (1:1) solution (100 mL) followed by ultrasonication at 70 °C for 0.5 h. The treated spores were filtered and washed with water (50 mL), water and ethanol (1:1) solution (50 mL), ethanol (50 mL), acetone and water (1:1) solution (50 mL) and acetone (50 mL) then air dried. The dried spores were transferred into DCM (100 mL) and treated by ultrasound at 35 °C for 0.5 h. The treated spores were filtered and washed with water (50 mL), water and ethanol (1:1) solution (50 mL), ethanol (50 mL), acetone and water (1:1) solution (50 mL) and acetone (50 mL). Finally, the treated spores were air dried. Yield 0.89 g (45%)

Bleached EICs (BE-1)⁸⁵

The EICs (**CM-1**, 76 g) were suspended in 7 % sodium hypochlorite solution (50 v/w) and the slurry warmed with stirring to 35 °C for 2 h. The slurry was then cooled to RT and immediately filtered and washed with water until a negative starch iodide test was obtained. The product was washed with EtOH (400 mL) and acetone (400 mL) then dried *in vacuo* over P₂O₅.

Yield 73.3 g (96%).

The other batches of BEICs used the same procedure described for **BE-1** but double the volume of solvent was used in the washing processes. The reagents used, quantities and yields are summarized in Table 4.1:

Table 4.1 Summary of reagent, quantities used and yield for BEICs.

Name	Batch name of EICs utilized	Weight of EICs/g	Concentration of aqueous Sodium hypochlorite solution/%	Yield/g
BE-2	CM-3	1.01	7.62	0.98
BE-3	CM-3	1.00	7.62	0.91
BE-4	CM-3	2.28	8.32	2.20
BE-5	BE-4	2.02	8.32	1.95
BE-6	CM-3	2.00	7.98	1.90
BE-7	CM-3	10.01	7.92	9.45

5. Exine and Intine

Capsule

Encapsulation

The passive method, the vacuum method and the centrifugation method were discussed previously in Chapter 1. These methods rely on the capillary action associated with intact exine shells, but they are distinguished by the conditions used to enhance encapsulation. The results of encapsulation were found to be mostly affected by the volume ratio between the material to be encapsulated and the EICs. The three methods introduced previously were all carried out with a small volume ratio of target material to exine microcapsules, where the mixture usually appeared as a paste or wet powder. These methods were collectively called the droplet method where the main variable for adsorption is the volume ratio of target material to microcapsule. The amount of target material that can be encapsulated by the microcapsules using the droplet method is primarily dependent on the physical capacity (inner space) of the microcapsules, however, the affinity between microcapsule and absorbate may also be of importance. When the volume ratio of the target material to exine microcapsules is sufficient for the mixture to appear fluid, the amount of target material that can be encapsulated by the microcapsules is not only dependent on physical capacity, but also on the strength of the chemical interaction between the absorbate and the microcapsules. These interactions vary depending on the target materials used. This method is called the suspension method and most subsequent research is achieved using this method. Wetting of particles and filling of particles has been studied intensively, particularly in soils^{86,87}, hollow particles^{88,89} and capillaries^{90,91}, where contact angle and surface morphology are important variables.

5.1 The droplet method

The droplet method is the most universally used encapsulation technique for exine microcapsules because, theoretically, it is possible to encapsulate most materials that can be easily converted to a molten form or a solution.^{22,43,44,55} The main procedure is described in Figure 5.1.

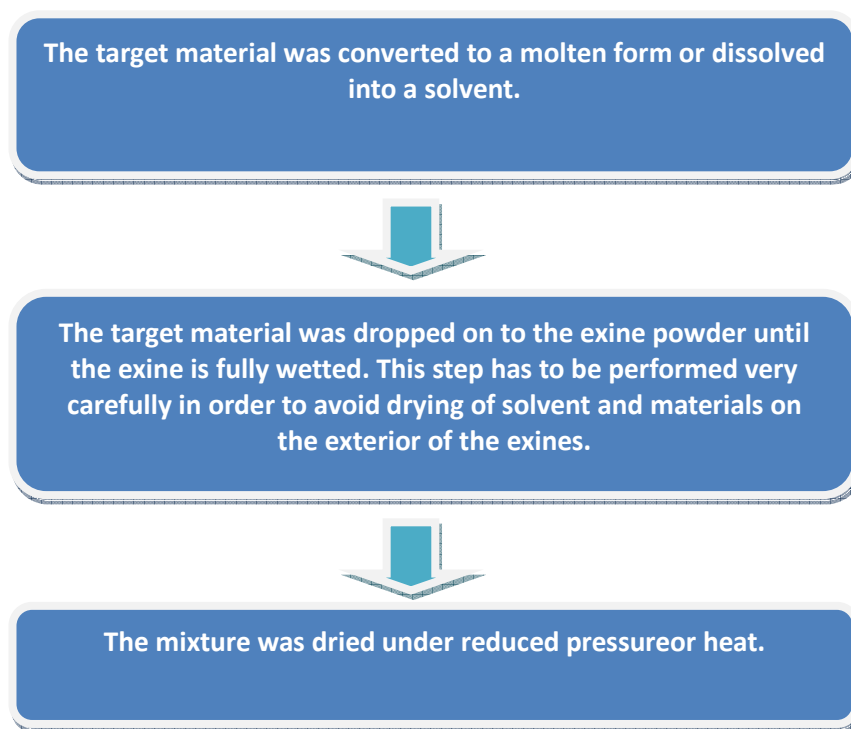


Figure5.1 Summary of droplet method

Depending on the target material, the droplet method can be carried out under a variety of encapsulation conditions to enhance the uptake of material by the microcapsules. The main variables for material encapsulation include heat, pressure (high or low pressure can both be helpful to absorption) and solvent. This method usually does not involve a washing process, as it has been found to have a negative influence on the result of encapsulation by virtue of removal of material from outside and inside the microcapsules.

The major disadvantage of this method is that some of target material remains on the outer surface of EICs, resulting in a contaminated final product. During encapsulation by the droplet method, it is unlikely that the microcapsules passively absorb all of the target material by capillary action alone. As an example, the target material may be deposited on the outer surface of EICs if the solvent evaporates before absorption by the EICs. In this case, the addition of extra solvent after the initial solvent has evaporated can increase the uptake and reduce the amount of non-encapsulated material. However, using this method the target material is not evenly encapsulated across all EICs; the EICs in the top layer absorb more target material than those in lower layers.

The droplet method is a simple procedure and encapsulation is achieved rapidly. This method was selected to carry out initial screening of materials to determine which materials were encapsulated with the greatest ease.

5.2 Suspension method

Most encapsulation experiments in this project were carried out using the suspension method. EICs were suspended in a solution of a target absorbate with additional stirring and the procedure used is summarized in Figure 5.2. The volume ratio between EICs and target material was in an excess of 1:7 during encapsulation. It has been found that when the volume ratio is low the EICs become damaged via mechanical stirring.⁹² This is the main reason such a high volume ratio is used in this work. The filling process is aided by the addition of solvents such as ethanol and water because they are easily able to access the internal part of the EIC. The filling process is also aided by increasing the temperature.⁹³

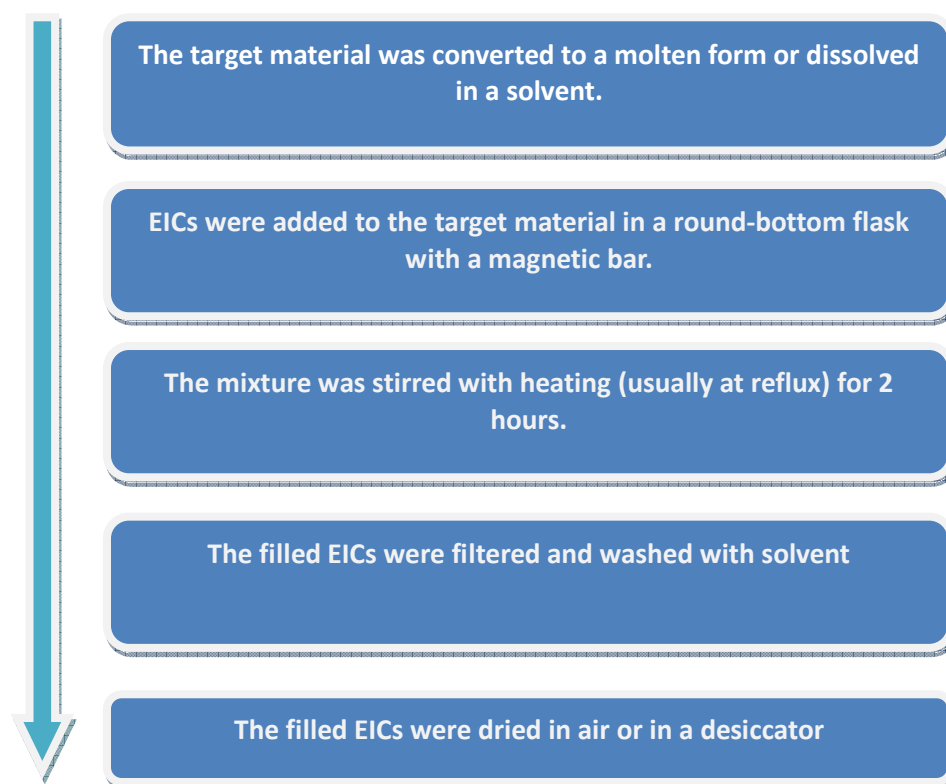


Figure5.2 Summary of the suspension method

The suspension method ensures that all of the microcapsules are equally exposed to the material to be encapsulated and as a result there is a strong tendency for filling to be

more consistent and uniform than the droplet method. Another advantage is that this method can be easily performed on a large scale. Using the suspension method enables a large excess of the target absorbate to be used ensuring that the potential to fill each EIC to saturation is high. Each method of filling largely depends on the physico-chemical interactions (e.g ionic interaction and Van der Waal force) between the target absorbate and the EICs. Once filled, the target material is expected to be bound tightly to the microcapsules.

One of the limitations of the suspension method is that materials that do not have strong interactions with the EICs do not fill to a high or saturation concentration. Additionally, these materials are easily removed during washing processes, which leads to a low concentration of absorbate in the isolated EICs.

5.3 Effect of concentration of the target material in suspension encapsulation

The advantage of using a solution of the material to be encapsulated over using it neat is that the solvent is able to penetrate the exine shell to a greater extent than the individual material. It has also been found that there is a strong concentration dependency on the amount of material that is isolated in the EICs.

Rhodamine B (RB) was used to investigate this hypothesis using a range of concentrations of RB in water. RB was used because it is inexpensive and easily fills into EICs. The concentrations of the aqueous RB solutions used were 0.001 (C0.001), 0.01(C0.01), 0.1(C0.1), 0.5 (C0.5), and 2 (C2) (all values in g L⁻¹).The encapsulation was allowed to proceed for two hours because EICs are sometimes damaged if this time is exceeded. However, it is noted that the maximum filling potential may not necessarily be achieved even after two hours. The procedure of sample preparation is summarized in Figure 5.3.

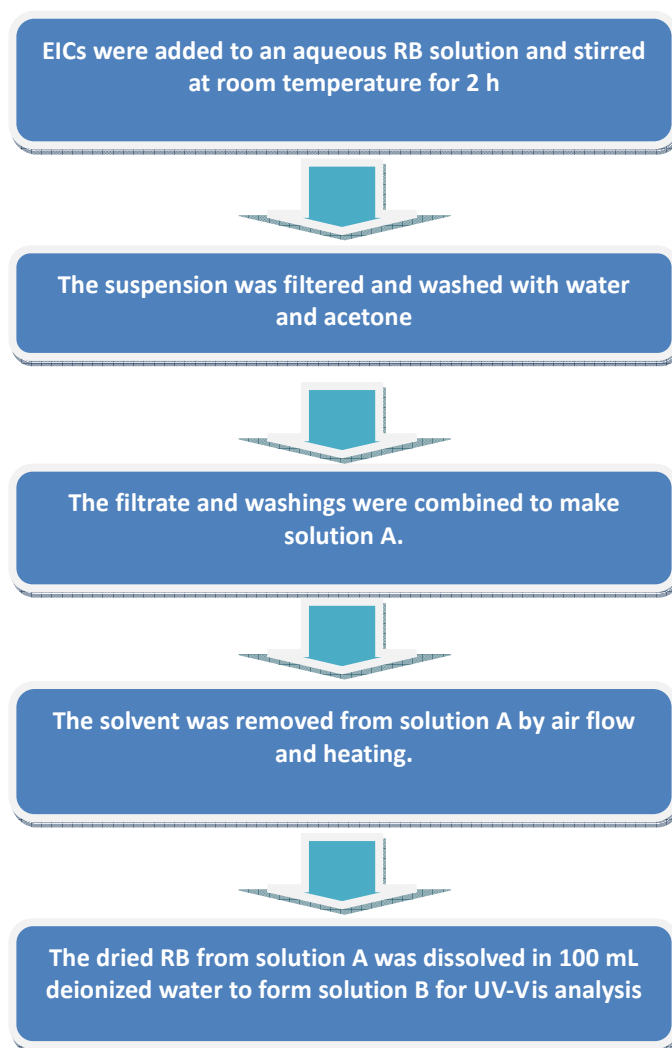


Figure 5.3 Summary of UV-Vis sample preparation for measurement of non-encapsulated RB from a RB encapsulation experiment.

In these experiments the amount of RB encapsulated by the EICs was determined by measuring the amount of non-encapsulated RB left in solution after isolation of the filled EICs. This process is summarized by equation 1.

Equation 1: $RB_{\text{encapsulated}} = RB_{\text{initial}} - (RB_{\text{filtrate}} + RB_{\text{wash}})$ where

- $RB_{\text{encapsulated}}$: the amount of RB encapsulated by EICs
- RB_{initial} : the amount of RB in initial RB solution before encapsulation
- RB_{filtrate} : the amount of RB remaining in solution after encapsulation
- RB_{wash} : the amount of RB washed from the filled EICs

UV-Vis spectroscopy was used to determine the amount of residual RB in the filtrate and the washings. Reference solutions were prepared in order to provide accurate concentration and absorbance determination by UV-Vis spectrometry. Thus, this data was used to create a calibration graph so that absorbance could be used to determine the quantity of RB remaining in solution after the spores had been filled. The concentrations prepared and their absorbances are given in Table 5.1. After filling the resultant solutions of C0.001, C0.01 and C0.1 (values in g L⁻¹) were measured and the absorbance value substituted into the equations of the trend line to give a concentration value, which is shown in Figure 5.4.

Table 5.1: Table of reference samples (Ref n) versus quantity, concentration and UV-vis absorbance of RB in water used as calibration data for the encapsulation experiments.

Sample Name	RB contained in the solution / mg	Concentration of RB solution / mg ml⁻¹	UV-Vis Absorbance
Ref 1	0.005215	5.22 x 10 ⁻⁵ ± 1.01 x 10 ⁻⁵	0.009
Ref 2	0.006258	6.26 x 10 ⁻⁵ ± 1.01 x 10 ⁻⁵	0.0125
Ref 3	0.007301	7.30 x 10 ⁻⁵ ± 1.01 x 10 ⁻⁵	0.013
Ref 4	0.008344	8.34 x 10 ⁻⁵ ± 1.02 x 10 ⁻⁵	0.016
Ref 5	0.009387	9.39 x 10 ⁻⁵ ± 1.02 x 10 ⁻⁵	0.02
Ref 6	0.286	0.00286 ± 1.57 x 10 ⁻⁵	0.465
Ref 7	0.5215	0.005215 ± 2.04 x 10 ⁻⁵	1.171
Ref 9	0.6258	0.006258 ± 2.25 x 10 ⁻⁵	1.355
Ref 10	0.7301	0.007301 ± 2.46 x 10 ⁻⁵	1.644
Ref 11	0.8344	0.008344 ± 2.67 x 10 ⁻⁵	1.833
Ref 12	0.9387	0.009387 ± 2.88 x 10 ⁻⁵	2.084
Ref 13	1.043	0.01043 ± 3.09 x 10 ⁻⁵	2.284

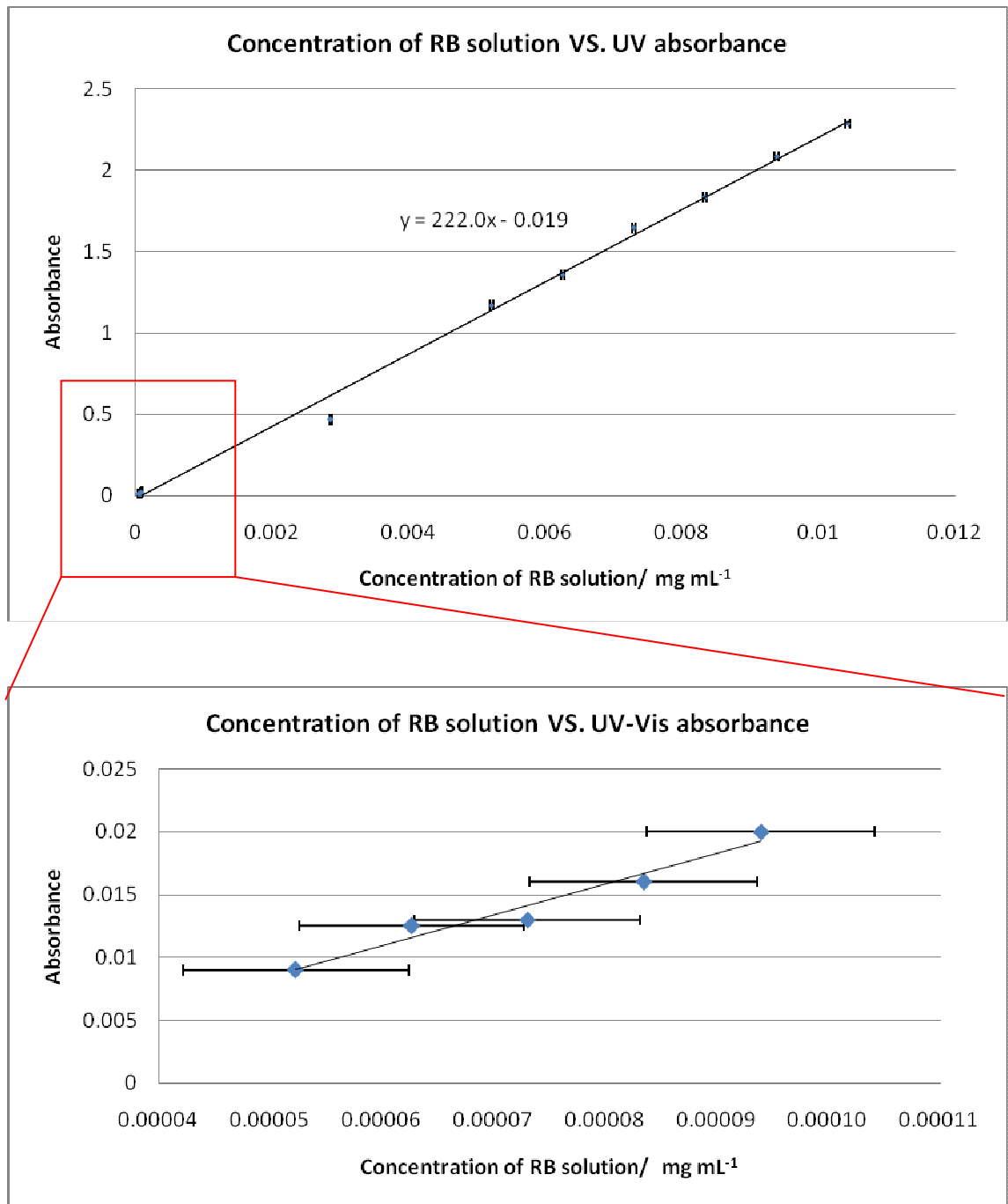


Figure 5.4 Calibration curve showing absorbance against concentration for RB in water.

Equation 2: $(RB_{\text{filtrate}} + RB_{\text{wash}}) = c_{\text{solution B}} \times 100$ where

- RB_{filtrate} the amount of RB remaining in solution after encapsulation
- RB_{wash} the amount of RB washed from the filled EICs
- $c_{\text{solution B}}$ Concentration of solution B

Table 5.2 RB left in the solution B.

Sample Name	RB contained in the solution B / mg	Concentration of solution B / mgml⁻¹	UV-Vis Absorbance
C0.001	7.7×10^{-4} $\pm 1.61 \times 10^{-4}$	1.54×10^{-4} $\pm 3.09 \times 10^{-5}$	0.015
C0.01	0.0402 \pm 0.0032	4.02×10^{-4} $\pm 3.09 \times 10^{-5}$	0.07
C0.1	0.3091 \pm 0.0037	0.0031 $\pm 3.09 \times 10^{-5}$	0.667

The amount of RB encapsulated per milligram of EICs was calculated using equation 3:

$$\text{RPE} = \text{RB}_{\text{encapsulated}} / \text{EIC}_{\text{Sused}}$$

RPE	RB per mg EICs
$\text{RB}_{\text{encapsulated}}$	Amount of RB encapsulated into EICs
$\text{EIC}_{\text{Sused}}$	Amount of EICs used in encapsulation

The results shown in Table 5.3 and Figure 5.5 indicate that the amount of RB absorbed by the BEICs increased as the concentration of the RB solution was increased from 0.001 to 2 g L⁻¹. Interestingly, the amount of RB that was encapsulated by the BEICs was 40 % wt to wt irrespective of the concentration of the solution. This value suggests that there is a limiting factor that prevents more than this quantity of absorbate entering or residing in the spore.

Table 5.3 RB encapsulated by EICs (mg mg⁻¹) by different concentrations of aqueous RB solutions.

Concentration of initial RB solution/ g L⁻¹	0.001	0.01	0.1	0.5	2
RB contained in the initial solution/ mg	0.005 ±6.10x10 ⁻⁵	0.0504 ±0.0008	0.5043 ±0.0051	2.5 ±0.001	10.26 ±0.001
RB remaining in filtrate and washings/mg	7.7 x 10 ⁻⁴ ±1.61x10 ⁻⁴	0.0402±0.0032	0.3091±0.0037	1.5501 ±0.0223	6.201 ±0.1078
RB encapsulated/mg	0.00423 ±2.22x10 ⁻⁴	0.0102 ±3.96x10 ⁻³	0.1952 ±8.79x10 ⁻³	0.955 ±0.0233	4.059 ±0.1088
Percentage of RB encapsulated	84.60%	20.24%	38.71%	38.2%	39.56%
EICs used/ mg	50.40±0.001	50.04 ±0.001	50.21 ±0.001	50.12 ±0.001	50.43 ±0.001
mg RB/ mg EIC	8.48 x 10 ⁻⁵ ±4.41x10 ⁻⁶	2.04 x 10 ⁻⁴ ±7.92x10 ⁻⁵	3.89 x 10 ⁻³ ±1.75x10 ⁻⁴	0.0191 ±4.65x10 ⁻⁴	0.0809 ±2.16x10 ⁻³
RB filled EICs/mg	40.72 ±0.001	37.95 ±0.001	39.25 ±0.001	37.65 ±0.001	38.15 ±0.001

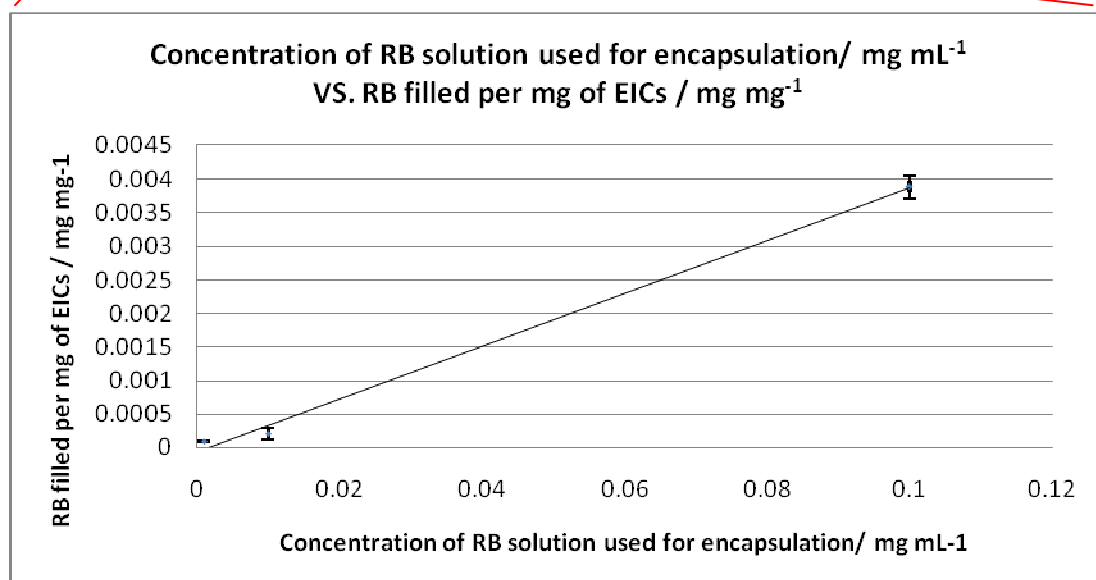
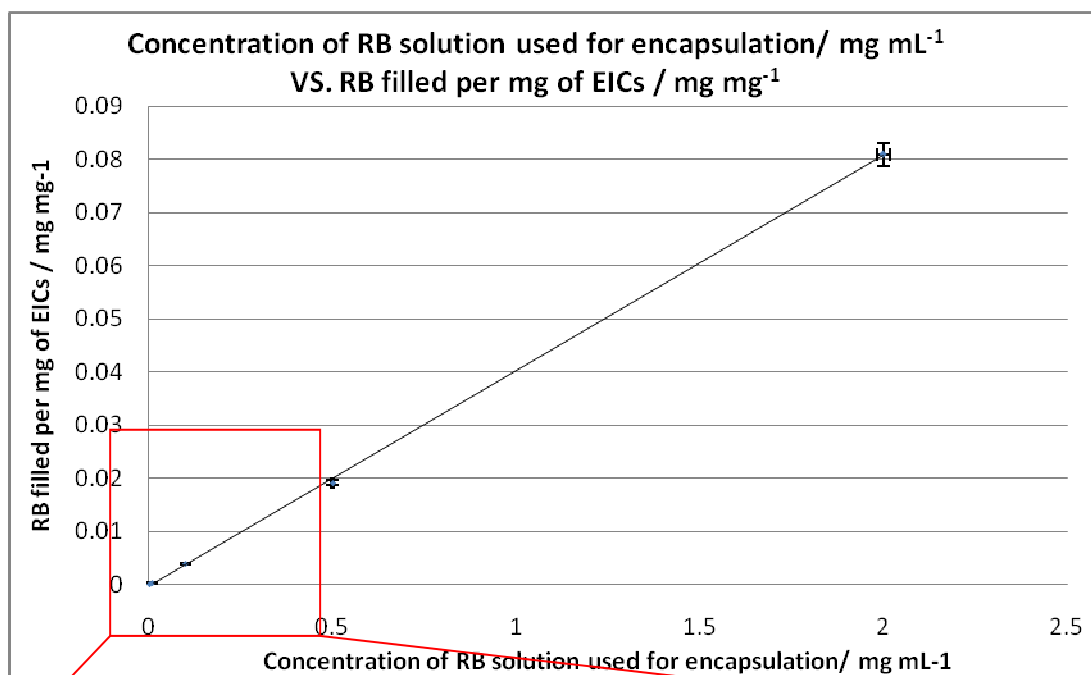


Figure 5.5 Amount of RB encapsulated versus the concentration of the RB solution used.

5.4 Effect of solvents on encapsulation

The maximum concentration of a target absorbate that can be achieved depends on the solubility of that material in a given solvent. Therefore, the choice of solvent is important in the process of encapsulation. However, the effects of solvent on the encapsulation process is not limited to the solubility of the encapsulant, or the concentration that can be achieved, but also to the chemical interactions between the solvent and the BEICs need to be considered. These variables make solvent selection complicated.

The effects of the chemical interactions between the solvent and EIC are mainly reflected by its influence on the chemical interactions between the absorbate and the EICs. For example, some solvents can wash out more encapsulated material from EICs than others. This could be for two reasons; (i) the solvent possesses a strong affinity for the absorbate and/or the solvent possesses a strong affinity for the EICs. The natures of the chemical interactions involved in BEIC encapsulations are demonstrated in a series of dye capture and release experiments, which are discussed in detail in Chapter 6.

It has been noted previously that the shapes of EICs can be affected by the type of solvent employed; this in turn may influence the amount of material that can be encapsulated. This observation was demonstrated by the suspension of EICs in a variety of solvents. The suspensions were analysed using optical microscopy after suspension of the EICs in the solvent on a microscope slide for 1 minute. The results are shown in Table 5.4.

When suspended in water, the EICs appear to be round in shape with a large internal volume. This shows that EICs can take up a large amount of water. Therefore, the amount of absorbate encapsulated using water as a solvent is relatively high, as demonstrated in this work. Methanol is another solvent that does not cause significant flattening of EICs. However, alcohols are able to negatively affect the affinity between target materials and EICs, so it is not normally used for EIC encapsulation. Except for water and methanol, the EICs appeared flattened when suspended in all the other solvents that were tested. However, the shape of EICs in a solvent is only a crude indication of the inflated volume of the EIC that could be achieved and filled with the absorbate or solution of absorbate in the encapsulation process. The major factor influencing the amount of material encapsulated into EICs is the relative strengths of the competing chemical interactions between solvent, target material and the EICs. For example, EICs have a similar appearance in ethanol and acetone, but these two solvents perform totally differently in the RB capture and release experiments as shown in Chapter 6. Therefore, it was concluded that the shape of EICs does not particularly affect the result of encapsulation using the suspension method.

Table 5.4-1 Appearance of EICs of *Lycopodium clavatum* in different solvents, when view from the top and side (x400)

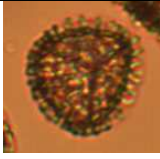
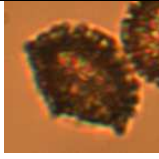
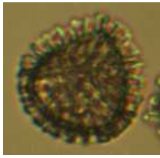
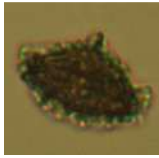
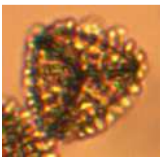
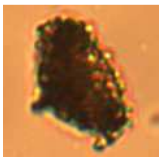
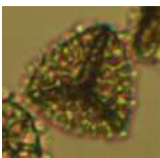
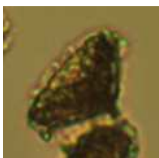
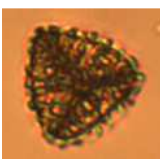
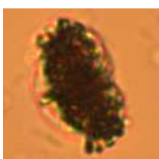
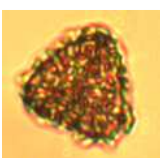

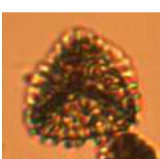
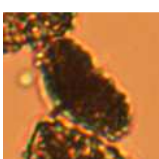
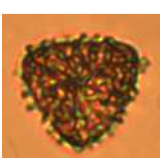

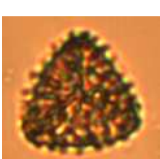

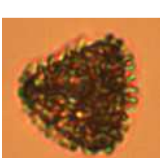
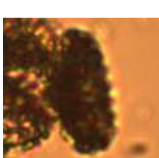
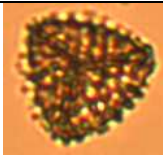


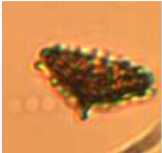
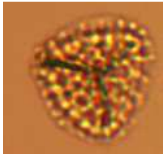

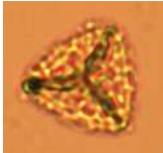
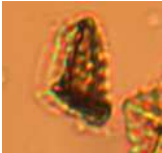
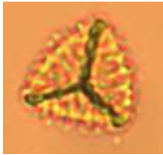
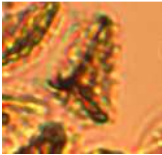


Solvent	Top View	Side View
Water		
Methanol		
Ethanol		
Ethandiol		
2-propanol		
Acetone		
Ethyl acetate		
Hexane		
THF		
Acetonitrile		

Table 5.4-2 Appearance of EICs of *Lycopodium clavatum* in different solvents, when view from the top and side (x400)

Solvent	Top View	Side View
DCM		
Chloroform		
Toluene		
Xylene		
Diethyl phthalate		
Sunflower oil		

In experiments using the suspension method, the EICs appear more transparent in some solvents than in others. For example, the EICs appear more transparent in solvents that have refractive indices of between 1.445 to 1.502, i.e., chloroform, 1.445⁹⁴, diethyl phthalate, 1.502⁹⁵, toluene, 1.496⁹⁶, and sunflower oil, 1.473⁹⁷. However, EICs are much less transparent in the solvents that have lower refractive indices, i.e., water, 1.340⁹⁸, methanol, 1.329⁹⁹, acetone, 1.359¹⁰⁰, and acetonitrile, 1.344¹⁰¹. Figure 5.6 shows a photomicrograph of “polymer-filled” EICs in toluene, where the EICs that possess some polymeric absorbate are easily distinguished (dark) from the EICs that do not possess polymeric absorbate. This is because there is a significant difference between the refractive indices (RI) of the filled and unfilled EICs and their respective index matching to the toluene (RI at 20 °C: 1.496). The same polymer filled EICs were examined in a water suspension and this time it was difficult to determine which EICs

contained polymer and which did not due to the large refractive index difference between the EIC and water (RI of water at 20 °C: 1.34), as shown in Figure 5.7.

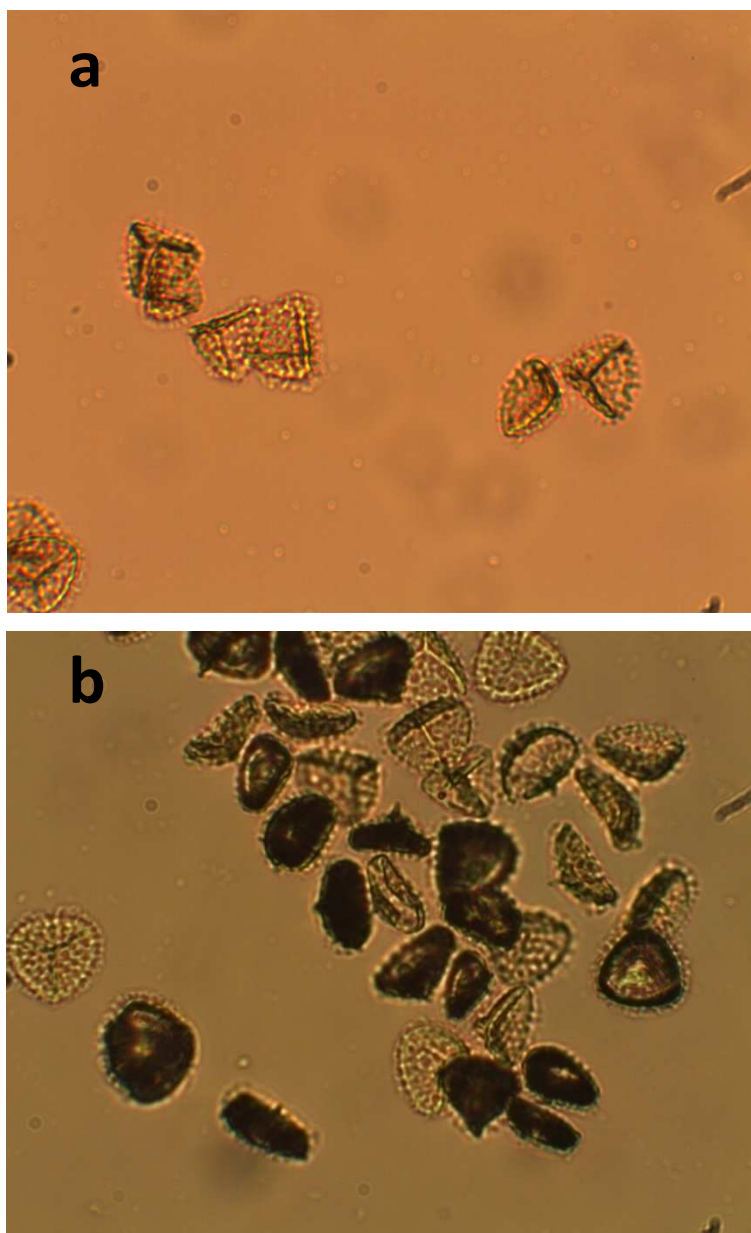


Figure 5.6 Photomicrographs of a) empty EICs in toluene and b) polymer absorbate encapsulated by EICs and suspended in toluene. (x400)

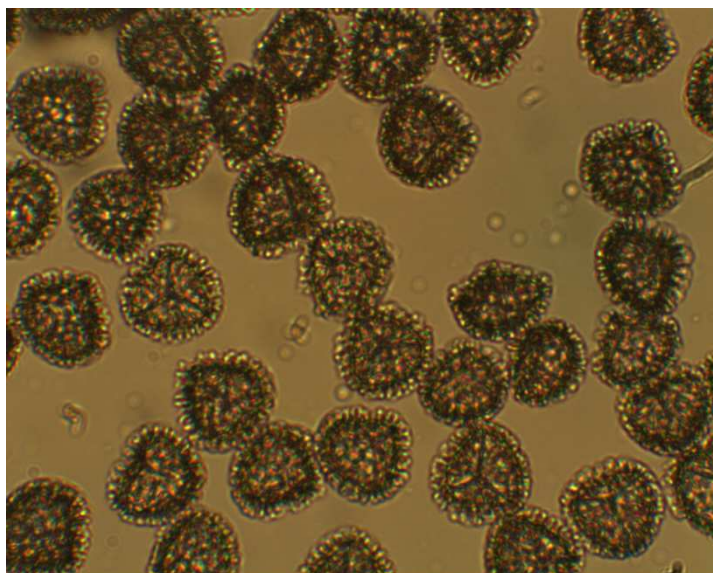


Figure 5.7 Polymeric absorbate encapsulated in EICs suspended in water.(x400)

5.5 Effect of temperature on encapsulation in suspension method

Temperature is another factor that can affect EIC encapsulation of a target absorbate. The solubility, and hence the concentration, of a target absorbate can be increased by heating the solution. This in turn may also enable a higher concentration of target material to be absorbed in the EICs.

An experiment was performed to demonstrate the effect of temperature on the encapsulation process by using a fixed concentration of a target absorbate. The experiments were carried out using aqueous solutions of RB at concentrations of 0.1 g L^{-1} . The amounts of RB encapsulated were calculated using the same approach discussed previously in section 5.2. The results of the experiment ($\text{RB } 0.1 \text{ g L}^{-1}$) with equipment errors are shown in Table 5.5 and graphically in Figure 5.8. The graph in Figure 5.8 shows that there is a general trend for greater absorption with increasing in temperature. However, it should be noted that there was consistently more material encapsulated at $45 \text{ }^\circ\text{C}$. On face value this trend indicates that there is a temperature dependence associated with the encapsulation process, although there may be additional factors that contribute to this which give rise to the unusually high uptake of absorbate at $45 \text{ }^\circ\text{C}$.

Table 5.5 Results of the experiments for temperature effect in RB encapsulation with 0.1 g L⁻¹ RB solution with water (Errors bar were come from equipment errors)

Temperature/ °C	25	45	60	80	100
Volume of solution B/ mL	50±0.12	50±0.12	50±0.12	50±0.12	50±0.12
UV absorbance	1.304	1.046	1.112	1.072	0.994
Concentration of solution B/ mg mL⁻¹	0.006 ±3.09 x 10 ⁻⁵	0.0048 ±3.09 x 10 ⁻⁵	0.0051 ±3.09x 10 ⁻⁵	0.0049 ±3.09 x 10 ⁻⁵	0.0046 ±3.09 x 10 ⁻⁵
RB contained in solution B/ mg	0.3000 ±2.27 x 10 ⁻³	0.2400 ±2.12 x 10 ⁻³	0.2550 ±2.16 x 10 ⁻³	0.2450 ±2.13 x 10 ⁻³	0.2282 ±2.10 x 10 ⁻³
RB used in encapsulation/ mg	0.517 ±2.12 x 10 ⁻⁴	0.517 ±2.12 x 10 ⁻⁴	0.517 ±2.12 x 10 ⁻⁴	0.517 ±2.12 x 10 ⁻⁴	0.517 ±2.12 x 10 ⁻⁴
RB encapsulated /mg	0.2170 ±2.05 x 10 ⁻³	0.2770 ±1.91 x 10 ⁻³	0.2620 ±1.95 x 10 ⁻³	0.2720 ±1.92 x 10 ⁻³	0.2870 ±1.89 x 10 ⁻³
EICs used/ mg	50.11 ±0.001	50.24 ±0.001	50.28 ±0.001	50.15 ±0.001	50.13 ±0.001
RB encapsulated per mg of EICs / mg mg⁻¹	0.0043 ±4.11 x 10 ⁻⁵	0.0055 ±3.81 x 10 ⁻⁵	0.0052 ±3.88 x 10 ⁻⁵	0.0054 ±3.84 x 10 ⁻⁵	0.0058 ±3.77 x 10 ⁻⁵

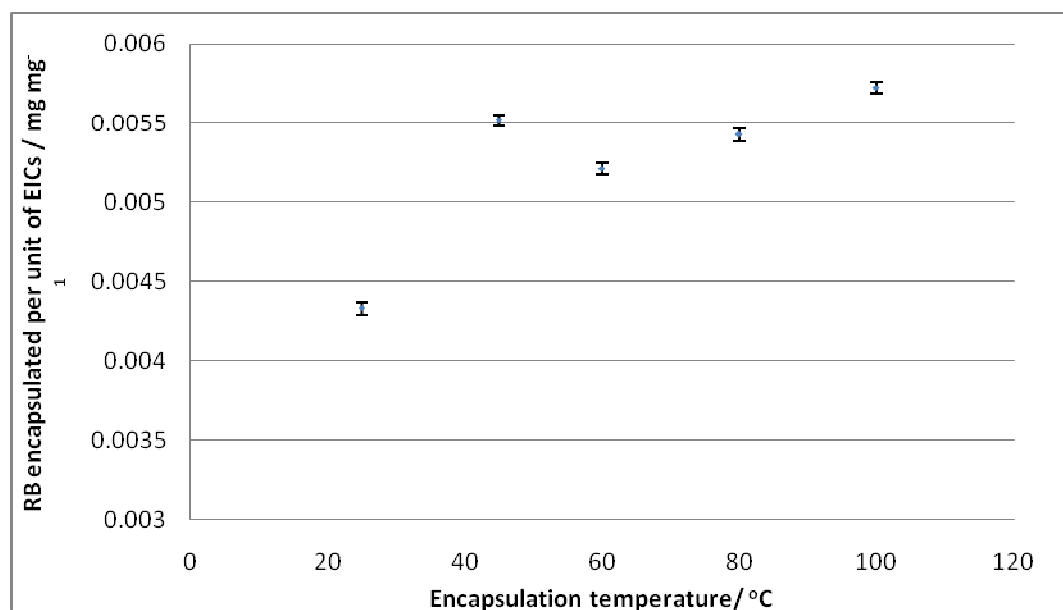


Figure 5.8 Amount of RB encapsulated per mg of EIC as a function of temperature.

5.6 Conclusion

The most commonly published method for encapsulation processes involving exine shells is the droplet method. This method can be aided with varying of conditions, such as low or high pressures, the temperature and concentration of the solution for encapsulation. Results of experiments, however, show that the droplet method had many disadvantages, such as uneven distribution of the adsorbates, and low purity of the materials. As a consequence, the major encapsulation method used in the subsequent research was the suspension method. This method achieves a better distribution of adsorbates, higher purities, and a process that could be adapted for large-scale production. However, the suspension method is largely dependent on the ionic properties of sporopollenin, so it may not be efficient if the chemical properties of adsorbate are not compatible.

A few common conditions that may influence results from the suspension method were listed and investigated. They included the concentration of the encapsulation solution, the solvent used in the encapsulation process, and the temperature of encapsulation. Increasing in concentration and temperature both cause higher uptake of the adsorbate. Furthermore, in some cases, the encapsulation solvent makes it easier for the adsorbate to access the exine shell and therefore to increase the uptake.

During the investigation of the effects of different solvents, it was discovered that the solvents that have a similar refractive index to that of the EICs increase the transparencies of the EICs, when viewed by microscopy, such that the interior appearance of the EICs can be seen with the application of a suitable solvent. These results should be of importance for further research.

5.7 Experimental

ET-1 Rhodamine B encapsulation

Bleached exine intine capsules (BEICs, **BE-1**, 50.40 mg) were added into a sample vial with an aqueous solution of rhodamine B (RB) (5 mL; 0.001 g L⁻¹). The sample vial was sealed and then placed in the dark. The BEICs and RB mixture was stirred at room temperature for 2 h, and the filled BEICs were isolated by filtration and then washed with water and acetone until no more RB appeared in the washings. The filtrate and washings were combined and retained for further UV-Vis analysis. The washed RB filled BEICs were dried under partial vacuum.

A similar procedure was used for each concentration (0.01, 0.1, 0.5, 2 and 10 g L⁻¹).

Table 5.6 Summary of **BE-1** used in aqueous RB solutions with different concentrations.

Concentration of aqueous RB solution(g L ⁻¹)	BE-1 used
0.001	50.40 mg
0.01	50.04 mg
0.1	50.11 mg
0.5	50.12 mg
2	50.43 mg

ET-2 Effect of temperature on rhodamine B encapsulation (0.1 g L⁻¹ rhodamine B aqueous solution)

BEICs (**BE-1**, 50 .49 g) were added to a sample vial with aqueous rhodamine B (RB) solution (5 mL, 0.1 g L⁻¹). The sample vial was sealed and placed in the dark. The mixture of BEICs and RB was stirred at 0 °C in an ice bath for 2 h. The filled BEICs were isolated by filtration and washed with water and acetone until no further RB appeared in the washings. The filtrate and washings were combined and retained for further UV-Vis analysis. The washed RB filled BEICs were dried under partial vacuum.

The procedure was repeated at different temperature using the following quantity of BEICs.

Table 5.7 Summary of **BE-1** used in the experiment to encapsulate RB with different temperatures.

Temperature	BE-1 used
25 °C	50.21 g
45 °C	50.39 g
60 °C	50.65 g
80 °C	50.61 g
100 °C	50.11 g

6. Dye encapsulation

One of the principal aims of this work is to produce coloured particles for use in display applications such as E-paper. All of the exine and intine capsules used in encapsulation experiments for this purpose have been bleached (BEICs, Figure 6.1) to ensure that they are colourless and do not alter the colour of the dye. The colours of dyes include the three primary colours (yellow, red and blue) and a range of dyes of each colour was used for comparison purposes. The structures of the dyes differ significantly which results in differences in their affinity to the BEICs. The dyes were further subdivided into water-insoluble or water-soluble dyes (Figure 6.2 and Figure 6.3). The water-insoluble dyes include TBBA (yellow), CT67 (blue), CT75 (purple), CT51 (orange) and Indigo (indigo); the water-soluble dyes include rhodamine B (RB), safranin O (SO), methylene blue (MB), naphthol blue black (NBB) and thiazole Yellow G (TYG).

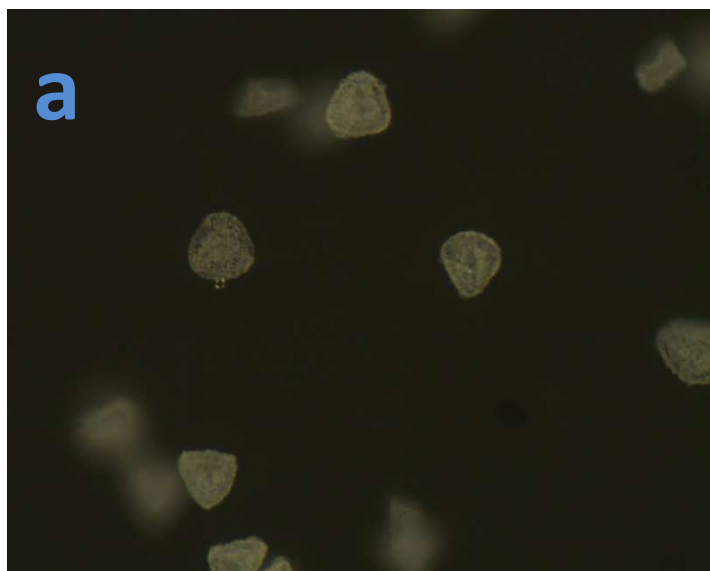
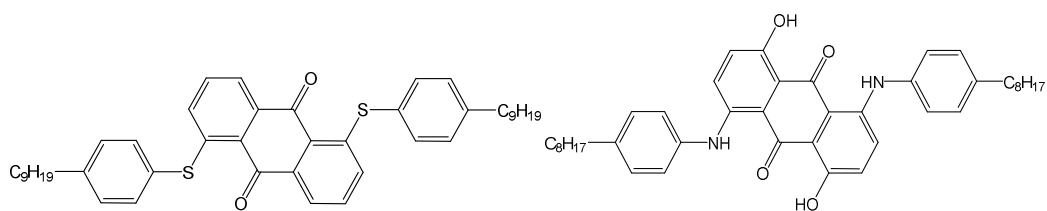


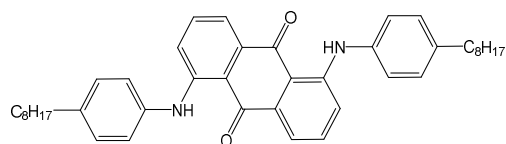
Figure 6.1 Photomicrographs of BEICs in a) crossed polars reflective mode and b) crossed polars transmissive mode (x200).

Water-insoluble dyes

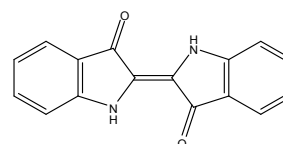


CT51

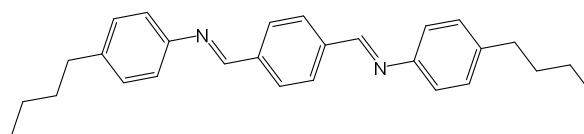
CT67



CT75



Indigo



TBBA

Figure 6.2 Structures of the water-insoluble dyes used.

Water-soluble dyes

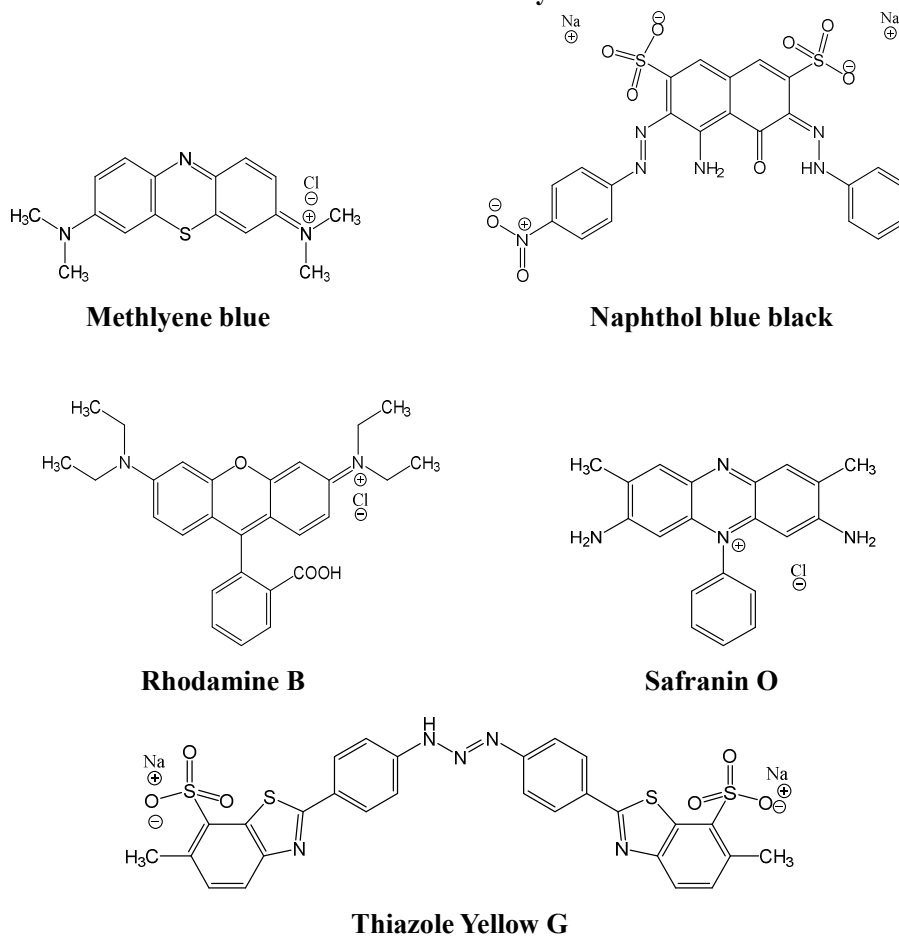


Figure 6.3 Structures of the water-soluble dyes used.

The production of coloured BEICs was divided into two steps. Firstly, the dyes were encapsulated into BEICs using the droplet method (step 1). This method was used to screen each of the dyes to ascertain which ones exhibited the most intense and stable coloured particles for the target application. A few drops of ethanol were added to the BEIC pads after the addition of dye solutions to facilitate dye uptake.²² Once it was established which were the most suitable dyes, the selected dyes were encapsulated into BEICs using the suspension method to yield the highest quality particles for the application (step 2).

Each of the drop-filled BEICs were analyzed by light microscopy and assessed for the quality of filling and colour intensity. For ease of discussion, each colour group is discussed in turn. The yellow dyes included CT51 (water-insoluble, orange), TBBA (water-insoluble yellow) and TYG (water-soluble, yellow). Figure 6.4a shows the TBBA filled EICs under reflective mode with crossed polars and Figure 6.4b shows the

same BEICs using transmission microscopy. Interestingly, the particles visually did not appear dyed and microscopy reveals that there is no significant difference to the unfilled BEICs, see Figure 6.1a and b. The conclusion from this study is that TBBA is not a suitable candidate to produce yellow BEICs.

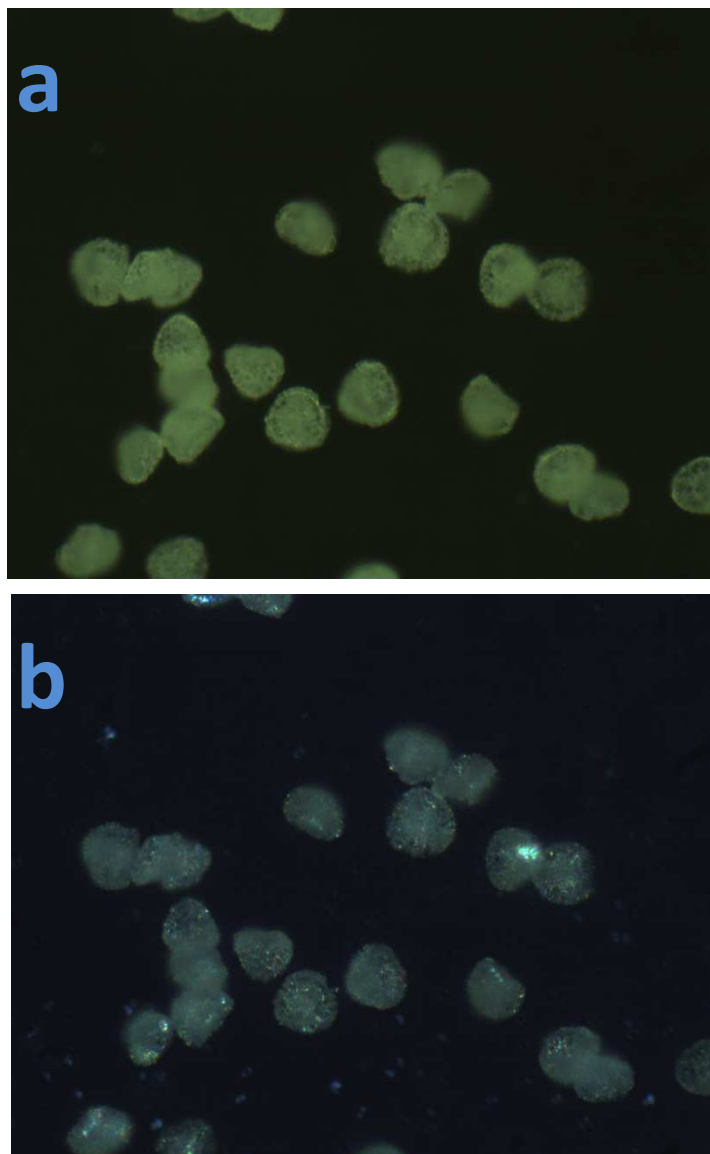


Figure 6.4 Photomicrographs of the TBBA filled BEICs viewed through a) crossed polars reflective mode and b) crossed polars transmissive mode. (x200)

The other water-insoluble dye, CT51 was drop filled into the BEICs. The studies revealed that a number of the particles had been dyed using this dye but the process gave an inhomogeneous mixture of dyed and unfilled particles, see Figure 6.5. For clarity, a dyed BEIC has been highlighted in Figure 6.5 with a red ring whereas an unfilled BEIC is highlighted with a yellow ring.

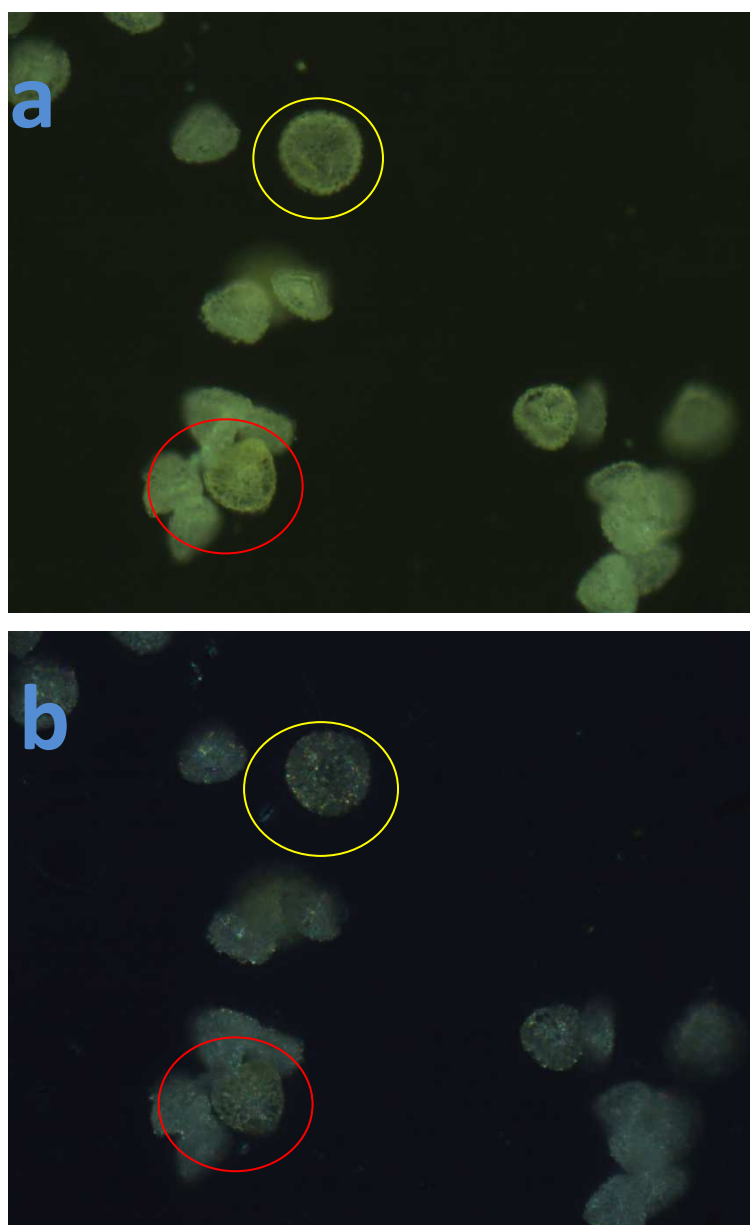


Figure 6.5 Photomicrographs of CT51 filled BEICs viewed through a) crossed polars reflective mode and b) crossed polars transmissive mode. (x200)

The BEICs filled with TYG were extremely well dyed and every particle had an intense yellow colouration. When the particles were viewed by optical microscopy (Figure 6.6) it was easy to see the intense colour of the dye using transmission light microscopy, Figure 6.6b. This dye was selected to be investigated using the suspension method.

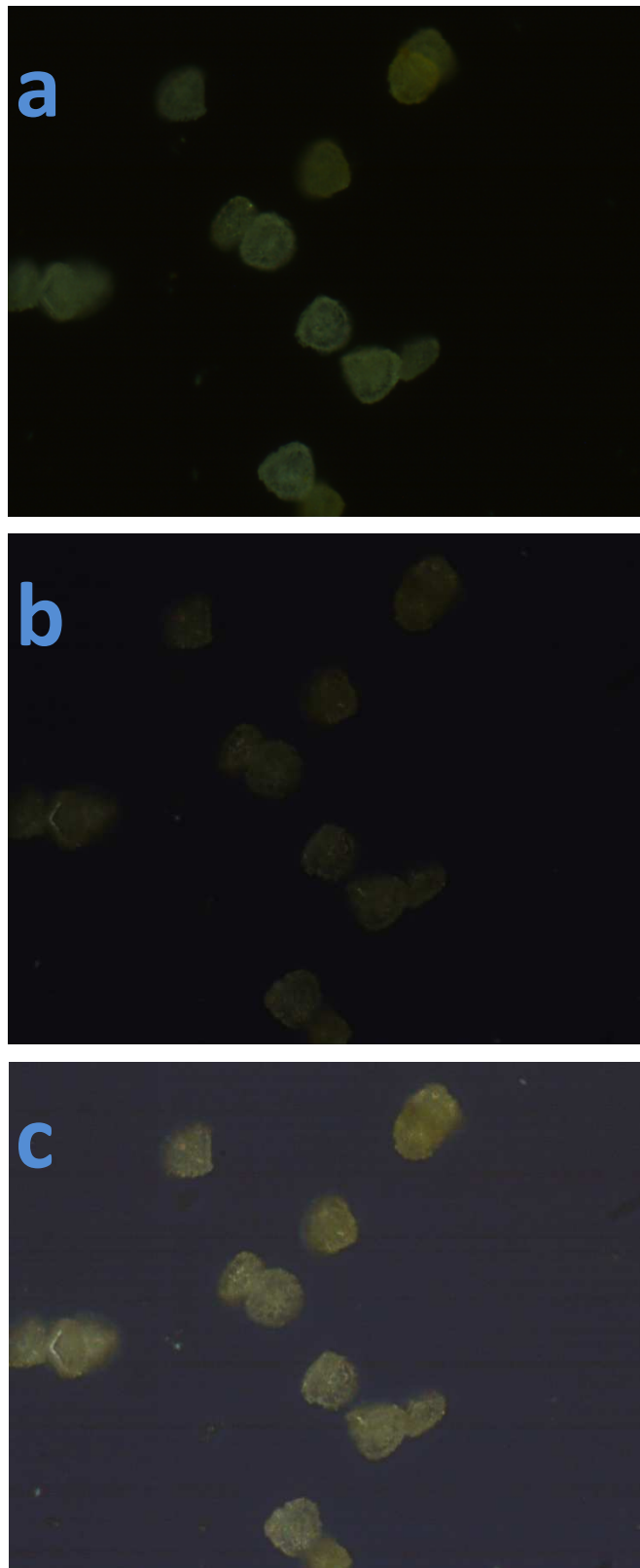


Figure 6.6 Photomicrographs of the TYG filled BEICs viewed through a) crossed polars reflective mode; b) crossed polars transmissive mode and c) computer enhanced brightness of the image of photomicrograph b. (x200)

The red dyes examined include CT75 (water-insoluble), RB (water-soluble) and SO

(water-soluble). The high contrast of the red dyes to the BEIC allowed for even subtle dyeing of the particle to be observed easily. CT75 is the only water-insoluble dye in this group and a similar result was obtained to the yellow dye CT51 whereby inhomogeneous filling was observed (see Figure 6.7).

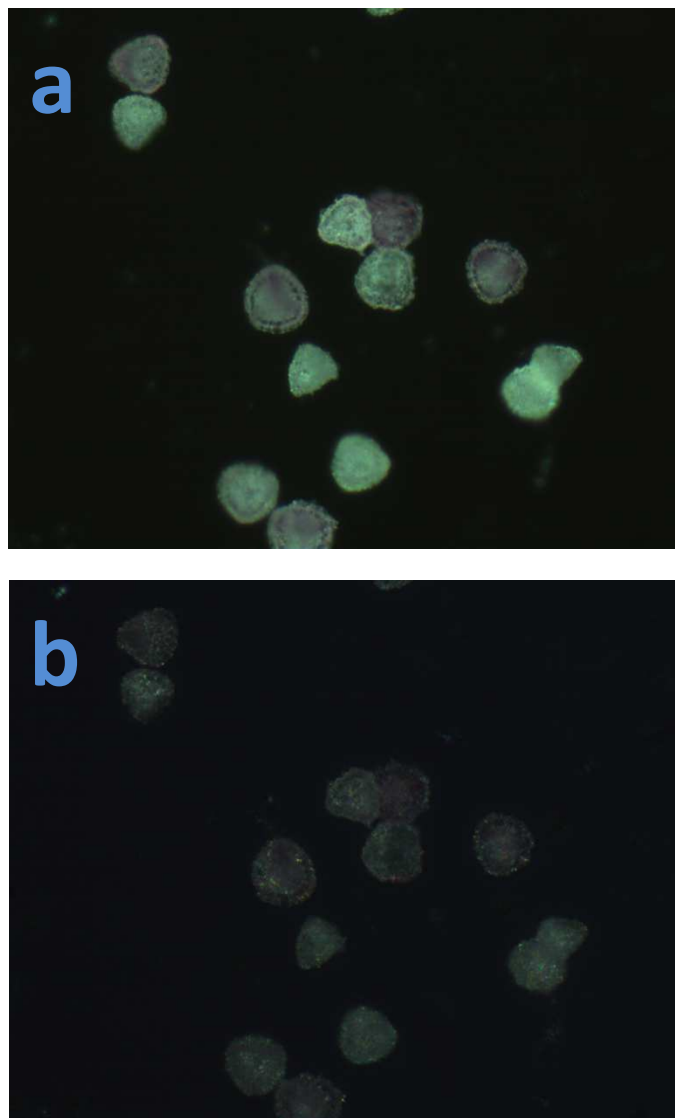


Figure 6.7 Photomicrographs of CT75 filled BEICs viewed through a) crossed polars reflective mode and b) crossed polars transmissive mode. (x200)

The other two dyes in this group, RB and SO, were both water-soluble dyes and resulted high colour intensity particles with a consistently high filling efficiency (Figure 6.8 and Figure 6.9). It was difficult to separate these two dyes from a visual inspection and the particles all had intense red appearances. It was interesting to note that due to the high affinity of these dyes to the BEICs very little dye was unused or washed off when the particles were washed with solvent.

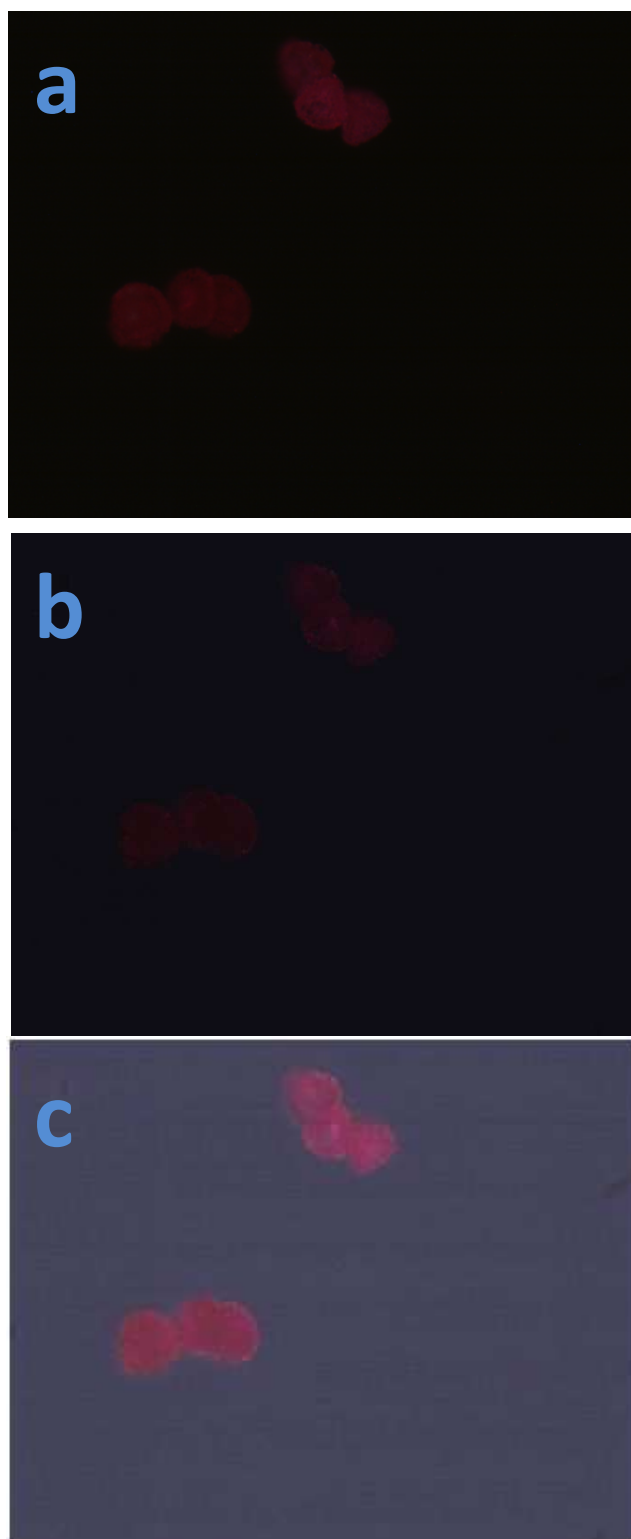


Figure 6.8 Photomicrographs of RB filled BEICs viewed through a) crossed polars reflective mode; b) crossed polars transmissive mode and c) computer enhanced brightness of the image of photomicrograph b. (x200)

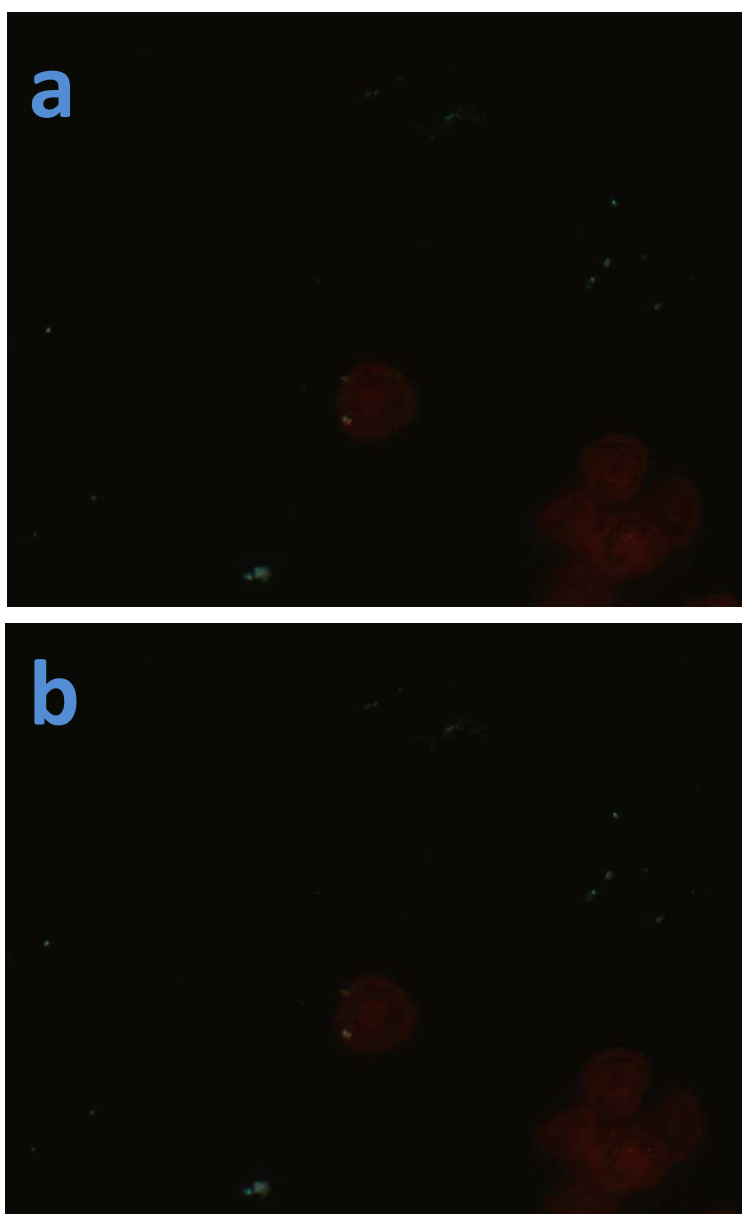


Figure 6.9 Photomicrographs of SO filled BEICs viewed through a) crossed polars reflective mode and b) crossed polars transmissive mode. (x200)

The final group of blue dyes examined included CT67 (water-insoluble), indigo (water-insoluble), MB (water-soluble) and NBB (water-soluble). CT67 did not fill the BEICs and the appearance of the particles after dye treatment, see Figure 6.10, was unaltered compared to the untreated spores shown in Figure 6.1.

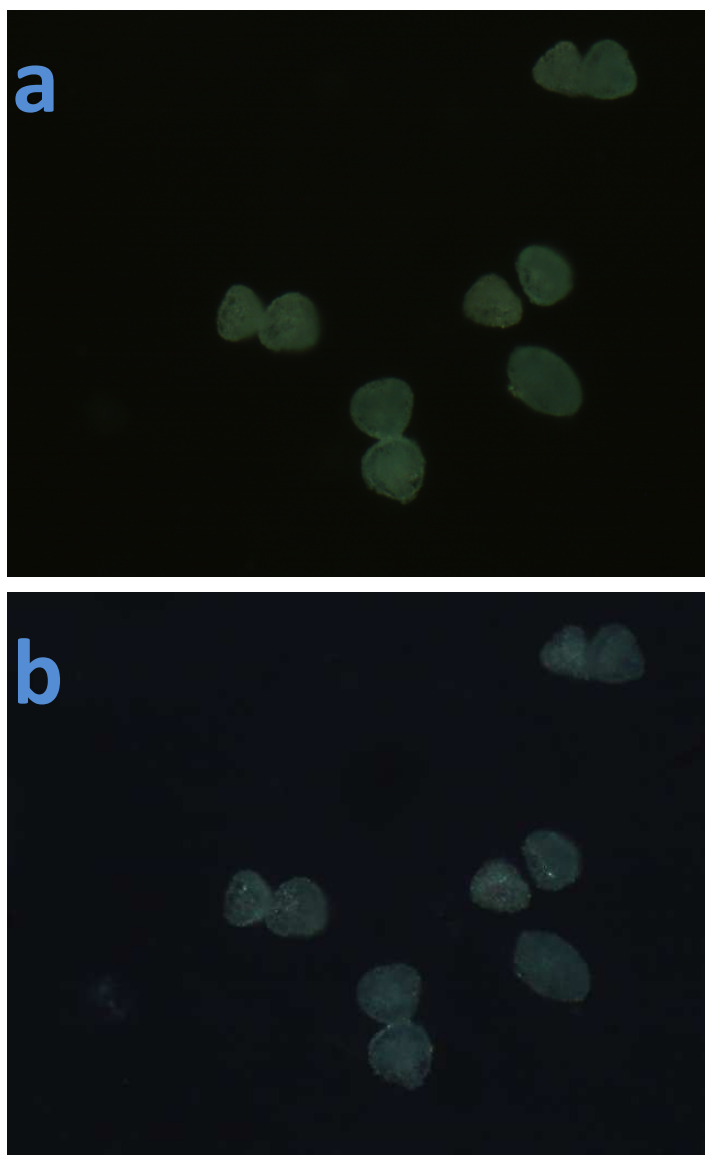


Figure 6.10 Photomicrographs of CT67 filled BEICs viewed through a) crossed polars reflective mode and b) crossed polars transmissive mode. (x200)

The indigo dye, which is also one of the water-insoluble dye appears to dye the BEICs to a far greater extent than any of the other water-insoluble dyes. The microscopy results are shown in Figure 6.11 and reveal that there is a strong concentration gradient in filling whereby some particles are more intensely coloured than others. This was most easily observed when the particles were viewed using reflective microscopy, Figure 6.11a.

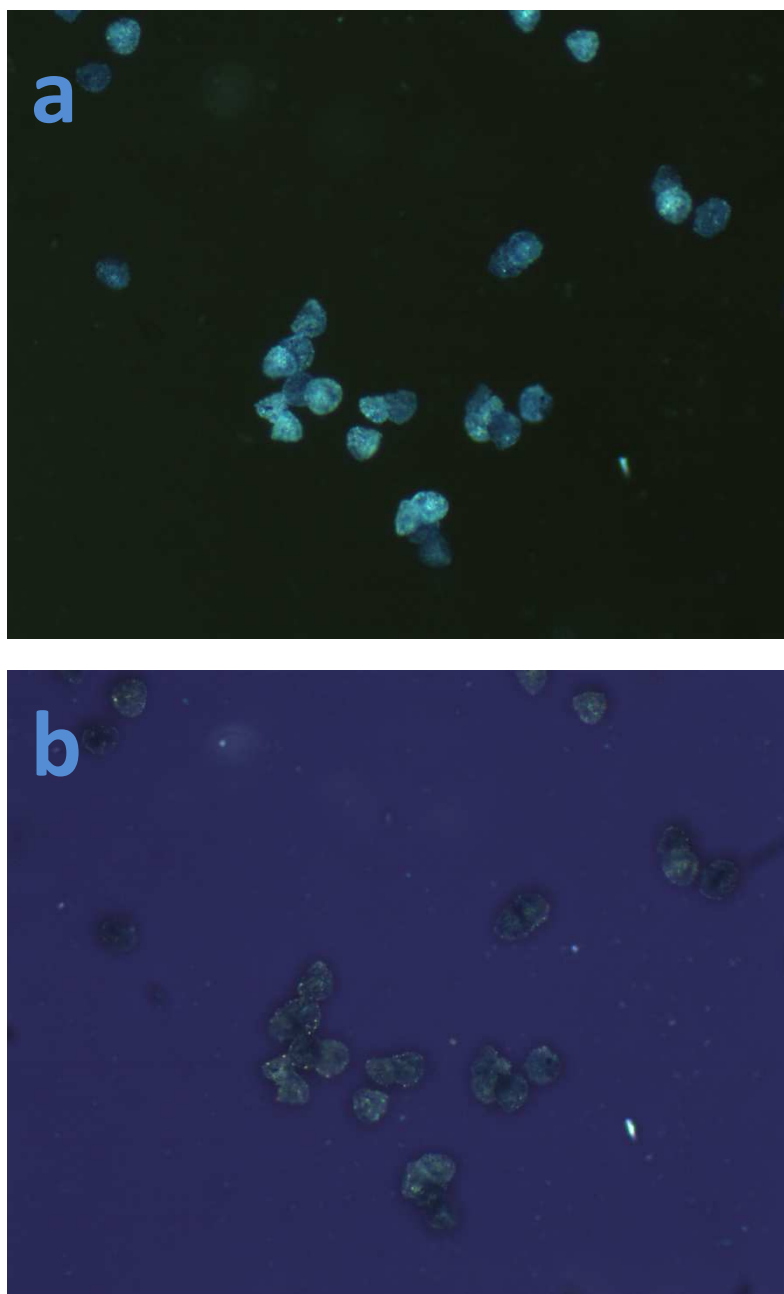


Figure 6.11 Photomicrographs of indigo filled BEICs viewed through a) crossed polars reflective mode and b) crossed polars transmissive mode. (x100)

The MB filled BEICs were similar to the indigo filled BEICs where a colour gradient was observed across a range of BEICs, (Figure 6.12). The colour gradient is derived from a concentration gradient of the dye in the BEICs. Where the concentration is low it is possible to see the particles by microscopy but when the concentration is high the particles are not easily observed and appear nearly black.

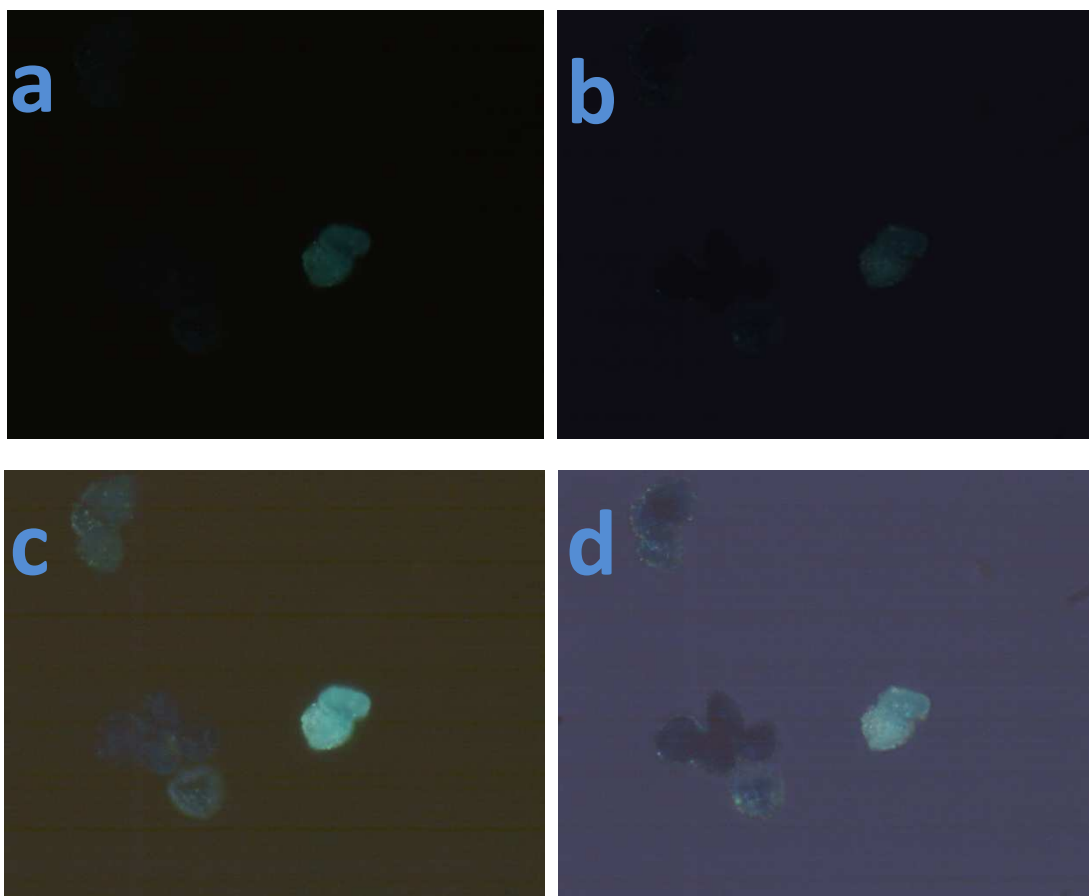


Figure 6.12 Photomicrographs of the MB filled BEICs viewed through a) crossed polars reflective mode; b) crossed polars transmissive mode; c) computer enhanced brightness of the image of photomicrograph a, and d) computer enhanced brightness of the image of photomicrograph b. (x200)

NBB homogeneously filled the particles but it was not clear that the encapsulated concentration of this dye in the BEICs was very high. Microscopy, see Figure 6.13, does not show an intense blue in the BEICs, rather the blue colouration was only slight.

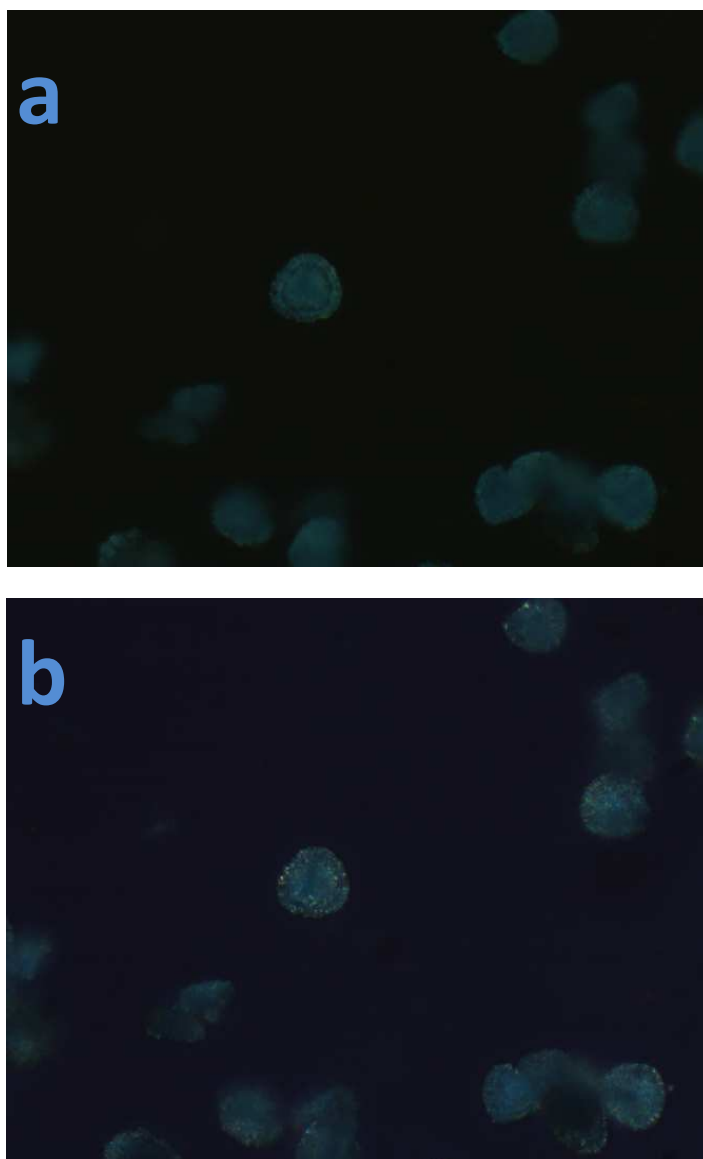


Figure 6.13 Photomicrographs of the NBB filled BEICs viewed through a) crossed polars reflective mode and b) crossed polars transmissive mode. (x200)

It was concluded from the BEIC studies that of the dyes examined, ionic water-soluble dyes more efficiently fill the particles than non-ionic water-insoluble dyes.

In order to produce yellow, red and blue particles *via* the suspension method the water-soluble dyes, TYG, RB and MB, were used. These encapsulations were carried with high concentration (RB: 40 mg.mL⁻¹; TYG: 13 mg.mL⁻¹ and MB: 24 mg.mL⁻¹) aqueous dye solutions at 90 °C to ensure that all BEICs were filled to saturation. Each of the dyes was successfully encapsulated into the BEICs and the visual appearances are presented in Figure 6.14.

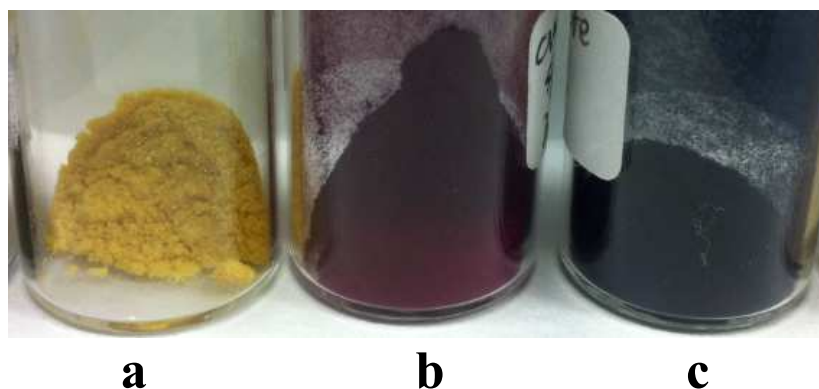


Figure 6.14 Visual appearance of the BEICs filled by a) TYG, b) RB and c) MB.

These coloured BEICs were also examined by microscopy to ensure that there was a homogeneous distribution of dye in the BEICs. Interestingly, the high concentration of dye in the BEICs meant that it was very difficult to observe the particles using transmission microscopy but they were visible using reflective mode. Images for each dye are shown in Figures 6.15-6.17 for TYG, RB and MB respectively.

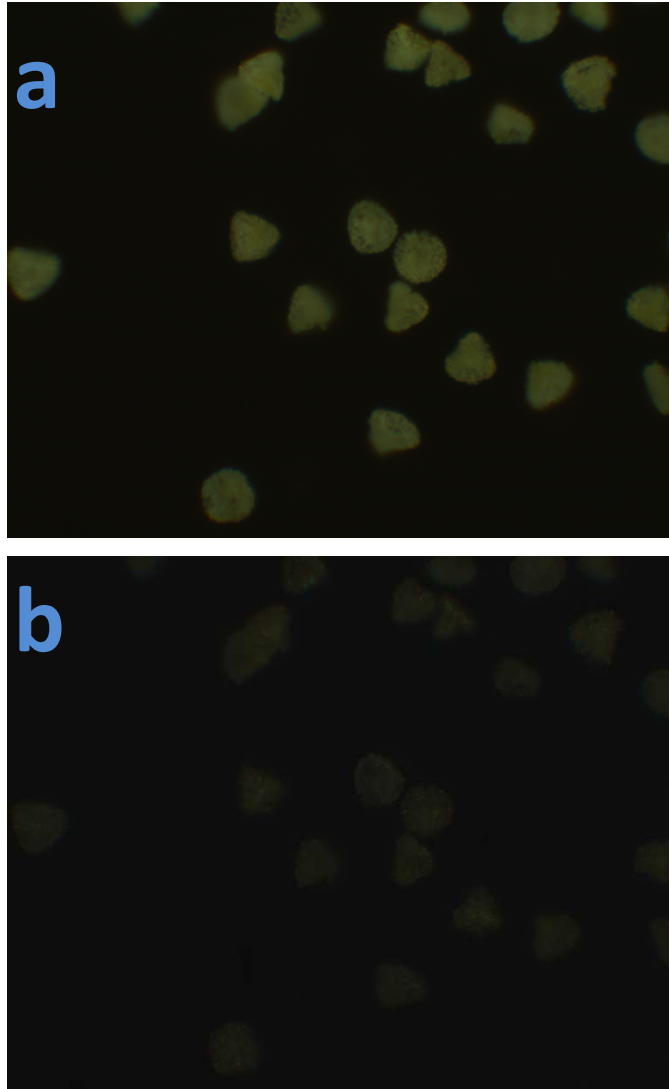


Figure 6.15 Photomicrographs of TYG filled BEICs (suspension method) viewed through a) crossed polars reflective mode and b) crossed polars transmissive mode. (x100)

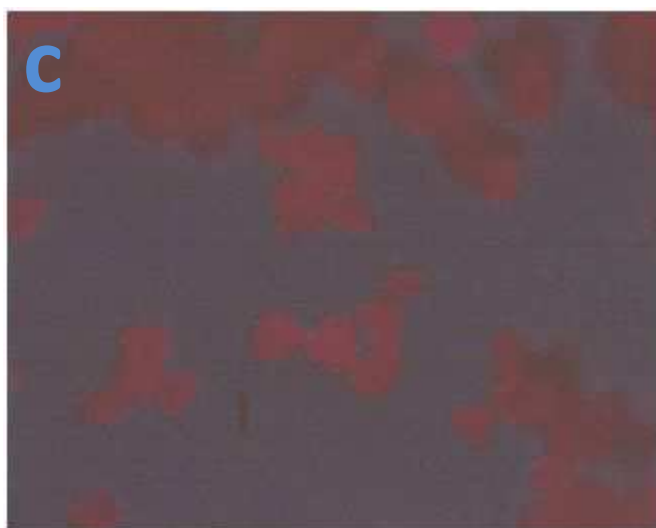
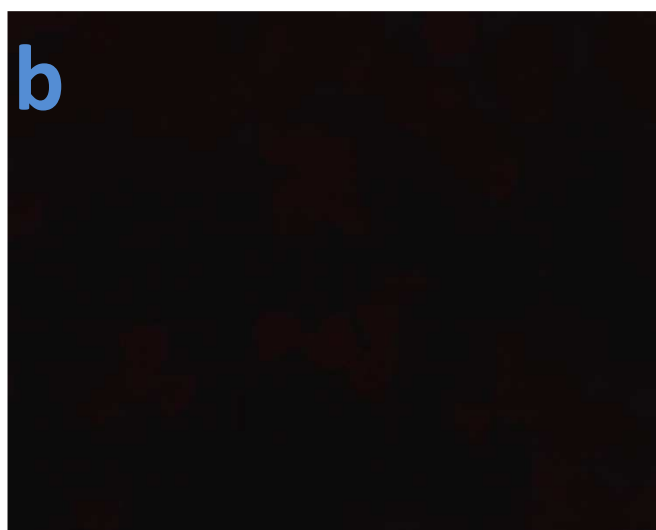
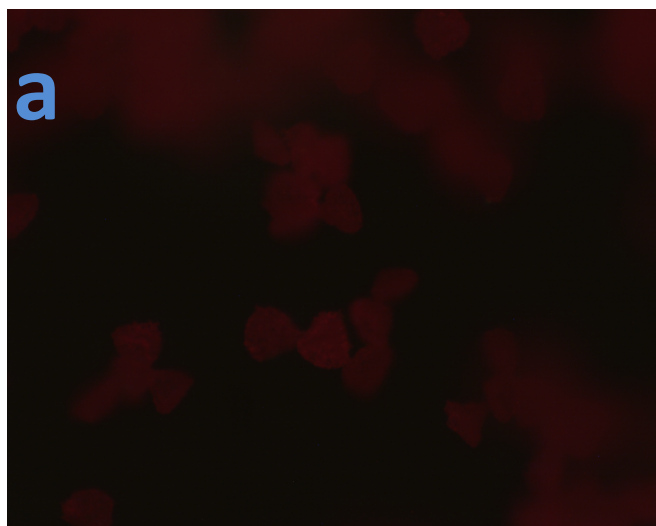


Figure 6.16 Photomicrographs of RB filled BEICs (suspension method) viewed through a) crossed polars reflective mode; b) crossed polars transmissive mode and computer enhanced brightness of the image of photomicrograph b. (x100)

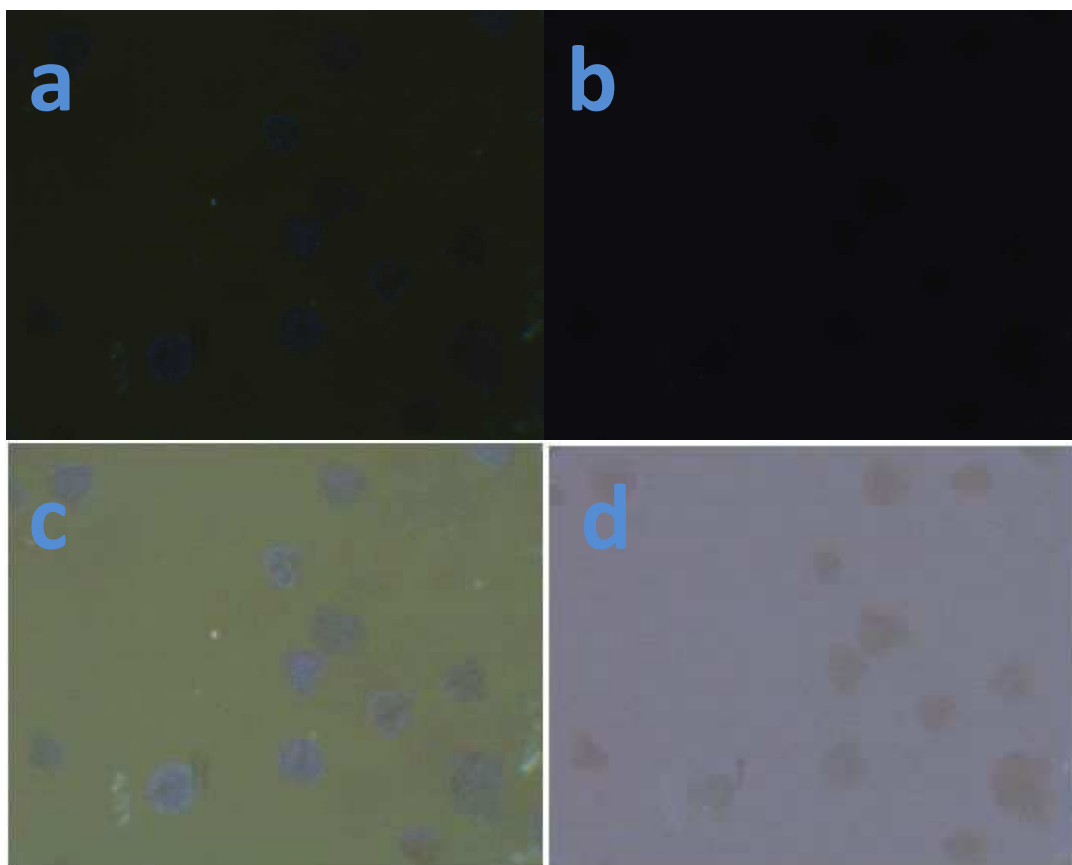


Figure 6.17 Photomicrographs of MB filled EICs (suspension method) viewed through a) crossed polars reflective mode; b) crossed polars transmissive mode; c) computer enhanced brightness of the image of photomicrograph a, and d) computer enhanced brightness of the image of photomicrograph b. (x100)

The concentration and location of the dye inside the BEICs were investigated by laser scanning confocal microscopy (LSCM). The results of LSCM analysis for BEICs filled using saturated solutions of RB and TYG respectively are shown in Figures 6.18a and 6.19a. These LSCM photomicrographs show that the internal cavities of the BEICs are completely filled by the dyes and the intensity of the fluorescence shows that the dye is at very high concentration; for contrast, the RB and TYG filled BEICs using a low concentration of dye are shown in Figures 6.18b and Figure 6.19b and it is possible to see that the internal cavity does not contain dye. At high concentration there is certain amount of dye that is extracted into the water, giving rise to a fluorescent background.

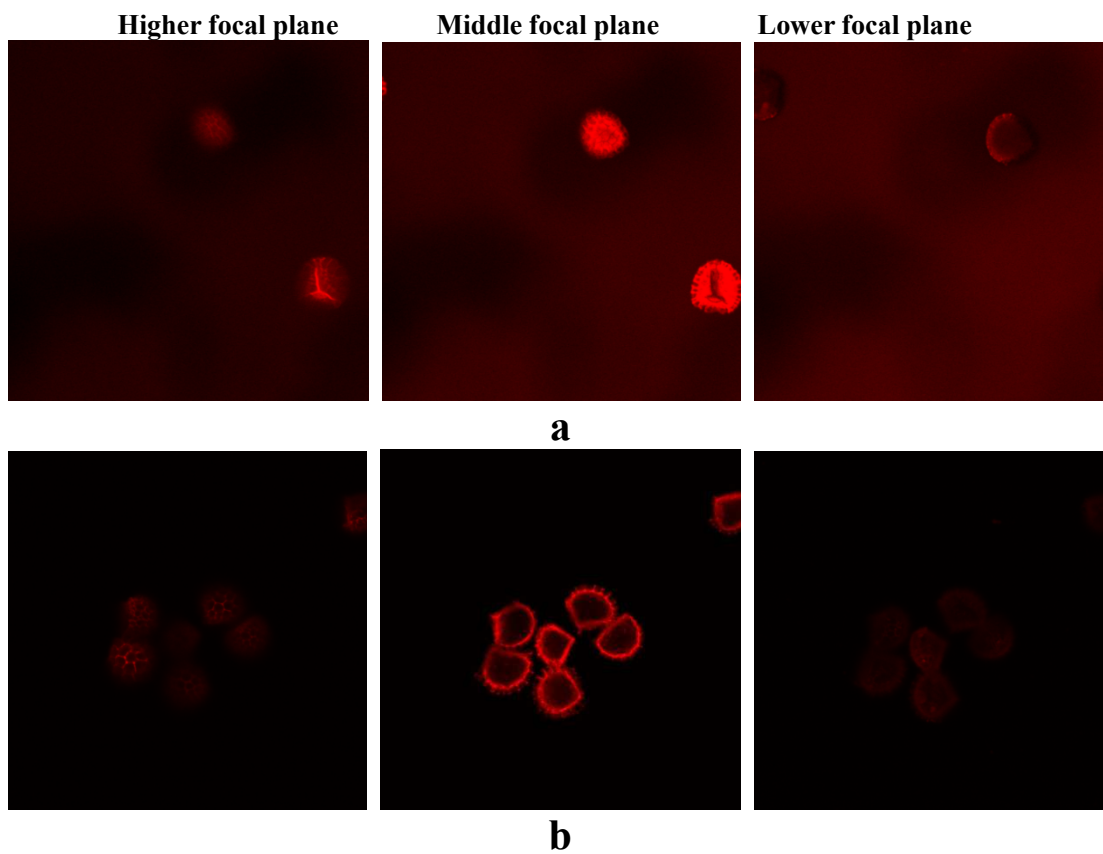


Figure 6.18 LSCM photomicrographs showing the RB filled BEICs viewed on different focal planes a) The encapsulation was carried out using a saturated RB solution and b) the encapsulation was carried out using a low concentration of RB solution. The sample was excited using a laser at 543 nm.

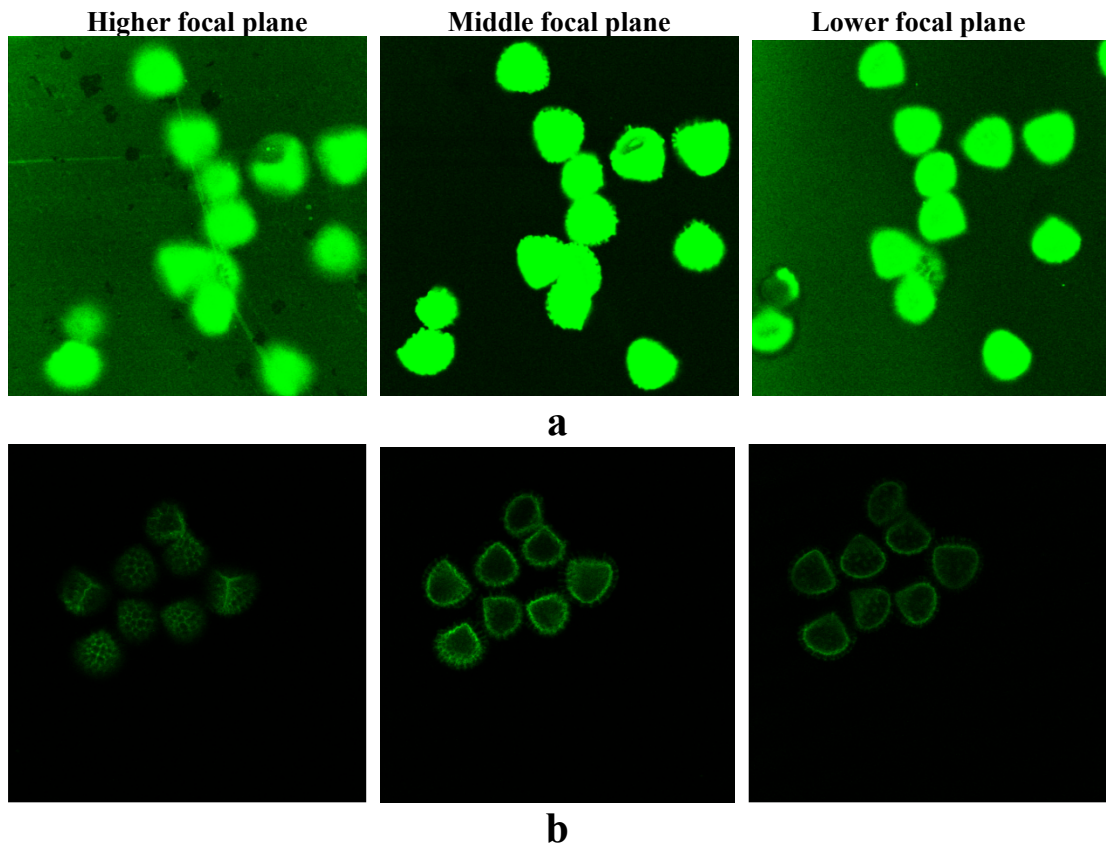


Figure 6.19 LSCM photomicrographs showing the TYG filled BEICs viewed on different focal planes a) The encapsulation was carried out using a saturated TYG solution and b) the encapsulation was carried out using a low concentration of TYG solution. The sample was excited using a laser at 488 nm.

This dyeing technique was also successfully employed on 40 μm *Clavatum* spores (see for example the spores in Figure 6.20). These filled spores were also examined using polarised light microscopy and it was possible to observe that they were filled to a similar extent to the BEICs filled by same dyes , see Figure 6.21.

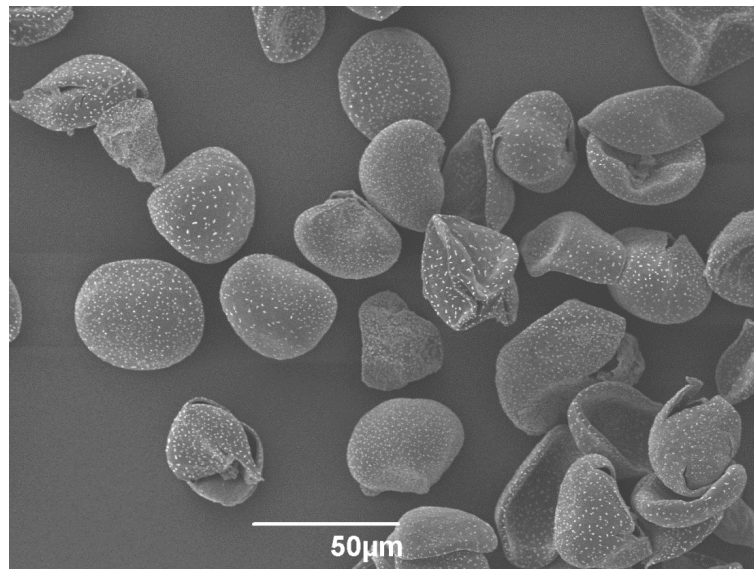


Figure 6.20 SEM image of *Clavatum* exines (40 μm).

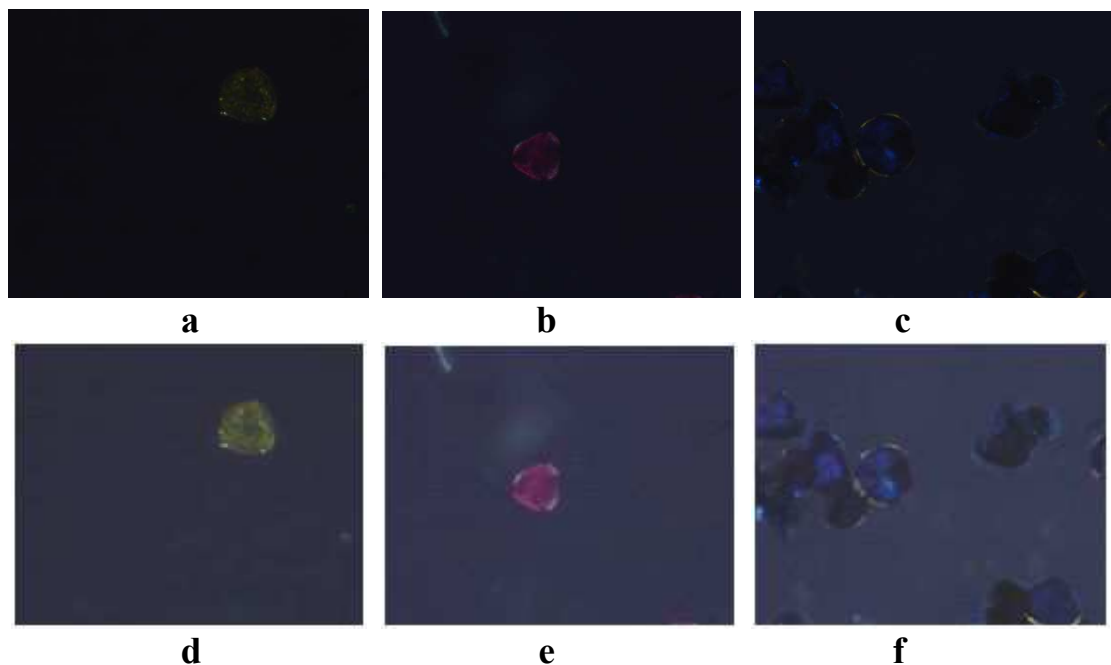


Figure 6.21 Photomicrographs of the *Clavatum* exines (40 μm) filled by a) TYG; b) RB; c) MB with crossed polars transmissive mode; d) computer enhanced brightness of the image of photomicrograph a; e) computer enhanced brightness of the image of photomicrograph b and f) computer enhanced brightness of the image of photomicrograph c. (x200)

6.1 Black particles produced by exine and intine capsules

Black particles would also be required for applications such as E-ink. A very high concentration of dye is required to be encapsulated in order for the particles to appear black otherwise the BEICs may only appear grey. Due to the ionic dyes filling the BEICs more successfully than non-polar dyes in the studies thus far, an ionic dye, NBB,

was chosen for encapsulation to give black particles. However, studies revealed that the concentration of Naphthol blue black (NBB) encapsulated in the BEICs was still insufficient to appear black and the particles always had a dark blue appearance. There are very few commercially available black ionic dyes. Attempts were made to combine different coloured ionic dyes to produce a black dye mixture. For this purpose, TYG, MB and SO were combined to give a black solution which was used in subsequent encapsulation experiments.

Initial studies gave rise to purple coloured particles because the red dye was preferentially encapsulated over the yellow and blue dyes leading to a separation of the dye mixture. In order to obtain a black particle a new encapsulation method was devised as shown in Figure 6.22

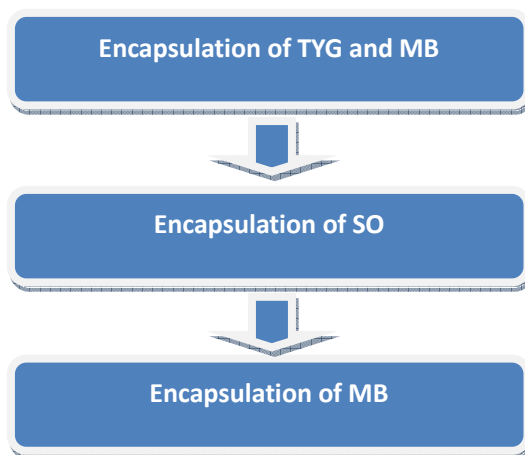


Figure 6.22 Procedure used to produce black BEICs.

It is very difficult to analyse the black particles using transmitted light polarised optical microscopy because the particle is black on a black background. The particles were suspended in water and observed using optical microscopy viewed through parallel polars. The particles dyed with the black dye mixture appeared as solid black objects (see Figure 6.23) whereas the raw spores suspended in water had a semi-transparent appearance (see Figure 6.24). No dye was observed to leak from the particles when suspended in water.

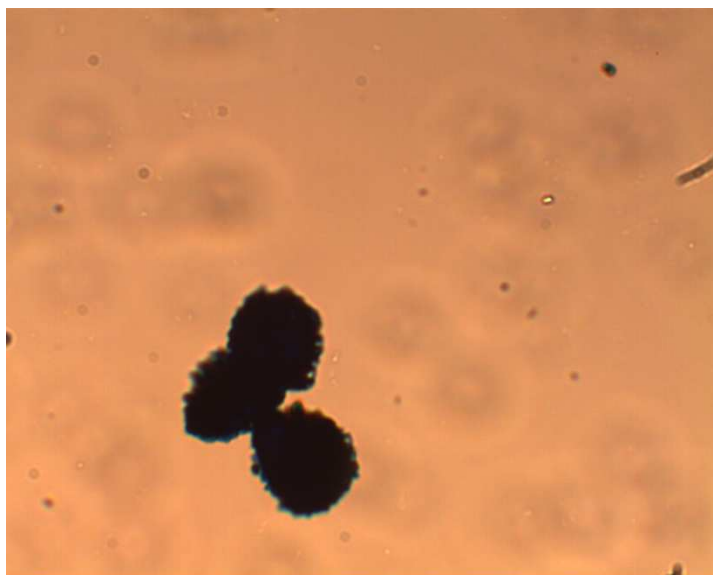


Figure 6.23 Photomicrograph of black BEICs in water viewed through parallel polars transmissive mode. (x400)

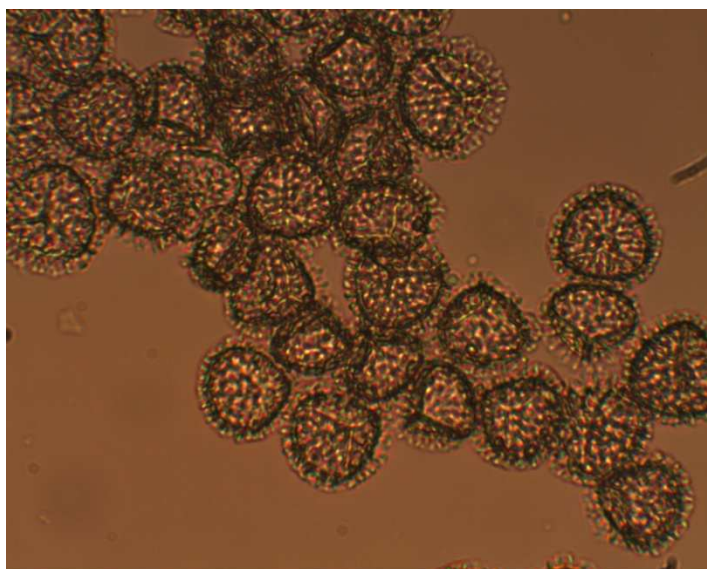


Figure 6.24 Photomicrograph of empty BEICs in water viewed through parallel polars transmissive mode. (x400)

This study has shown that it is possible to encapsulate a complex mixture of components in the BEICs in a stepwise manner. This study opens up the opportunity to study complex systems such as leuco dyes for thermochromic applications.

6.2 White particles produced by exine and intine capsules

Although the BEICs have been bleached they appear slightly off white which is not good enough for display applications. Therefore, a well known white pigment, TiO_2 , was chosen to improve the whiteness of BEICs. The encapsulation of TiO_2 was

successfully achieved using the suspension method even though the TiO_2 was insoluble in water. The whitened BEICs with TiO_2 are shown in figure 6.25.



Figure 6.25 Photographs of the white BEICs a) dry and b) suspended in water.

These white BEICs were analyzed by microscopy and it was noted that the particles filled with TiO_2 were opaque when viewed through crossed polars in transmission microscopy (Figure 6.26b) whereas they exhibited intense brightness when viewed using reflective microscopy (Figure 6.26a).

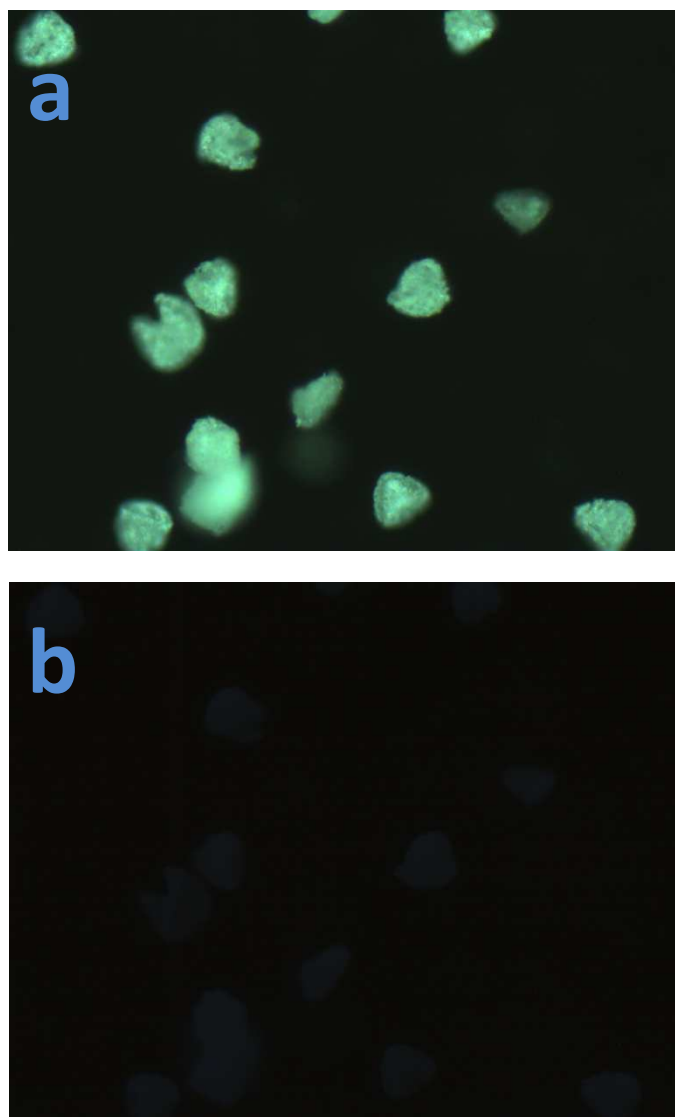
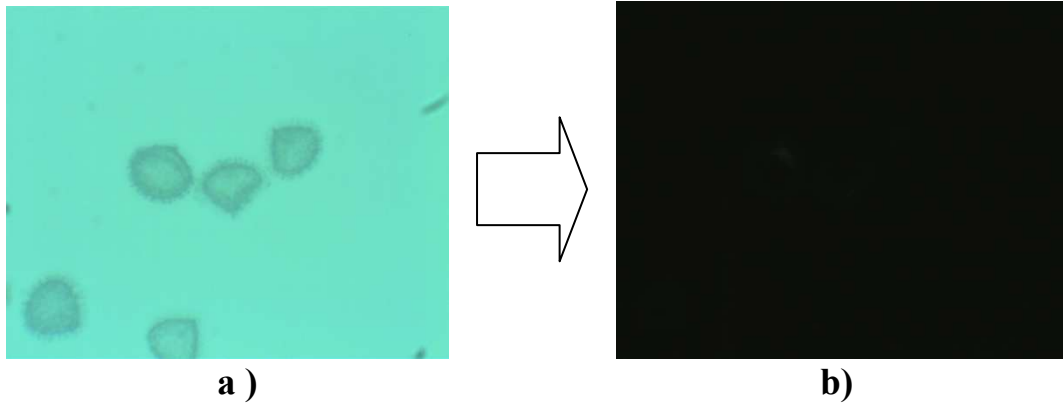


Figure 6.26 Photomicrographs of the white BEICs viewed through a) crossed polars reflective mode and b) crossed polars transmissive mode. (x200)

When unfilled BEICs are suspended in water it is difficult to observe them using reflective microscopy with crossed polars (Figure 6.27). Therefore, the intensely bright appearance of the white BEICs suspended in water observed via reflective microscopy (Figure 6.28) was attributed to the presence of TiO_2 . This experiment clearly demonstrates an effect based on the presence of TiO_2 but it cannot distinguish between particles encapsulated within the BEIC or associated with the surface. The appearance of the particles does not alter over time even when suspended in water suggesting a stable association of TiO_2 with BEICs. However, TEM studies would need to be carried out to conclusively determine the location of the TiO_2 particles in the BEICs.



a) **b)**
Figure 6.27 Photomicrographs of empty BEICs in, a) 40° crossed polars and b) crossed polars, reflective mode.

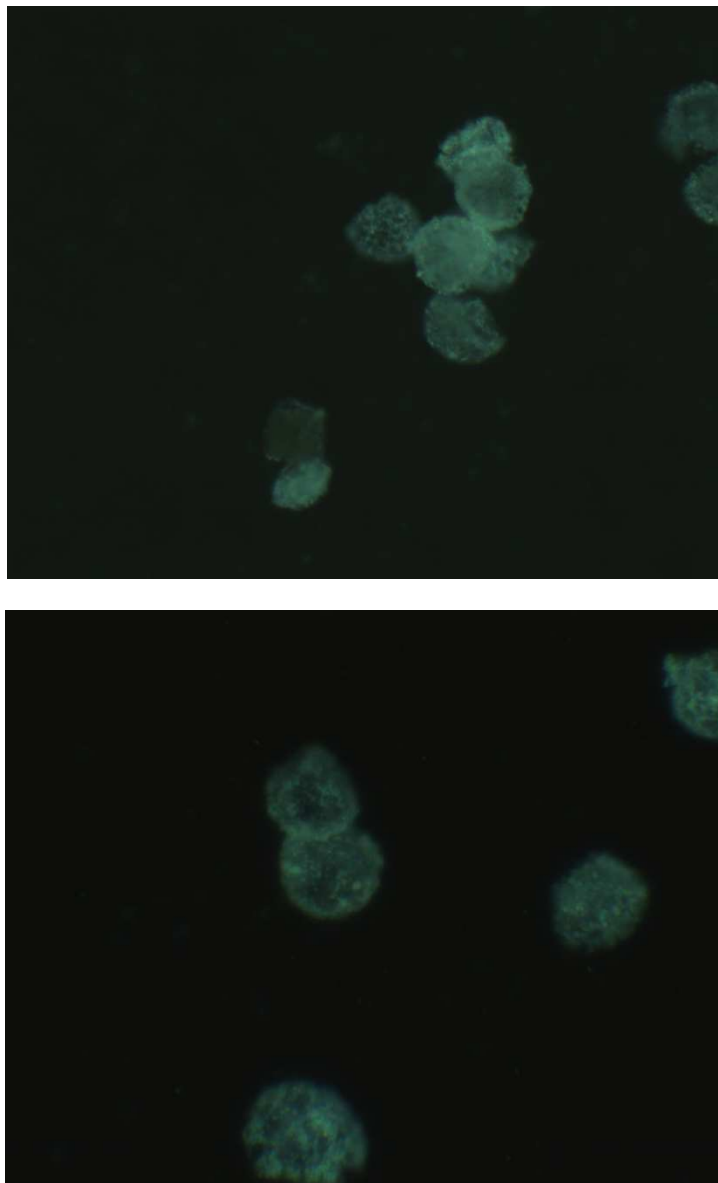


Figure 6.28 Photomicrographs of the white BEICs in crossed polars reflective mode.

Although it appears that the TiO₂ has not been encapsulated by the BEICs in the classical sense, there is evidence to suggest that it has associated at the surface of the particles. Studies in solution revealed that this association appears stable and no TiO₂ was observed to disassociate. This study has focused on 1 μm TiO₂ and it is not clear if size is a critical factor in this type of encapsulation.

6.3 Isolation and recovery of dyes by exine and intine capsules

Due to the stability of sporopollenin and the wide variety of functionality present, it is possible to further functionalize the surface using a range of different reagents to change the nature of the sporopollenin. For example, reaction of sporopollenin from *Lycopodium Clavatum* with ethylenediamine yields a diamino-sporopollenin, which can be further modified by reacting the amine groups present with bromoacetic acid to generate carboxylic acid functionalized diamino-sporopollenin. Such modified sporopollenin has been investigated as solid substrates for ligand-exchange chromatography. Furthermore, these sporopollenins have been investigated as an adsorbent for dye and metal ions (see chapter 1). However, the following research indicates that the raw spores, specially treated spores and EICs prepared by the Chm-method can be used as adsorbent materials and that it is not restricted to functionalized spores.

A pre-weighed ‘column’ of raw untreated spores or BEICs was prepared in a pasteur pipette whereby the neck of the pipette was plugged with glass wool to prevent loss of spore material. The column prepared for this study is shown graphically in Figure 6.29. The sand layer ensured that there was minimum disturbance to the spores layer while the dye solution was added.

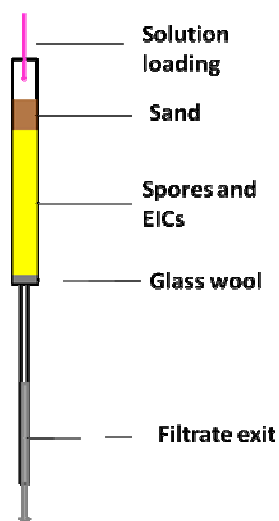








Figure 6.29 Graphical representation of the spores ‘column’ used in this study.

Prior to use, the exine ‘column’ was packed using either a vacuum or positive air pressure to ensure that no voids remained between the exines. When eluent was passed through the column under positive pressure the ‘column’ fragmented upon the release of the pressure and hence the eluent was passed through the column using a vacuum.

Initial studies to compare raw spores to EICs yielded some interesting results. There was a direct correlation to the amount of RB which absorbed onto the spores/exines to how deflated or empty the spores were. The raw spores absorbed very low quantities of dye from the aqueous solutions whereas the spores compressed using a vacuum retained nearly all of the dye. The exines that had been emptied and hence possessed the greatest capacity retained all the dye and a colourless filtrate was isolated. The results are shown in Table 6.1. This result indicates that the absorption efficiency is directly related to the available volume of the exine/spores. Additionally, it would appear that, the functional groups which interact more strongly with the dye are located within the exine shell rather than on the outer surface.

Table 6.1 Comparison of the capture efficiency of raw spores and exines with different pre- and post-packing treatments.

Spore treatment	UV intensity (Absorbance)	Filtrate	% dye captured
0.1g.L ⁻¹ RB in acetone	0.442		N/A
normal spores	0.158		64%
vacuum treated spores after leaving in air for 3 hours	0.033		93%
weak vacuum treated spores	0.018		96%
vacuum treated spores	0.014		97%
empty exines	0		100%

Following the successful isolation of RB, the experiment was extended to encompass a wide range of dyes including cationic dyes (RB, MB and SO), anionic dyes (TYG and NBB) and a neutral dye (CT69). Figure 6.30 shows a comparison of the initial solutions to the filtrates after they had been passed through the exine “column”. Interestingly, the cationic dyes (RB, MB and SO) were all completely isolated by the exines, but the

anionic (TYG and NBB) and the neutral dye (CT69) remained in solution and were either partially or not isolated by the EIC “column”. However, CT69 was not soluble in water and therefore, acetone was used as the solvent. Figure 6.31 shows a summary of the structures of the dyes and whether they are isolated or not by the exine column. All of the cationic dyes contain a quaternary ammonium ion as the cationic species with a chloride counter ion. Therefore, it is possible to conclude that there is a strong interaction between cationic dyes and the functional groups forming the inner and outer surfaces of the exines but weak interaction in the case of neutral dyes or possibly repulsion for anionic dyes.

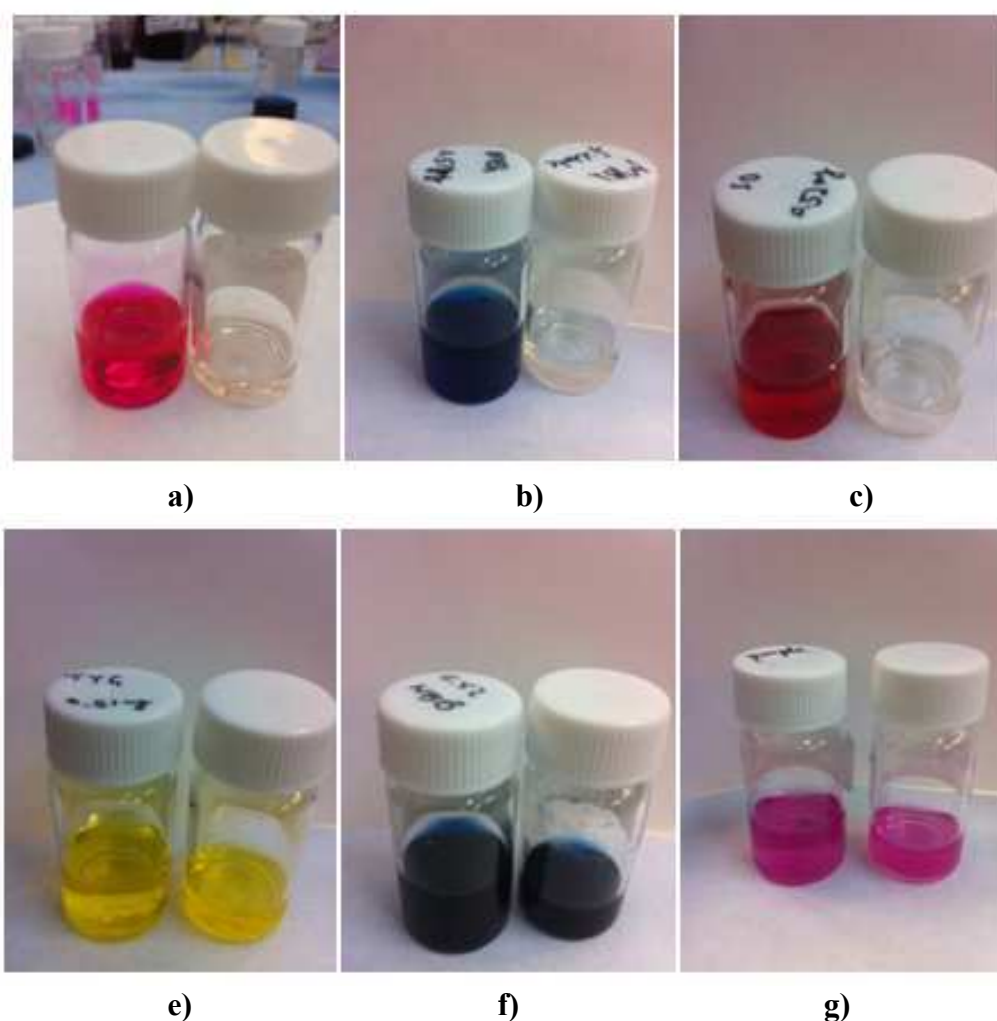


Figure 6.30 Photographs showing a comparison of the initial aqueous solutions (left) and filtrates (right) of a) RB, b) MB, c) SO, d) TYG, e) NBB and f) CT69 (in acetone)

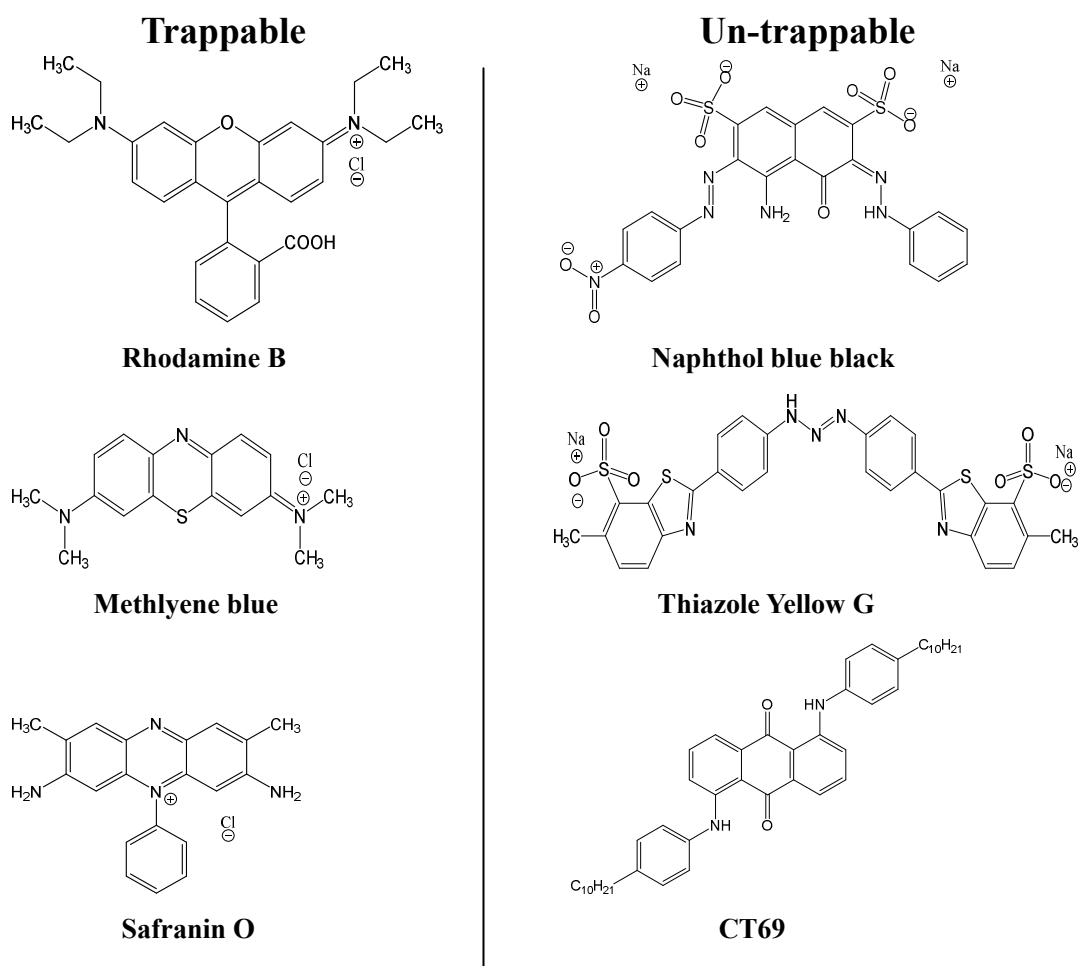


Figure 6.31 Molecular structures of dyes that were isolated compared to dyes that were not isolated.

In order to determine if the nature of the solvent would affect the capture of dyes by the EICs, the experiment was repeated for RB using a range of solvents including acetone, DCM and ethanol. RB was successfully isolated by the EICs from acetone and DCM, but interestingly it was not isolated when ethanol was used as the solvent. Figure 6.32 shows comparisons of the initial solutions and the filtrates from this experiment. It was reported by Atkin *et al*, that ethanol aids the encapsulation process for exines which is in contrast to these results (see chapter 1).²² By careful consideration of all these results it is possible to postulate that ethanol can both increase the ability of exines to capture material, but additionally, it may also facilitate the release of cationic materials from the exines by interrupting the interactions between the cationic dye and the exine.

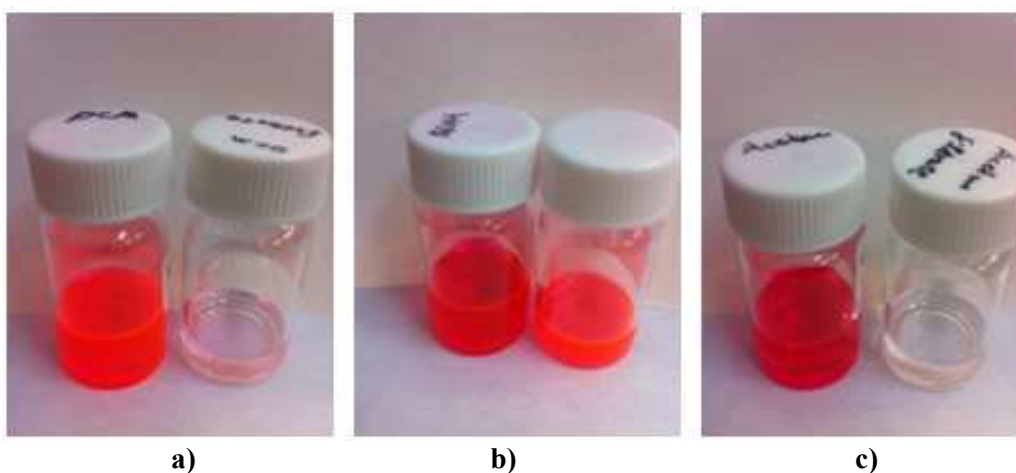


Figure 6.32 Photographs showing comparisons of the initial solutions of RB (left) and the filtrates (right) for a) Acetone, b) Ethanol and c) DCM

To investigate if this theory held true RB was isolated in an exine “column” from aqueous solution. The ‘column’ was washed with water and no dye was evident in the aqueous washings (Figure 6.33a). The “column” was then washed with ethanol and the dye was released from the “column” into the ethanol (Figure 6.33b). The exine column also returned back to its original colour indicating that the dye had been removed.

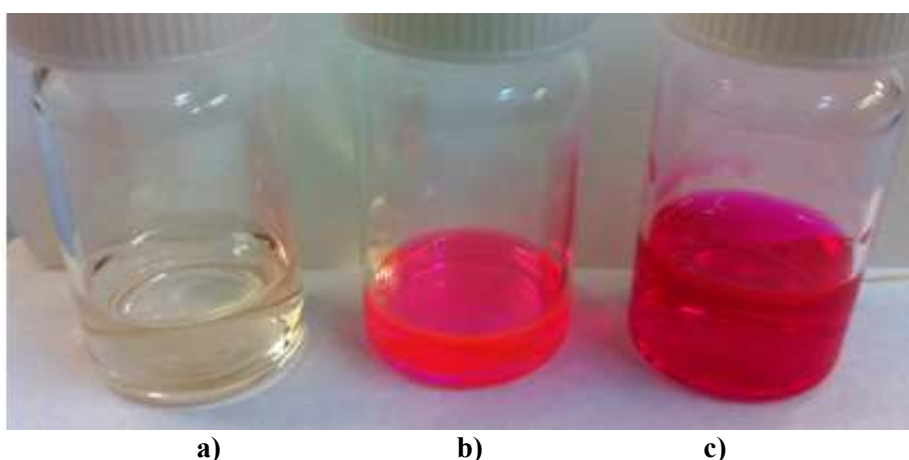



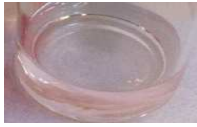

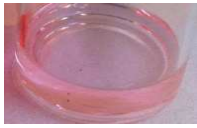


















Figure 6.33 Photographs showing a) the deionized water washings, b) ethanol washings and c) initial 0.1g.L^{-1} aqueous solution of RB

These studies revealed that cationic dyes can be isolated by the exines from certain solvents and released using ethanol showing the potential of the exines to be used as capture, storage and release vehicles. The study was expanded to consider a much wider range of solvents, see Table 6.2. RB was dissolved in each solvent and passed through the exine ‘column’. Solvents including water, acetone, dichloromethane, acetonitrile,

chloroform and diethyl phthalate resulted in isolation of the dye by the exines while all alcoholic solvents including ethanol, methanol, ethanediol and propanol prevented isolation of the dye. These results suggest that the hydroxy group must play a role in releasing the dye from the exine. One possible explanation for this behaviour is that there is a greater affinity between the dye and solvent than between the dye and the EIC or that alcoholic solvents have a greater affinity with the EIC than the dye and this leads to a disassociation of the dye from the EIC.

Table 6.2 Comparison of initial solutions of RB and filtrates for a range of solvents. All the initial solutions have a concentration of 0.1g.L^{-1}

Solvent	pKa	Initial Solution	Filtrate
Water	15.7		
Acetone	24.2		
DCM	N/A		
Acetonitrile	25		
Chloroform	25		
Diethyl phthalate	N/A		
Acetone:Water (1:1)			
Ethanol	15.9		
Ethenediol	14.2		
Propan-2-ol	16.5		
Methanol	15.5		

To understand if this result was universal for all cationic dyes, the experiment was repeated using SO. It was found that SO has lower solubility than RB in ethanol and it was absorbed onto the EIC column from ethanol just like it was from water. Due to the lower solubility of SO in ethanol it is possible that the affinity for SO to ethanol is much lower than the affinity of RB to ethanol. Figure 6.34 shows (a) the initial ethanol filtrate, (b) the subsequent ethanol washings and (c) HCl washings. HCl was used to protonate the hydroxyl groups present in the exine shells and to create a cationic surface. In this way the functionalisation can release any isolated cationic materials from the exine shells by creating a similarly charged surface that would repel rather than attract. The proposed scheme for the addition of HCl and release of dye is shown in Figure 6.35.

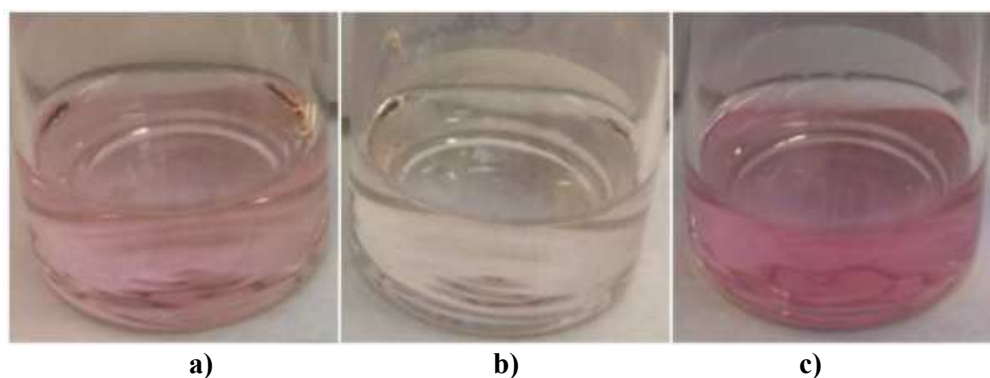


Figure 6.34 Photographs of a) initial ethanol filtrate containing little SO, b) subsequent ethanol washings and c) HCl washing continuing to release SO.

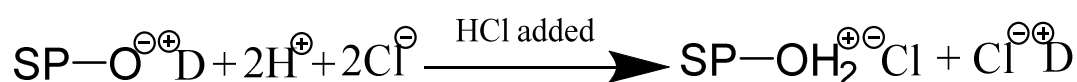


Figure 6.35 Protonation of the exine shell and release of dye (D^{\oplus}).

In order to determine if the exine shells could be protonated in order to change their behaviour, they were pretreated using HCl. HCl was flowed through a short exine “column” and immediately followed by either a solution of RB in acetone or in ethanol. Remarkably it appeared that this experiment was successful and the dye was not totally isolated. In both cases a lot dye remained in solution as shown in Figure 6.36 One suggestion to explain the small quantity of dye that was absorbed onto the exine “column” is that the HCl did not completely protonate all of the functional groups on the exine shells and some interactions were still possible.



Figure 6.36 Photographs showing the initial solutions of RB and the resulting filtrates using a) acetone and b) ethanol.

In previous experiments using untreated EICs it was not possible to isolate any anionic dyes. However, after pre-treatment of the EIC ‘column’ with HCl it became possible to isolate anionic dyes. Figure 6.37 shows an initial solution of NBB in acetone and the filtrate from the EIC “column” whereby the dye has been isolated on the “column”. This result clearly demonstrates that it is possible to alter the nature of the exine and to tailor its properties so that either cationic or anionic species can be isolated. In order to verify that this behaviour was caused by the HCl pretreatment, the experiment was repeated, but the exine ‘column’ was only pretreated with dichloromethane instead of HCl. In this experiment ‘normal’ behaviour was observed and NBB was not isolated, see Figure 6.38.

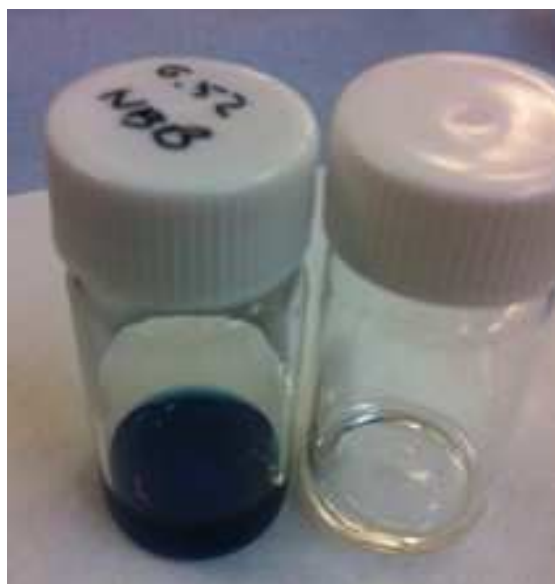


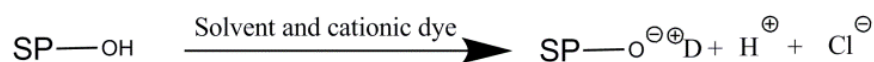
Figure 6.37 Photograph showing the initial solution of NBB in acetone (left) and the clear filtrate from the HCl pretreated exine “column” (right).



Figure 6.38 Photograph showing the initial solution of NBB in acetone (left) and the filtrate from the DCM pretreated exine “column” (right).

Based on these experiments the capture and release of dyes using exines has been demonstrated. In order to understand the processes for isolation of the dye using untreated exines or HCl pretreated exines, the mechanism for capture is summarised using the schemes shown in Figure 6.39.

A: Cationic dye trapping interaction:



B: Anionic dye trapping interaction:

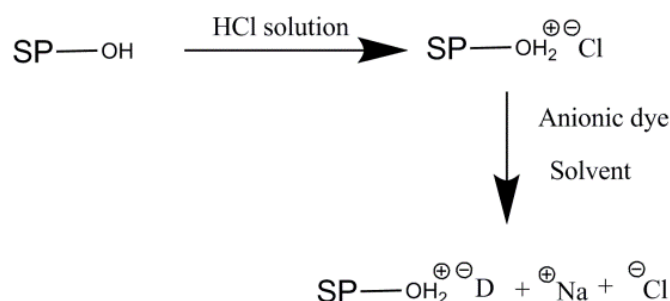


Figure 6.39 Proposed mechanism for the interaction of A) the untreated sporopollenin and dye for capture of cationic dyes. B) HCl pretreated sporopollenin and dye for capture of anionic dyes.

In this research, the use of EICs from *Lycopodium Clavatum* for capture and release vehicles for dyes was examined. It was demonstrated that raw spores have a capacity to absorb dyes onto their surface but sporopollenin exines have a much greater void-volume, due to the removal of the biological centre, which allows for greater uptake of dye. The exines preferentially absorb cationic dyes over anionic and neutral dyes from a range of solvents and the release mechanism was investigated using ethanol,

methanol, propan-2-ol and ethanediol.

The behaviour of the exines was inverted by pretreating the exines with hydrochloric acid and in this case, the exines were able to preferentially capture anionic dyes over cationic or neutral dyes indicating that the ionic nature of the sporopollenin exine is important for determining the affinity of the dye to the exine.

Experimental

Encapsulation of dyes via the droplet method

Encapsulation of TBBA in EICs at room temperature

TBBA (4.81 mg) was dissolved in DCM (4 mL). The TBBA solution was added dropwise to exines (3.39 mg) until the dry powder became a paste and then followed with a drop of ethanol. The mixture was dried in vacuum over CaCl₂ until all solvent gone. Subsequently, the filled exines were transferred on to a filter paper and washed with dichloromethane (2 x 10 mL) and then dried in vacuum.

Other water-insoluble dyes were encapsulated into *Lycopodium Clavatum* exines (25µm, bleached, Sporomex) in an analogous way to the encapsulation of TBBA and the reagents used are summarized in Table 6.3.

Table 6.3 Summary of reagents used in encapsulations of water-insoluble dyes via the droplet method.

Dye name	Dye used /mg	Exines used/ mg	Volume of DCM used for encapsulation / mL	Volume of DCM used for washing/ mL
CT51	3.8	2.7	4	2 x 10
CT75	14.8	2.9	10	2 x 10
CT67	6.7	2.1	3	2 x 10
Indigo	10.6	4.2	10	2 x 10

Water-soluble dyes were encapsulated into *Lycopodium Clavatum* exines (25µm, bleached, Sporomex) in an analogous way to the encapsulation of TBBA, but

encapsulation solvent and washing solvent were changed to deionized water. Reagents used in encapsulations are summarized in Table 6.4.

Table 6.4 Summary of reagents used in encapsulations of water-soluble dyes via the droplet method.

Dye name	Dye used /mg	Exines used/ mg	Volume of Deionized water used for encapsulation / mL	Volume of Deionized water used for washing/ mL
Thiazole yellow G	22.0	4.6	4	5 x 10
Rhodamine B	12.6	4.8	6	Washed until no dye observed in the washings
Safranin O	26.0	3.6	6	Washed until no dye observed in the washings
Methylene blue hydrate	15.1	3.7	7	Washed until no dye observed in the washings
Naphthol blue black	36.8	3.5	7	Washed until no dye observed in the washings

Water-soluble dyes were encapsulated into *Clavatum* exines (40µm, bleached, Sporomex) in an analogous way to the encapsulation of TBBA, but encapsulation solvent and washing solvent were changed to deionized water. Reagents used in encapsulations are summarized in Table 6.5.

Table 6.5 Summary of reagents used in encapsulations of water-soluble dyes via the droplet method (40 μ m exine microcapsule).

Dye name	Dye used /mg	40 μm Exines used/ mg	Volume of Deionized water used for encapsulation / mL	Volume of Deionized water used for washing/ mL
Thiazole yellow G	34.8	4.6	10	Washed until no dye observed in the washings
Rhodamine B	16.7	3.9	7	Washed until no dye observed in the washings
Safranin O	37.5	4.7	10	Washed until no dye observed in the washings
Methylene blue hydrate	29.8	3.5	8	Washed until no dye observed in the washings
Naphthol blue black	38.1	5.0	10	Washed until no dye observed in the washings

Encapsulation of dyes via the suspension method:

Encapsulation of RB by the suspension method in BEICs

RB (5 g) was dissolved in deionized water (125 mL) and heated to 90 °C. BEICs (3 g) were added and the suspension stirred at 90 °C for 2 hours. The mixture was filtered and the filled bleached EICs were washed with acetone until no RB was observed in the washings. The product was dried in air.

Other water-soluble dyes were encapsulated into BEICs in an analogous way to the encapsulation of RB (the suspension method) and reagents used in encapsulations were summarized in Table 6.6.

Table 6.6 Summary of reagents used in encapsulations of water-soluble dyes via the suspension method.

Dye name	Dye used /g	BEICs used/ g	Volume of Deionized water used for encapsulation / mL	Volume of acetone used for washing/ mL
Thiazole yellow G	1.39	3.00	100	Washed until no dye observed in the washings
Methylene blue hydrate	3.09	3.03	125	Washed until no dye observed in the washings

Black and white BEICs:

Encapsulation of Ionic black dye mixture in BEICs (Black BEICs)

BEICs (0.2 g) were added to an aqueous solution of TYG & MB (20 mL). The mixture was stirred at 70 °C for 1 hour. The filled BEICs were isolated by filtration and washed with water and then acetone. These BEICs were then added to an aqueous solution of SO (20 mL) and stirred at 70 °C for 0.5 hours. The BEICs were isolated by filtration and washed with water and acetone. Subsequently, the filled BEICs were stirred in an aqueous solution of MB (20 mL) at 100 °C for 0.5 hours. The black BEICs were isolated by filtration and washed with water and then acetone until no dye was observed in the washings. The product was dried in vacuo over CaCl₂.

Encapsulation of TiO₂ in BEICs (White BEICs)

TiO₂ (5 g) was dispersed in water (50 ml) and ultrasonicated for half hour at room temperature. The mixture was filtered and then the solution (20 ml) was added dropwise to BEICs (0.21 g) with stirring and then ethanol (1ml) was added. The mixture was heated to reflux with stirring for 2 hours. The product was isolated by filtration and then washed with water (100 mL), acetone (2 x 50 mL) and ethanol (2 x 50 mL). Finally, the product was dried in vacuo over CaCl₂.

Dye capture and release:

Isolation of Rhodamine B from solution using raw spores

Raw spores (0.4 g) were packed in a mini “column” without any further treatment. An aqueous solution of RB (0.1 g L⁻¹, 2 mL) was drawn through the column under vacuum.

The filtrate was collected for evaluation.

Using the same quantity of RB solution, the process was repeated with different column packing conditions as follows:

- The 'column' was packed and then compacted using a weak vacuum.
- The spores were subjected to a vacuum, left in air for 3h and then packed into a "column".
- The spores were subjected to a vacuum, packed into a 'column and then compacted using a vacuum.

The process described above was repeated using EICs (EICs batch: **CM-2**). Details of quantities of materials and the solvents used are given in Table 6.7.

Table 6.7 Experimental detail of dye isolation using EIC “columns”.

Dye	Solvent	Dye concentration (g L⁻¹)	Volume (mL)	Weight of exine (g)
RB	Deionized water	0.1	2	0.2
RB	Acetone	0.1	2	0.2
RB	Ethanol	0.1	2	0.2
RB	Dichloromethane	0.1	2	0.2
RB	Water/acetone (1:1)	0.1	2	0.2
RB	Acetonitrile	0.1	1	0.1
RB	Chloroform	0.1	1	0.1
RB	Diethyl phthalate	0.1	1	0.1
RB	Ethenediol	0.1	2	0.2
RB	2-propanol	0.1	2	0.2
RB	Methanol	0.1	1	0.1
MBh	Deionized water	0.1	2	0.2
SO	Deionized water	0.1	2	0.2
SO	Ethanol	0.1	2	0.2
TYG	Deionized water	0.1	2	0.2
NBB	Deionized water	0.1	2	0.2
NBB	Acetone	0.1	2	0.2
NBB	Ethanol	0.1	2	0.2
CT69	Acetone	>0.1	2	0.2

A series of experiments were carried out to isolate dye on EIC “columns” that were pre-treated with HCl, ethanol or dichloromethane. After pretreatment of the exine “column” a solution of dye (2 mL, 1 g.L⁻¹) in a solvent was drawn through the column using a vacuum. The filtrate was isolated for further evaluation. The details of solvents, dyes, concentration and ‘column’ size are given in Table 6.8.

Table 6.8 Experimental detail of dye isolation using pretreated EIC “columns”

Dye	Pre-treatment solvent	Volume of pre-treat solvent used (ml)	Solvent	Volume (mL)	weight of exine (g)
RB	5 M HCl	3	Ethanol	2	0.2
RB	5 M HCl	3	Acetone	2	0.2
NBB	Ethanol	1	Acetone	2	0.2
NBB	5 M HCl	3	Acetone	2	0.2
NBB	5 M HCl	3	Ethanol	2	0.2
NBB	DCM	3	Ethanol	2	0.2
CT69	5 M HCl	3	Acetone	2	0.2

7. Properties of Functional dye Encapsulated Microcapsules

In the previous chapters the encapsulation of dyes by exines has been described. In this chapter the potential for using BEICs as optical containers for the production of optically functional materials is described and evaluated. Thus, in the subsequent sections, the feasibilities of creating BEICs possessing properties such as fluorescence, pH sensitivity, and thermochromism are described.

7.1 Fluorescent microcapsules produced from bleached exine and intine capsules

Spores and pollen are known to autofluoresce and sporopollenin is one of the chromophores within their structures.¹⁰² Furthermore, it was noted that sporopollenin can still autofluoresce after it has been treated by the Chm-method and subsequently bleached. The fluorescence of exine and intine capsules (EICs) and bleached exine and intine capsules (BEICs) was examined. In order to probe the interactions between fluorescent dyes and BEICs, BEICs were filled with rhodamine B (RB) (Figure 7.1), and their fluorescence emission measured. Rhodamine B is a well-studied fluorescent dye, frequently used in research.¹⁰³

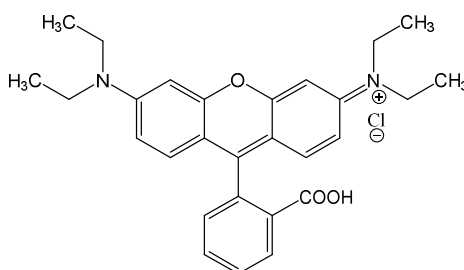


Figure 7.1 Molecular structure of Rhodamine B (RB).

Under short-wavelength ultraviolet (UV) light (365nm), photomicrographs show that BEICs exhibit much more intense fluorescence compared to non-bleached EICs and untreated spores (see Figure 7.2). This illustrates that, even before rhodamine B (RB) was added, the chemical treatments applied to spores and EICs alter their fluorescent properties.

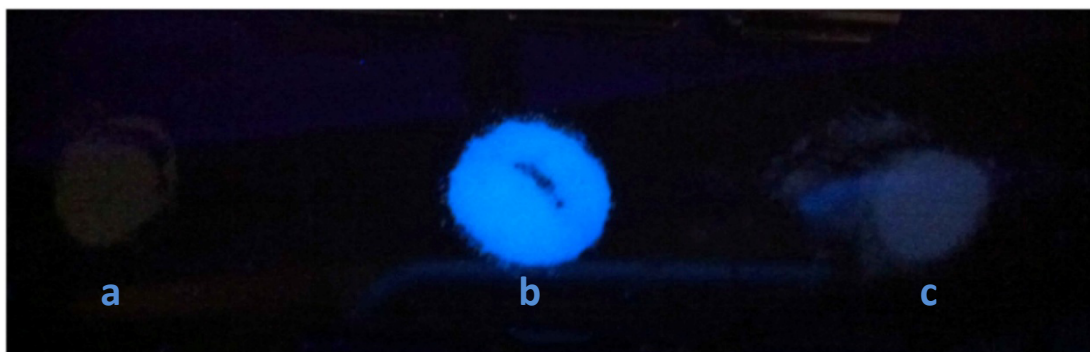


Figure 7.2 Photomicrographs of samples of *Lycopodium clavatum* under a 365 nm UV lamp. a) Non-bleached EICs, b) BEICs, and c) untreated spores.

The fluorescence of BEICs (**BE-1** and **BE-7**) was measured using spectrofluorometry with a front-face excitation geometry. It was observed by visual inspection that two batches of BEICs (both prepared using the same method, see Chapter 4) were slightly different colours. **BE-1** was slightly whiter than **BE-7**, although the difference was very small. Samples from both batches were analyzed using spectrofluorometry and the results are shown in Figure 7.3. Both samples exhibit two peaks in their spectra; one between 380-500 nm and the other at 729 nm. The peaks between 380-500 nm are likely to be due to the autofluorescence of sporopollenin, as well as fluorescence from other components of the spores, such as the intine and protoplast.^{104,105} Conversely, the peaks at 729 nm are probably due to second order diffraction and are caused by the excitation light. Second order diffraction usually occurs from strongly scattering surfaces, such as from the samples prepared for this experiment.¹⁰⁶ These peaks can be eliminated if a 350 nm long-pass filter is situated between the sample and the detector. This filter blocks any fluorescence emitted from the sample below 350 nm, as well as light resulting from scattering of the excitation beam. However, a long-pass filter was not used in this work. Thus, peaks situated at ~729 nm can be excluded from analysis when a 365 nm excitation beam was used. Furthermore, it should be noted that although **BE-7** and **BE-1** appeared slightly different visually, their emission profiles are broadly similar.

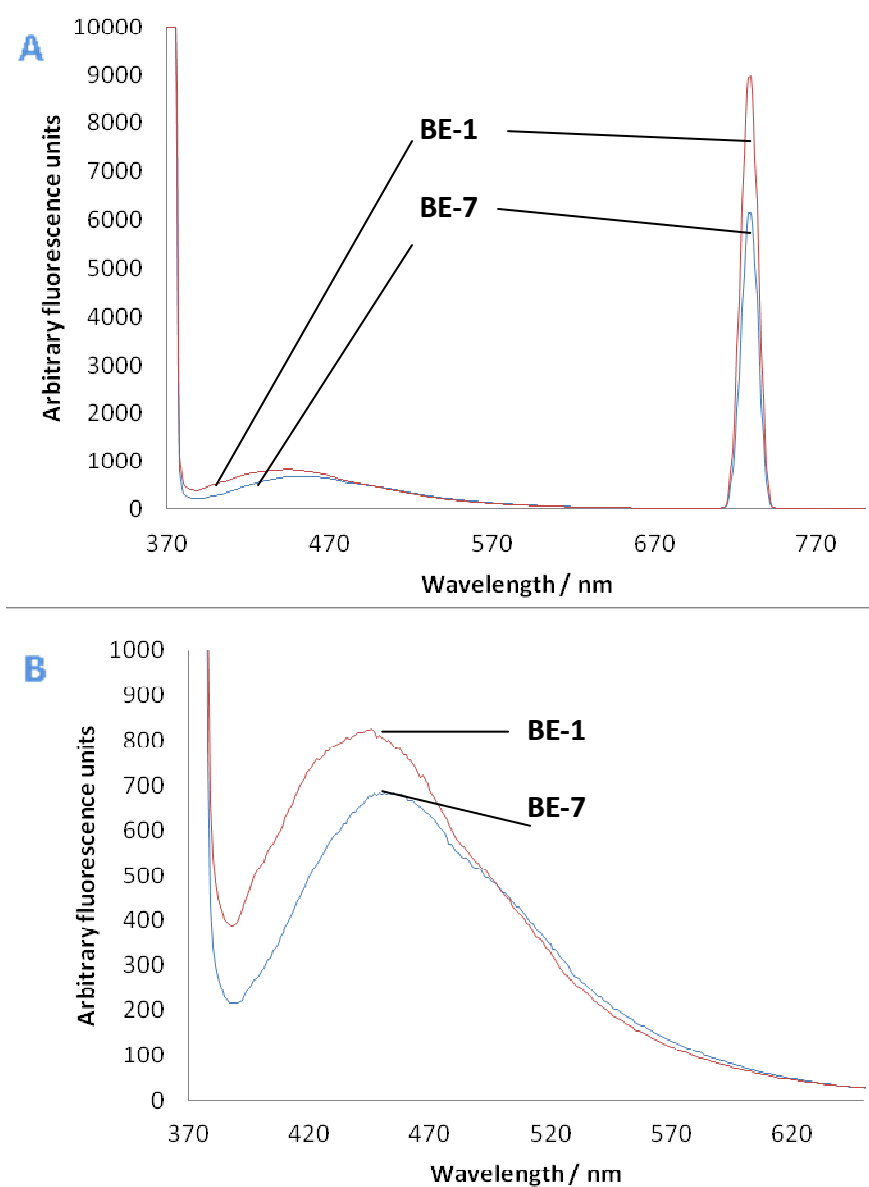
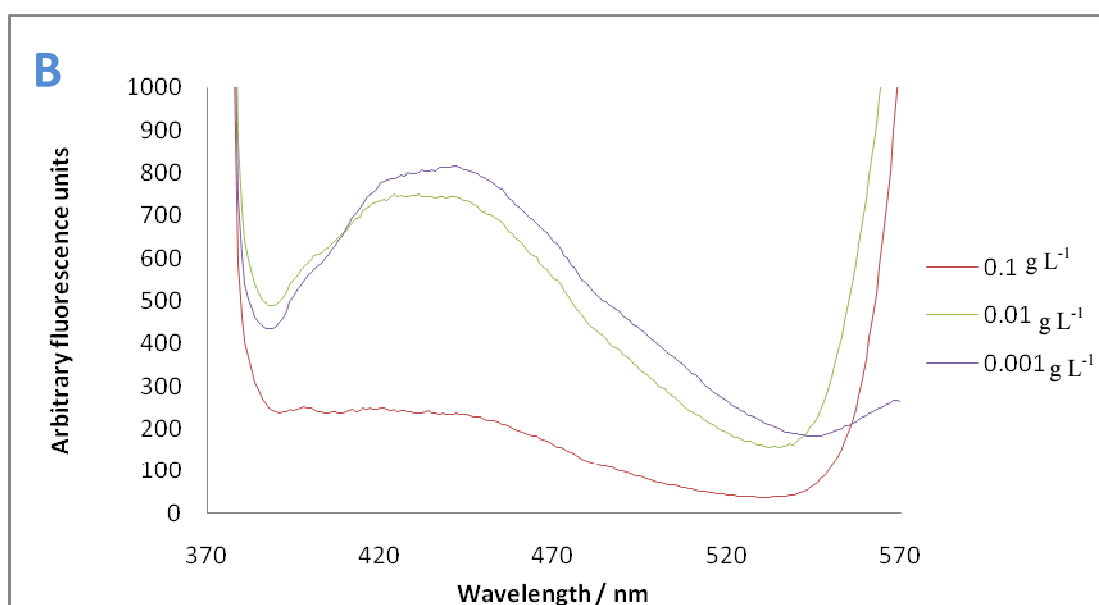
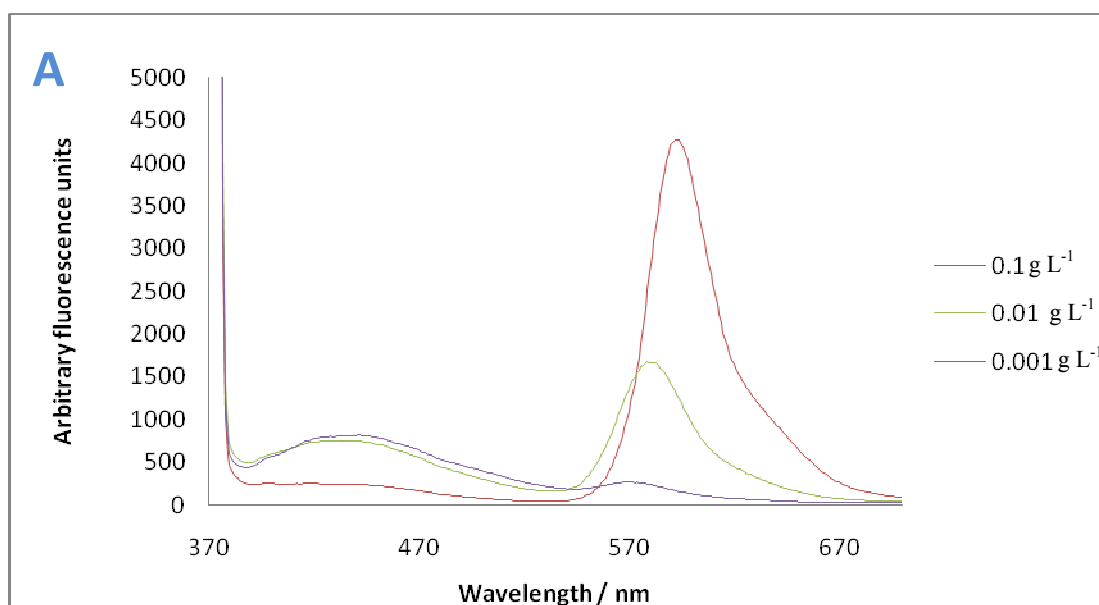


Figure 7.3 Emission spectra of BEICs from two different batches (**BE-1** and **BE-7**), Spectrum B is an expansion of the 370-650 nm range in spectrum A. The excitation wavelength is 365 nm, the peak emission wavelength for **BE-7** is 444 nm and for the **BE-1** 449 nm

The BEICs were filled with RB and their fluorescence emission measured (see Figure 7.4). Peaks attributed to autofluorescence of BEICs still remain in the spectra (between 370-530 nm), but the peak emission wavelength of these bands appears to shift to shorter wavelengths at higher RB concentrations. These are very broad bands, so assigning maxima is difficult, meaning that very small shifts in peak emission wavelengths, may be insignificant. The peak area of BEICs' emission decreases relative to that of RB as the concentration of RB is increased. Therefore, the emission from the BEICs is quenched in the presence of RB.



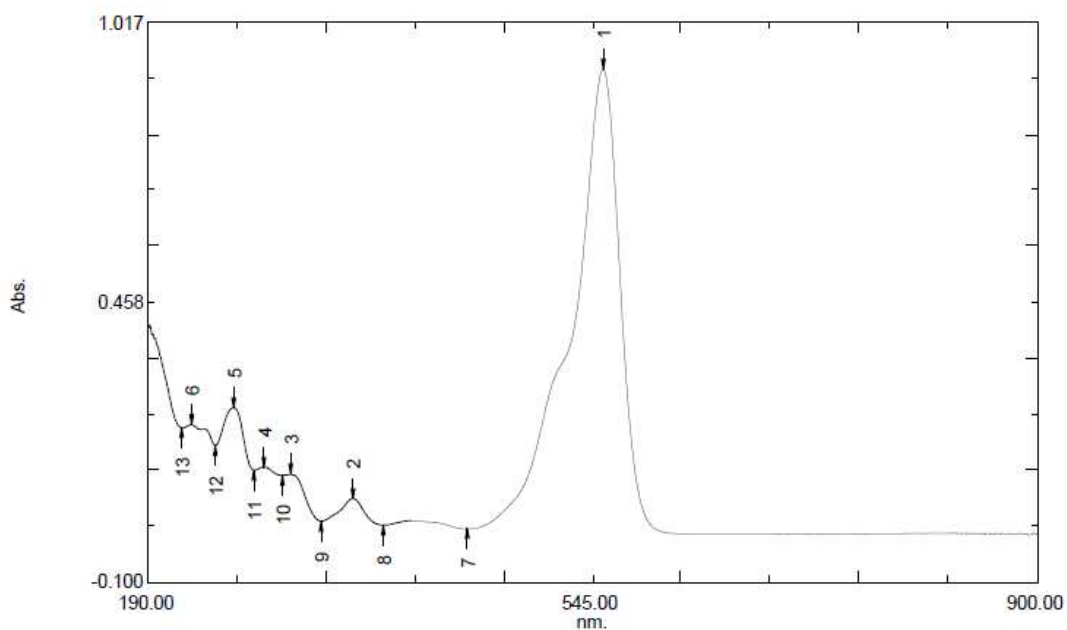
Concentration of RB aqueous solution applied to BEICs (g L^{-1})	Peak emission wavelength of BEICs (nm)	Peak emission wavelength of RB (nm)
0.1	420	594
0.01	424	579
0.001	442	571

Figure 7.4 Graph A: Fluorescence emission spectra of BEICs treated with aqueous solutions of RB at different concentrations. Graph B: Expansion of the region 370–570 nm of graph A. Excitation wavelength 365 nm

The primary cause of the observed quenching is likely to be the change in concentration of the RB solution applied to the BEICs. During the fluorescence process, it is possible

that energy is transferred between different RB molecules, as well as RB and components of the BEICs. During quenching, energy from the higher energy species (e.g. BEICs) is absorbed by or transferred to the lower energy species. This point is supported by the overlap of emission wavelength of BEICs (Figure 7.3, 370–650 nm) and absorption wavelength of RB (see Figure 7.5, 445–600 nm); Also, the overlap of emission wavelength of BEICs and excitation wavelength of RB (500–570 nm).¹⁰⁷

Another possible reason for the decreased emission of BEICs at high RB concentrations is the potential change in their intine composition and concentration. RB is an acidic species,¹⁰⁸ and its addition could act to decompose any remaining intine material inside the BEICs (acid treatment is a standard approach used to remove intine from *Lycopodium Clavatum* spores, see Chapter 1). The amount of intine removed may be proportional to the concentration of RB, although this has not been measured. However, because the intine material is usually removed by particularly strong acids, such as sulfuric acid or phosphoric acid, RB is unlikely to remove significant amounts of intine due to its relatively low acidity. In addition, the washing process after the encapsulation of RB could remove any intine remaining inside the BEICs, which may previously have been broken down by the bleaching process. However, the washing process was thorough, meaning the amount of intine remaining should have been very small, although this was not measured.

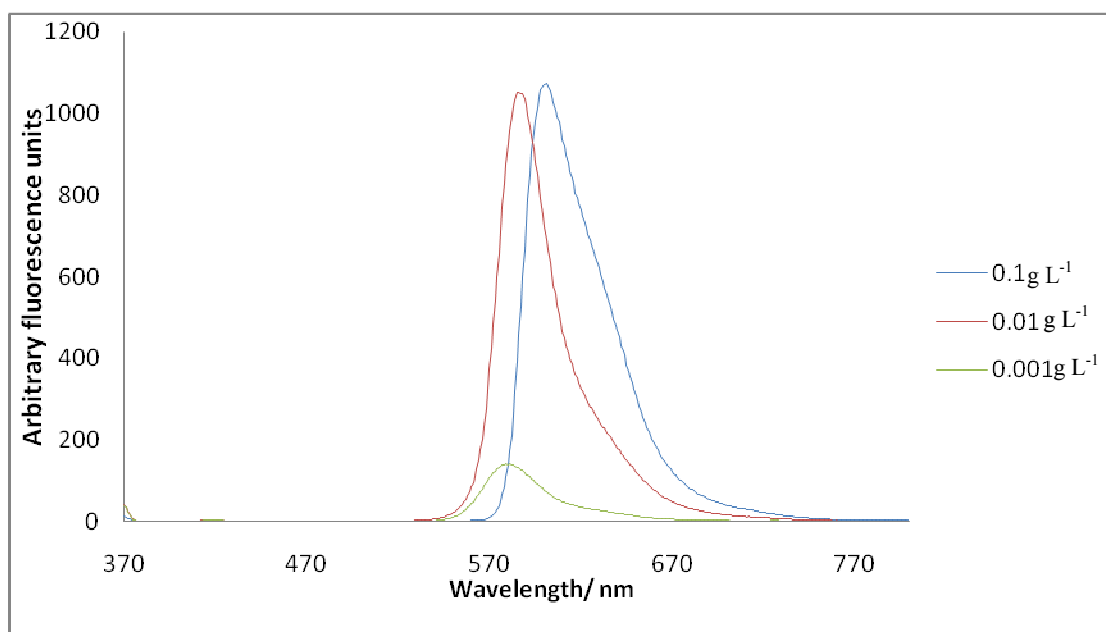


Peak No.	Wavelength/ nm	Absorbance
1	553.50	0.924
2	353.50	0.066
3	304.00	0.114
4	282.50	0.129
5	258.00	0.248
6	224.50	0.214
7	445.00	0.005
8	378.50	0.013
9	328.00	0.021
10	297.50	0.112
11	274.50	0.122
12	243.50	0.172
13	217.00	0.206

Figure 7.5 UV spectrum of 0.01 gL⁻¹ aqueous solution of RB

RB emission occurs in the region 550 to 670 nm. As the concentration of the RB solution used to fill BEICs is increased, the peak emission wavelength in the range 550-700 nm (corresponding to the encapsulated RB) shifts to longer wavelengths. However, this observation is not particular to encapsulated RB, but also occurs in aqueous solutions (see Figure 7.6). This observation might be caused by the fluorescence re-absorption between rhodamine B molecules.^{109, 110} This shift is therefore not solely related to the presence of BEICs. Furthermore, the proportion of

BEICs' emission quenched by encapsulated RB increases as the concentration of the RB solution used during encapsulation was increased. This suggests more energy should be absorbed by or transferred to encapsulated RB from BEICs. Therefore the interaction between BEICs and RB should shift the RB peaks to higher frequency. However, the fact that this does not happen supports the argument that the presence of BEICs has either a very limited, or no effect on the fluorescent behaviour of RB.



Concentration of RB solution (g L ⁻¹)	Peak emission wavelength (nm)
0.1	601
0.01	586
0.001	579

Figure 7.6 Emission spectra of aqueous solutions of RB at different concentrations. Excitation wavelength 365 nm.

7.1.1 Conclusion

In conclusion, BEICs from different production batches display broadly similar emission spectra, despite appearing slightly different colours by visual inspection. BEICs display more intense emission compared to untreated spores and unbleached EICs when examined under a UV lamp. RB filled BEICs show distinct emission peaks arising from both BEICs and RB. As the concentration of RB solution used to fill BEICs was raised, the emission of encapsulated RB exines shifts to longer wavelengths. Simultaneously, the longer wavelength components of the EICs' emissions are quenched. Overall, the influence on the emissions between BEICs to RB is very weak,

and the fluorescent properties of the RB filled BEICs is mainly decided by the encapsulated RB. Therefore, *via* the incorporation of fluorescent dyes, BEICs could be good materials for the production of fluorescent microparticles.

7.2pH responsive microparticles based on exine and intine capsules

Devices, or materials, that give an optical response as a function of changing pH value are useful in many areas of the chemical and biological sciences. Modern pH indicators can be divided into two groups that are digital pH indicators and chemical-based indicators. Digital pH indicators can measure almost all pH conditions with better precision than chemical-based indicators, but their relatively expensive price makes the chemical-based indicators still popular in scientific experiments. However, the practical applicability of many the commercially available chemical-based pH indicators is limited by the fact that such devices are relatively large (< 1 cm) and typically show a non-reversible response to changes in pH.

It was, however, anticipated that an BEIC-based, and therefore micrometer sized, pH responsive material could be realized via the encapsulation of a suitable pH responsive material. The approach taken in order to produce pH responsive BEICs, in addition to the responsive properties of the resulting materials, is discussed in the sections that follow.

7.2.1 Approach

pH Responsive materials usually respond to pH by altering their colour appearance. Therefore, for an encapsulated system to be useful it must be transparent and allow for chemical exchange between the outer and inner environment. BEICs were found possess both of these properties, so it was anticipated that they could exhibit a particle colour change on change in pH.

Phenolphthalein is a cheap and commercially available pH responsive material. It undergoes a continuous change in appearance from colourless to purple within the pH range of 8-10, also its structure is altered from non-ionic to ionic with increasing pH, thereby resulting in a change of colour (see Figure 7.7).¹¹¹ Also, the colour change is found to be reversible as the pH changes. It was therefore anticipated that the encapsulation of phenolphthalein would result in BEICs that exhibited an optical response in response to changes in pH.

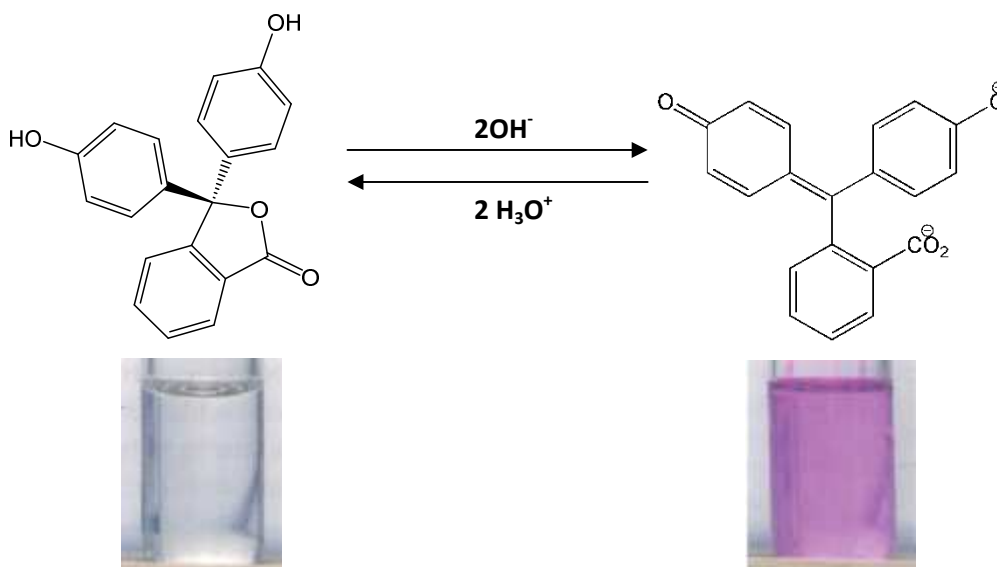


Figure 7.7 Molecular structure altering and optical observation of phenolphthalein in the pH 8-10.

Thus, phenolphthalein was encapsulated in BEICs *via* the suspension method. After encapsulation, the product appeared as white powder and none of the non-encapsulated phenolphthalein was observed *via* visual inspection (see Figure 7.8).



Figure 7.8 The appearance of phenolphthalein based pH responsive BEICs (pH-EICs).

When analyzed by light microscopy (Figure 7.9), the dry phenolphthalein filled EICs (pH-EIC) are similar in appearance to empty BEIC in both transmissive and reflective modes. However, as can be seen in Figure 7.9a, small, unencapsulated particles surround the filled BEICs. These particles are likely to be non-encapsulated phenolphthalein that was not successfully removed by the washing process. Owing to the small sizes of these crystals and their poor reflectivity, the particles were not observed in reflective modes (Figure 7.9b).

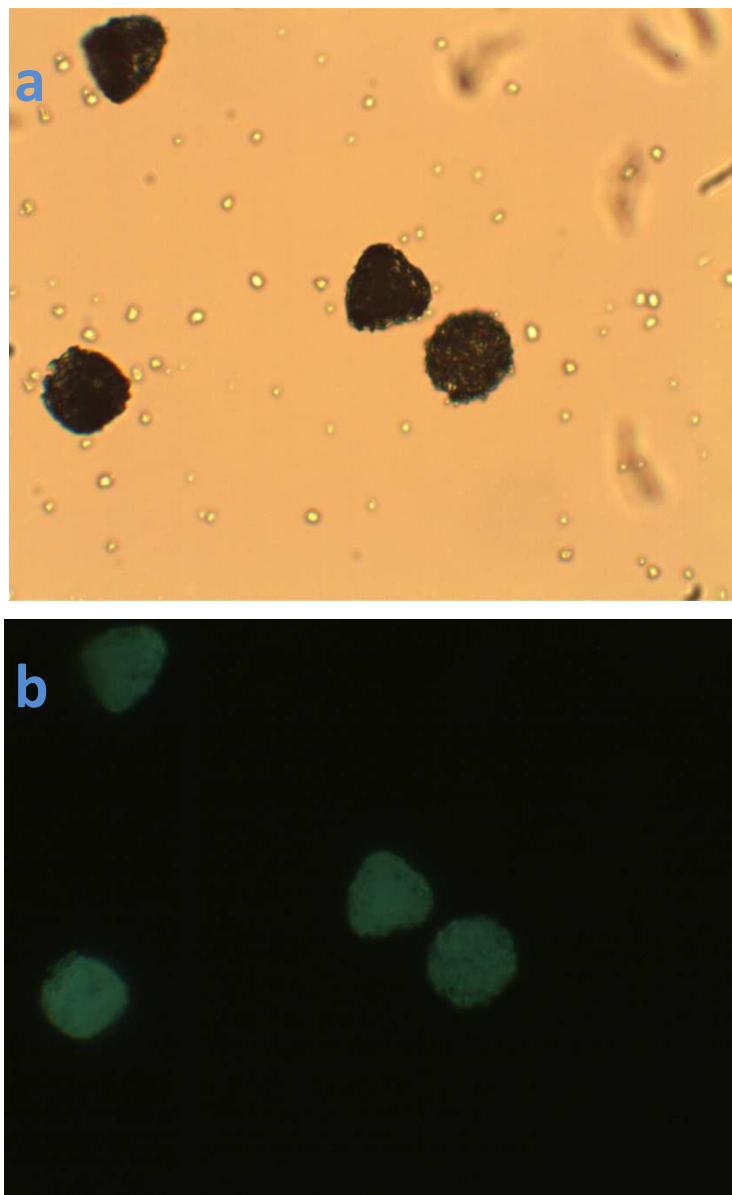


Figure 7.9 Photomicrographs of dry phenolphthalein filled BEICs, a) parallel polars in transmissive mode and b) crossed polars in reflective. (x400)

Preparations of the pH-EICs suspended in deionized water exhibited a pink appearance when observed microscopically, as shown in Figure 7.10, thereby implying that the surround environment is not at pH 7, as expected, but instead is basic. It is possible that this observation could be due to the presence of residual sodium hypochlorite used in the production of BEICs. Alternatively, the interactions between encapsulated phenolphthalein and the BEICs possibly result the pink colour due to the ionic properties of sporopollenin. The reason was clarified by an experiment that disperses empty BEICs in phenolphthalein aqueous solution (see Figure 7.11). The image shows that the solution of phenolphthalein was turned to pink after the addition of empty

BEICs, which indicates that the major reason for the unusual pink colouration is the presence of remaining sodium hypochlorite. Fortunately, the pH response of the pH-EICs is not apparently affected by this residual basic contaminant.

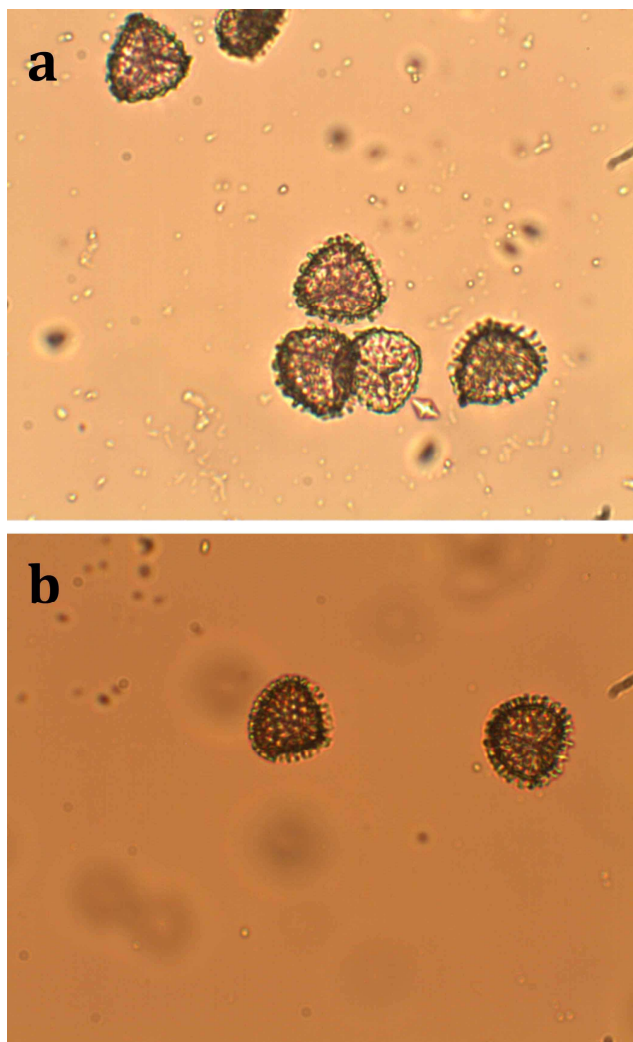


Figure 7.10 Photomicrographs of a) pH-EICs and b) BEICs suspended in deionized water. (x400).



Figure 7.11 The appearance of BEIC in an aqueous solution of phenolphthalein after shaking.

The dry pH-EICs were added to an aqueous solution of NaOH (pH 9) and their

appearance quickly changed from white to pink (Figure 7.12). However, the change in colour of the BEICs was accompanied by a change in the appearance of the solution from colourless to an intense pink colour. Owing to the intensity of the resulting colour of the solution it can be inferred that this change is probably not exclusively caused by the non-encapsulated phenolphthalein, but also via leaking of the encapsulated material from the pH-EICs.



Figure 7.12 Photograph of pH-EICs in pH 9 solution.

In order to further investigate this effect, the experiment was repeated and observed via microscopy (see Figure 7.13). Pink was only observed in the pH-EICs, but not in the solution. However, these differing observations may be caused by the thin sample preparation. Therefore, another experiment was performed in which the pH-EICs were pressurised by gently pressing the cover slip while in an aqueous NaOH solution (pH 9). The pink content of the pH-EICs disappeared after pressing (see Figure 7.14). This observation indicates phenolphthalein is released from the BEICs, thus it likely suggests the chemical interaction between phenolphthalein and BEICs is weakened by the presence of base or by the change in chemical structure of phenolphthalein, otherwise the BEICs should still appear pink

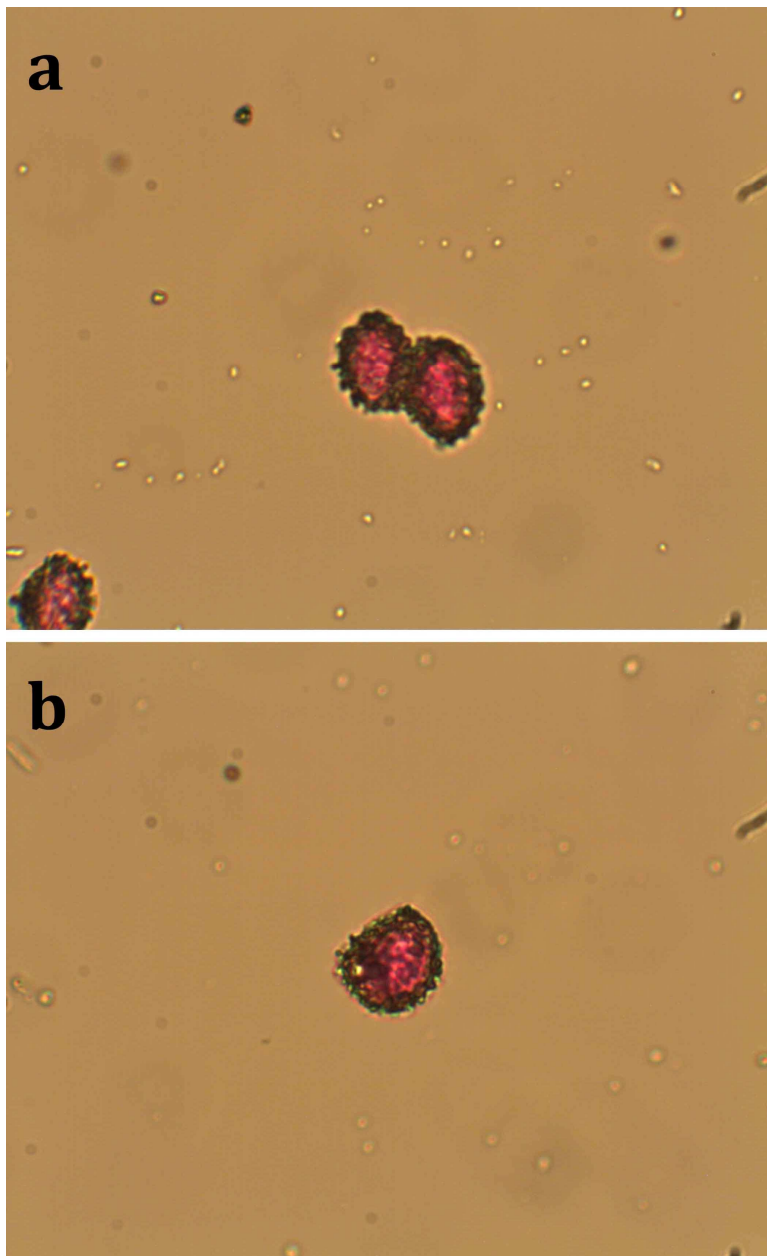


Figure 7.13 Photomicrographs of pH-EICs in a NaOH aqueous solution (pH 9). (x400)

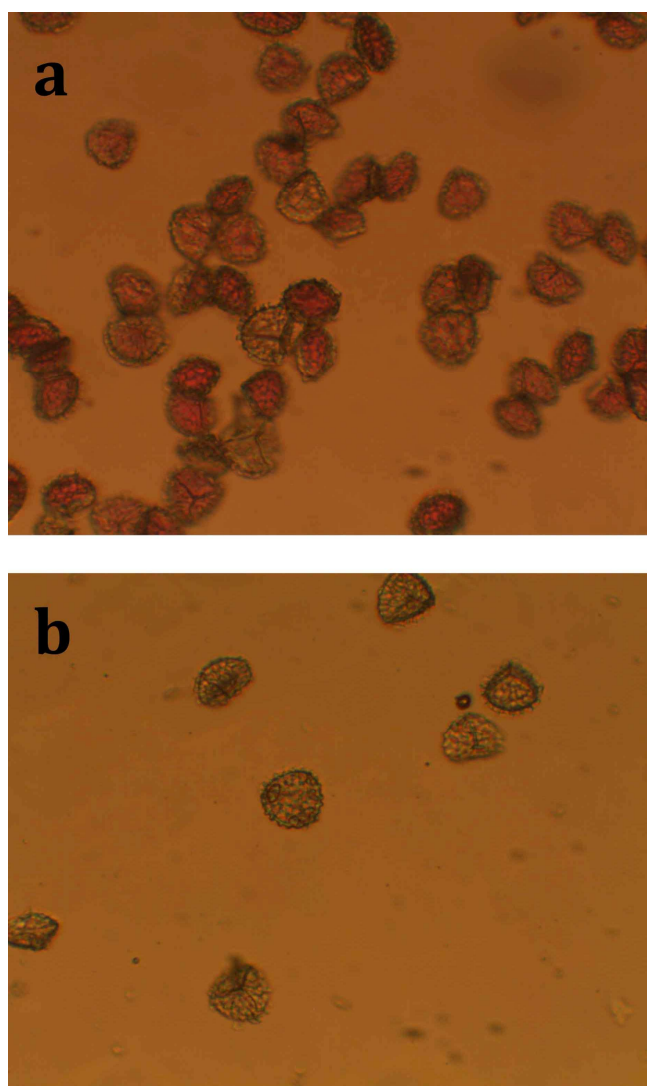


Figure 7.14 Photomicrographs of pH-EICs; a) before pressing, and b) after being pressed.
(x100)

The change in the chemical structure of phenolphthalein is reversible, and this reversibility is maintained after it is encapsulated into BEICs. The reversibility of pH-EICs was demonstrated experimentally by adding aqueous HCl solution (pH 4) to these microcapsules in an aqueous NaOH solution (pH 9) until the solution became colourless (pH6). As expected, all of suspended pH EICs turned colourless when the colour of solution changed as shown in Figure 7.15.



Figure 7.15 Photograph of an aqueous solution (pH 6) with pH EICs suspended.

This experiment was also repeated under microscopy. After a droplet of HCl solution (pH 1) was added to the sample (same microscopic sample used in Figure 7.13), the pH EICs became completely colourless after 1-3 minutes (see Figure 7.16). The time delay may be related to slow diffusion of the HCl solution or by the ionic influence from the EICs.

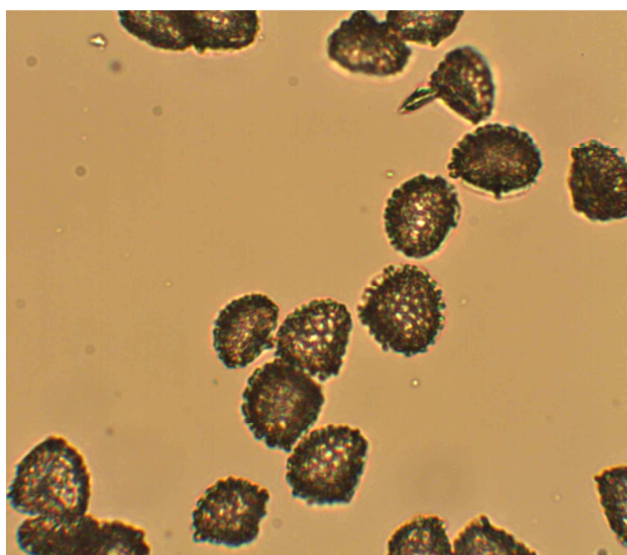


Figure 7.16 Photomicrographs of pH-EICs in a solution after the pH was changed from 9 to 6.
(x200)

7.2.2 Conclusion

pH-EICs were successfully prepared based on the encapsulation of phenolphthalein. Moreover, the pH-EICs show the potential for being recyclable, due to the reversible properties of phenolphthalein, although the lifetime of the process has not yet been determined. As with the successes of multi-functional materials encapsulation (e.g black EICs), pH-EICs have the potential to incorporate other pH responsive materials (e.g. methyl red) by encapsulation, thereby expanding the range of pH-EICs available.

However, a disadvantage of these pH-EICs is also apparent. The ionic interactions between the encapsulated phenolphthalein and the EICs appears to be weakened by the presence of base, and leaking therefore occurs during colour change. This can be largely avoided by gentle handling, as evidenced by the fact that the majority of the leakage occurred only after pressurisation when observed *via* light microscopy. Alternatively, functionalization of the sporopollenin may solve this problem permanently.

7.3 Temperature responsive EICs based on a Leuco dye

The main response of temperature responsive BEIC (named as TCS, thermochromic spores) to temperature stimuli is colour change, a phenomenon that is very easy to observe. The colour appearances of TCS are derived from leuco dyes, a type of compound that can exist in two forms. Crucially, these two forms result from the rearrangement of the molecular structure in response to external stimuli. The rearrangement causes a colour change that can be easily observed as one form is usually colourless and the other is not. However, in order for a leuco dye to alter its molecular architecture as a function of temperature two additional components are usually required; a solvent, and an H⁺ donor. Thus, in this case the thermochromic function of a leuco dye, and consequently of TCS, is actually performed by the interaction of three components. The objective of incorporating leuco dyes into exines is to use the oxidative protection of the exine to prevent the dyes from deteriorating. In the first instance the possibility of encapsulating a leuco-dye system into exine shells and eliciting a thermochromic response was investigated.

The leuco dye used in this study is crystal violet lactone, which in the presence of phenolphthalein (H⁺ donor) and hexadecanol (solvent) exhibits a colour change from blue to colourless in response to temperature stimuli. This mixture exists in its leuco form (blue) at room temperature due to the H⁺ donated by phenolphthalein. As such, the TCS are also blue at room temperature. Furthermore, the TCS appears to be different strengths of blue depending on the amount of the compounds encapsulated and the amount will vary with the encapsulation method used (Figure 7.17 a and b).

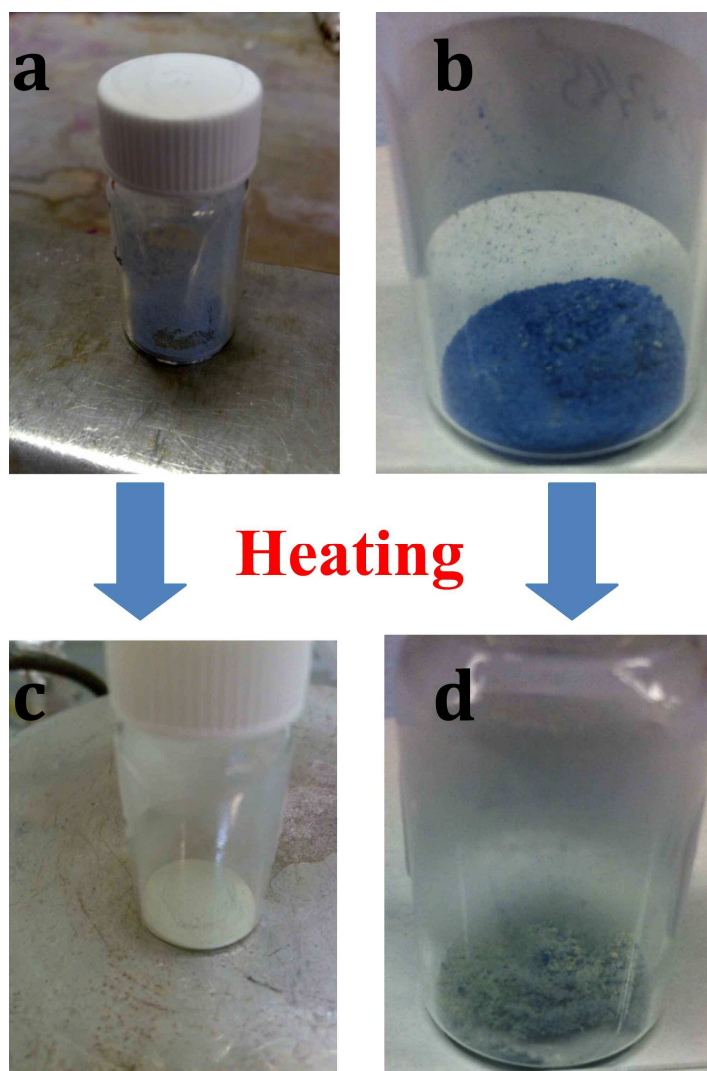


Figure 7.17 Photographs of a) TCS-1 and b) TCS-2 at room temperature, and c) TCS-1 and d) TCS-2 after the thermal stimuli.

The sample of TCS shown in Figure 7.17a is TCS-1. In the procedure, the crystal violet lactone, phenolphthalein and hexadecanol are encapsulated by the BEICs without the use of an additional solvent. The hexadecanol acts as the solvent, dissolving the other two components, allowing them to be encapsulated by BEICs. Conversely, the TCS shown in Figure 7.17b is TCS-2. To produce it, all three components were dissolved in acetone prior to encapsulation. The use of acetone as a solvent results in a much higher uptake of the components by the BEICs compared with encapsulation in the absence of an additional solvent. However, the amount of hexadecanol encapsulated by BEICs with acetone is less than without it. As a result, TCS-2 appears to be much more vivid blue in colour than TCS-1.

After temperature stimuli, both TCS-1 and TCS-2 experience a colour change, but to

various degrees as shown in Figure 7.17c and d. The observed colour change of TCS-1 is much more pronounced than for TCS-2. For TCS-1, the encapsulation procedure used hexadecanol as the solvent, and so some of it would be expected to remain inside of the BEIC even after washing with small amounts of organic solvent. Moreover, crystal violet lactone and phenolphthalein are evenly dispersed in hexadecanol before and after encapsulated by BEICs. This even dispersion is maintained upon crystallization of the hexadecanol, allowing the components to be dissolved easily upon subsequent heating. This resulted in a sharp and total colour change, with all TCS-1 particles turning white when the temperature stimuli exceeded the melting point of hexadecanol.

In contrast, TCS-2 utilized acetone as the encapsulation solvent and carrier. During the encapsulation, crystal violet lactone and phenolphthalein are both ionic and have ionic interactions with sporopollenin. This interaction allows the two compounds to be easily retained by the BEICs after uptake. However, alcohols normally have poor affinity to sporopollenin because of the absence of ionic interactions. Therefore, only a small amount of the hexadecanol may be retained inside the BEICs after encapsulation. This results in a low hexadecanol/leuco dye ratio within the BEICs, and there is not enough hexadecanol present to dissolve the other two compounds when heated beyond the melting point. As the molecules of crystal violet lactone and phenolphthalein cannot fully interact with the 1-hexadecanol, the sample does not go completely white. Although crystal violet lactone and phenolphthalein both are white crystals at room temperature, their mixture is blue after dissolving in acetone, and the colour can be maintained after the acetone has evaporated.

The response to the thermal stimuli of TCS-1 and TCS-2 were also checked by light microscopy, see Figures 7.18 and 7.19. When TCS-1 was observed at room temperature, over half of the treated BEICs did not show the desired blue colour due to the absence of solvent (hexadecanol). The amounts of crystal violet lactone and phenolphthalein may not be great enough in these white BEICs, since part of them may gone with the hexadecanol after encapsulation. Moreover, the washing process will have removed a portion of the encapsulated compounds. However, the washing process is an essential step that cannot be bypassed. Despite there being a mixture of filled, partially filled and unfilled BEICs, the normal inspection of the entire sample is not affected, and the appearance is still blue as shown in Figure 7.17a.

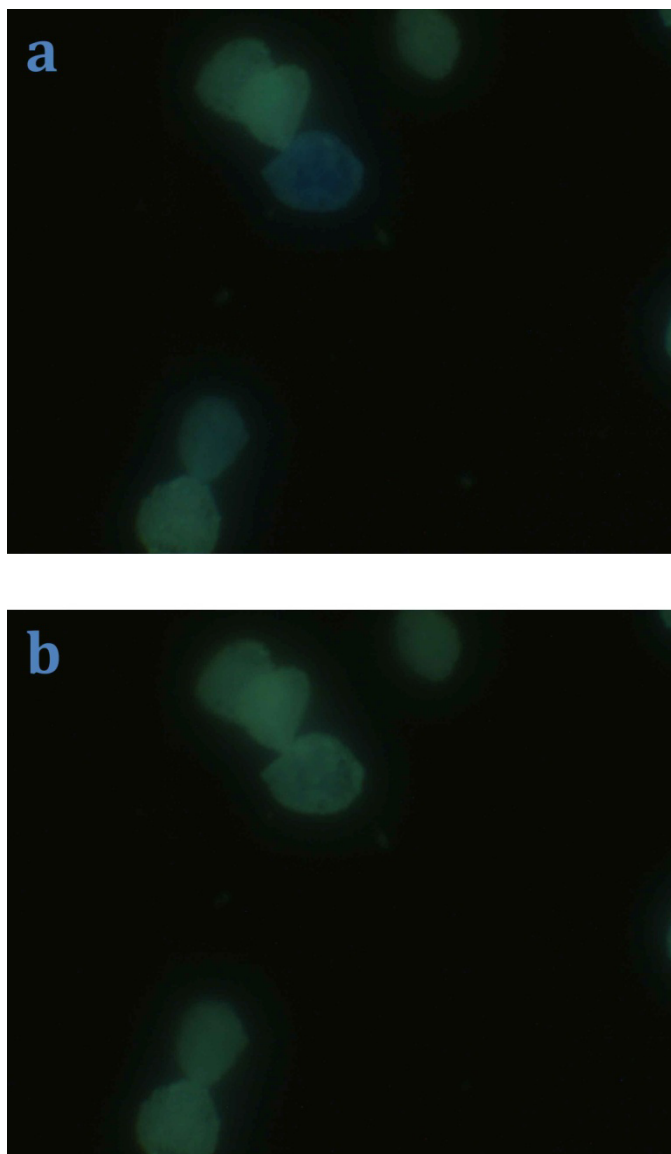


Figure 7.18 Photomicrographs of TCS-1 in reflective mode with crossed polars. a) TCS-1 at room temperature and b) TCS-1 at 55 °C. (x400)

In comparison to TCS-1, most of the BEICs in TCS-2 exhibit a blue colour at room temperature under the microscope, although the colour varies in intensity (see Figure 7.19). The colour change of some TCS-2 BEICs upon heating is not very pronounced, giving only a slight reduction in the intensity of the blue. This is due to the low uptake of hexadecanol and the resulting failure for the crystal violet lactone and phenolphthalein to become dissolved. This non-pronounced colour change, found by microscopy, can be used to explain why TCS-2 retains some blue colour when heated beyond the transition temperature under normal inspection (see Figure 7.17d).

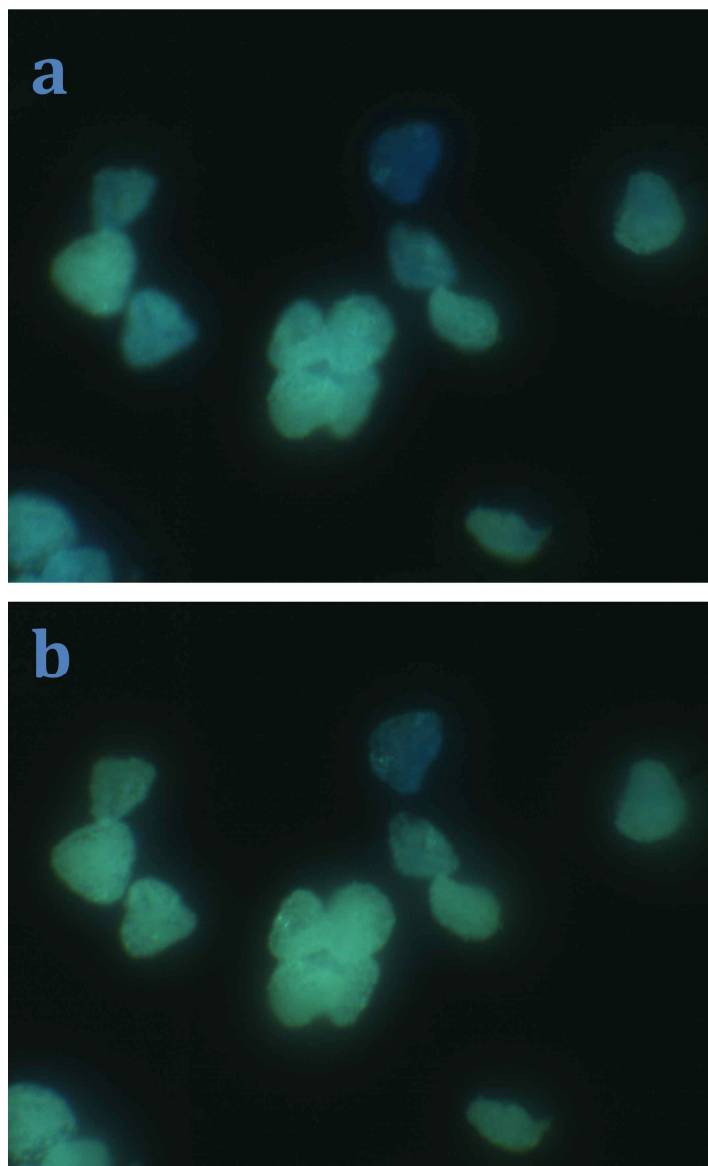


Figure 7.19 Photomicrographs of TCS-2 in reflective mode with crossed polars. a) TCS-2 at room temperature, and b) TCS-2 at 55 °C. (x400)

The thermochromic transition temperatures of TCS-1 and TCS-2 were carefully determined by microscopy. Figure 7.20 very clearly shows the change observed for TCS-1 when the temperature is increased. The change started at 43 °C with a very slight colour change (compare with the image taken at 42 °C). The TCS-1 BEICs became gradually less coloured until the temperature reached 46 °C, at which point the treated BEICs became white. As the first obvious change observed was at 44 °C, this point is considered to be the thermochromic transition temperature for TCS-1. The same experiment was carried out for TCS-2 (Figure 7.21). The only colour change for the TCS-2 BEICs was observed at 44 °C, and the change was only slight with a reduction in the intensity of the blue colour. After heating beyond 44 °C, TCS-2 maintained the blue colour with the same intensity. The thermochromic transition temperature of TCS-2 is

therefore confirmed as 44 °C, which corresponds with that of TCS-1. It also shows the transition temperature of TCS is not affected by the encapsulation method.

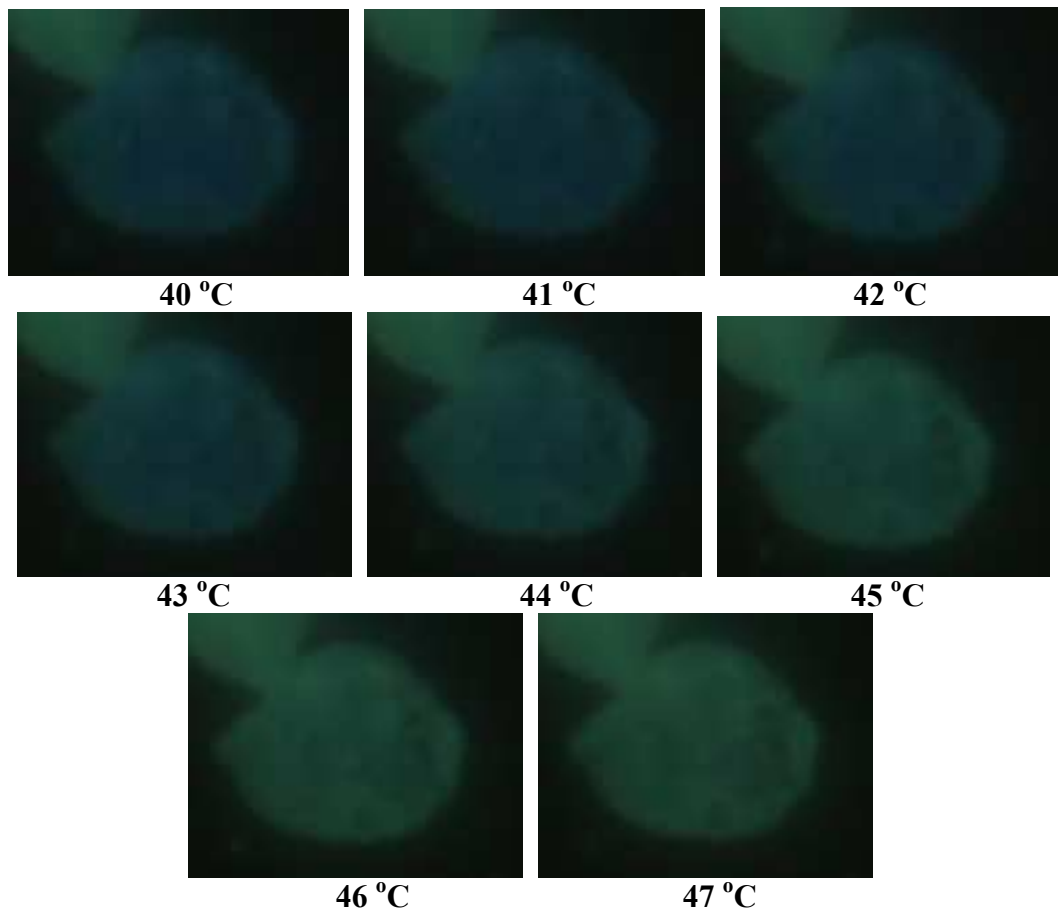


Figure 7.20 Photomicrographs of TCS-1 across a temperature range in reflective mode with crossed polars.

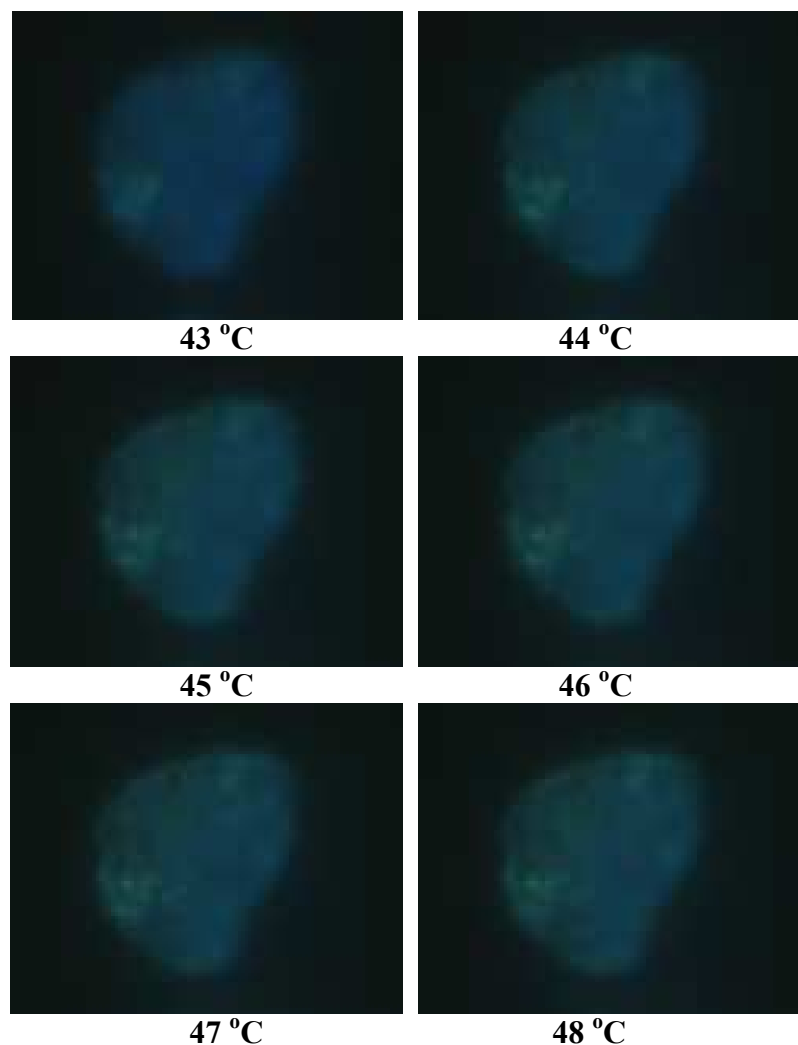


Figure 7.21 Photomicrographs of TCS-2 across a temperature range in reflective mode with crossed polars.

When TCS-2 was cooled below the transition temperature, a small proportion of the treated BEICs did not return to their blue state. An experiment was carried out to determine the reversibility of thermochromism of TCS-2. Four samples of TSC-2 were heated to 40, 60, 80 and 90 °C respectively, and held at that temperature for an hour. The results are shown in Figure 7.22. As expected, the reversibility of the colour change degenerated quickly as the temperature was increased. The sample that was heated to 40 °C is the only one did not show degeneration, however, this is below the transition temperature. The samples that were heated to 60 and 80 °C showed some degree of degeneration and most of the sample lost all reversibility when heated to 90°C for an hour.

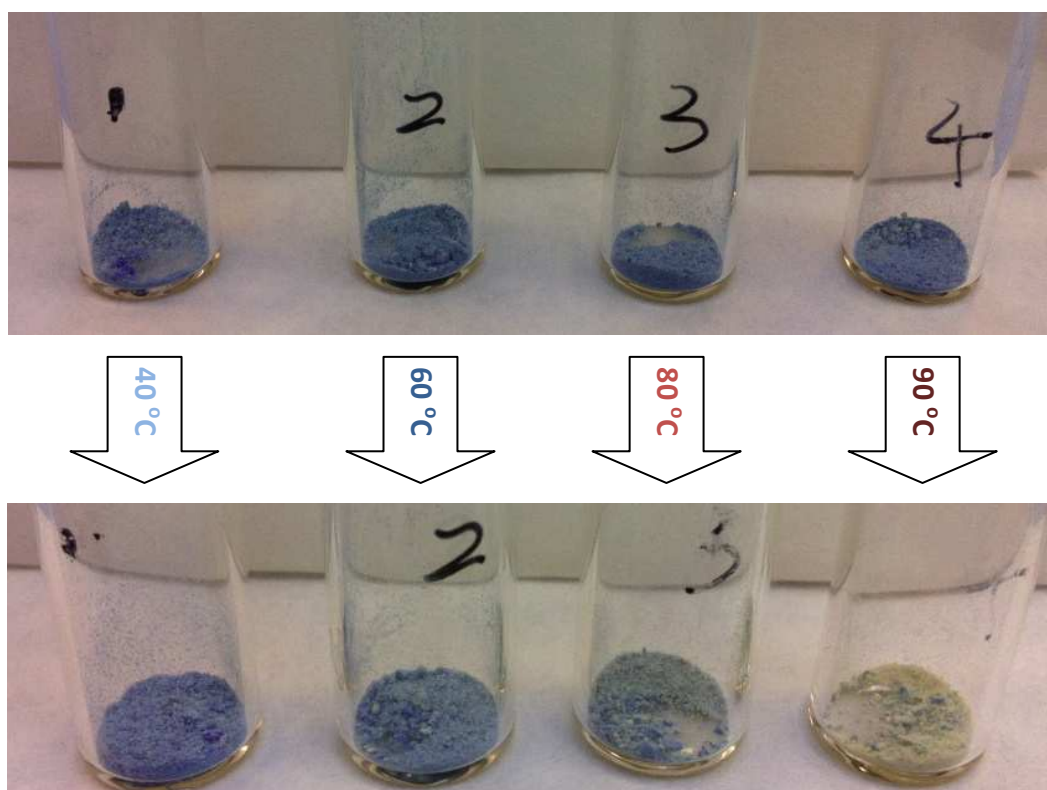


Figure 7.22 Four samples of TCS-2 were heated at different temperature for 1 h, all photographs were taken at room temperature.

From microscopy, a more accurate observation can be made, as shown in Figure 7.27. TCS-2 was observed by light microscopy with crossed polars in reflective mode. This mode relies on light being reflected by the sample, so it can be viewed and the transparency of the sample indicates the intensity of light reflected. When the TCS-2 BEICs were heated to 50 °C, the blue appearance was changed, resulting in a white outer circle containing a black centre. This is a result of the centre of the BEIC becoming completely transparent. It is believed that the melting of hexadecanol at 50°C causes wetting of the BEIC, as it is the only compound that can melt at this temperature among the compounds encapsulated. The wetting of the BEIC allows light to pass through it completely and be transmitted.

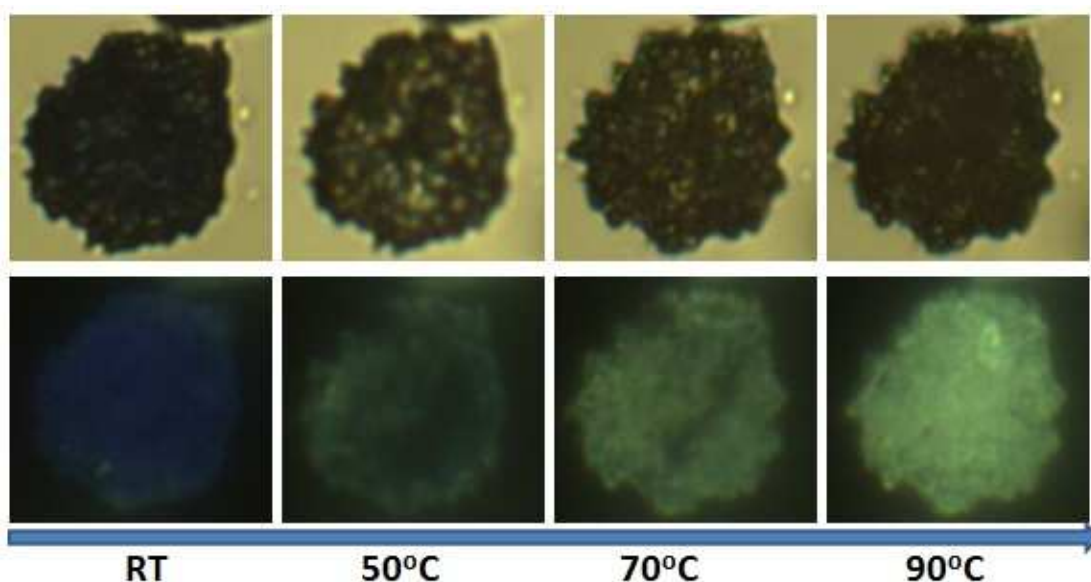


Figure 7.23 Photomicrographs of TCS-2 across a temperature range from room temperature to ninety °C. The upper images were taken in transmissive mode with parallel polars, and the lower images were taken in reflective mode with crossed polars.

Upon heating to 90 °C, this transparency disappears and the treated BEICs appear white. This is a result of the hexadecanol no longer wetting the BEIC. Despite being below the boiling point of hexadecanol, it is believed this volatile liquid evaporates readily at these elevated temperatures. This is confirmed by the presence of hexadecanol condensation on the inner surface of the sample vials (see Figure 7.17d). This can also explain the degeneration of thermochromic reversibility of TCS-2. The reduction of hexadecanol reduces the amount of crystal violet lactone and phenolphthalein dissolved, so the colour reversibility degenerates as the temperature and time of heating are increased.

The reversibility of the colour change for TCS-2 slightly degenerated after heating to 60 °C for 1 hour. Experiments were carried out to determine if the degeneration at this relatively low temperature was time dependant. Five samples of TCS-2 were heated to 55 °C for 2, 4, 8, 12 and 16 h, respectively in a sample cell. Figure 7.24 shows that all of the specimens of TCS-2 were reversible after cooling to room temperature from 2 h at 55 °C. This result is obviously different with respect to the experiment in which TCS-2 is heated to 60 °C for an hour (see Figure 7.22) When TCS-2 is heated to 60 °C for an hour, the blue appearance of some of the treated BEICs are weaker in colour than before they were heated.

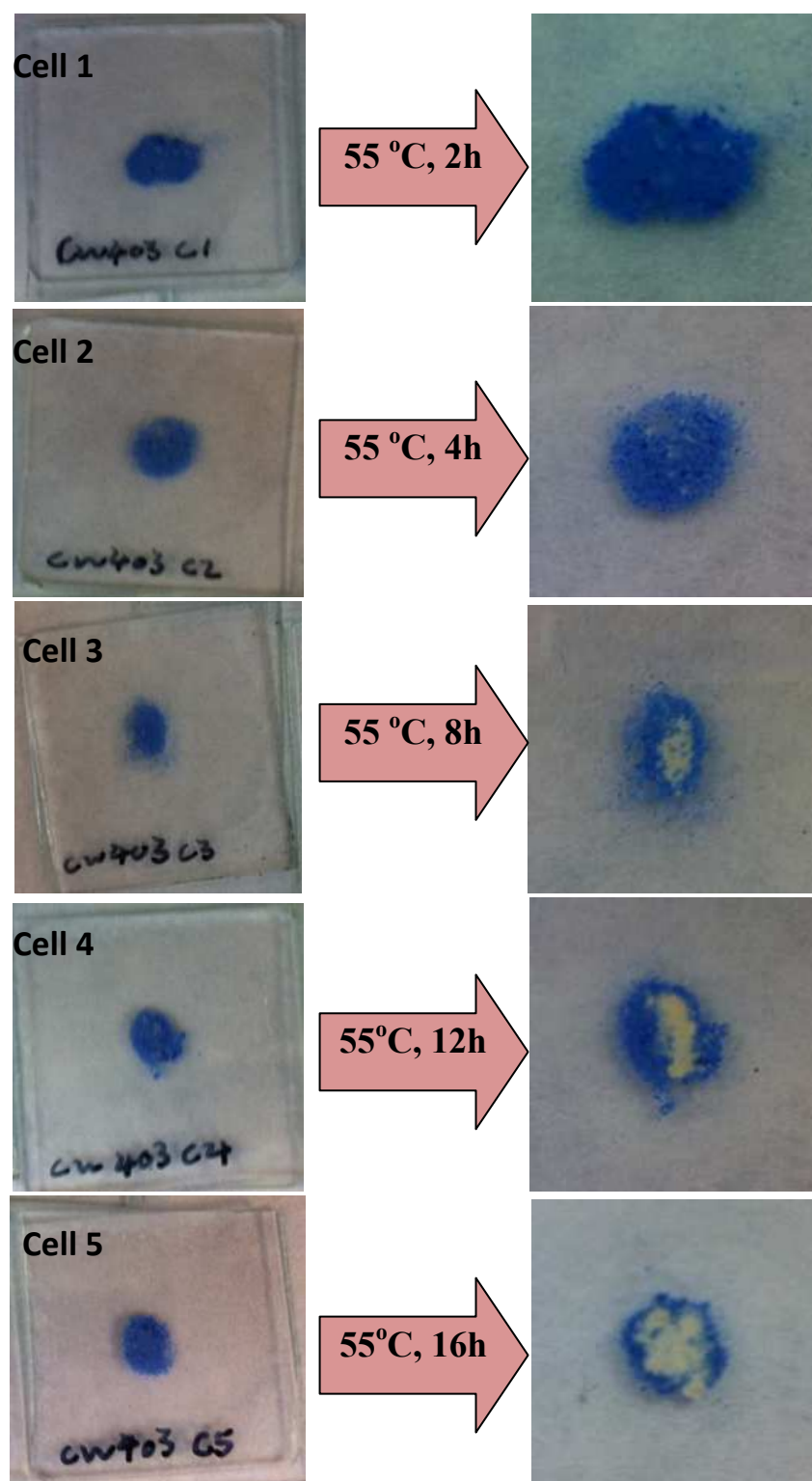


Figure 7.24 The comparison for the TCS-2 samples before and after being heated at 55 °C for different lengths of time. All of the photographs were taken at room temperature.

In the initial experiment, the sample was placed in a normal sample vial, any hexadecanol that evaporated was found to crystallize on the inner surfaces of the sample vial as shown in Figure 7.17d. However, when a sample is placed in a cell, there is more containment of volatile substances that have leached out of the BEICs. Therefore, it is

proposed that in the “cell” experiments, the path of hexadecanol is very similar to that with reflux. It is evaporated by heating and crystallizes on the upper cover of the cell. The solid on the upper cover is then melted again by heating, and due to the very small gap between the BEICs and the cell surface, the melted hexadecanol is drawn back into the BEICs. Therefore, the hexadecanol inside of BEICs does not experience a reduction in quantity after 2 h of 55 °C heating in cell, and therefore the reversibility is maintained better than 1 h of 60 °C heating in a sample vial.

After heating for 4 h, i.e. for cell 2, a few white dots appeared in the sample, but most of the BEICs still maintained their reversible behaviour, see Figure 7.24. For Cell 3, after 8 h of heating some of treated BEICs in the middle region of sample are no longer able to show reversal from white to blue at room temperature. The irreversible area increases as the heating time is extended (Figure 7.24 cells 4 and 5). It was noticed that the irreversible areas in Figure 7.24 for cells 3, 4 and 5 were always located in the middle of the sample, whereas for the TCS-2 BEICs at the edge of the sample reversibility is maintained. This may be the result of the evaporation of hexadecanol. For instance, after heating, the hexadecanol evaporates and the vapor moves upward. However, the upper surface of the cell forces the evaporated hexadecanol to move in the plane of the cell as shown in Figure 7.25a. Thus the result is depletion of hexadecanol from the centre of the specimen that becomes white at the centre, in comparison to the edges which still exhibit a blue colour.

These experiments suggest that the stability of TCS-2 can be affected by the mechanics of the loss of hexadecanol by evaporation. For instance, the movement of the evaporating hexadecanol described previously is achievable only when the cell is laid flat (horizontal). However, when the direction of the cell is changed, the direction of the evaporated hexadecanol will change too. For example, when the orientation of the cell is changed from horizontal to vertical, the direction of evaporating hexadecanol will flow along the centre of the cell as shown in Figure 7.25b). In case, the reversibility of TCS-2 BEICs in the upper region of the cell degenerates slower than the lower region, and as a consequence the irreversible area expands from bottom to top.

These observations suggest that it might be possible to use TCS as a temperature marker by measuring the size of the irreversible area, the time for which the TCS has been heated at a given temperature can determined. Such a relationship could be used as the

basis for a device to evaluate the storage history for food and drugs.

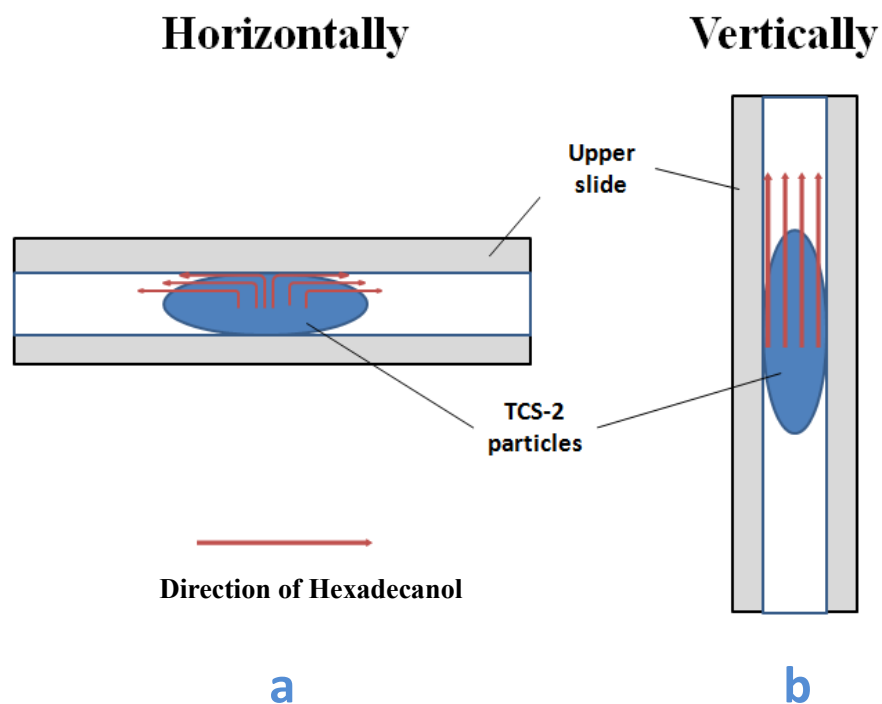


Figure 7.25 Illustration for the directions of evaporating hexadecanol movement in a cell with different orientations; a) the cell laid flat, b) the cell laid vertically.

It has been shown that the thermochromic nature of the TCSs is lost by evaporation of hexadecanol. Therefore theoretically, this ability should be reinstated by re-filling with hexadecanol. In order to confirm this, a TSC-2 sample was heated until the colour reversibility was lost, then suspended in hexadecanol/acetone solution; the sample was dried in air without application of the washing process and labelled as refTCS-2. The entire sample reverted to blue upon removal of the acetone (see Figure 7.26) and it again exhibited colour reversibility (see Figure 7.27). The sample was heated to 60 °C and showed a colour change from blue to white upon cooling to room temperature. The leuco form of refTCS-2 is quite pure with no blue particles found in the photographs due to there being an excess of hexadecanol.

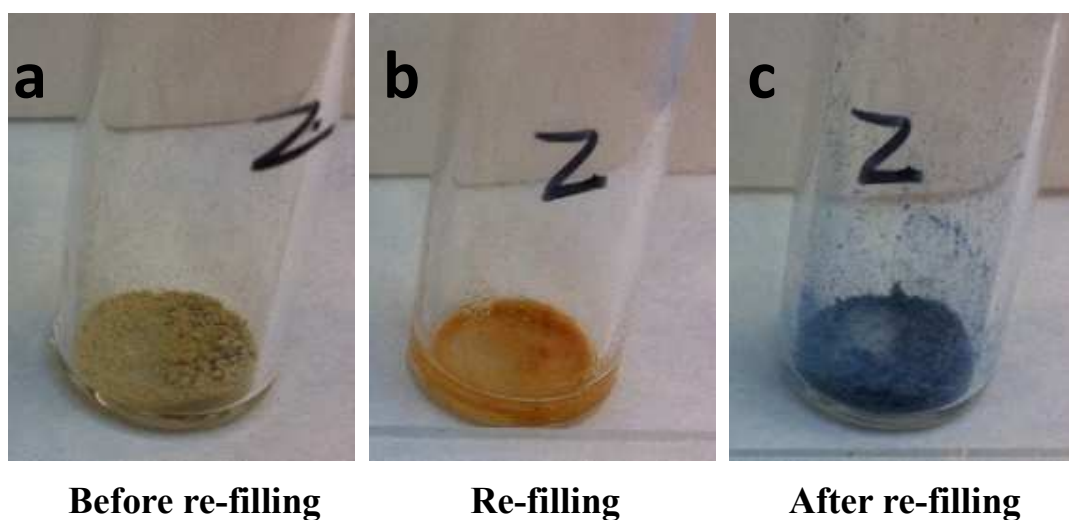


Figure 7.26 Re-encapsulation of 1-hexadecanol to regenerate irreversible TCS-2 BEICs.

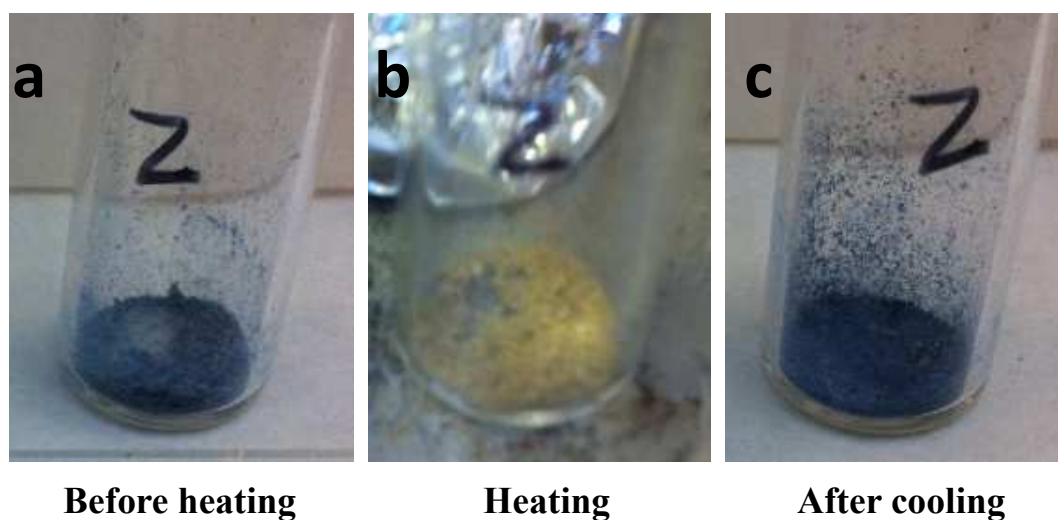


Figure 7.27 Test for the thermochromic reversibility of refTCS-2, a) and c) were taken at room temperature, and b) was taken at roughly 60 °C.

Another experiment was performed in order to determine if any hexadecanol remains on the surface of TCS-2 that has lost thermochromic reversibility. A sample of TCS-2 was heated until the colour reversibility was lost, and then it was suspended in acetone. The solvent TCS-2 was then allowed to evaporate in air to give restored TCS (named as resTCS-2 in this study). Similarly with refTCS-2, resTCS-2 showed reversibility to blue, see Figure 7.28. Subsequently, resTCS-2 was heated to 60 °C and cooled to room temperature (see Figure 7.29). The resTCS-2 BEICs are partially changed to white when heating, but some of them remain blue due to the absence of hexadecanol. This result proves the hypothesis that some of the hexadecanol remains on the surface of resTCS-2, although these TCSs have lost their thermochromic reversibility by heating. Therefore,

the degeneration of the reversibility of TCS-2 is not only due to the disappearance of hexadecanol by evaporation, but also the phase separation of hexadecanol from crystal violet lactone and phenolphthalein.

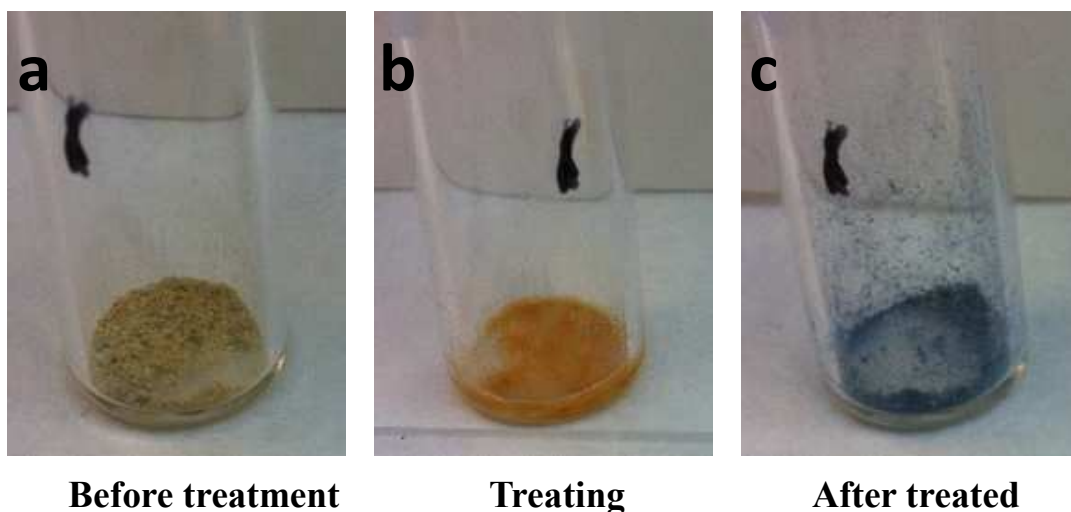


Figure 7.28 Irreversible TCS-2 treated with acetone; a) Irreversible TCS-2, b) Irreversible TCS-2 was suspended in acetone without hexadecanol, and c) resTCS-2.

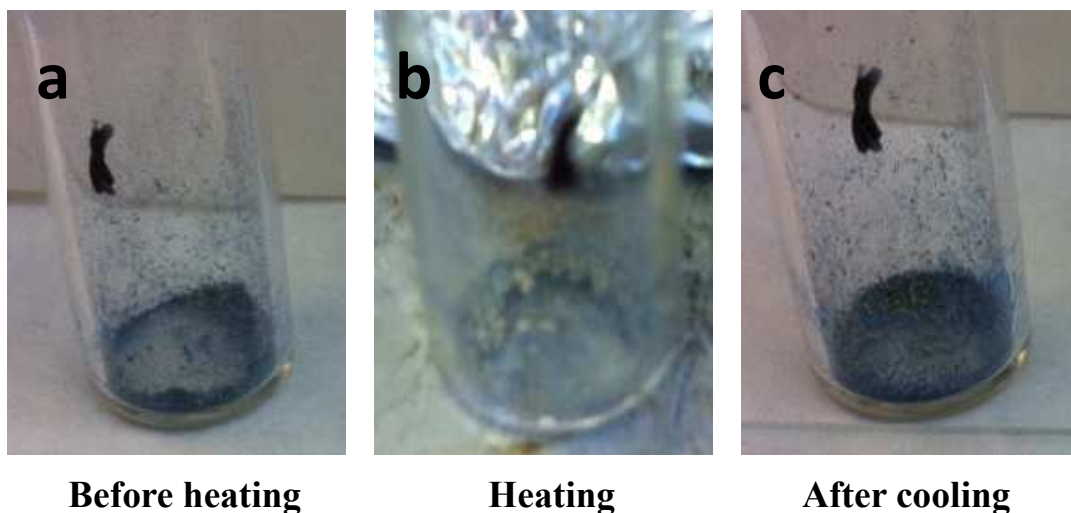


Figure 7.29 Test for the thermochromic reversibility of resTCS-2; a) and c) were taken at room temperature, and b) was taken at roughly 60 °C.

The results show that TCS-1 has a longer life-time than TCS-2, but the thermochromic reversibility still degrades. Figure 7.30 shows contrasting photographs of a TCS-1 sample before and after 2 years. The colour intensity of the sample after two years is obviously weaker than before. Whatever the encapsulation method applied, the thermochromic reversibility degrades on exposure to heat and over time. Fortunately, they can be regenerated and re-used after re-filling and re-location of 1-hexadecanol.

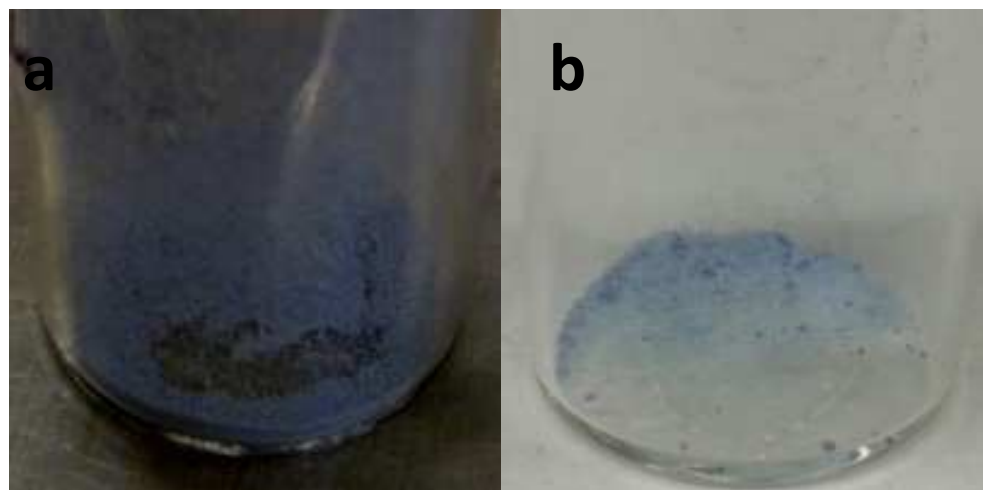


Figure 7.30 Photographs of the same TCS-1 sample, a) before and b) after 2 years.

7.3.1 Conclusion

TCS-1 and TCS-2 were found to be responsive to thermal stimuli, and the temperature at which the colour change occurred was not sensitive to the method of preparation. However, the encapsulated 1-hexadecanol was found to evaporate when the TCSs were heated causing degeneration of the reversibility of the colour effect. This problem was solved by re-filling and re-locating of the 1-hexadecanol in the TCSs. Also, a two year old TCS-1 sample demonstrated the strength of the colour of TCS slowly becomes weaker when it stored for a long time, although this sample was heated for many times during the two years.

7.4 Experimental

Fluorescent microparticles produced by rhodamine B encapsulated exine and intine capsules.

See Chapter 5, The RB encapsulated BEICs were directly analyzed by fluorometry without any further treatment.

Phenolphthalein encapsulate by BEICs

Phenolphthalein (0.7 g) was dissolved in ethanol (20 mL) and heated to 70°C. BEICs (0.1g) were added to the flask and stirred under reflux for 1 h. Then the filled spores were filtered and washed with ethanol (20 mL) and then water (20 mL) (x3). Finally, the product was washed with acetone (30 mL) and dried in a flow of air.

TCS-1

Leuco dye encapsulate by BEICs

1-Hexadecanol (3.5 g) was heated to 80°C until it melted. Crystal violet lactone (0.15 g) and phenolphthalein (0.2 g) were added to the hexadecanol and stirred until a solution resulted. The temperature of the solution was heated to 90 °C. BEIC (**BE-1**, 0.2 g) were added to the solution and the mixture was stirred overnight at 90 °C. Then the filled BEICs were filtered very quickly, and then carefully washed with ethanol (30 mL), acetone (30 mL), water(30 mL) and dichloromethane (30 mL). Finally, the product was dried in air.

TCS-2

Leuco dye encapsulate by BEICs with acetone

1-Hexadecanol (4.03), crystal violet lactone (0.11 g) and phenolphthalein (2.01) were dissolved in acetone (100 mL) and stirred at 50 °C until all of materials dissolved. BEICs (**BE-6**, 0.2 g) were added to the solution and the resultant mixture was stirred under reflux for 2 h. Then the filled EICs were filtered through a warm sinter funnel and washed with 10 mL acetone x2. Finally, the product was dried in air.

**8. Magnetic
Capsules Produced
by Doping Exine
Shells**

Magnetic nanoparticles and vessels have been studied extensively, owing to their usefulness for a variety of potential applications, such as drug delivery,^{112,113,114} mRNA isolation,¹¹⁵ information storage.¹¹⁶ In this chapter, two methods are applied to make EICs that are responsive to magnetic fields. Such EICs were created by the direct synthesis of a magnetic material inside the exine microcapsules using the “micro-reactor” method, or by doping of magnetic nanoparticles into or onto sporopollenin, which is called the “doping” method.

8.1 Synthesis of magnetic nanoparticles inside exine and intine capsules

Fe₃O₄ nanoparticles were chosen as the magnetic material to be encapsulated into EICs because, compared to other magnetic materials, their production is relatively simple, and the reactants are relatively cheap and readily available. Also, *Paunov et al.* have reported a successful case for the encapsulation of Fe₃O₄ into exine microcapsules.⁴⁴ In the experiment, FeCl₂ and FeCl₃ were encapsulated into Bleached EICs (BEICs) firstly, and then the salt encapsulated BEICs were added to ammonia solution after quick washing with deionized water. Finally, the magnetic particles encapsulated BEICs (Magnetic spores I, MS I) were washed with water and dried in air.

Figure 8.1 shows visual comparisons of dry BEICs, MS I, and their water suspensions. The encapsulation of Fe₃O₄ makes the BEICs turn to brown, which may be caused by the reaction of ammonia and/or the presence of Fe₂O₃. There is no direct evidence to verify if the colour change of the BEICs is caused by the introduction of an amino group, or if it is due to the formation of nanoparticles. However, an experiment has been carried out in which BEICs are reacted with diaminoethane. The BEICs change from white to brown and the introduction of an amino group is considered the only likely reason for the colour change in that experiment. Furthermore, although Fe₃O₄ is a black material, it may further oxidized to form Fe₂O₃, which is a brown red compound, after being encapsulated in BEICs.¹¹⁷

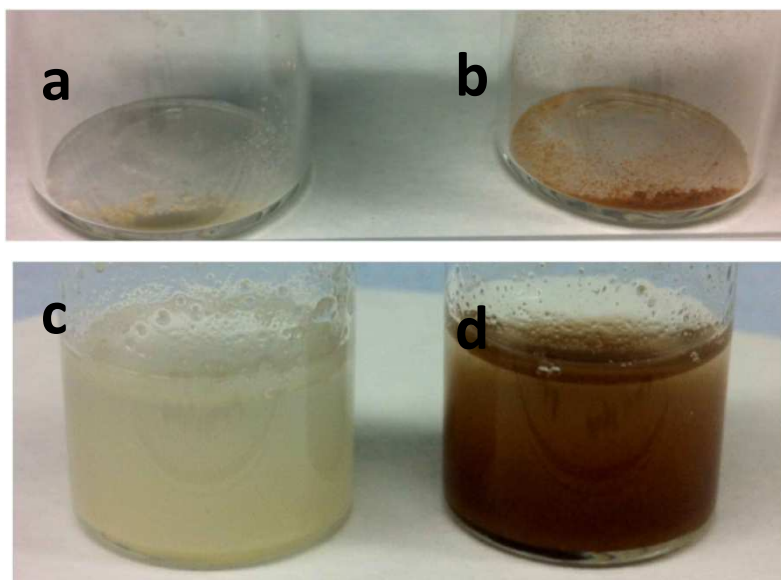


Figure 8.1 Photographs of empty BEICs and MS I. a) Dried bleached EIC; b) Dried MS I; c) BEIC suspended in water and d) MS I suspended in water.

Under light microscopy, apart from the colour, the dry MS I particles had no perceived difference from the empty BEICs (see Chapter 6 for images of BEICs), and no apparent damage was detected on this length scale, as shown in Figure 8.2. For magnetic nanoparticles obtained using a similar method, but in the absence of spores, aggregation can occur causing them to stick together to form aggregates that can be observed *via* microscopy. However, in the MS I, there is no evidence of this using optical microscopy (Figure 8.2). The object highlighted in both photomicrographs is not recognizable as an aggregate of Fe_3O_4 nanoparticles, because it does not exhibit the colour resulting from Fe_3O_4 and/or Fe_2O_3 in reflection mode with parallel polars.

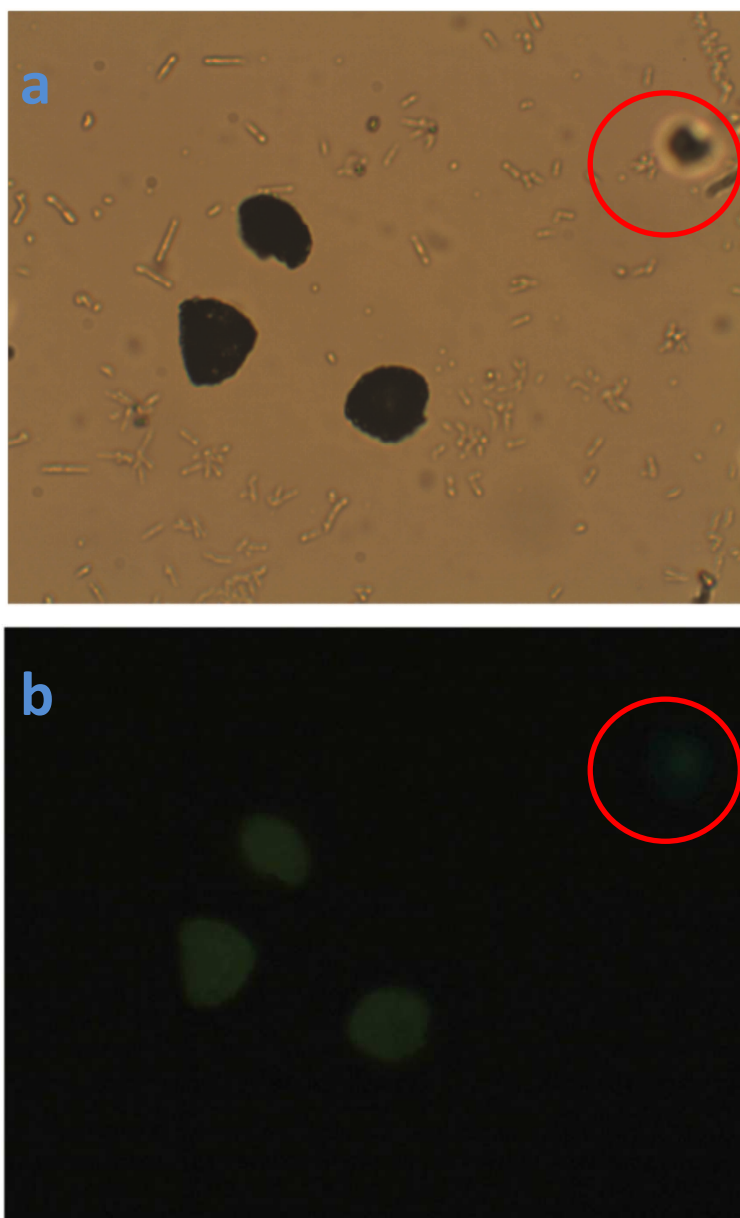


Figure 8.2 Photomicrographs for MS I in a) transmissive mode with parallel polars, b) reflective mode with crossed polars (x400).

In a suspension of MS I in toluene, some small dark red regions were observed under microscopy at random locations on the BEICs, as shown in Figure 8.3. Such observations are not achieved with empty BEICs (see Figure 8.4) because, due to the excess ammonia used in the reaction, the encapsulated FeCl_2 and FeCl_3 are mostly converted to Fe_3O_4 . Therefore, the dark red regions may be caused by the presence of magnetic nanoparticles. However, it is hard to determine whether they are located inside or on the surface of the exine shells by optical microscopy alone.



Figure 8.3 Photomicrograph of MS I in toluene in transmissive mode with parallel polars (x 400).

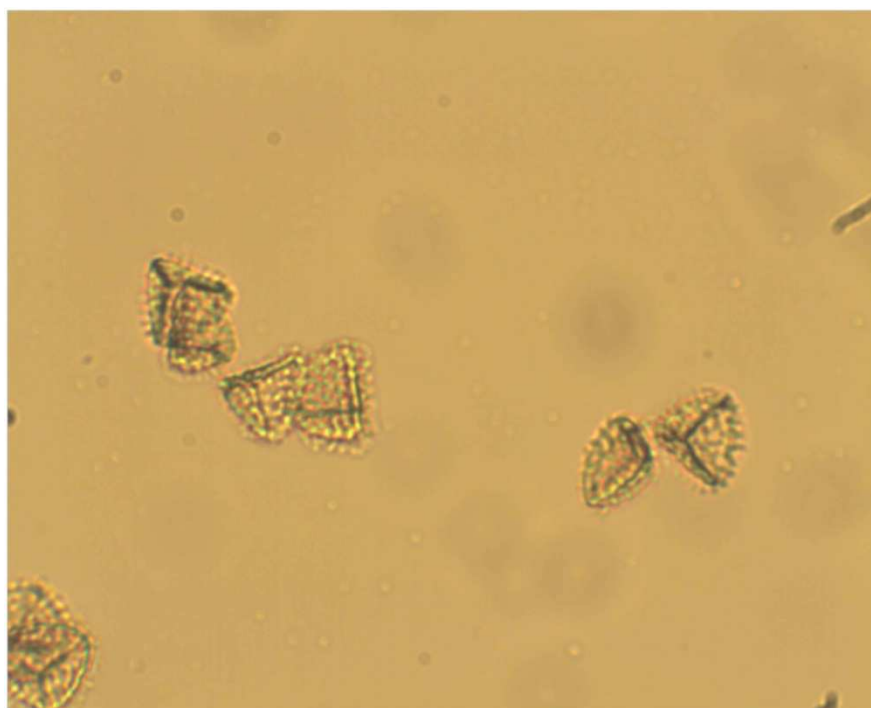


Figure 8.4 Photomicrograph of empty BEICs in toluene in transmissive mode with parallel polars (x400).

The purpose of the micro-reactor encapsulation method is to produce magnetic nanoparticles inside exine shells directly, bypassing the difficult process of filling the BEICs with an insoluble material. As described in the method reported by *Paunov et al.* (see Chapter 1), the starting reactants were firstly encapsulated by the BEICs and then the filled BEICs were transferred into an ammonia solution for the formation of magnetic nanoparticles. It was expected that the ammonia solution would permeate the exine wall and react with the materials inside the exine microcapsules, resulting in the formation of magnetic nanoparticles. Upon investigation by TEM, however, the Fe_3O_4 particles were only found to be present on the outer surface of the exine shells. Figure 8.5a shows the middle region of the cross-section of a flattened MS I BEIC and illustrates the presence of magnetic particles on the surface of exine shell only. All the TEM photomicrographs of this sample show aggregated clusters and individual particles distributed randomly on the exine shell surface, covering a large proportion of the surface.

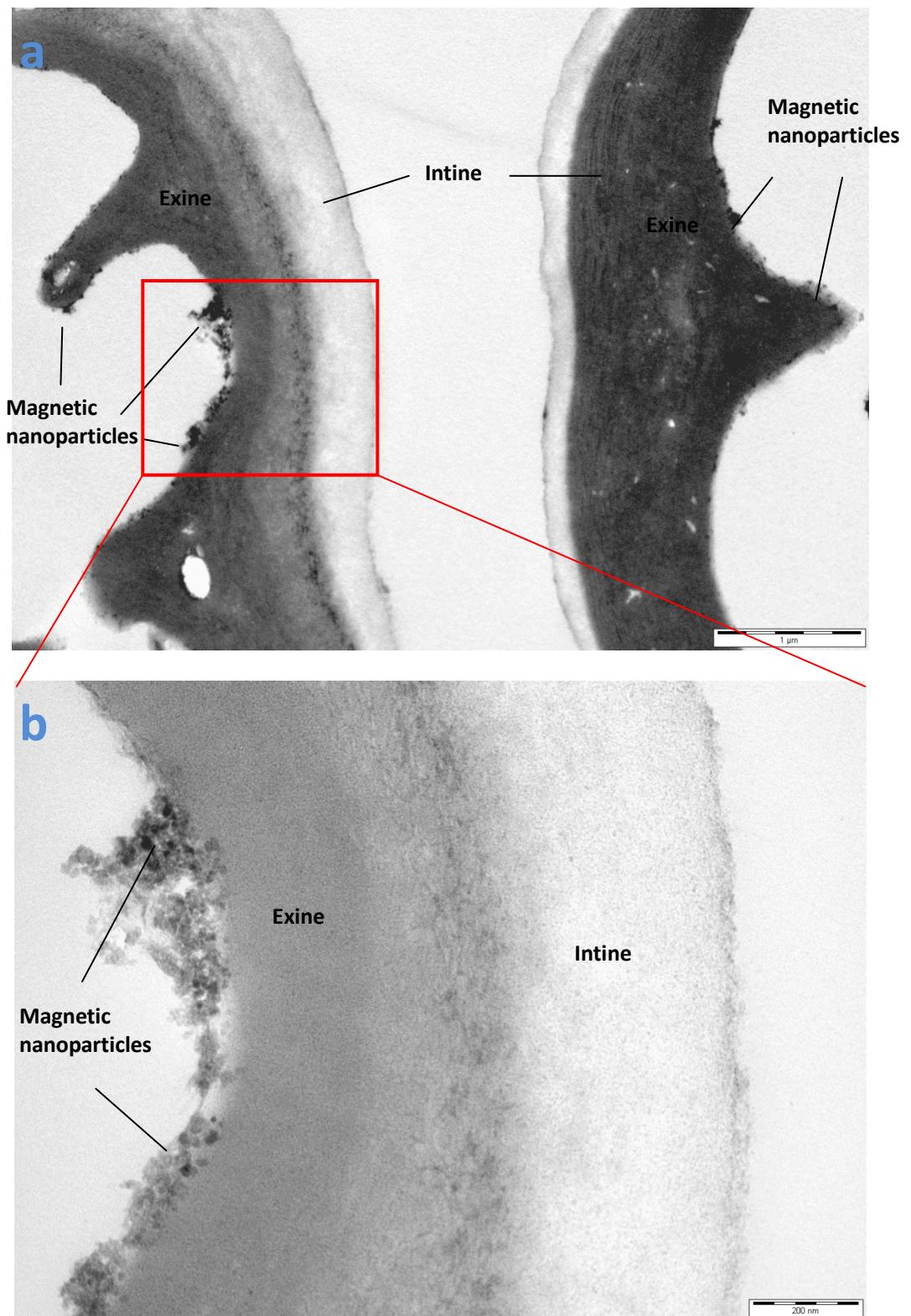


Figure 8.5 TEM images of MS I, a) the middle part of a slightly flattened MS I and b) close up for the red square marked area in a. Scale bar in a) 1 μm and b) 200 nm.

There are three possible reasons why the nanoparticles are not encapsulated: (i) The absence of magnetic nanoparticles may be due to the materials exiting the spore prior to the reaction. However, this is unlikely as the target material is a salt and therefore would

experience strong interactions with sporopollenin. (ii) The reactants are not encapsulated in the exine microcapsules in the first place, but are deposited on the surface of exines because of the high affinity of sporopollenin to ionic salts. (iii) The environment inside of the exines is not suitable for the formation of these types of particles.

The magnetic nanoparticles that form on the surface of MS I are in the size range of 15 to 40 nm and possess irregular morphologies, as shown in Figures 8.5b and 8.6. The nanoparticles must either interact strongly with, or be attached to, the surfaces of the exine walls because the exine capsules can be moved in relatively weak applied magnetic fields. For example, Figure 8.7 shows dry MS I can be moved using an exterior magnet to a sample vial. All of the exines in the sample of MS I responded in response to the magnetic field, indicating a relative uniformity in the distribution of the particles achieved in the encapsulation process. Upon movement of the magnet, the motions of some of the MS I particles are hindered by friction and static charge on the inner surfaces of sample vial. This problem was resolved by suspending the sample in water or other solvents, such as acetone and ethanol.

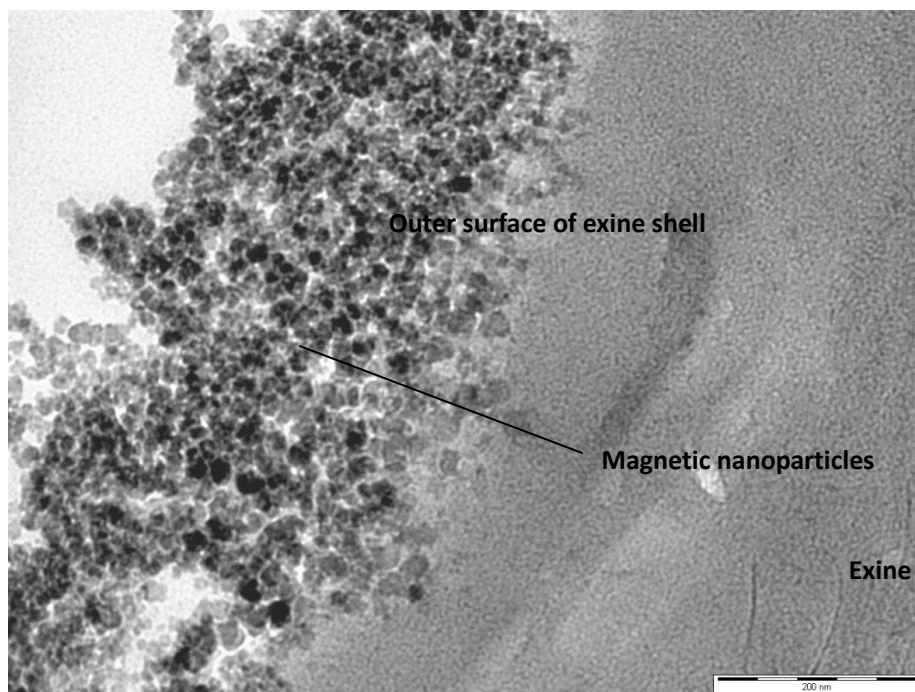


Figure 8.6 TEM photograph for the close up of Fe₃O₄ magnetic nanoparticles in MS I. Scale bar 200 nm.

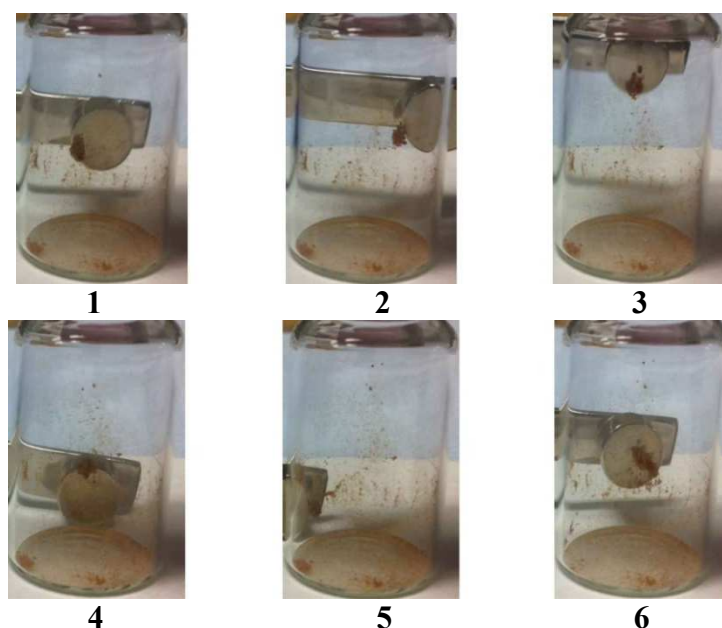


Figure 8.7 Pictures taken from a video of MS I moving by application of a magnet

The behaviour of MS I was also observed in water as a selected solvent. MS I was dispersed in water by shaking, and a magnet was placed on the surface of the side of the vial, as shown in Figure 8.8. The BEICs of MS I moved quickly toward the magnet in the first instance, but as the cluster of MS I BEICs became bigger, the movement of the MS I BEICs toward the magnet slowed. After 3 min in the presence of a magnet, most of the MS I sample gathered on the side of the vial, although a small number of exines remained suspended in the water.

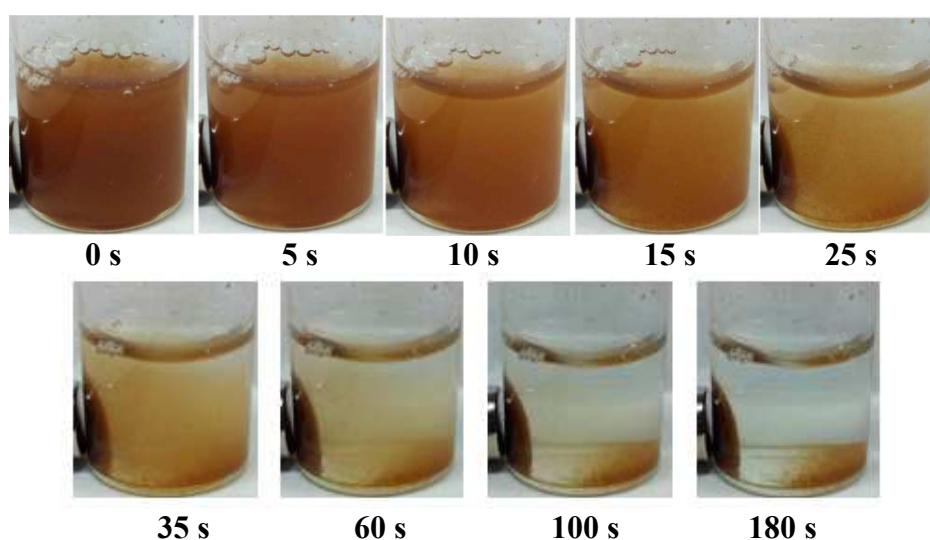


Figure 8.8 Photographs of MS I suspended in water and subjected to a magnetic field as a function of time (seconds)

An experiment was carried out to see if the rotation of the magnet had an effect on the clusters of MS I BEICs nearby, the results for which are shown in Figure 8.9. Upon

rotation, slight movement of the spores can be observed and none of them appear to fall to the bottom of the vial, see Figure 8.9.

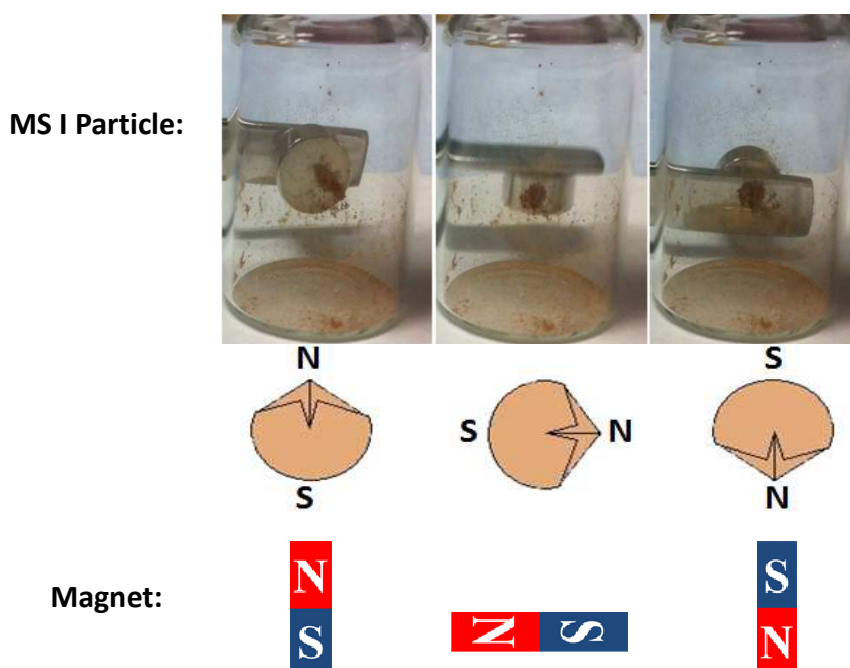


Figure 8.9 General inspection of MS I when the magnet is rotated. ‘N’ and ‘S’ represent the north and south poles of the magnet, respectively.

In order to investigate the qualitative details of the rotation MS I BEICs, a similar experiment was carried out under light microscopy. Figure 8.10 shows the MS I EICs being rotated when the orientation of the magnetic field is changed. The rotation is very rapid and continuous. The MS I BEICs stay in the same position during rotation, and do not move toward the magnet. There are three possibilities for this effect as follows; (i) the viscosity of the water is too high for the exines to move any linear distance with respect to the rotation of the magnet, (ii) the magnet was too far away and hence the field was too weak to induce linear motion, (iii) the separation between the cover-slip and the slide was comparable to the dimensions of the exines, and therefore surfaces played a role, (iv) the magnetic field induced turbulence in the motions of the exines due to non-uniform distributions of magnetic particles on the surfaces of the exine shells, (v) the flow of the particles in the water was itself turbulent. Because of these possibilities the rotation was hard to control. A solution to this may be to use multiple magnetic fields, so the strength of the combined magnetic field can be controlled by fixing the distance between each magnet as well as the direction of each magnetic field. Using a higher viscosity solvent may also aid control of the rotation and reduce the attraction of the magnetic BEICs to the magnets.

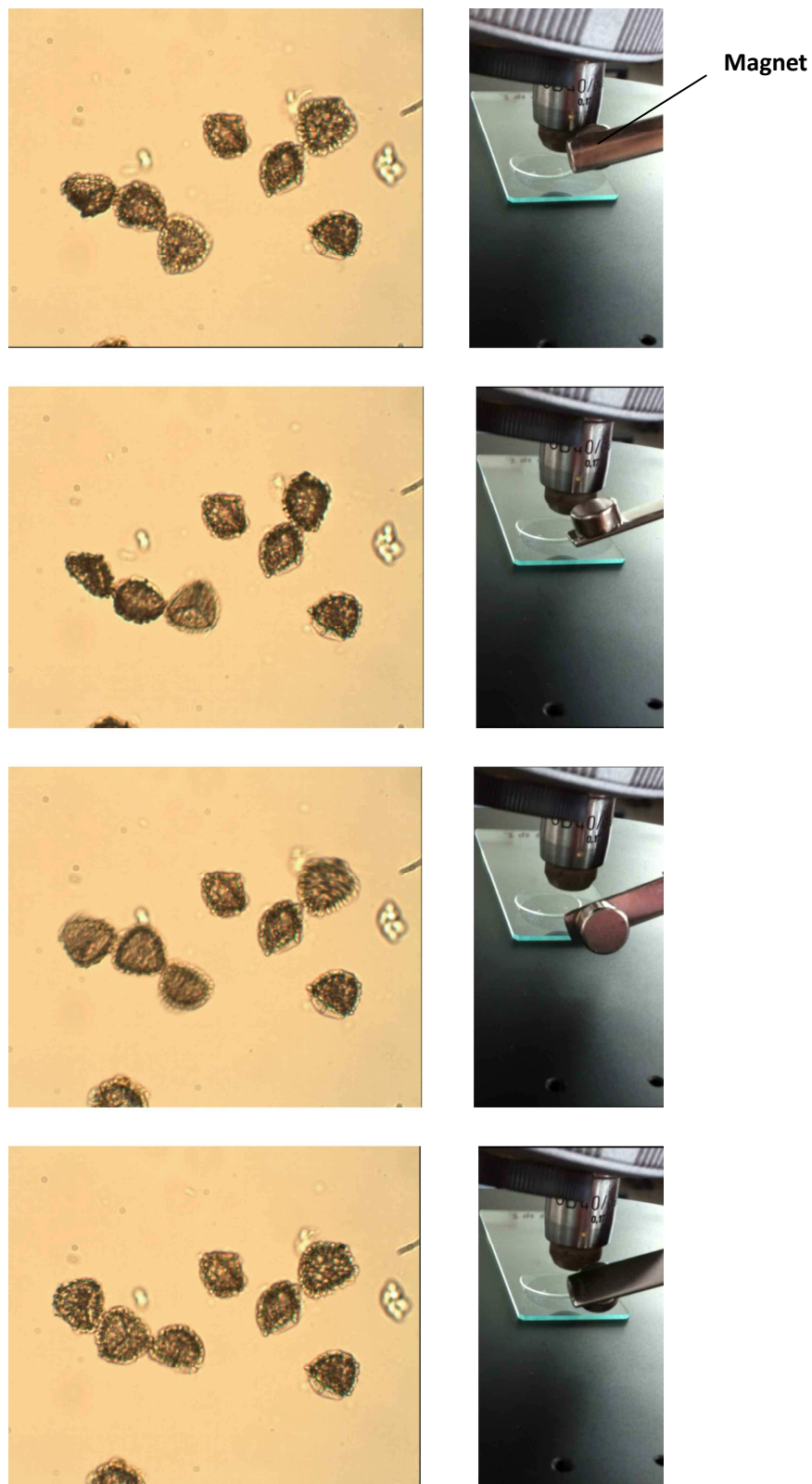


Figure 8.10 Photomicrograph of MS I rotating in water by a magnet.

Due to the MS I BEICs being paramagnetic, they can be easily separated from a mixture with non-magnetic materials. Thus an experiment was performed to isolate MS I BEICs from a mixture of MS I and empty BEICs. None of the experiments used to investigate

the behaviour of MS I resulted in removal of magnetic nanoparticles from the MS I BEICs, thus the BEICs were not expected to be contaminated by magnetic nanoparticles when mixed with MS I. The experiment is demonstrated in Figure 8.11.

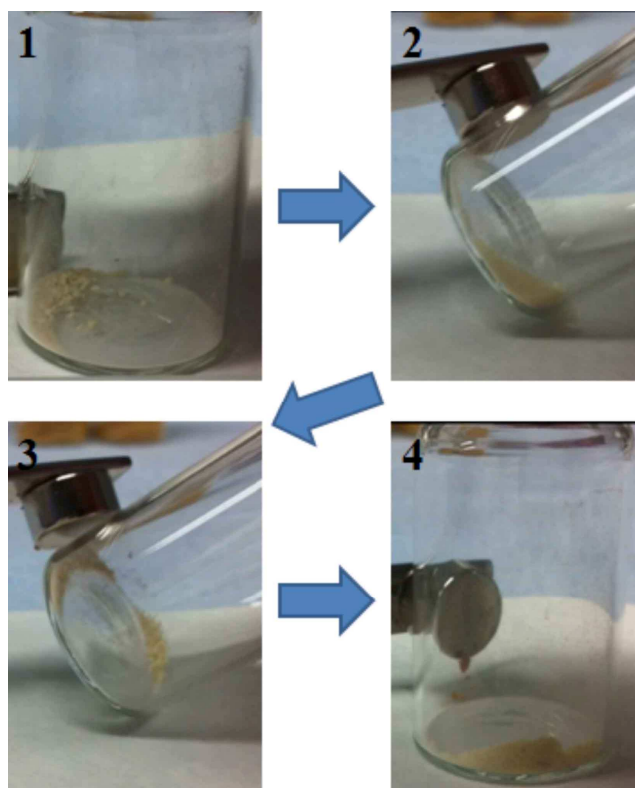


Figure 8.11 Isolation of MS I from BEIC in the absence of solvent.

The MS I BEICs were well mixed with empty BEICs and a magnetic field applied in order to selectively isolate MS I BEICs from the mixture. Initially the separation process was slow, i.e., there was a barrier to the isolation due to the friction that occurs upon movement of the spores past each other, see Figure 8.12. Gentle shaking or slow rotation of the sample aided separation. Although this process was repeated several times, complete isolation was not achieved. After isolation of the MS I BEICs from the empty BEICs, a gentle knock on the sample vial can remove the empty BEICs that gather with the isolated MS I BEICs.

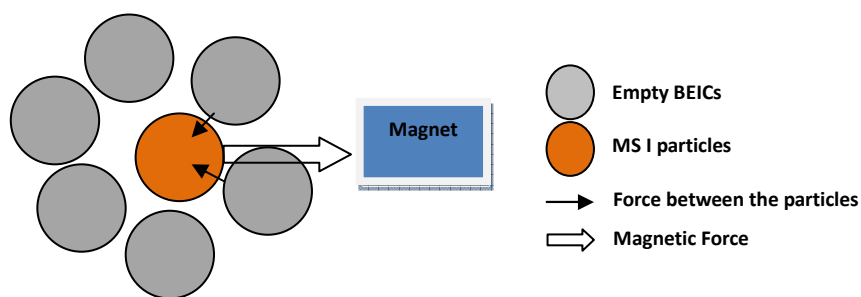


Figure 8.12 Simplified diagram showing the isolation of MS I from empty BEICs in the absence of solvent

Complete separation of MS I BEICs from the BEICs is challenging when the mixture is dry, so the separation was carried out in water. The process is shown in Figure 8.13. To begin with the suspension is entirely brown since MS I is well dispersed with empty BEICs. As the isolation proceeds, the suspension turns yellow white (the inherent colour of empty BEICs), within 30 s of the magnetic field being applied. Thus, MS I isolation using a solvent is much more efficient than isolation from a dry mixture because the force from empty BEICs on MS I is partially reduced by their separation into the solvent (see Figure 8.14a). Moreover, the empty BEICs gathered in isolated MS I were fewer when the separation proceeded in water. When the mixture is suspended in water, water acts as a filter to partially stop empty BEICs in the mixture moving with the MS I particles when the magnetic field is applied (Figure 8.14b).

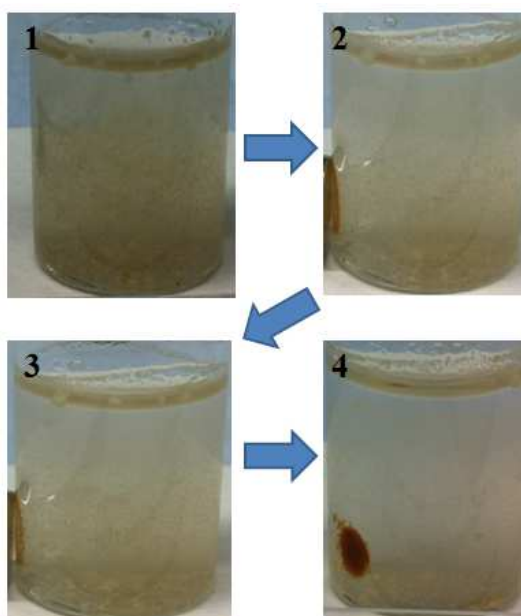


Figure 8.13 Isolation of MS I from normal BEIC in water.

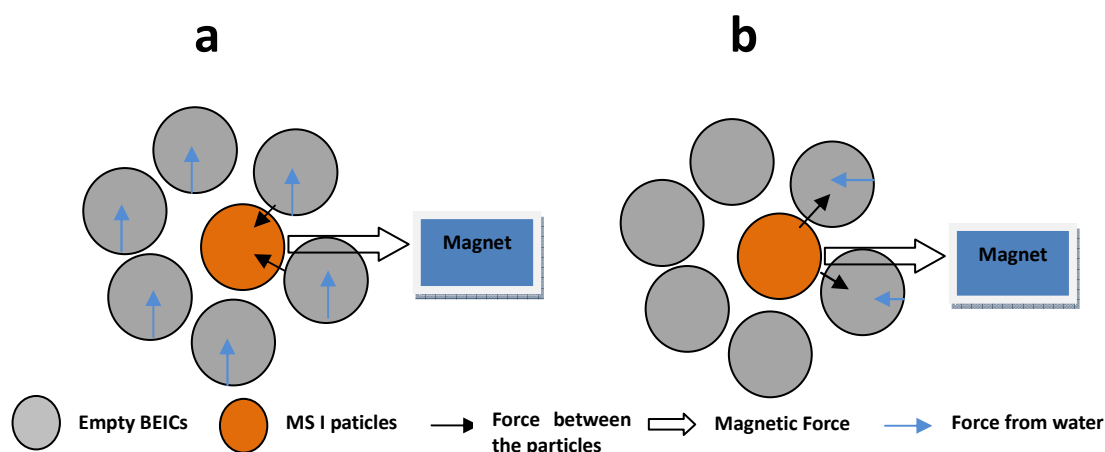


Figure 8.14 Simplified diagram showing the isolation of MS I from empty BEICs in solvent

8.2 Doping of magnetic nanoparticles onto BEIC

The second method used to produce magnetic BEICs is by directly doping magnetic nanoparticles onto the BEICs (magnetic spores II, MS II). This process is much simpler than that used for MS I. The nanoparticles can be adhered to the surface of the exine shells using a variety of treatments, such as ultrasound and the “column” method. Each of the methods achieves similar results, but in the following the subsequent analyses have all been completed using the magnetic BEICs produced by the “column” method. This method involves packing the BEICs in a pipette and compressing them with the use of a vacuum, the suspension of magnetic nanoparticles is added to the “column” and drawn through by reduced pressure until dry. The magnetic nanoparticles used for MS II were $\gamma\text{-Fe}_2\text{O}_3$; they have a much smaller size, i.e., roughly 10 nm, than the nanoparticles that form on MS I. The visual appearance of MS II is similar to MS I, as shown in Figure 8.15.



Figure 8.15 Photographs for MS II.

MS II was successfully moved by the same magnet as used for MS I. However, a small number of magnetic nanoparticles could not be doped onto the BEICs, even though the non-encapsulated magnetic nanoparticles appear in all samples, whatever the encapsulation method used and the amount of nanoparticles used in encapsulation process. Therefore, the MS II samples required further purification/isolation. The nanoparticles that were attached to the surface of the exines form aggregates that are positioned randomly over the surfaces of the exine shells. The non-encapsulated magnetic nanoparticles, which are not attached onto exine microcapsules, would be expected to move more easily moved by a magnet than magnetic BEICs. It was therefore expected that they easily isolated from the MS II sample. Nevertheless, isolation proved to be difficult, see Figure 8.16.



Figure 8.16 Photographs showing purification of MS II, the black powder highlighted by red circle is thought to show an area composed of free magnetic nanoparticles.

After the sample of MS II was purified by exposure to a magnet field, some loose aggregates of nanoparticles could still be observed by microscopy (see Figure 8.17). In transmissive mode with a parallel polar, BEICs and magnetic nanoparticles appear to be of a similar colour, so it was difficult to distinguish BEICs fragments and aggregates of nanoparticles (Figure 8.17a). For example Figure 8.17b (left – centre) shows the association between a BEIC and a nanoparticles aggregate. With both appearing dark due to the presence of $\gamma\text{-Fe}_2\text{O}_3$ nanoparticles it is difficult to see if the exine and nanoparticles cluster are actually attached or not. Some of MS II BEICs do not appear this dark yellow in their dry state in reflective mode (crossed polars), so they were suspended in toluene and observed by microscopy. In transmissive mode with parallel polars, all of the MS II spores appear to have varying amounts of small particles doped (see Figure 8.18) and none of them were found to detach from the BEICs during the observation period. Although some aggregated nanoparticles appeared, under microscopy, to be on the surface of BEIC, this was still not enough to determine the positions of the nanoparticles, and so further investigations were required, by TEM analysis, for confirmation.

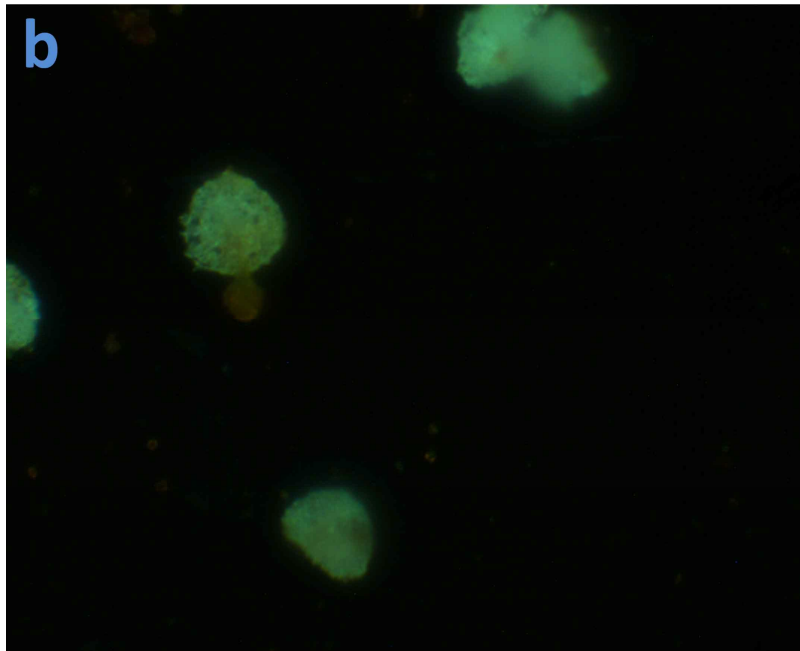
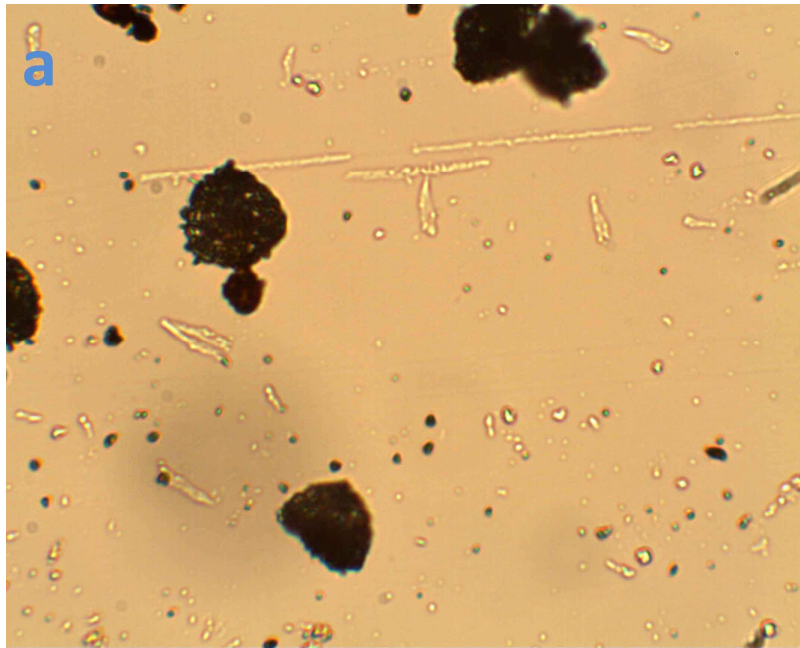


Figure 8.17 Photomicrographs of MS II a) in transmissive mode with parallel polars and b) in reflective mode with crossed polars.

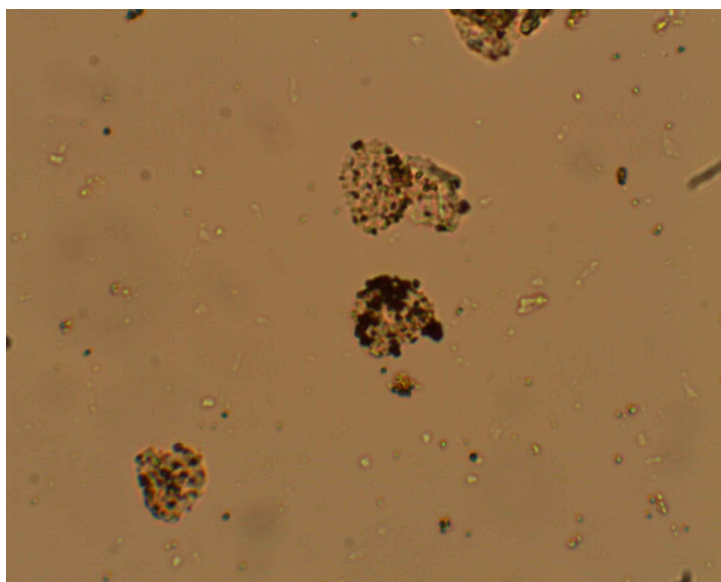


Figure 8.18 Photomicrographs of MS II in toluene in transmissive mode with parallel polars.

The TEM images demonstrate that no magnetic nanoparticles were found in the inside of the BEICs, and all are located on the outer surface of the exine shells, as shown in Figure 8.19. Figure 8.19b shows an aggregate of nanoparticles that are partially doped into the exine shells, but unlike the nanoparticles for MS I that only stay on the surface of exine wall. The reason for this is difficult to rationalize; for instance, it may be caused in the preparation of the TEM sample or any step in the procedure for MS II. The TEM sample of MS I was prepared by the same method as for MS II, but uses a completely different approach to coating nanoparticles onto BEICs. However, TEMs for MS I show that some of nanoparticles can also be doped into the exine wall, but much to a much shallower depth than for MS II (see Figures 8.5 and 8.6). Therefore, the preparation of TEM sample is the more likely reason for doping nanoparticles into exine the wall.

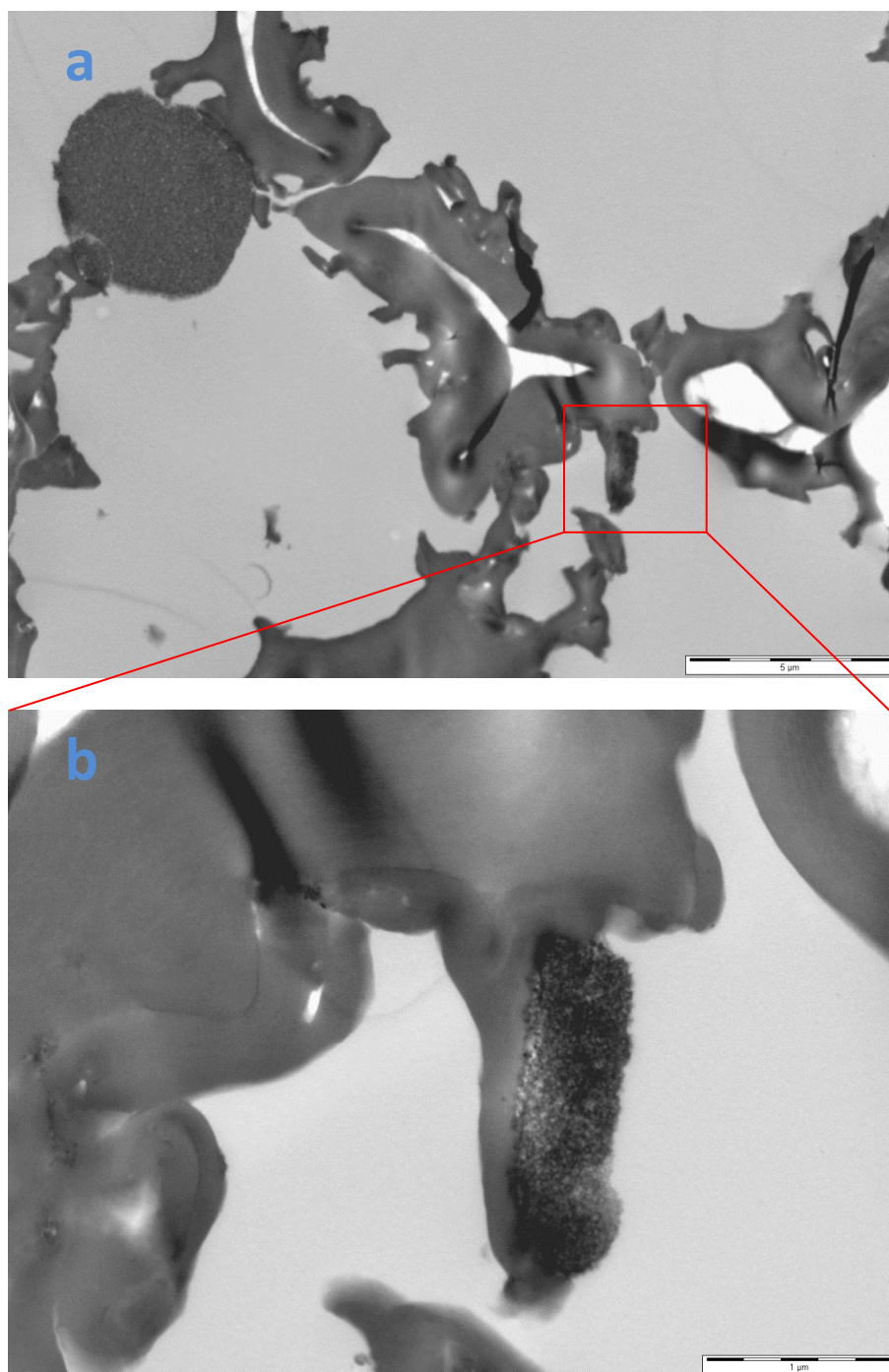


Figure 8.19 TEM images of MS II showing the nanoparticles on the surfaces of the exine walls.
Scale a) 5 μm and b) 1 μm .

Despite the difference in the purities and the sizes of the nanoparticle clusters on the BEICs, the behaviour of MS II and MS I are similar in their responses to magnetic fields. For example, Figure 8.20 shows a sample of MS II can be moved in various directions by a magnet. The number of MS II particles that respond to magnetic field appeared to be constant, and so some MS II particles always remained on the bottom of the vial. There are two possible factors that may be related this behaviour. Firstly, the

magnetic field applied to the non-responsive MS II BEICs is partially shielded by the MS II particles that already respond to the field. Secondly, the magnetic field is weakened by the by the thicknesses of the clustered responsive MS II BEICs. Both of these factors could have an influence on whether the magnetic field is strong enough to move and hold some of the MS II particles. Figure 8.21 shows the movement of MS II in water toward the magnet and most of MS II BEICs move very fast. But again, some of the MS II BEICs remain at the bottom of the vial and far from the magnet. The very small amount of MS II remains suspended in the water at various distances from the magnet and unlikely to be affected by the magnetic field. This suggests that the nanoparticles are not very well distributed on the surfaces of the BEICs. The MS II BEICs no longer, therefore, respond to a magnetic field, and so they are treated as impurities in the product. Fortunately, they can be easily separated from functional MS II particles due to their lack of magnetic response.

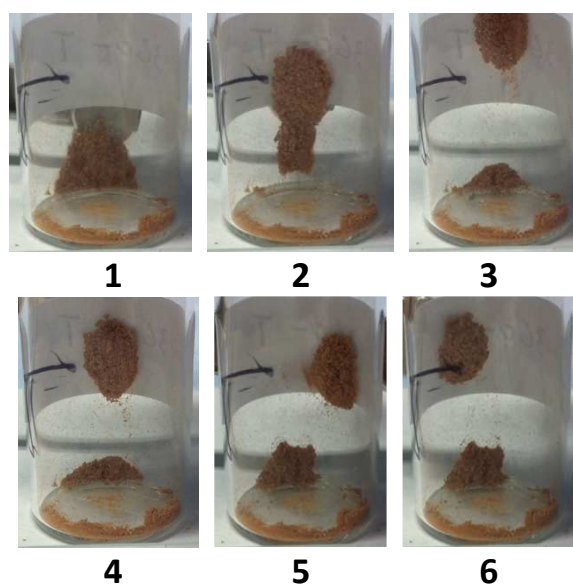


Figure 8.20 Moving MS II by a magnetic field in a sample vial

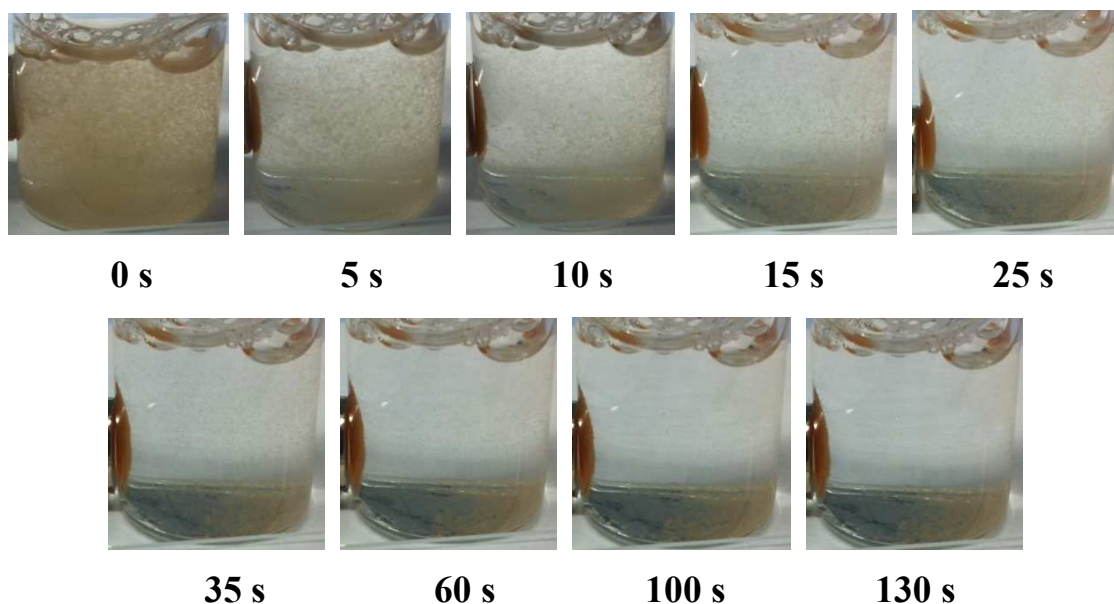


Figure 8.21 Pictures taken from a video of MS II being collected by a magnet in a solvent (water).

As with MS I, it is possible to isolate the MS II particles from empty BEICs using either dry or wet methods in the presence of a magnetic field (Figures 8.22 and 8.23). The difference with isolation of MS II is the possibility of contamination of the surrounding empty BEICs by remaining free $\gamma\text{-Fe}_2\text{O}_3$ nanoparticles when the isolation procedure is enacted and the doped exines move towards the magnet. However, it should be noted that in order to effectively coat EIC and BEIC by nanoparticles, a treatment such as ultrasound is usually required, which in turn limits the contamination from free nanoparticles to a certain degree.

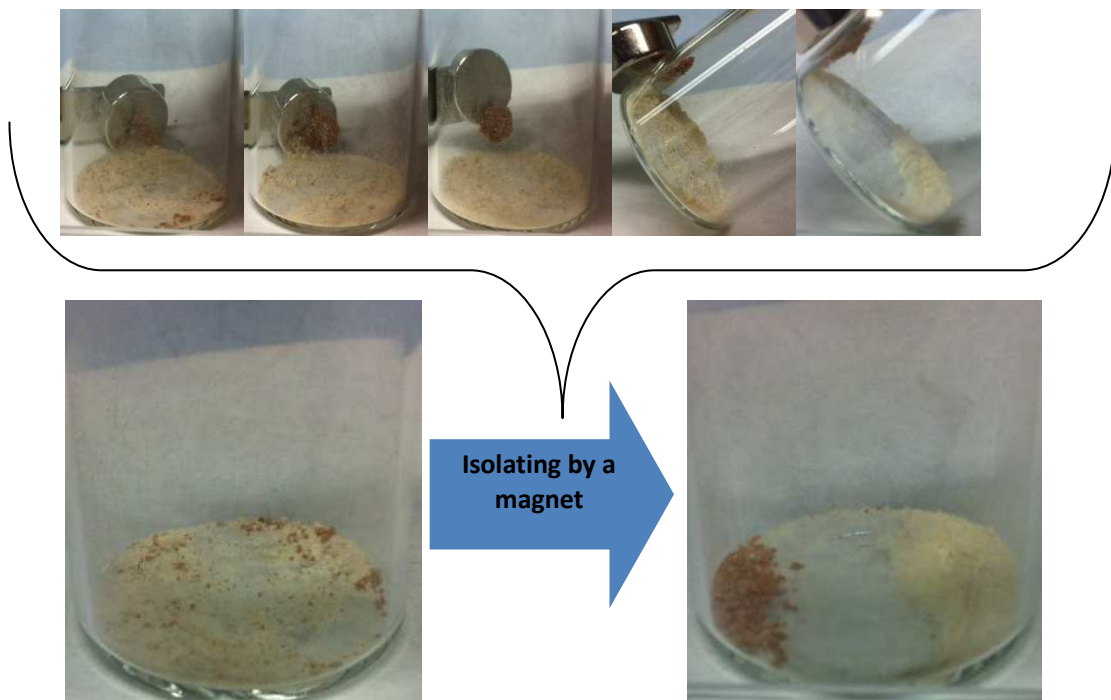


Figure 8.22 Isolation of MS II from BEIC by a magnet without solvent.

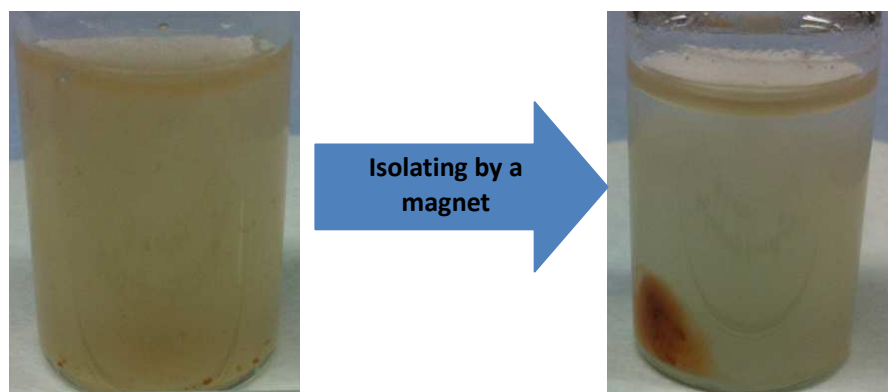


Figure 8.23 Isolation of MS II from BEICs in solvent (water) by a magnet.

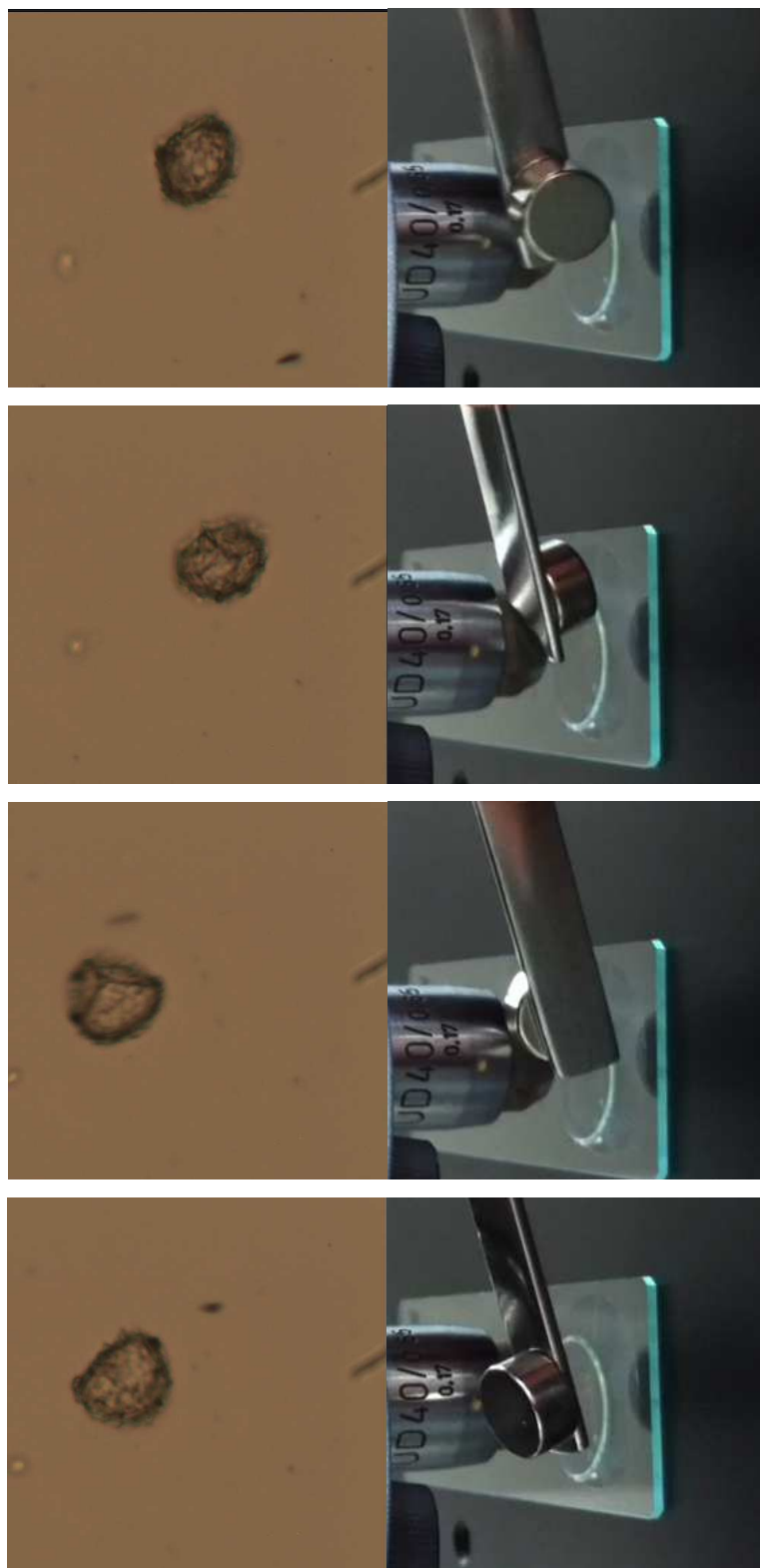


Figure 8.24 MS II rotation by magnetic field under microscope.

Although some of the nanoparticles that attach to the BEICs in MS II do so as aggregates not individual particles, this does not appear to have an apparent effect on the response of MS II to the rotation of the magnetic field. They can still rotate as MS I did under microscopy. Figure 8.24 shows pictures taken from a video of the magnetic

induced rotation of MS II. The MS II BEICs move easier toward the magnet than the comparative MS I, and, consequently, the doped exines not necessarily remain in the same local position when they are rotated.

Compared with MS I, the preparation process of MS II is relatively straight-forward. It is possible to avoid altering the chemical structure of sporopollenin and the bio-content (e.g residue of intine material and protoplast) by the materials used, such as ammonia, achieving the similar effect as for MS I. However, MS II, possesses a relatively lower purity, which is mainly a result of free magnetic nanoparticles mixed within the product. Furthermore, the method of doping magnetic nanoparticles onto exine shells may also be used to dope magnetic nanoparticles onto other micro-scale objects, such as cells, using a simple procedure. After doping of magnetic nanoparticles, this micro-object might be rotated and moved by a magnetic field, allowing the observation of all sides for the object.

8.3 Experimental

MS I Magnetic nanoparticles synthesize in BEICs

A solution was prepared by mixing FeCl_3 (8.11 g), $\text{FeCl}_2 \cdot \text{H}_2\text{O}$ (19.88), HCl (5 M, 5 mL), deionized water (40 mL) and ethanol (5 mL). The mixture was heated to 40 °C until all of the solids dissolved. BEICs (0.2 g) were placed under a vacuum for 10 min, and then they were added to 15mL of the prepared solution and stirred for 2h at RT. Subsequently, the iron-salt-BEICs admixtures were filtered off and washed very quickly with water (10 mL). Then they were placed in an ammonia solution (water : ammonia = 94:6, 100 mL) and stirred for one h. The product was filtered off and washed with water (100 mL). Finally, the product was dried under vacuum.

MS II-1 Magnetic nanoparticles doped onto BEICs by ultrasonic bath

Magnetic nanoparticles ($\gamma\text{-Fe}_2\text{O}_3$, half spatula) were dispersed in water (5 mL) by ultrasonic at 50 °C. The BEICs (0.1124g) were added to the fluid and treated with ultrasound at 50 °C for 2 h. Then the filled BEICs were washed with acetone and re-dispersed in acetone (5 mL) using ultrasound for 10 min. Finally, they were filtered and dried in air for overnight.

MS II-2 Magnetic nanoparticles doped onto Bs using the “coloum” method.

Magnetic nanoparticles (γ -Fe₂O₃, 0.0193 g) were dispersed in water (5 mL) in a sample vial using ultrasound for 1 h at 30 °C. Meanwhile, BEICs (0.1003 g) were packed in a mini “column”. The magnetic nanoparticle fluid mixture (2 mL) was dropped onto the “column” and forced to progress down the column under vacuum. Then the magnetic nanoparticle fluid mixture (2 mL) was added to the “column” again and allowed to flow through it overnight without any extra treatment. Finally, the “column” was washed with acetone (2 mL) and treated under vacuum until the product dried.

9. Multi-functional Exine and Intine Microcapsules

In previously published work and elsewhere in this thesis, bleached exine and intine microcapsules (BEICs) have only been filled with a single type of material that possesses only one function. For example, exine microcapsules have been filled with a magnetic resonance imaging (MRI) contrast agent and evaluated *via in vitro* studies.⁵⁵ However, it is possible to encapsulate more than one functional material inside BEICs, thereby producing multi-functional microcapsules. For example, multiple dyes have been mixed and then encapsulated inside BEICs to produce black microcapsules (see chapter 6). Three materials were combined inside BEICs to produce thermochromic microcapsules (see chapter 7). These two examples demonstrate that several materials have been encapsulated inside BEICs to produce mono-functional microcapsules. Therefore, it should be possible by careful combination of materials to produce multi-functional microcapsules.

If multiple materials are to be simultaneously encapsulated inside BEICs there are several considerations. Materials to be encapsulated should be carefully selected, so as to produce optimum physical properties and avoid any undesirable chemical reactions between the encapsulated materials and/or BEICs. It is desirable to encapsulate materials in the minimum number of steps. Otherwise, problems may be encountered, such as the leaking of encapsulated material caused by the next encapsulation steps and loss of product by transferring steps. For example, experience has shown that a dye mixture may be encapsulated, but differential dye leakage can occur when the functionalised microcapsules are suspended in various solvents.

In this work two multi-functional BEICs were successfully produced as follows; (i) coloured magnetic BEICs (cmEICs), and (ii) thermochromic magnetic BEICs (tmEICs). The multi-functionality of the cmEICs was achieved by the encapsulation of rhodamine B (RB) and the addition of magnetic nanoparticles (Fe_3O_4 , MNPs). The tmEICs were prepared by the co-encapsulation of RB and a thermochromic material, which was a mixture of crystal violet lactone, phenolphthalein and 1-hexadecanol. In these studies the BEICs had been previously bleached, as described in Chapter 4.

In order to produce cmEICs, RB was added to MS II (magnetic spores II, see Chapter 8). The magnetic BEICs (MS II) that were used to produce the cmEICs were light brown in colour as shown in Chapter 8. After encapsulation of RB the brown colour was no longer

observed and the bright pink colour of the RB could be clearly seen, thereby producing bright pink microcapsules as shown in Figure 9.1.



Figure 9.1 Photograph of cmEICs.

The cmEICs were analyzed by light microscopy (Figure 9.2). The reflective mode, with crossed polars, was used for the analytical studies because the dry cmEICs were too opaque to be observed using the microscope in standard transmissive mode. The dry cmEICs appeared similar to the empty BEICs, except for the colour, see Figure 9.2a, where the RB encapsulated BEICs appeared red in the reflective mode with the colour appearance being continuous on the surface of each filled BEICs. However, some small regions still appeared a little yellow, which was assumed to be due to doped MNPs because they cannot be dyed by RB.

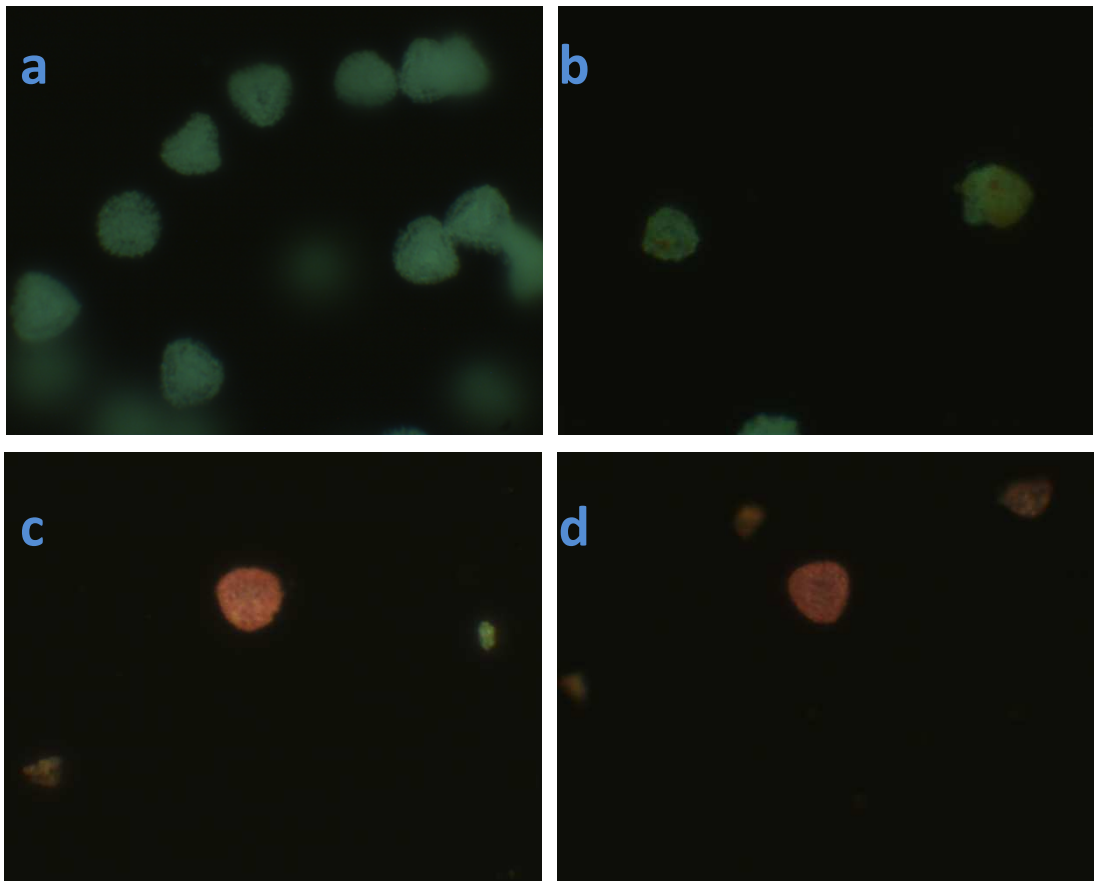


Figure 9.2 Photomicrographs using crossed polars in reflective mode for; a) empty BEICs, b) MS II, c), and d) cmEICs.(x400)

The cmEICs were suspended in water and analyzed by light microscopy (Figure 9.3). Unlike dry cmEICs, the cmEICs suspended in water were transparent enough to allow analysis using standard transmissive mode. Cracked BEICs were observed, that could have been due to damage caused by stirring in the encapsulation process (see Figure 9.3a). As explained in Chapter 6, in the absence of MNPs, the BEICs usually cannot be observed using the reflective mode, see Figure 9.3b. This suggested that the faint outlines of the BEICs seen in Figure 9.3c, are probably due to the presence of MNPs.

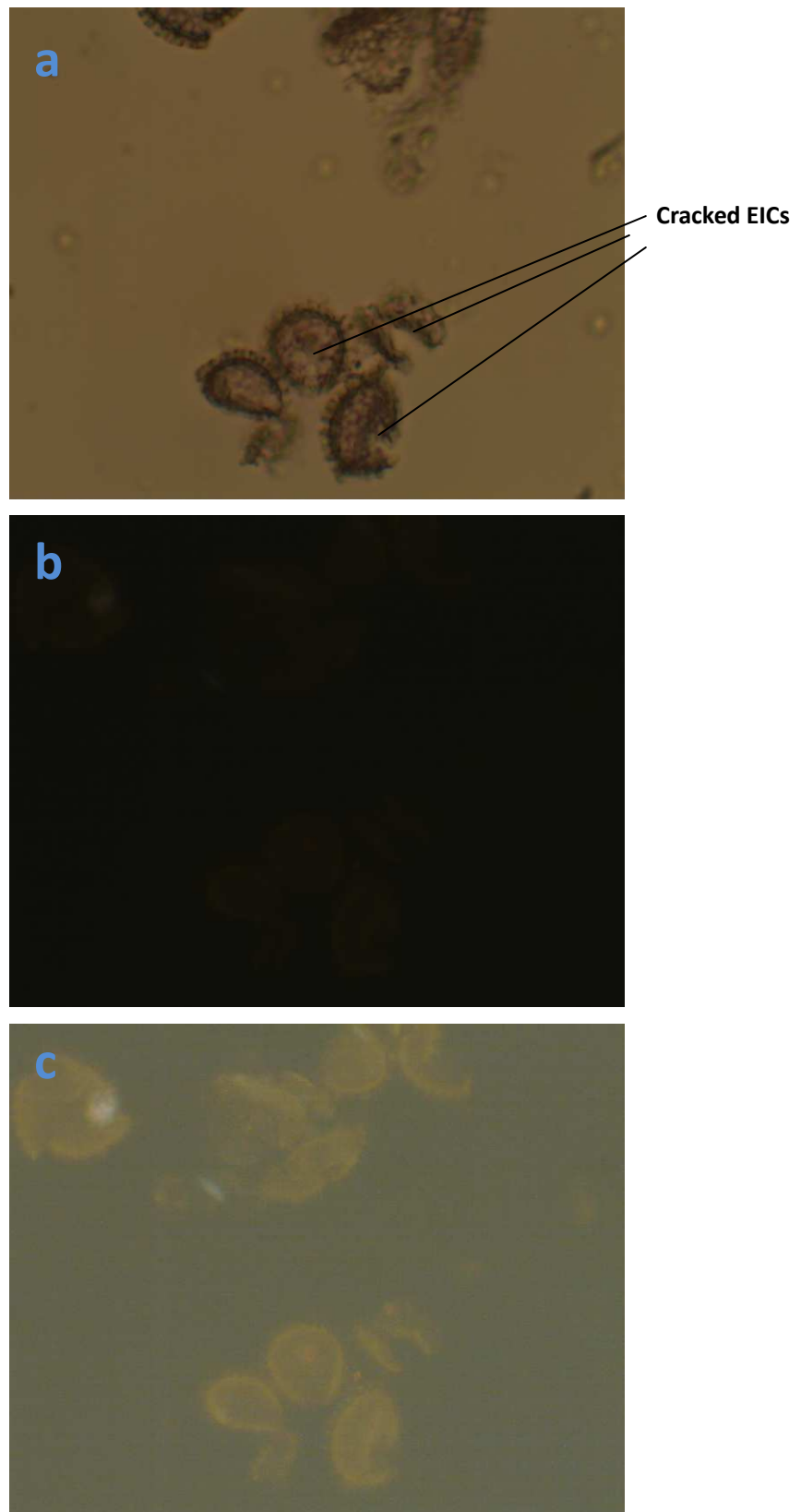


Figure 9.3 Photomicrograph of cmEICs with a) transmissive mode with parallel polars, b) reflective mode with crossed polars and c) computer enhanced brightness of the image of photomicrograph b.(x400)

The magnetic response of cmEICs is very similar to that of MS II BEICs, i.e. in the presence of a magnet, both move towards the magnet (see Figure 9.4 and Chapter 8). This suggests that the additional encapsulation of RB does not alter the observed magnetic properties of the microcapsules. The cmEICs fluoresce due to the presence of the fluorochromic RB and sporopollenin (Figure 9.5). Two peaks observed from this spectra, the sharp peak at 550-560 is probably from excitation light beam (554 nm); another broad peak at 560-650 is the signal from encapsulated RB. However, signal of BEICs cannot be observed from this spectra, may due to it is too weak to appear compare to other obvious peaks (peaks at 550-560 nm and 560-650 nm).

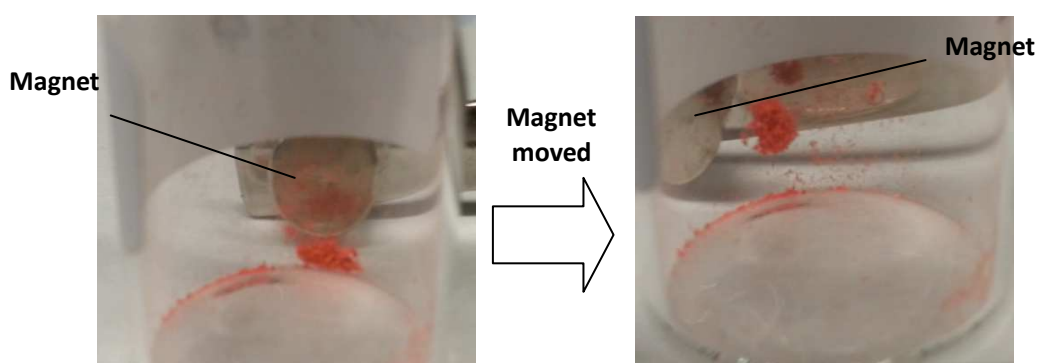


Figure 9.4 cmEICs moving in the presence of a magnet.

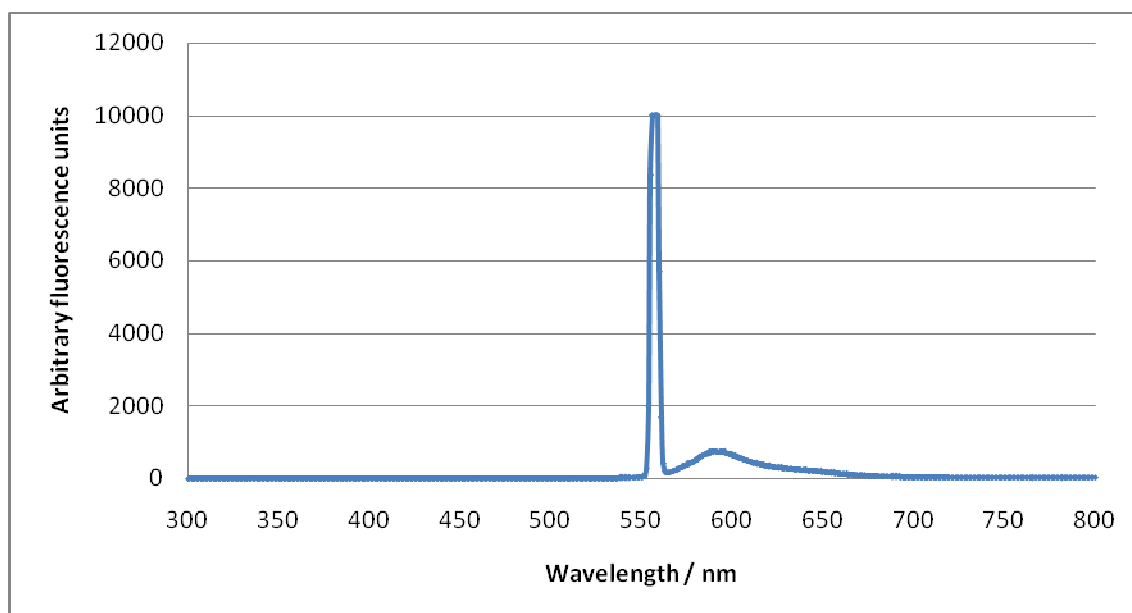


Figure 9.5 Fluorescence emission spectra of cmEIC. Excitation wavelength: 554 nm.

The cmEICs were further functionalized to produce tmEICs, by the addition of a leuco dye-based thermochromic material (LTM) that exhibits thermochromic properties. This mixture included 1-hexadecanol, phenolphthalein and crystal violet lactone. The colour

changes observed for this dye system upon temperature change were discussed in Chapter 7. As the LTM used is blue at room temperature and RB is red (see Chapters 7 and 6), the tmEICs were purple at room temperature, as shown in Figure 9.6.



Figure 9.6 Photograph of tmEICs at room temperature.

Dry tmEICs were analyzed by light microscopy undercrossed polars using reflective, as shown in Figure 9.7. Figure 9.7a shows purple-coloured BEICs, suggestive of a MNP-coated BEIC filled with both RB and LTM (highlighted by a red circle). In this case, the purple colour probably arises from the mixing of red RB and blue LTM. Figure 9.7b and c are from the same sample shown in Figure 9.7a, but are blue and red respectively, suggesting that both RB and the LTM were not successfully encapsulated together on all occasions. A blue BEIC suggests the encapsulation of the LTM and a red BEIC indicates the encapsulation of RB. Trace amounts of other encapsulants may be present in these BEICs, but the quantities were too small to observe via light microscopy. Figure 9.7 only shows a single BEIC (circled) taken from a much larger sample, however, it demonstrates the bulk behaviour observed in Figure 9.6. Other BEICs in this photomicrograph appear white to yellow in colour, indicating the absence of RB and the coloured components of the LTM (i.e. phenolphthalein and crystal violet). MNPs are almost certainly always present, due to the presence of small red regions observed in these yellow-white BEICs. A similar appearance can be observed from the BEICs of MS II.



Figure 9.7 Photomicrographs of a single exine (circled) of tmEICs a), the tmEICs with both RB and LTM encapsulated, b) and c) tmEICs where encapsulation did not occur are highlighted in a difference in colour.(x400)

The tmEICs were suspended in water and analyzed by light microscopy in transmissive mode using parallel polars. Their appearance is different to that of empty BEICs as shown in Figure 9.8 and cmEICs as shown in Figure 9.3, although it is unclear why this is the case. Under reflective with crossed polars, the tmEICs are difficult to see, with only small areas of them appearing very faintly red (see Figure 9.9), and possessing a similar outline appearance to cmEICs (see Figure 9.3). It is possible that the 1-hexadecanol component of the LTM coats the aggregated MNPs on the surface of the BEICs, causing the MNPs to become easier to observe than in cmEICs under reflective light. Although other components of the LTM could possibly cause a similar effect, these are added in much smaller amounts compared to 1-hexadecanol thereby making

this scenario much less likely. Alternatively, the red clusters could be 1-hexadecanol together with RB. However, owing to the positive affinity between RB and BEICs, the previously discussed RB encapsulated BEICs always appeared red all over their surfaces. However, in the Figure 9.9, only a small number of the red clusters were observed.

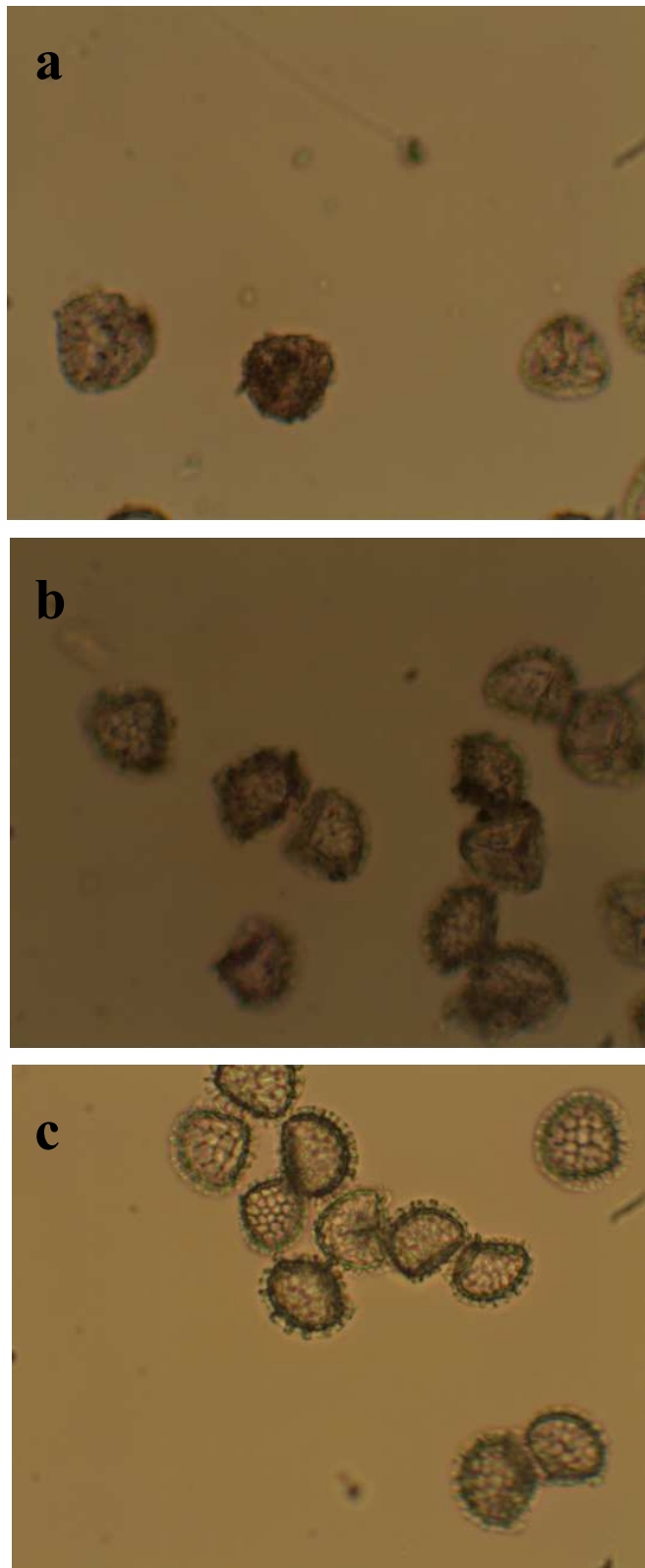


Figure 9.8 Photomicrograph of a) and b) tmEICs suspended in water, and c) empty BEICs suspended in water with parallel polarsintransmissive mode.
(x400)

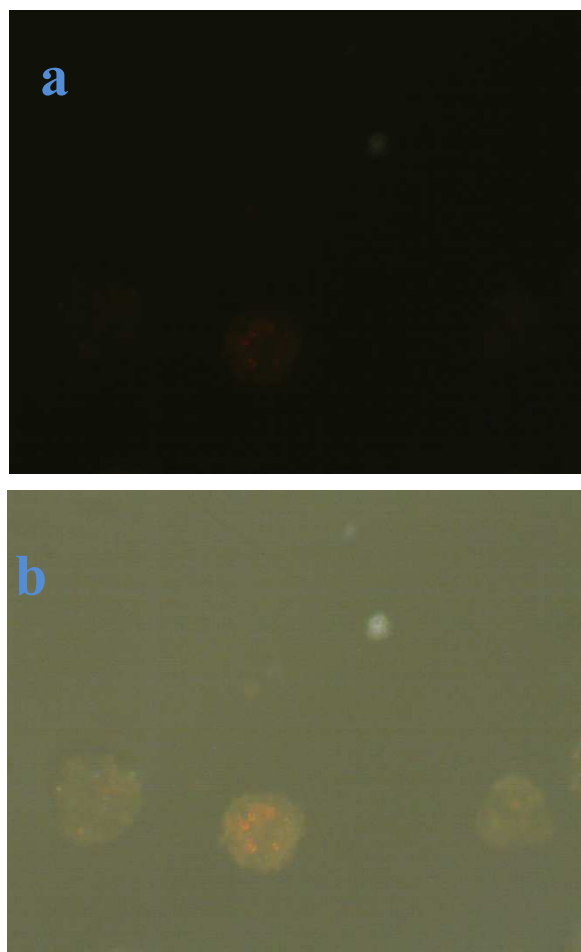


Figure 9.9 Photomicrograph of a) tmEICs suspended in water with crossed polars using reflective and b) computer enhanced brightness image of a).(x400)

When heated from room temperature to 50 °C, the tmEICs changed colour from purple to red, as shown in Figure 9.10. TCSs (thermochromic spores, see Chapter 7) and tmEICs use the same LTM which exhibits a reversible thermochromic change.

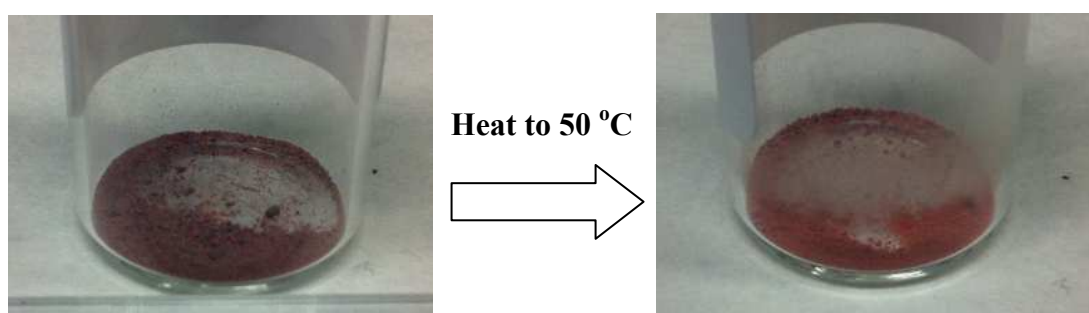


Figure 9.10 Photographs of tmEICs heated from room temperature to 50 °C.

Yellow BEICs were prepared by encapsulating thiazole yellow G (TYG) into BEICs. These were mixed with tmEICs in order to give a magnetic/non-magnetic exine composition, and the mixture was then exposed to a magnet. The tmEICs were attracted

towards the magnet, while the yellow BEICs were not (see Figure 9.11). As a result, the different microcapsules were successfully separated. The increased weight of tmEICs (due to the addition of RB and LTM) compared to MS II, required an increased magnetic force to move these microcapsules. However, quantitative measurements were not made, as only a qualitative result was required to demonstrate the principle.

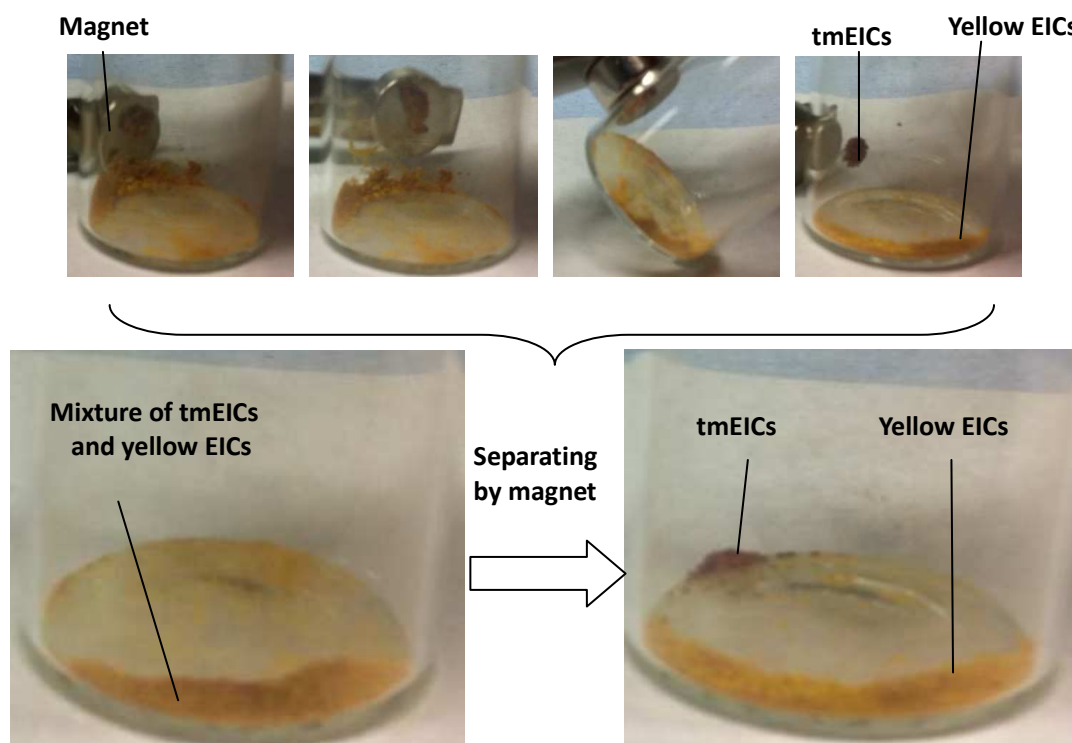


Figure 9.11 Photographs of the separation of tmEICs and yellow BEICs by a magnet.

9.1 Conclusion

Multi-functional cmEICs and tmEICs were successfully prepared and their properties demonstrated. However, it may be possible to further improve the quality of these multi-functional microcapsules. For example, cmEICs were found to be cracked, and it is thought that stirring caused the cracking during the encapsulation process. By reducing the speed of the magnetic stirring during the encapsulation process, damage to the exine shell may be reduced. By increasing the volume ratio between BEICs and the encapsulation solution of the functional material, it may be possible to further limit cracking of the BEICs.

In all cases, photomicrographs of tmEICs and cmEICs taken in reflective mode with crossed polars, indicate that encapsulated materials were not evenly distributed throughout the samples (see Figure 9.2 and 9.6). Some multi-functional BEICs contain encapsulant material, whereas others clearly do not. Quite why this is the case is unclear.

Although BEICs sometimes do not contain encapsulant material, the designed properties arising from this encapsulant material are seen in bulk samples as shown in Figure 9.6.

Five materials were encapsulated into BEICs and it may be possible to load more materials into BEICs, thus increasing their diverse functionality even further. For example, encapsulating a pH sensitive dye with MNPs, would lead to a solid, re-usable pH sensor that could be easily recovered from a suspension.

9.2 Experimental

cmEICs Coloured magnetic BEIC based on rhodamine B

Rhodamine B (0.6 mg) was dissolved in water (5 mL) in a sample vial with a magnetic stirrer. Then MS II was added to the solution and the mixture was stirred at 30 °C for 4.5 h. Finally, the treated BEICs were filtered and washed by with acetone until no dyewas washed out of the BEICs. The washed product was dried in air.

tmEICs Thermochromic magnetic BEICs

1-Hexadecanol (0.29 g), crystal violet lactone (0.016 g), phenolphthalein (0.12 g) and rhodamine B (half spatula) were dissolved in acetone (5 mL) and labeled as solution A. MS II was packed as a mini-column in a short pipette. Then 5 mL of solution A was loaded by the column and sucked by vacuum until the solution flowed through the column. Finally, the treated BEICs were dried under vacuum and collected by a sample vial.

10. Conclusion

This thesis presented the results from three research areas concerning the materials properties of spore exines as follows; (i) exine production, (ii) encapsulation of absorbates that have functional properties, and (iii) the applications of doped spore microcapsules. All of the techniques used for the preparation of spore capsules in this project were based on the literature acid and base treatment,²² but all excluded the acid methodology in order to simplify and shorten the time for the procedure. The major microcapsule production method, the Chm-method, successfully produced intact spore microcapsules (EICs) with all of protoplast and part of intine removed. Moreover, these EICs were successfully bleached using sodium hypochlorite without significant damage to the exine shells. However, the washing process required further improvement due to the small amount of residual material remaining inside the bleached exines (BEICs).

The procedure for producing intact exine shells was further developed using the simplified Chm-method (S-method) which employed an ultrasonic bath to further shorten the processing time. The resulting spores had a relatively more intact intine layer, and so a larger amount of intine material remained than for the EICs prepared by the Chm method. It was proposed that the intact intine layer may actually aid the release of encapsulated material employing the autoclave and sucrose method described in Chapter 1. Therefore, the S-method, and its treated spores, were considered to have good potential for future development.

Subsequent research on the processing of spores (simplified S-method, DS-method) demonstrated the removal of intine and protoplast without harsh chemical treatments (e.g acid and base). The result shows potential for using only common organic solvents, aided by an ultrasonic bath, in order to achieve similar effects to the 4-methylmorpholine N-oxide monohydrate (MMNO) methodology (which can detach the intine from the exine shell). Therefore, this method may be improved by the addition of an enzyme treatment as an alternative to the MMNO method, and the gentle nature of the treatment is expected to maintain the initial chemical integrity of sporopollenin.

The most commonly published method for encapsulation involving exine shells is the droplet method. This method can be supported by varying conditions, such as low or high pressures, and/or change in temperature and concentration of the solution for encapsulation. The results obtained from various experiments, however, show that the droplet method has many disadvantages, such as the uneven distribution of the

adsorbate, and low purity of the resulting materials. As a consequence, the major encapsulation method used in the research work was the “suspension” method. This method achieved a better distribution of the adsorbate(s), higher purities, and a process that could be adapted for large-scale production. However, the suspension method was largely dependent on the ionic properties of sporopollenin, so it may not be as efficient if the chemical properties of the adsorbate and exine shells are not compatible.

A few conditions in common that could influence results from the suspension method were defined and investigated. They included the concentration of the encapsulation solution, the solvent used in the encapsulation process, and the temperature at which encapsulation was conducted. Increasing the concentration and/or temperature caused higher uptake of the adsorbate. Furthermore, in some cases, the encapsulation solvent made it easier for the adsorbate to access the exine shell and therefore to increase the uptake.

During the investigation of the effects of different solvents, it was discovered that the solvents that had similar refractive indexes to those of the EICs increased the transparencies of the EICs, when viewed by microscopy, such that the interior appearance of the EICs could be seen with the use of a suitable refractive index matching solvent. These results should be of importance to further research.

The applications of spore microcapsules were demonstrated starting with the production of coloured microparticles. This included simple encapsulation procedures for single coloured adsorbates, and for multicoloured adsorbate mixtures of three dyes to give microcapsules of any desired colour. For example, rhodamine B (RB, red), thiazole yellow G (TYG, yellow) and methylene blue hydrate (MB, blue) were mixed together to give an adsorbate of desired colour. Furthermore, white microparticles were successfully produced *via* the encapsulation of TiO₂. This also demonstrated the potential for BEICs to encapsulate none-soluble small particles/pigments. Additionally, black microparticles were successfully produced by multi-encapsulation of safranin O (SO), RB, TYG and MB. This study showed that it is possible to encapsulate a complex mixture of components in the BEICs in a stepwise manner, thereby opening up the opportunity to study complex systems such as leuco dyes for thermochromic applications.

The affinity between sporopollenin and ionic compounds was used in separation techniques based on BEICs. In this research, EICs derived from *Lycopodium Clavatum* were examined as capture and release vehicles for dyes. It was demonstrated that raw spores have a capacity to absorb dyes onto their surface, but that sporopollenin exines had a much greater void-volume, due to the removal of the biological centre, which allowed for a greater uptake of dye. The exines absorbed cationic dyes over in preference to anionic and neutral dyes in a range of solvents. The release mechanism was investigated using the following solvents; ethanol, methanol, propan-2-ol and ethanediol. The behaviour of the exines was inverted by pretreating the exines with hydrochloric acid, and in this case, the exines were able to preferentially capture anionic dyes over cationic or neutral dyes, thereby indicating that the ionic nature of the sporopollenin exine is important for determining the affinity of the dye in relation to the exine.

The fluorescence properties of bleached EICs (BEICs) were studied for undoped samples and also for those with RB as the absorbate. BEICs from different production batches were found to display broadly similar emission spectra, despite appearing slightly different colours by visual inspection. BEICs displayed more intense emissions compared to untreated spores and unbleached EICs when examined under a UV source. BEICs filled with RB showed distinct emission peaks arising from both the BEICs and the RB. As the concentration of the RB solution used to fill BEICs was increased, the emission of the encapsulated RB exines shifted to longer wavelengths. Simultaneously, the longer wavelength components of the BEICs' emissions were quenched. Overall, the influence on the emissions between the BEICs and RB was found to be weak. The fluorescent properties of the RB filled BEICs were therefore found to be mainly due to the encapsulated RB. Thus, with the incorporation of fluorescent dyes, the BEICs could be useful materials for the production of fluorescent microparticles.

BEICs responsive to change in pH (pH-EICs) were successfully prepared based on the encapsulation of the indicator phenolphthalein. Although the lifetime of the process had not been determined, the pH-EICs showed the potential for being recyclable because of the reversible properties of phenolphthalein. As with the successes of the encapsulation of multi-functional materials (e.g. black EICs), pH-EICs have the potential to incorporate other pH responsive materials (e.g. methyl red) by encapsulation, thereby expanding the range of pH-EICs available. However, a disadvantage of the pH-EICs

was found to be apparent. The ionic interactions between the encapsulated phenolphthalein and the BEICs appeared to be weakened by the presence of base, and leakage therefore occurred during colour change. This was largely avoided by gentle handling, as evidenced by the fact that the majority of the leakage occurred only after pressurisation.

Thermochromic BEICs (TCS) were successfully produced by the encapsulation of a thermochromic dye mixture, which included phenolphthalein, 1-hexadecanol and crystal violet lactone. This mixture was encapsulated into BEICs by two methods; one that used 1-hexadecanol as the encapsulation solvent (thermochromic spore-1, TCS-1), and another that used acetone as the encapsulation solvent (thermochromic spore-2, TCS-2). TCS-1 and TCS-2 were found to be responsive to thermal stimuli, and the temperature at which the colour change occurred was not sensitive to the method of preparation. However, the encapsulated 1-hexadecanol was found to evaporate when the TCSs were heated causing degeneration of the reversibility of the colour effect. This problem was solved by re-filling, and re-location, of the 1-hexadecanol in the TCSs. Also, a two year old TCS-1 sample demonstrated the strength of the colour of TCS by slowly becoming weaker when it was stored for a long time (although one sample was heated and cooled many times over a two year period).

Magnetic responsive microparticles based on BEICs were successfully produced *via* two methods; one involved the synthesis of Fe_3O_4 inside BEICs (magnetic spore I, MS I) and the other by doping of $\gamma\text{-Fe}_2\text{O}_3$ onto BEICs (magnetic spore II, MS II). The locations of the magnetic material in MS I and MS II were investigated *via* TEM, and both were found to have magnetic materials only on the outer surfaces of the exines. However, the location of the magnetic material was found not to affect the movement of MS I and MS II in an applied magnetic field. Furthermore, separation tests demonstrated that it was possible, with and without solvent, to isolate MS I and MS II exines from non-magnetic BEICs.

Finally, multi-functional cmEICs and tmEICs were successfully prepared and their properties investigated. For example, cmEICs were found to crack, and it is thought that stirring caused the cracking during the encapsulation process. By reducing the speed of the magnetic stirring during the process, damage to the exine shell could be reduced. By increasing the volume ratio between the BEICs and the encapsulation solution of the

functional material, it might be possible to further limit cracking of the BEICs.

In all cases, photomicrographs of tmEICs and cmEICs taken in reflective mode with crossed polars, indicated that encapsulated materials were not evenly distributed throughout the samples. Some multi-functional BEICs contained encapsulant material, whereas others clearly did not. Quite why this was the case is unclear. However, although BEICs sometimes do not contain encapsulant material, the desired properties arising from this encapsulant material were seen in bulk samples.

Five materials were encapsulated into BEICs and it may be possible to load more materials into BEICs, thereby increasing the diverse functionality even further. For example, encapsulating a pH sensitive dye with MNPs, would lead to a solid, re-usable pH sensor that could be easily recovered from a suspension.

11. Definitions

List of Abbreviations

FT-IR	Fourier transform-infrared spectroscopy
SEM	Scanning electron microscopy
TEM	Transmission electron microscopy
MMNO	4-Methylmorpholine N-oxide monohydrate
LSCM	Laser scanning confocal microscopy
ALP	Alkaline phosphatase
sHRP	Streptavidin-horseradish peroxidase
MRI	Magnetic resonance imaging
SP	Spores
DMSP	Diaminosporopollenin
CDMSP	Carboxylated diaminoethylsporopollenin
UV-Vis	Ultraviolet-Visible spectroscopy
EIC	Exine and intine capsule
DCM	Dichloromethane
BEIC or BE	Bleached exine and intine capsule
RB	Rhodamine B
TYG	Thiazole yellow G
MB	Methylene blue hydrate
SO	Safranin O
NBB	Naphthol blue black
TCS	Thermochromic spore
MNP	Magnetic nanoparticle
MS	Magnetic spore
MS I	Magnetic spore I

MS II	Magnetic spores II
cmEIC	Coloured magnetic EIC
tmEIC	Thermochromic magnetic
pH- EICs	pH responsive EICs
CM	EICs produced by Chm Method
S-Method	Simplified Chm method
DS-Method	Simplified S-method
SM	Spore treated by S-method
DSM	Spore treated by DS-method
ET	Encapsulation condition test

12. References

-
- ¹ W.R. Strohl, J.M. Larkin, B. H. Good and R.L. Chapman, *Can J Microbiol*, 1977, **8**, 1080-1083.
- ² G. W. Gooday, *Journal of General Microbiology*, 1973, **74**, 233-239.
- ³ S. S. Kim and C. J. Douglas, *J. Plant Biol.*, 2013, **56**, 1-6
- ⁴ M. Q. Sutton, K. D. Sobolik and J. K. Gardner, *Paleonutrition*, The University of Arizona Press, Tucson, 2010, ch. 4, pp. 109-110.
- ⁵ P. Sreedevi, G. S. Pillai and A. N. Namboodiri, *Curr. Sci. India.*, 1990, **59**, 324-325.
- ⁶ F. Ahlers, J. Lambert and R. Wiermann, *Z. Naturforsch. C.*, 2003, **58**, 807-811.
- ⁷ J. Brooks and G. Shaw, *Grana*, 1978, **17**, 91-97.
- ⁸ G. Shaw, *Phytochemical Phylogeny*, ed. J. B. Harborne, Academic Press, London and New York, 1997, ch. 3, pp. 31-35.
- ⁹ T. Ariizumi and K. Toriyama, *Annu. Rev. Plant Biol.*, 2011, **62**, 437-460.
- ¹⁰ A. K. Chauhan and A. Varma, *A Textbook of Molecular Biotechnology*, I.K. International Publishing House Pvt. Ltd, New Delhi, 2009, Ch. 1, pp. 64-65.
- ¹¹ R. B. Knox, *Studies in Biology no. 107: Pollen and Allergy*, Edward Arnold Limited, London, 1979, Ch. 1, pp. 19.
- ¹² V.B. Gema and A. W. Zoe, *J. Exp. Bot.*, 2006, **57**, 2709-2717.
- ¹³ D. Twell, *Handbook of Plant Science*, ed. K. Roberts, John Wiley & Sons Ltd, Chichester, 2007, pp. 484-485
- ¹⁴ J. R. Rowley, J. J. Skvarla and G. EI-Ghazaly, *Can. J. Bot.*, 2003, **81**, 1070-1082.
- ¹⁵ S. Gubatz and R. Wiermann, *Z. Naturforsch. C.*, 1993, **48**, 10-15.
- ¹⁶ J. Brooks and G. Shaw, *Nature*, 1969, **223**, 754-756.
- ¹⁷ E. Dominguez, J. A. Mercado, M. A. Quesada and A. Heredia, *Sex Plant reprod.*, 1999, **12**, 171-178.
- ¹⁸ P. Piffanelli, J. H. E. Ross and D. J. Murphy, *Sex. Plant Reprod.*, 1998, **11**, 65-80.
- ¹⁹ S. Barrier, A. Lobbert, A. J. Boasman, A. N. Boa, M. Lorch, S. L. Atkin and G. Mackenzie, *Green Chem.*, 2009, **12**, 234-240.
- ²⁰ K. S. Osthoff and R. Wiermann, *J. Plant Physiol.*, 1987, **131**, 5-15.
- ²¹ <http://www.saps.plantsci.cam.ac.uk/pollen/index.htm> [accessed 8th/04/2014]
- ²² S. L. Atkin, S. T. Beckett and G. Mackenzie, *Dosage Form*, US patent,

- ²³ F. Zetzsche and K. Huggler, *Liebigs. Ann. Chem.*, 1928, **461**, 89-109.
- ²⁴ F. Zetzsche, P. Kalt, J. Liechti and E. Ziegler, *J. Prakt. Chem*, 1937, 148, 267-286.
- ²⁵ J. Brook, P. R. Grant, M. Muir, P. V. Gijzel and G. Shaw, *Sporopollenin*, Academic press, London and New York, 1979, pp. 305-350.
- ²⁶ G. Shaw and D. C. Apperley, *Grana*, 1996, **35**, 125-127.
- ²⁷ B. P. Binks, A. N. Boa, M. A. Kibble, G. Mackenzie and A. Rocher, *Soft Matter*, 2011, **7**, 4017-4024
- ²⁸ S. Barrier, A. S. Rigby, A. Diego-Taboada, M. J. Thomasson, G. Mackenzie and S. L. Atkin, *LWT-food Sci. Technol.*, 2010, **43**, 73-76,
- ²⁹ G. Erdtman, *The acetolysis method*, Svensk Botanisk Tidskrift, pp. 561-564.
- ³⁰ G. Erdtman, *Handbook of Palynology: Morphology, Taxonomy, Ecology. An introduction to the study of pollen grains and spores*, Munksgaard, 1969, pp. 213-216.
- ³¹ E. B. Leopold, J. Birkebak, L. Reinink-Smith, A. P. Jayachandar, P. Narvaez and S. Zaborac-Reed, *Palynology*, 2012, **36**, 131-151.
- ³² Y. F. Kuang, B. K. Kirchoff and J. P. Liao, *Grana*, 2012, **51**, 253-262.
- ³³ M. Hesse, H. Halbritter, R. Zetter, M. Weber, R. Buchner, A. Rroshch-Radivo and M. S. Ulrich, *Pollen Terminology: An illustrated handbook*, SpringerWienNewYork, 2009, pp. 51.
- ³⁴ E. Dominguez, J. A. Mercada, M. A. Quesada and A. Herdia, *Grana*, 1998, **37**, 93-96.
- ³⁵ F. A. Loewus, B. G. Baldi, V. R. Franceschi, L. D. Meinert and J. J. Mccollum, *Plant Physiol.*, 1985, **78**, 652-654.
- ³⁶ H. Lin, I. Gomez and J. C. Meredith, *Langmuir*, 2013, **29**, 3012-3023.
- ³⁷ B. G. Baldi, V.R. Franceschi, and F.A. Loewus, *Protoplasma*, 1987, **141**, 47-55.
- ³⁸ N. M. Tarlyn, V. R. Franceschi, J. D. Everard and Frank A. Loewus, *Plant Sci.*, 1993, **90**, 224.
- ³⁹ D. Southworth, *Amer. J. Bot.*, 1988, **75**, 15-21.
- ⁴⁰ U. S. Vural, M. Ersoz, E. Pehlivan, *J. Appl. Polym. Sci.*, 1995, **58**, 2423-2428.
- ⁴¹ T. M. S Chang, *Science*, 1964, **146**, 524-525
- ⁴² G. Bohne, H. Woehlecke and R. Ehwald, *Ann. Bot-London.* , 2005, **96**, 201-208.

-
- ⁴³ S. Barrier, A. D. Taboada, M. J. Thomasson, L. Madden, J. C. Pointon, J. D. Wadhwan, S. T. Beckett, S. L. Atkin and G. Mackenzie, *J. Mater. Chem.*, 2011, **21**, 975-981.
- ⁴⁴ V. N. Paunov, G. Mackenzie and S. D. Stoyanov, *J. Mater. Chem.*, 2007, **17**, 609-612.
- ⁴⁵ T. Engen, *Am. Sci.*, 1987, **75**, 497-503.
- ⁴⁶ W. R. Gombotz and S. F. Wee, *Adv. Drug Deliver. Rev.*, 1998, **31**, 267-285
- ⁴⁷ P. Walde and S. Ichikawa, *Biomol Eng*, 2001, **18**, 143-177.
- ⁴⁸ R. Haag and F. Kratz, *Angew. Chem. Int. Ed.*, 2006, **45**, 1198-1215.
- ⁴⁹ S. Gouin, *Trends Food Sci. Tech.*, 2004, **15**, 330-347.
- ⁵⁰ Q. Chen, F. Zhong, J. Y. Wen, D. McGillivray and S. Y. Quek, *Dry. Technol.*, 2013, **31**, 707-716.
- ⁵¹ Y. D. Kim and C. V. Morr, *J. Agr. Food Chem.*, 1996, **44**, 1314-1320.
- ⁵² Y. Minemoto, K. Hakamata, S. Adachi and R. Matsuno, *J. Microencapsul.*, 2002, **19**, 181-189.
- ⁵³ P. Caravan, C. Comuzzi, W. Crooks, T. J. McMurry, G. R. Choppin and S. R. Woulfe, *Inorg. Chem.*, 2001, **40**, 2170-2176.
- ⁵⁴ A. L. Doiron, K. Chu, A. Ali and L. Brannon-Peppas, *P. Natl. Acad. Sci. USA*, 2008, **105**, 17232-17237.
- ⁵⁵ M. Lorch, M. J. Thomasson, A. Diego-Taboada, S. Barrier, S. L. Atkin, G. Mackenzie and S. J. Archibald, *Chem. Comm.*, 2009, 6442-6444.
- ⁵⁶ S. K. Morcos, *Brit. J. Radiol.*, 2007, **80**, 73-76.
- ⁵⁷ Q. A. Pankhurst, J. Connolly, S. K. Jones and J. Dobson, *J. Phys. D. Appl. Phys.*, 2003, **36**, R167-R181.
- ⁵⁸ B. Zebli, A. S. Susha, G. B. Sukhorukov, A. L. Rogach and W. J. Parak, *Langmuir*, 2005, **21**, 4262-4265.
- ⁵⁹ K. Adhikar, A. Mustapha, I. U. Grun and L. Fernando, *J. Dairy. Sci.*, 2000, **83**, 1946-1951.
- ⁶⁰ T. Wang, L. Lacik, M. Brissova, A. V. Anilkumar, Ales. Prokop, D. Hunkeler, R. Green, K. Shahrokhi and A. C. Powers, *Nat. Biotechnol.*, 1997, **15**, 358-362.
- ⁶¹ N. T. Annan, A. D. Borza, L. T. Hansen, *Food Res Int.*, 2008, **41**, 184-193
- ⁶² S. A. Hamad, A. F. K. Dyab, S. D. Stoyanov and V. N. paunov, *J. Mater. Chem.*, 2011,

21, 18018-18023.

⁶³<http://www.sigmaaldrich.com/catalog/product/sial/p1379?lang=en®ion=GB>
[accessed 29th/03/2014]

⁶⁴ G. Shaw, M. Sykes, R. W. Humble, G. Mackenzie, D. Marsden, E. Pehlivan, *React Funct. Polym.*, 1988, **9**, 211-217.

⁶⁵ M. Kucukosmanoglu, O. Gezici, A. Ayar, *Sep. Purif. Technol.*, 2006, **52**, 280-287.

⁶⁶ O. Gezici, M. Kucukosmanoglu and A. Ayar, *J. Colloid interf Sci.*, 2006, **304**, 307-316.

⁶⁷ S. Sayin, I. H. Gubbuk and M. Yilmaz, *J. Incl. Phenom. Macro.*, 2013, **75**, 111-118.

⁶⁸ N. Kocak, M. Sahin and I. H. Gubbuk, *J. inorg. Organomet. P.*, 2012, **22**, 852-859.

⁶⁹ M. Sahin, I. Gubbuk and N. Kocak, *J. inorg. Organomet. P.*, 2012, **22**, 1279-1286.

⁷⁰ H. Tutar, E. Yilmaz, E. Pehlivan and M. Yilmaz, *Int. J. Biol. Macromol.*, 2009, **15**, 315-320

⁷¹ I. H. Gubbuk, M. Ozmen and E. Maltas, *Int. J. Biol. Macromol.*, 2012, **50**, 1346-1352.

⁷²<http://phx.corporate-ir.net/phoenix.zhtml?c=176060&p=irol-newsArticle&ID=1453463&highlight=>
[accessed 30th/03/2014]

⁷³http://tw.eink.com/display_products_triton.html [accessed 3th/04/2014]

⁷⁴ D. G. Yu, J. H. An, J. Y. Bae, D. J. Jung, S. Kim, S. D. Ahn, S. Y. Kang and K. S. Suh, *Chem. Mater.*, 2004, **16**, 4693-4698.

⁷⁵ B. Comiskey, J. D. Albert, H. Yoshizawa and J. Jacobson, *Nature*, 1998, **394**, 253-255.

⁷⁶ C. M. Lu and C. L. Wey, *J. Disp. Technol.*, 2011, **7**, 482-489.

⁷⁷ Y. Kwak, J. Park, D. S. Park and J. B. Park, *Appl. Opt.*, 2008, **47**, 4491-4500.

⁷⁸ Y. H. Lu and C. H. Tien, *J. Disp. Technol.*, 2013, **9**, 807-813.

⁷⁹ J. Heikenfeld, P. Drzaic, J. S. Yeo and T. Koch, *Journal of the SID*, 2011, **19**, 129-156.

⁸⁰ G. C. Hill and J. S. Holman, Chemistry in context, *Sunbury-on-Thames Nelson*, 1978, Chapter 7, 326-327.

⁸¹ I. Malherbe, R. D. Sanderson and E. Smit, *Polymer*, 2010, **51**, 5037-5043

⁸² C. F. Zhu, A. B. Wu, *Thermochimica Acta*, 2005, **425**, 7-12.

⁸³ S. Atkin, S. beckett and G. Mackenzie, 2009, US20110117148 A1.

-
- ⁸⁴ Private correspondence, Katrina Bakker, Univeristy of York, 2011
- ⁸⁵ Private correspondence, Charles Bradbury, University of York, 2009.
- ⁸⁶ A. N. Zhou, *Comput. Geotech.*, 2013,**49**,36-42.
- ⁸⁷ H. Czachor, M. Flis-Bujak, M. Kafarski and A. Krol, *Soil & Water Res.*. 2008, **3**, S52-S57
- ⁸⁸ X. Zhang, X. Yao, X. Wang, L. Feng, J. Qu and P. Liu, *Soft Matter*, 2014, **10**, 873-881.
- ⁸⁹ S. Komura and Y. Hirose, *J. Chem. Phys.*, 2006, **124**, 241104-1 – 241104-2.
- ⁹⁰ H. T. Xue, Z. N. Fang, Y. Yang, J. P. Huang, L. W. Zhou, *Chem. Phys. Lett.*, 2006, **432**, 326-330.
- ⁹¹ V. D. Sobolev, N. V. Churaev, M. G. Velarde and Z. M. Zorin, *J. Colloid Interf. Sci.*, 2000, **222**, 51-54.
- ⁹² Private correspondence, unpublished work, Katrina Bakker, University of York, 2011.
- ⁹³ G. K. Batchelor, *An Introduction to Fluid Dynamics*, Cambridge university press, New York, 2000, Ch. 1.9, pp. 67-68.
- ⁹⁴ <http://www.sigmaaldrich.com/chemistry/solvents/chloroform-center.html>
[accessed 8th/ 04/2014]
- ⁹⁵ http://www.chemicalbook.com/ChemicalProductProperty_EN_CB3349654.htm
[accessed 8th/ 04/2014]
- ⁹⁶ <http://www.sigmaaldrich.com/chemistry/solvents/toluene-center.html>
[accessed 8th/ 04/2014]
- ⁹⁷ I. Nita, A. Neagu, S. Geacai, A. Dumitru and A. Sterpu, *Ovidius University Annals of Chemistry*, 2010, **21**, 5-8.
http://anale-chimie.univ-ovidius.ro/anale-chimie/chemistry/2010-1/full/1_nita.pdf
[accessed 8th/ 04/2014]
- ⁹⁸ <http://www.sigmaaldrich.com/chemistry/solvents/water-center.html>
[accessed 8th/ 04/2014]
- ⁹⁹ <http://www.sigmaaldrich.com/chemistry/solvents/methanol-center.html>
[accessed 8th/ 04/2014]
- ¹⁰⁰ <http://www.sigmaaldrich.com/chemistry/solvents/acetone-center.html>
[accessed 8th/ 04/2014]
- ¹⁰¹ <http://www.sigmaaldrich.com/chemistry/solvents/acetonitrile-center.html>

[accessed 8th/ 04/2014]

- ¹⁰² D. J. O'Connor, D. Iacopino, D. A. Healy, D. O'Sullivan, J. R. Sodeau, *Atmospheric Environment*, 2011, **45**, 6451-6458.
- ¹⁰³ T. Karstens and K. Kobs, *J. Phys. Chem.*, 1980, **84**, 1871-1872.
- ¹⁰⁴ C. P. C. Lin, C. Kim, S. O. Smith and A. M. Neiman, *PLOS Genetics*, 2013, **9**, page e1003700.
- ¹⁰⁵ J. C. Audran and M. T. M. Willemse, *Protoplasma*, 1982, **110**, 106-111.
- ¹⁰⁶ Private correspondence, Dr. Laurence Abbott, University of York, 6th Feb 2013.
- ¹⁰⁷ F. A. Saeed and J. R. G. Evans, *Anal Chimica Acta*, 2010, **677**, 79-89
- ¹⁰⁸ S. Merouani, O. Hamdaoui, F. Saoudi and M. Chiha, *Chem. Eng. J.*, 2010, **158**, 550-557.
- ¹⁰⁹ C. Wurth, M. Grabolle, J. Pauli, M. Spieles and U. R. Genger, *Nature Protocols*, 2013, **8**, 1535-1550.
- ¹¹⁰ M. F. Al-Kadhemy, I. F. Alsharuee and A. A. D. Al-Zuky, *J. Phys. Sci.*, 2011, **22**, 77-86.
- ¹¹¹ I. Malherbe, R. D. Sanderson and E. Smit, *Polymer*, 2010, **51**, 5037-5043.
- ¹¹² A. Wittrup, S. H. Zhang, K. J. Svensson, P. Kucharzewska, M. C. Johansson, M. Morgelin and M. Belting, *proceedings of the National academy of sciences of the USA*, 2010, 107, 13342-13347
- ¹¹³ X. Gong, S. Peng, W. Wen, P. Sheng and W. Li, *Adv. Funct. Mater.*, 2009, **19**, 292-297.
- ¹¹⁴ Y. K. Hwang, J. N. Choi, J. H. Cho, H. Kwon and S. Huh, *Eur. J. Inorg. Chem.*, 2012, **21**, 3379-3383.
- ¹¹⁵ T. R. Sarkar and J. Irudayaraj, *Anal. Biochem.*, 2008, **379**, 130-132.
- ¹¹⁶ T. Fried, G. shemer and G. Markovich, *Adv. Mater.*, 2001, **13**, 1158-1161.
- ¹¹⁷ A. H. Lu, E. L. Salabas and F. Schuth, *Angew. Chem. Int. Ed*, 2007, **46**, 1222-1244.